

**Life detection and taxonomic characterization with MinION sequencing in Mars and
icy worlds analogue environments**

By Catherine Maggiori

Department of Natural Resource Sciences

Faculty of Agricultural and Environmental Sciences

McGill University

September 2022

A thesis submitted to McGill University in partial fulfillment of the requirements of the degree

of Doctor of Philosophy

© Catherine Maggiori, 2022

*We have
a microscopic anatomy
of the whale
this
gives
Man
assurance*

– William Carlos Williams

We have
a map of the universe
for microbes,
we have
a map of a microbe
for the universe.

we have
a Grand Master of chess
made of electronic circuits.

But above all
we have
the ability
to sort peas,
to cup water in our hands,
to seek
the right screw
under the sofa
for hours

This
gives us
wings.

– Miroslav Holub, “*Wings*”

You look at science (or at least talk of it) as some sort of demoralizing invention of man, something apart from real life, and which must be cautiously guarded and kept separate from everyday existence. But science and everyday life cannot and should not be separated. Science, for me, gives a partial explanation of life.

– Rosalind Franklin

Detailed table of contents

Abstract	9
Résumé	11
Acknowledgments	14
Contribution to original knowledge	15
Contributions of Authors	17
List of Figures and Tables	19
List of Abbreviations	22
Chapter 1. Introduction and Literature Review	23
1.1 Objectives of this thesis	23
1.2 Habitability and the search for life in our Solar System	25
1.2.1 Martian habitability.....	26
1.2.2 The Viking biological experiments.....	27
1.2.3 Habitability of icy moons in our Solar System.....	31
1.3 Biosignatures in our Solar System	32
1.4 DNA detection with MinION sequencing	35
1.4.1 MinION sequencing: advantages and disadvantages.....	35
1.4.2 MinION utilization in remote field work and space science.....	38
1.5 Mars and icy moons analogue environments	40
1.5.1 Hanksville inverted paleochannels.....	40
1.5.2 Lithobionts and University Valley cryptoendoliths.....	44
1.5.3 Cryoconites and sea ice.....	47

1.6 Extraterrestrial simulation experiments	50
1.6.1 Mars simulation chambers.....	51
1.6.2 Previous experiments in Mars simulation chambers.....	53
1.7 Conclusion	61
Connecting Text	62
Chapter 2. The Limits, Capabilities, and Potential for Life Detection with MinION Sequencing in a Paleochannel Mars Analog	63
2.1 Abstract	64
2.2 Introduction	65
2.3 Materials and Methods	69
2.3.1 Site and sample collection	69
2.3.2 DNA extraction and MinION sequencing.....	71
2.3.3 Powder X-ray diffraction (XRD).....	73
2.3.4 Reflectance spectroscopy (UV-VIS-NIR, 350–2500 nm).....	73
2.3.5 Raman Spectroscopy (532 nm).....	74
2.3.6 LDChip biomolecule detection.....	74
2.4 Results	76
2.4.1 MinION sequencing produced diverse metagenomes from the Hanksville paleochannels.....	76
2.4.2 Illumina 16S rRNA gene sequencing revealed a rich bacterial community in the Hanksville paleochannels.....	78
2.4.3 Determination of putative DNA detection limits for MinION sequencing.....	83

2.4.4 Powder XRD revealed a quartz-rich environment.....	85
2.4.5 Reflectance spectra showed hydrated minerals and some organic features.....	85
2.4.6 Prominent bands of chlorophyll and quartz are observed in the Raman spectra.....	87
2.4.7 LDChip immunoassays detected a wide variety of potential metabolisms and taxa.....	89
2.5 Discussion.....	91
2.5.1 MinION metagenomes complement and support XRD data, reflectance spectra, Raman spectra, and LDChip immunoassays.....	91
2.5.2 Putative MinION DNA detection limits and suitability for life detection.....	97
2.6. Conclusion.....	100
2.7 References.....	101
Connecting Text.....	108
Chapter 3. Biosignature detection and MinION sequencing of Antarctic cryptoendoliths after exposure to Mars simulation conditions.....	109
3.1 Abstract.....	110
3.2 Introduction.....	111
3.3 Methods.....	114
3.3.1 Sample site and collection.....	114
3.3.2 Mars chamber (MARTE) exposure.....	116
3.3.3 UVC chamber construction and exposure.....	119

3.3.4 DNA extraction and MinION sequencing.....	122
3.3.5 Life Detector Chip (LDChip) biomolecule detection.....	123
3.3.6 Lipid extraction and analysis.....	124
3.4 Results.....	125
3.4.1 DNA remained detectable and sequenceable after exposure in MARTE and in the UVC chamber.....	125
3.4.2 Protein profile changes in MARTE as revealed by LDChip immunoassays.....	127
3.4.3 MARTE exposure altered the lipid content of the University Valley cryptoendoliths.....	130
3.5 Discussion.....	132
3.5.1 Changes in DNA content post-MARTE and UVC chamber exposure.....	132
3.5.2 Protein and lipid biomolecule changes during the MARTE exposure.....	135
3.5.3 The University Valley cryptoendolith community may be dominated by photoautotrophs.....	137
3.5.4 Implications for extant life detection with MinION sequencing.....	138
3.6 Conclusion.....	141
3.7 References.....	142
Connecting Text.....	151
Chapter 4. MinION sequencing from sea ice cryoconites leads to de novo genome reconstruction from metagenomes.....	152

4.1 Abstract	153
4.2 Introduction	154
4.3 Results	159
4.3.1 Geochemistry of the Allen Bay sea ice collection site.....	159
4.3.2 The Allen Bay sea ice cryoconite metagenome is dominated by Bacteroidetes.....	159
4.3.3 Metagenome-assembled genome (MAG) properties from HiSeq, hybrid, and MinION assemblies.....	164
4.3.4 Hybrid_5: A potential novel species of Octadecabacter.....	167
4.4 Discussion	173
4.5 Conclusion	182
4.6 Methods	183
4.6.1 Sample site and collection.....	183
4.6.2 Geochemical analyses.....	184
4.6.3 DNA extraction and MinION sequencing.....	184
4.6.4 DNA extraction and HiSeq sequencing.....	186
4.6.5 Contig assembly and binning.....	187
4.7 References	190
Chapter 5. Discussion	198
5.1 The taxonomy of Mars analogue environments as revealed by MinION sequencing	198
5.2 MinION utility in space science	202

5.3 MinION sequencing complements and supports results from other space mission techniques.....	205
5.4 Utility of MinION sequencing in microbial ecology.....	208
5.5 Future work.....	213
Conclusion.....	217
References.....	219
Appendix.....	244

Abstract

The search for life beyond Earth is a top priority for space science and a fundamental human curiosity. Our Solar System comprises diverse worlds, some of which have the potential to harbour past or present life based on their possession of habitable qualities, including organic molecules and liquid water. These include the rocky inner planet Mars and icy moons Enceladus and Europa. Searching for ancient biosignatures on Mars is a primary objective of both Mars 2020 and the upcoming ExoMars mission, yet neither mission contains instrumentation capable of detecting definitive biosignatures, which are substances, objects, or patterns that could not form via abiotic processes. DNA is one such definitive biosignature, as it is virtually impossible to be produced without extant or recently extinct life. Robust instrumentation for detecting DNA exists in the form of the Oxford Nanopore Technologies' (ONT) MinION, a portable and miniaturized sequencing device. However, the MinION needs to be tested in a diverse set of analogue environments to establish its utility for life detection and metagenomics in extreme environments.

I first evaluated the MinION's performance on paleochannel samples from Hanksville, UT, USA. The MinION was able to directly detect DNA from this paleochannel site analogous to Martian sinuous ridges. Additionally, a putative lower detection limit of 0.001 ng of DNA was established, which corresponds to ~100 cells/g, a biomass common in extreme Mars analogue environments. Other space mission instruments and techniques (i.e. X-ray diffraction, reflectance spectroscopy, Raman spectroscopy, immunoassay microarrays) detected biosignatures such as pigments, other organics, and water-related features. However, when these techniques are combined with the MinION, the potential for biosignature identification and environmental

characterization was greatly increased; the MinION linked these environmental features with potential microorganisms and metabolisms.

Following this proof-of-concept utilization of the MinION for direct life detection, I then tested if DNA was detectable from Mars analogue samples after exposure to multiple extreme pressures analogous to Martian environmental conditions (i.e. a Mars environmental chamber). DNA remained detectable with MinION sequencing after a ~58-sol Mars chamber exposure, as did proteins and lipids (i.e. other definitive biosignatures). Of the many destructive environmental conditions on Mars (e.g. freezing temperatures, low atmospheric pressure, CO₂-rich atmosphere), UVC radiation is the most biocidal (i.e. it is the most likely to destroy cells and degrade DNA, preventing detection with the MinION). As such, I also used a custom-built UVC chamber to establish if an extreme radiation dose corresponding to ~278 Martian years prevents the ability of the MinION to detect DNA. While the amount of DNA decreased over the UVC exposure, DNA detection with the MinION was not prohibited, demonstrating its suitability for extant life detection on Mars analogue samples after exposure to Mars-like conditions.

Finally, I evaluated the MinION's potential for genome reconstruction from metagenomes in extreme analogue environments. Using samples from sea ice cryoconites in the Canadian high Arctic, I compared different approaches for producing metagenome-assembled genomes (MAGs) and found that combination MinION + HiSeq (i.e. hybrid) MAGs had the highest completeness, lowest contamination, and highest N50 of all datasets. A potential novel genome of *Octadecabacter* was also produced. The hybrid assembly also produced longer contigs, more coding sequences, and more total MAGs, leading to more accurate descriptions of microorganisms in this extreme environment.

Résumé

La recherche de la vie au-delà de la Terre est une priorité absolue pour la science spatiale et une curiosité humaine fondamentale. Notre système solaire comprend divers mondes, dont certains ont le potentiel d'abriter une vie passée ou présente en raison de leurs qualités d'habitabilité, notamment des molécules organiques et de l'eau liquide. Il s'agit particulièrement de la planète interne rocheuse Mars et des lunes glacées Encelade et Europe. La recherche d'anciennes biosignatures sur Mars est l'un des principaux objectifs de la mission Mars 2020 et de la prochaine mission ExoMars. Pourtant, aucune de ces deux missions ne dispose d'instruments capables de détecter des biosignatures définitives, c'est-à-dire des substances, des objets ou des motifs qui ne pourraient pas se former par des processus abiotiques. L'ADN est l'une de ces biosignatures définitives, car il est pratiquement impossible de le produire sans vie existante ou récemment éteinte. Il existe des instruments robustes pour détecter l'ADN, comme le MinION d'Oxford Nanopore Technologies (ONT), un appareil de séquençage portable et miniaturisé. Cependant, le MinION doit être testé dans un ensemble diversifié d'environnements analogues afin d'établir son utilité pour la détection de la vie et la métagénomique dans les environnements extrêmes.

J'ai d'abord évalué les performances du MinION en matière de détection de la vie sur des échantillons de paléo-canaux provenant de Hanksville, UT, États-Unis. Le MinION a été capable de détecter directement l'ADN de ce site de paléo-canaux analogue aux crêtes sinueuses martiennes. De plus, une limite inférieure de détection putative de 0,001 ng d'ADN a été établie, ce qui correspond à ~100 cellules/g, une biomasse commune dans les environnements extrêmes analogues à Mars. D'autres instruments et techniques de mission spatiale (c.-à-d. la diffraction des

rayons X, la spectroscopie de réflectance, la spectroscopie Raman, les microréseaux d'immuno-essais) ont détecté des biosignatures telles que des pigments, d'autres matières organiques et des caractéristiques liées à l'eau. Néanmoins, lorsque ces techniques sont combinées avec le MinION, le potentiel d'identification et de caractérisation des biosignatures est considérablement accru; le MinION relie ces caractéristiques environnementales à des micro-organismes et métabolismes potentiels.

Après cette preuve du concept de l'utilisation du séquenceur MinION pour la détection directe de la vie, j'ai ensuite testé si l'ADN était détectable à partir d'échantillons analogues à ceux de Mars après exposition à de multiples pressions extrêmes analogues aux conditions environnementales martiennes (c.-à-d. une chambre environnementale martienne). L'ADN est resté détectable avec le séquençage MinION après une exposition à une chambre martienne de ~58-sol, tout comme les protéines et les lipides (c.-à-d. d'autres biosignatures définitives). Parmi les nombreuses conditions environnementales destructrices sur Mars (p. ex. températures glaciales, faible pression atmosphérique, atmosphère riche en CO₂), le rayonnement UVC est le plus biocide (c.-à-d. qu'il est le plus susceptible de détruire les cellules et de dégrader l'ADN, empêchant ainsi la détection avec le MinION). C'est pourquoi j'ai également utilisé une chambre UVC sur mesure pour déterminer si une dose extrême de rayonnement empêche complètement le MinION de détecter l'ADN. Bien que la quantité d'ADN ait diminué au cours de l'exposition aux UVC, la détection avec le MinION n'était pas prohibée, ce qui démontre son aptitude à détecter la vie existante sur des échantillons analogues à ceux de Mars après une exposition à des conditions semblables à celles de Mars.

Enfin, j'ai évalué le potentiel du MinION pour la reconstruction de génomes à partir de métagénomes dans des environnements analogues extrêmes. En utilisant des échantillons de

cryoconites de glace de mer dans le Haut-Arctique canadien, j'ai comparé différentes approches pour produire des génomes assemblés de métagénome (MAGs) et j'ai trouvé que la combinaison MinION + HiSeq (c.-à-d. hybride) MAGs avait la plus grande complétude, la plus faible contamination, et le plus grand N50 de tous les ensembles de données. Un nouveau génome potentiel d'*Octadecabacter* a également été produit. L'assemblage hybride a également produit des contigs plus longs, avec plus de séquences codantes et plus de MAGs totaux, ce qui a permis de décrire plus précisément les microorganismes de cet environnement extrême.

Acknowledgments

There are many people I would like to thank and without whose support, this thesis would not have been possible.

To my supervisor, Lyle Whyte. Lyle, I want to express my sincere gratitude for giving me the opportunity to work in your lab. Thank you for exposing me to so many exciting projects in microbiology and astrobiology, for encouraging my application to fast-track to the Ph.D. program, for including me on field campaigns to the high Arctic and Utah, and for your guidance and support over the last six years. I will always be thankful for the opportunities and growth I've achieved in your lab, both as a scientist and as a person.

To my supervisory committee, Jennifer Ronholm, Richard Léveillé, and Sébastien Faucher. Thank you for your support, expertise, and answering my many (many...) questions.

To Isabelle Raymond-Bouchard. Isabelle, thank you for being my unofficial second supervisor. You have made me a better, more confident scientist and I am forever grateful.

To my funding sources NSERC PGS-D and CGS-D, FRQNT, the McGill Space Institute, and the Northern Scientific Training Program that supported this work.

To my dear colleagues in the Whyte lab and the Natural Resource Sciences department. By far you have been the best part of my graduate studies. Esteban Góngora Bernoske, Mariam Saad, Evan Marcolef, Ianina Altshuler, Miguel Angel Fernández-Martínez, Brady O'Connor, David Touchette, Elisse Magnuson, Olivia Blenner-Hassett, Madison Ellis, Louis-Jacques Bourdages, Nastasia Freyria, Helena Chan, and Antoine Lirette. Thank you for your insight, advice, and encouragement to keep going. I feel immeasurably lucky to call you all my friends.

To all my co-authors and collaborators, especially Jacqueline Goordial, Jessica Stromberg, Ed Cloutis, Laura Sánchez-García, Mercedes Moreno-Paz, Yolanda Blanco, Victor Parro, and the CanMars 2016 field team. Thank you for your patience and invaluable advice.

To my undergraduate supervisor, Kirsten Müller. Thank you for being my first mentor and giving me a chance to try academic science.

To my parents, Patricia and Jerry. Mom and Dad, I love you and I hope you're proud of this work.

To my sister Jasmine, brother-in-law Tom, and nieces Cecilia and Lily. Jasmine, you've been my hero since I was born. You're the smartest and coolest person I've ever met and ever since I was a kid, I wanted to be just like you. I hope this thesis brings me a little closer.

To Emily Wicks, Derek Godin, and Noah Century. Thank you for being my friends.

To Ethan Morrill-Ploum. Thank you for being my family. Thank you for everything.

Contribution to original knowledge

This thesis contributes to the current knowledge of direct life detection in analogue environments and genome reconstruction from metagenomes with MinION sequencing. Specifically:

1. In Chapter 2, I report successful DNA detection from a Mars analogue environment (the Hanksville paleochannels), as well as the integration of MinION sequencing results with spectral data and immunoassays. This work has produced the first determination of putative DNA detection limits for the MinION and the first whole metagenome analysis of an ancient paleochannel environment.
2. In Chapter 3, I investigated DNA detection with the MinION from Antarctic cryptoendolith samples after exposure to a Mars environmental chamber and a custom UVC chamber. I determined that these exposures corresponding to ~58 Martian sols and ~278 Martian years, respectively, did not preclude successful DNA detection. This work is the first evaluation of MinION sequencing on samples that have experienced the harshness of a Mars-like environment, which is an important step in establishing the MinION's utility in extant life detection missions.
3. In Chapter 4, I describe three separate approaches for metagenome-assembled genome (MAG) generation from Allen Bay, Nunavut sea ice cryoconites: HiSeq-only, MinION-only, and hybrid (HiSeq + MinION). I found that the hybrid approach produced longer contigs, more coding sequences, and more total MAGs; these MAGs had the highest completeness, lowest

contamination, highest N50, and include a putatively novel species of *Octadecabacter*. This work has produced the first hybrid MAGs from an extreme environment.

Contribution of Authors

1. In Chapter 2, I am the first author of the associated published paper. I designed and oversaw the overall experiment. I performed all sample collection, MinION sequencing, and data analysis of the MinION, immunoassay, and spectral results. I wrote and edited the manuscript. Jessica Stromberg and Edward Cloutis performed the X-ray diffraction (XRD), reflectance spectroscopy, and Raman spectroscopy experiments. Yolanda Blanco, Miriam García-Villadangos, and Victor Parro performed the Life Detector Chip (LDChip) experiment. Jacqueline Goordial and Lyle Whyte provided guidance and helped to oversee the experimental design.
2. In Chapter 3, I am the first author of the associated manuscript. I designed and oversaw the overall experiment. I performed all MinION sequencing and data analysis, as well as DNA extraction and management of the UVC chamber exposure. I also contributed to the design and specifications of the UVC chamber. I wrote and edited the manuscript. Miguel Angel Fernández-Martínez performed the MARTE exposure and associated DNA extractions. Mercedes Moreno-Paz and Yolanda Blanco performed the LDChip experiment. Laura Sánchez-García and Daniel Carrizo performed the lipid extraction and gas chromatography-mass spectrometry (GC-MS). Álvaro Vicente-Retortillo performed the UV radiation model calculations. Jesus Sobrado provided access to the MARTE environmental chamber. Louis-Jacques Bourdages constructed the UVC chamber. Lyle Whyte provided guidance and helped to oversee the experimental design.
3. In Chapter 4, I am the first author of the associated published paper. I designed and oversaw the overall experiment. I collected samples, carried out DNA extractions, MinION sequencing,

HiSeq sequencing, bioinformatics analyses, and wrote and edited the manuscript. Isabelle Raymond-Bouchard also contributed to overall experimental design, sample collection, DNA extractions, and HiSeq sequencing. Laura Brennan carried out some DNA extractions. David Touchette performed *in situ* geochemical analyses. Lyle Whyte provided guidance and helped to oversee the experimental design.

List of Tables and Figures

Table 1.1. Missions to Mars focused on characterizing its habitability.....	28
Table 1.2. List of biosignatures that can be used as targets in the search for life beyond Earth.....	33
Table 1.3. Terrestrial environments that can act as analogues for Mars and the icy moons.....	41
Table 1.4. List of Mars simulation chambers and their environmental parameters.....	52
Table 1.5. List of organisms tested in low Earth orbit and Mars simulation chambers.....	54
Table 2.1. Input DNA and MinION sequence details.....	77
Table 2.2. DNA detection limit trial details with endolith sample E4.....	83
Table 2.3. Relationship between MinION sequences, XRD data, reflectance spectra, Raman spectra, and LDChip immunoassays.....	94
Table 3.1. Environmental conditions in MARTE and on Mars.....	117
Table 3.2. Exposure time and DNA content in the MARTE samples.....	118
Table 3.3. UV irradiation and doses for MARTE from the Xenon source emissions.....	119
Table 3.4. Irradiation doses at the Phoenix lander site on Mars.....	120
Table 3.5. UVC chamber and Mars conditions.....	120
Table 3.6. UVC chamber exposure time and DNA content.....	122
Table 4.1. Physico-chemical characteristics of the Allen Bay collection site.....	159
Table 4.2. Sequencing information.....	160
Table 4.3. MAGs produced with HiSeq and hybrid assembly with >50% completeness and <10% contamination.....	161
Supplementary Table 2.1. XRD results of the mineralogy of the Hanksville paleochannel samples.....	244

Supplementary Table 3.1. UVC irradiation values for the UVC chamber.....	245
Supplementary Table 4.1. MAGs produced with MinION assembly.....	246
Supplementary Table 4.2. Stress response genes present in Hybrid_5.....	247
Supplementary Table 4.3. DNA extraction details for MinION-sequenced cryoconites.....	251
Supplementary Table 4.4. DNA extraction details for HiSeq-sequenced samples.....	252
Figure 1.1. Overview of MinION sequencing approach and steps.....	36
Figure 1.2. Hanksville inverted paleochannel site.....	43
Figure 1.3. Sandstone from University Valley, Antarctica containing a cryptoendolithic community.....	46
Figure 1.4. Allen Bay sea ice cryoconites.....	48
Figure 2.1. Hanksville paleochannel site and samples.....	70
Figure 2.2. Metagenomes of the Hanksville paleochannel samples generated by MinION sequencing.....	79
Figure 2.3. (A) Bacterial 16S rRNA community profile of the Hanksville paleochannels.....	80
Figure 2.3. (B) Bacterial content of MinION metagenome of the Hanksville paleochannels.....	81
Figure 2.4. Weighted UniFrac principal coordinates analysis (PCoA) of the 16S rRNA sequencing data of the Hanksville paleochannels.....	82
Figure 2.5. Detection limit trials with endolith sample E4 at the phyla level.....	84
Figure 2.6. Reflectance spectra of the Hanksville paleochannels.....	86
Figure 2.7. Raman spectra of the Hanksville paleochannels.....	88
Figure 2.8. Heat map comparing positive LDChip and MinION results at the phylum level.....	90
Figure 2.9. Heat map comparing positive LDChip and MinION results for specific protein detection.....	91

Figure 3.1. Study and sampling site in the McMurdo Dry Valleys, Antarctica.....	115
Figure 3.2. The MARTE vacuum chamber.....	118
Figure 3.3. Custom UVC chamber containing University Valley cryptoendoliths.....	121
Figure 3.4. Community composition at the phylum level of the University Valley cryptoendoliths after MARTE exposure.....	127
Figure 3.5. Community composition at the phylum level of the University Valley cryptoendoliths after UVC exposure.....	128
Figure 3.6. Heat map displaying the protein content and microbial diversity of T0 _M and T3 _M from the University Valley cryptoendoliths.....	129
Figure 3.7. Molecular lipid profile of the University Valley cryptoendoliths at T0 _M and T3 _M	131
Figure 4.1. Allen Bay sea ice location and cryoconites.....	158
Figure 4.2. Community composition from metagenomes of the Allen Bay sea ice.....	162
Figure 4.3. IDEEL plots of frequency vs. query length:hit length.....	166
Figure 4.4. mummer2circo alignment of Hybrid_5 and HiSeq_31 to the <i>Octadecabacter arcticus</i> genome.....	169
Figure 4.5. Model of Hybrid_5 cellular systems based on genomic data.....	171
Supplementary Figure 2.1. PHRED quality distribution of the detection limit trials with endolith sample E4.....	253
Supplementary Figure 3.1. Statistically significant differences between antibodies from the LDChip.....	254
Supplementary Figure 4.1. Details of the hybrid and HiSeq high-quality and medium-quality MAGs.....	255

List of Abbreviations

CAB: Centro de Astrobiología
CDS: Coding sequences
COMIMART: COMplutense and MICHigan MARS Radiative Transfer model
CPD: Cyclobutane pyrimidine dimer
EPS: Extracellular polymeric substances
ESA: European Space Agency
GCMS: Gas Chromatograph-Mass Spectrometer
GC-MS: Gas chromatography-mass spectrometry
GEx: Gas Exchange
HMW: High molecular weight
ISS: International Space Station
JAXA: Japanese Aerospace Exploration Agency
JGI IMG/M ER: Joint Genome Institute Integrated Microbial Genomes & Microbiomes Expert Review
LDChip: Life Detector Chip
LMC: Life Marker Chip
LR: Labeled release
MAG: Metagenome-assembled genome
MA-MISS: Mars Multispectral Imager for Subsurface Studies
MARC: MinION Analysis and Reference Consortium
MDRS: Mars Desert Research Station
MUFA: Monounsaturated fatty acid
NASA: National Aeronautics and Space Administration
ND: Not detected
OM: Organic matter
ONT: Oxford Nanopore Technologies
PCR: Polymerase chain reaction
PCoA: Principal coordinates analysis
POP: Persistent organic pollutant
PR: Pyrolytic Release
RLS: Raman Laser Spectrometer
ROS: Reactive oxygen species
SOLID: Signs of Life Detector
SOLID-SPU: Signs of Life Detector Sample Preparation Unit
SHERLOC: Scanning Habitable Environments with Raman and Luminescence for Organics and Chemicals
SRB: Sulfate-reducing bacteria
XRD: X-ray diffraction

Chapter 1. Introduction and literature review

1.1 Objectives of this thesis

The overall goals of my research are to determine the efficacy of DNA as a target biosignature using MinION sequencing and to understand how microbial life can survive in analogue environments at a molecular level. The specific questions that my research seeks to answer are as follows:

1. Is MinION sequencing a viable tool for life detection? What are the limits of its detection? What is the microbial community composition of the Hanksville paleochannels?
2. Is DNA detectable with MinION sequencing in Mars analogue samples after exposure to Mars-like conditions? Are other unambiguous biosignatures (i.e. proteins, cell membrane-derived lipids) also detectable? How do these biosignatures change over the exposure?
3. Can MinION sequencing be used to aid in the reconstruction of individual microbial genomes from extreme environmental metagenomes? Are there novel members of cryoconite microbial communities in Canadian high Arctic sea ice? What are the main metabolisms present? What are their genomic adaptations for survival in this extreme cryoenvironment?

Each group of questions corresponds to a specific section of my doctoral project, which are described in the following chapters. In Chapter 2, I present a proof-of-concept utilization of

the MinION sequencer for direct life detection and show how its results complement established space mission instruments. Additionally, I determined putative detection limits for MinION sequencing, an important factor for life detection missions, given the extremely low biomass encountered in high fidelity (i.e. highly similar to extraterrestrial locations) terrestrial analogue environments. I also used Illumina sequencing to generate a 16S rRNA community profile of the Hanksville paleochannel site for comparison with the MinION metagenome.

In Chapter 3, I determined if DNA is detectable with MinION sequencing in Mars analogue samples exposed to Mars-like conditions; I exposed cryptoendolith samples from University Valley to an environmental chamber mimicking conditions found on Mars (e.g. extremely low temperatures and high radiation). Additionally, I determined if proteins and cell membrane-derived lipids remained detectable after exposure. Of the extreme conditions on Mars (which include desiccation, freezing temperatures, and low atmospheric pressure), strong UVC radiation has been identified as the most limiting for microorganisms and is particularly damaging to DNA, causing crosslinks and breakages. I supplemented the main exposure with a secondary UVC exposure and used MinION sequencing to ascertain if DNA is still detectable after exposure to intense UVC radiation.

In Chapter 4, I performed genome binning using MinION-generated sequences to reconstruct genomes of individual community members, identify potentially novel microorganisms, and study metabolic adaptations to cryoconite holes in the Canadian high Arctic. A putatively novel member of the *Octadecabacter* genus is discussed in depth to characterize its potential metabolic activities and survival adaptations.

1.2 Habitability and the search for life in our Solar System

The search for life in our Solar System is among the highest priorities for modern space missions and seeks to answer a fundamental human question: are we alone in the universe? Mars is an especially promising target in the search for life given its proximity and physical/geochemical similarities to Earth (Mustard *et al.* 2013). The surface of Mars is currently characterized by environmental conditions inhospitable to life, including freezing temperatures (average surface temperatures of -123 to $+25$ °C), low atmospheric pressure (~ 8 mbar), anaerobic atmospheric composition ($\sim 95\%$ CO₂), and high UV and ionizing radiation (total surface UV of ~ 50 W/m²) (Horneck 2000; Schuerger *et al.* 2003; Sobrado *et al.* 2014). While the present-day atmospheric pressure (~ 168 x less than that of Earth) and lack of a magnetosphere on Mars prevent effective liquid water retention on the surface, heat transfer, and protective shielding from solar winds, UV, and gamma ray bombardment, Mars had a much warmer and wetter climate $\sim 2 - 4.5$ bya (Johnson *et al.* 2011; McKay *et al.* 1992) that could have supported microbial life. During the Noachian ($\sim 4.5 - 3.5$ bya) and Hesperian ($\sim 3.5 - 2.9$ bya) epochs, Mars' climate would have allowed for widespread water-rich surface reservoirs and local water zones, respectively. This past water availability is evidenced geomorphologically by lake and river deltas (Mangold *et al.* 2021), lake basins (Ehlmann *et al.* 2008; Irwin III *et al.* 2002; Rapin *et al.* 2019), valley networks (Fassett and Head III 2008), inverted relief features (Balme *et al.* 2016; Williams *et al.* 2009), and alluvial fans (Moore and Howard 2005; Morgan *et al.* 2014).

1.2.1 Martian habitability

Any putative extant Martian life would be bound to localized high areas of water availability (Fairén *et al.* 2010; Leuko *et al.* 2017); as such, the presence of liquid water is a strong indicator of Mars' habitability (i.e. ability to harbour life) (Westall *et al.* 2013). While the current Amazonian (~2.9 bya – present) period is characterized by hyperaridity on the surface (Leuko *et al.* 2017), surface waters may have persisted until 2 – 2.5 bya (Leask and Ehlmann 2022). Liquid water may still exist today on Mars in subsurface reservoirs (e.g. subglacial lakes) (Orosei *et al.* 2018; Scheller *et al.* 2021) and could be present in local recesses (e.g. cryptoendoliths, lava tubes, ice caves) where life may have retreated as Mars transitioned to its present-day cold desert conditions (de Vera *et al.* 2014b; McKay *et al.* 1992; O'Connor *et al.* 2021). Liquid brines may also exist near the Martian surface due to hygroscopic salt activity (Cesur *et al.* 2022). MgSO₄, (per)chlorates, and NaCl are present on the Martian surface and can absorb moisture from the atmosphere that is capable of deliquescing into liquid brines (Davila *et al.* 2010; Rivera-Valentín *et al.* 2020) and may be responsible for seasonal flows on warm, steep Martian slopes (i.e. recurring slope lineae) (McEwen *et al.* 2014; Ojha *et al.* 2015). Deliquescence could also support the metabolic activity of methanogenic archaea (Maus *et al.* 2020) and ¹³C-depleted methane in Gale crater could be the result of photolyzed biogenic methane (House *et al.* 2022).

There have been numerous Martian missions focused on characterizing its past and present habitability (Table 1.1); these include the *Mariner* and *Mars* mission orbiters, which provided the first glimpses of the Martian surface from orbit and revealed a frigid, cratered landscape. Results from *Mariner* 4 (1964 – 1967) and *Mariner* 9 (1971 – 1972) in particular re-framed the interpretation of Martian habitability as an environment capable of supporting multicellular life to

microbial organisms (Sagan and Fox 1975; Sagan and Lederberg 1976). Further orbiters (e.g. *Mars Global Surveyor*, *2001 Mars Odyssey*, *Mars Reconnaissance Orbiter*) have mapped signs of water on Mars (Garvin 2001; Malin and Edgett 2001; Mustard *et al.* 2008; Saunders *et al.* 2004). Martian rovers (twin rovers *Spirit* and *Opportunity*, *Curiosity*, *Zhurong*, and *Perseverance*) have documented rocks and soils containing water-related minerals, as well as searched for signs of ancient microbial life (Eigenbrode *et al.* 2018; Haskin *et al.* 2005; Hays *et al.* 2017; Millan *et al.* 2016; Neveu *et al.* 2018; Squyres *et al.* 2009; Szopa *et al.* 2020; Wan *et al.* 2020). The National Research Council (USA) and the Mars 2020 Science Definition Team both state that determining if life is, or ever was, present on Mars is the prime focus of the 2013 – 2022 decade and a high priority of the Mars Exploration Program Analysis Group (MEPAG) (Banfield *et al.* 2021; Hays *et al.* 2017; Mustard *et al.* 2013); however, no mission has ever searched for signs of extant life on Mars, save the Viking missions (1975 – 1982).

1.2.2 The Viking biological experiments

In 1976, the *Viking 1* and *Viking 2* landers each performed four types of experiments to search for life on Mars, three of which attempted to directly measure microbial metabolism on Mars (Klein 1978a; Levin and Straat 2016). The Gas Chromatograph-Mass Spectrometer (GCMS) experiment was performed to identify organic molecules in the Martian soil and atmosphere (Biemann 1979; Biemann *et al.* 1977). The Gas Exchange (GEx) experiment analyzed gases released from Martian soil after the addition of water, a nutrient solution, and water vapour from the nutrient solution (Oyama and Berdahl 1977). The Pyrolytic Release (PR) experiment incubated Martian soil with radiolabelled $^{14}\text{CO}_2$ and ^{14}CO , followed by pyrolytic analysis of any ^{14}C

Table 1.1. Missions to Mars focused on characterizing its past and present habitability.

Mission/program name	Years active	Country of origin	Goals	References
Mars program	1960 – 1973	Soviet Union	Provide information on Martian surface conditions	(Smith 1988)
Mariner program	1962 – 1975	USA	Provide information on Martian surface conditions; return close-up pictures of the Martian surface	(Sagan and Fox 1975; Sagan and Lederberg 1976)
Viking program	1975 – 1982	USA	Characterize the Martian surface and atmosphere; generate high-resolution images of the Martian surface; search for signs of life	(Klein 1977; Klein 1978a; Klein 1978b)
<i>Mars Global Surveyor</i>	1996 – 2007	USA	Characterize the Martian surface and geological processes	(Garvin 2001; Malin and Edgett 2001)
<i>2001 Mars Odyssey</i>	2001 – present	USA	Characterize the Martian surface; detect evidence of water and ice	(Saunders <i>et al.</i> 2004)
Mars Exploration Rover mission (<i>Spirit</i> and <i>Opportunity</i>)	2003 – 2018	USA	Characterize Martian rocks and soils that provide evidence for past water activity	(Haskin <i>et al.</i> 2005)
<i>Mars Reconnaissance Orbiter</i>	2005 – present	USA	Search for signs of past and present water activity	(Mustard <i>et al.</i> 2008)
<i>Phoenix</i> lander	2008	USA	Search for signs of past and present water activity; evaluate Martian habitability	(Hecht <i>et al.</i> 2009)
Mars Science Laboratory (<i>Curiosity</i>)	2011 – present	USA	Search for organic compounds and ancient biosignatures; investigate water cycling on Mars	(Eigenbrode <i>et al.</i> 2018; Szopa <i>et al.</i> 2020)
Mars 2020 (<i>Perseverance</i>)	2020 – present	USA	Search for ancient biosignatures; evaluate Martian habitability; cache samples for return to Earth	(Mangold <i>et al.</i> 2021)

assimilation into organic constituents in the Martian soil (Horowitz *et al.* 1977). The Labeled Release (LR) experiment injected ^{14}C -labeled Miller-Urey compounds into Martian soil and monitored it for evolution of ^{14}C -labeled gases (Levin and Straat 1976; Levin and Straat 1977). These latter three tests (GEx, PR, and LR) comprise the Viking biological experiments.

Results at that time stated that the GCMS failed to detect significant amounts organic compounds in the Martian soil and atmosphere (Biemann 1979; Biemann *et al.* 1977). Humidified Martian soil in the GEx experiment rapidly released O_2 gas, although subsequent addition of water and nutrient solution failed to produce any evolution of oxygen, and O_2 was also released from the heat-sterilized control. These results were attributed instead to the presence of superoxides in the Martian surface regolith rather than biology (Oyama and Berdahl 1977). The PR experiment showed a small amount of ^{14}C fixation in both light and dark conditions; however, these results were also obtained with samples heated to 90°C and could also be explained by the presence of oxidants in Martian soil (Horowitz *et al.* 1977; Klein 1978b). The LR experiment produced the most controversial results; it found that $^{14}\text{CO}_2$ was swiftly released after the addition of ^{14}C -labeled organics and this reaction did not occur in the 160°C -heated controls. Heating to $45 - 50^\circ\text{C}$ partially reduced the reaction activity and long-term storage at $10 - 26^\circ\text{C}$ resulted in complete inactivity from the soil, which would be expected from a biological agent (Levin and Straat 2016). Radiolabelled gas was not released with subsequent nutrient additions to the Martian soil (contrary to terrestrial biological activity) and the initial release of radiolabelled carbon dioxide could be explained again by organic oxidation (Klein 1978a; Klein 1978b).

The Viking biological experiment results were largely viewed as resulting from chemical rather than biological activity, especially since the GCMS experiment had failed to detect organic molecules (Biemann 1979; Horowitz *et al.* 1977; Klein 1977; Klein 1978a; Klein 1978b; Oyama

and Berdahl 1977). Oxidants (perchlorate) were later detected on the Martian surface in 2008 by the *Phoenix* lander (Hecht *et al.* 2009) and may be widespread on the Martian surface (Clark and Kounaves 2016; Glavin *et al.* 2013); however, their presence renders some Viking results interpretations inconclusive. Chlorinated hydrocarbons were in fact detected by the GCMS but at a very low abundance (0.04 – 40 ppb) and with a terrestrial chlorine isotopic ratio; these were assumed to be laboratory contaminants, although no chlorohydrocarbons were detected in the controls (Navarro-González *et al.* 2010). When the GCMS experiment was recreated with Atacama Desert soil samples inoculated with organics and perchlorate, the majority of the organics present were destroyed, but a small amount of chlorinated hydrocarbons were produced, similar to the GCMS results (Navarro-González *et al.* 2006; Navarro-González *et al.* 2010). Additionally, the ExoMars Trace Gas Orbiter has recently found that chlorine in the Martian atmosphere has the same isotopic ratio as on Earth (Trokhimovskiy *et al.* 2021).

When some organics are oxidized (e.g. salts of aliphatic and aromatic polycarboxylic acids), they become refractory and can accumulate; the GCMS could detect only volatilized material (Benner *et al.* 2000). Organic molecules have since been detected on Mars (Eigenbrode *et al.* 2018; Stern *et al.* 2022; Szopa *et al.* 2020) and the GCMS experiment could have missed any putative organics present at the Viking lander sites when they were destroyed via perchlorate oxidation or if they remained undetectable in refractory form (Benner *et al.* 2000; Navarro-González *et al.* 2006; Navarro-González *et al.* 2010).

There is neither a completely biological nor nonbiological interpretation that satisfies 100% of the Viking biological experiment results. Further extant life detection experiments are needed to better contextualize and interpret the Viking results, as well as determine if life is truly present on the Red Planet (Banfield *et al.* 2021). This is especially crucial with both private and public

space sectors that seek to develop relatively affordable space travel and land humans on Mars potentially before 2040 (Linck *et al.* 2019; Musk 2017). These activities could result in backward contamination (i.e. Martian life with the potential to harm humanity) and forward contamination (i.e. terrestrial contamination of the putative Martian biosphere), compromising future life detection and science activities on Mars (Spry *et al.* 2018). The arrival of human explorers or settlements would irrevocably contaminate the Martian environment and the ability to detect native microbial Martian life would be lost (Fairén *et al.* 2017; Rummel and Conley 2018).

1.2.3 Habitability of icy moons in our Solar System

Besides Mars, there are other bodies in our Solar System with the potential for habitability based on their possession of liquid water oceans; these include Enceladus, Europa, Titan, Callisto, and Ganymede (Hendrix *et al.* 2019). The icy moons Enceladus, a moon of Saturn, and Europa, a moon of Jupiter, are particularly promising targets because of their relatively thin outer ice crusts and direct ocean contact with their rocky cores (McKay *et al.* 2014; Nimmo and Pappalardo 2016; Spencer *et al.* 2006).

In 2005, the *Cassini* orbiter observed water-rich plumes spraying from Enceladus' south polar region (i.e. the "tiger stripes") (Spencer *et al.* 2006) and later found evidence of a southern subsurface water ocean (10 km thick and capped with ~40 km of ice) (Iess *et al.* 2014). The plumes contain water vapour, carbon dioxide, molecular hydrogen, silica, organics, salts, and amines, indicating contact between the ocean and Enceladus' silicate core (Khawaja *et al.* 2019; McKay *et al.* 2014). Enceladus' southern region is measurably hotter than the rest of the moon (Spencer *et al.* 2006), suggesting interior heating and potential hydrothermal activity (e.g. tidal flexing,

radioactive decay) (Nimmo and Pappalardo 2016; Shoji *et al.* 2014). Core heating that dissolves minerals from the seafloor could be responsible for the particles emitted from Enceladus' plumes, some of which represent sources of electrons for microbial metabolism (e.g. H₂) (Deamer and Damer 2017).

Like Enceladus, Europa has also been observed to have water plume activity and a subsurface water ocean (up to 150 km thick under ~20 km of ice) (Khurana *et al.* 1998; Roth *et al.* 2014). The plume composition is unknown, but Europa undergoes strong tidal flexing effects from Jupiter (Nimmo and Pappalardo 2016) and its icy shell contains salt impurities (Trumbo *et al.* 2019), signifying potential contact between ocean water and the European core, although cryovolcanism may also be responsible for plume generation on Europa (Steinbrügge *et al.* 2020). Both Enceladus and Europa bear further exploration and will be the subject of future missions to investigate their habitability (e.g. Jupiter Icy Moons Explorer, *Europa Clipper*, Enceladus Orbilander mission concept) (Hendrix *et al.* 2019; MacKenzie *et al.* 2021).

1.3 Biosignatures in our Solar System

Biosignatures are a broad category of signs, substances, phenomena, and/or processes that indicate the presence or past presence of life (Table 1.2) (Hays *et al.* 2017; Neveu *et al.* 2018; Schwieterman *et al.* 2018). As all known life is organic and carbon-based, organic molecules are particularly promising indicators of life and are common in interstellar space (Pace 2001). Amino acids and nucleosides have been detected in meteorites, and riboses have been shown to naturally synthesize in early solar system conditions (Meinert *et al.* 2016; Pace 2001). Organic molecules are commonly used for assessing habitability and as ancient biosignature detection targets for

Table 1.2. List of biosignatures that can be used as targets in the search for life beyond Earth. This list is neither exhaustive nor conclusive.

Biosignature types	Example	Ambiguity	Reference
Microbial fossils	Diatom frustules	Ambiguous	(Bower <i>et al.</i> 2015; Crosby and Bailey 2018)
Microbialites	Stromatolites, microbial mats	Ambiguous	(Menon <i>et al.</i> 2016; Pace <i>et al.</i> 2016; Perri <i>et al.</i> 2013)
Biominerals	Biogenic silica, magnetite	Ambiguous	(Barber and Scott 2002; Chan <i>et al.</i> 2019)
Organic matter	Amino acids, carbonaceous chondrites	Ambiguous	(Kvenvolden <i>et al.</i> 1970; Parro and Munoz-Caro 2010)
Isomerism preference	Enantiomeric excess, proteinogenic vs. non-proteinogenic amino acids	Ambiguous	(Glavin <i>et al.</i> 2019; Glavin <i>et al.</i> 2012; Ilardo <i>et al.</i> 2015)
Bulk isotopic fractionation	$^{13}\text{C}/^{12}\text{C}$ ratios	Ambiguous	(Summons <i>et al.</i> 2011; Vago <i>et al.</i> 2017)
Atmospheric disequilibrium	Excess atmospheric methane	Ambiguous	(Krissansen-Totton <i>et al.</i> 2016; Meadows <i>et al.</i> 2018)
Biomolecules	DNA, RNA, proteins, cell membrane-derived lipids, pigments	Unambiguous	(Benner 2017; Chan <i>et al.</i> 2019; Schwieterman <i>et al.</i> 2018)

Martian missions (e.g. Mars Science Laboratory and *Curiosity*; Mars 2020; ExoMars and *Rosalind Franklin*) (Eigenbrode *et al.* 2018; Maurice *et al.* 2021; Rull *et al.* 2017) and thiophenes, aromatic and aliphatic hydrocarbons have been detected on Mars (Eigenbrode *et al.* 2018; Szopa *et al.* 2020). However, on their own, simple organic molecules are not definitive signs of life and can be generated abiotically (Eigenbrode *et al.* 2018), although their degree of diagenesis can indicate the relative age of the initial polymer.

Darwinism is likely necessary in the genesis of life (i.e. the transition of a chemical system to a biological one) and is a key feature of life as defined by the National Aeronautics and Space Administration (NASA): “Life is a self-sustaining chemical system capable of Darwinian evolution” (Council 2019). As such, features that enable Darwinism (e.g. genetic biopolymers) may be universal and are thus strong biosignatures. Darwinism-supporting genetic biopolymers must also be polyelectrolytic (i.e. have a repeating backbone charge) and aperiodic (i.e. subunits do not reoccur at regular intervals) (Benner 2017; Schrodinger 1951).

Unlike other organic molecules (e.g. hydrocarbons, amino acids), DNA is an unambiguous biosignature, demonstrates the presence of extant or recently extinct life, is extremely unlikely to be generated without life, is a repeating, aperiodic polyelectrolytic biopolymer, and enables Darwinism (rather than being produced by Darwinism) (Benner 2017; Mustard *et al.* 2013; Neveu *et al.* 2018). In addition, DNA is especially ideal for missions targeting Mars because meteoritic exchange during the Late Heavy Bombardment period ~4 billion years ago could have seeded microbe-carrying rocks from Earth to Mars (i.e. lithopanspermia) when the Martian environment was relatively warm and wet (Mileikowsky *et al.* 2000). The universality of organic molecules in our Solar System and relative similarities between Earth and Mars also indicates a plausibility that any extant Martian life could present its hereditary polymers as repeating organic subunits to form long, complex chains (e.g. DNA-like) (Mustard *et al.* 2013; Pace 2001; Sephton 2018). However, for DNA to be an effective biosignature, there needs to exist robust instrumentation capable of its detection.

1.4 DNA detection with MinION sequencing

Instrumentation for detecting DNA should have relatively low energy requirements and a small mass/physical footprint to simplify operation and launch on an exploratory probe (Ellery *et al.* 2002); the Oxford Nanopore Technologies' (ONT) MinION Mk1b sequencer fulfills these requirements (hereafter referred to as the MinION). The MinION is a miniaturized device (~ 90 g, 105 x 23 x 33 mm) for sequencing DNA, RNA, and potentially proteins (Goordial *et al.* 2017; Leggett and Clark 2017; Loman and Watson 2015), directly detecting unambiguous signs of life through sequencing. The MinION produces sequences via nanopore technology, whereby biomolecules are ratcheted through a proprietary protein nanopore embedded in a flow cell sensor array. As the biomolecules passes through the pore, a current change is generated that is characteristic of the specific subunits within the pore and stored as fast5 files. The MinION software can then decode the fast5 files into fastq files real-time during the run, after its completion, or a combination thereof, generating up to 50 Gb of data from a single run (sequencing overview depicted in Figure 1.1) (Leggett and Clark 2017; Loman *et al.* 2015; Loman and Watson 2015).

1.4.1 MinION sequencing: advantages and disadvantages

The MinION is a third-generation sequencer that generates reads directly from biological samples (i.e. a single-molecule sequencer) (Thompson and Milos 2011). As a single-molecule sequencer, the MinION can produce ultra-long (>50 000 bp) and even genome-spanning contigs (Cuscó *et al.* 2021; Jain *et al.* 2018; Loman *et al.* 2015; Stewart *et al.* 2019), in contrast to second-

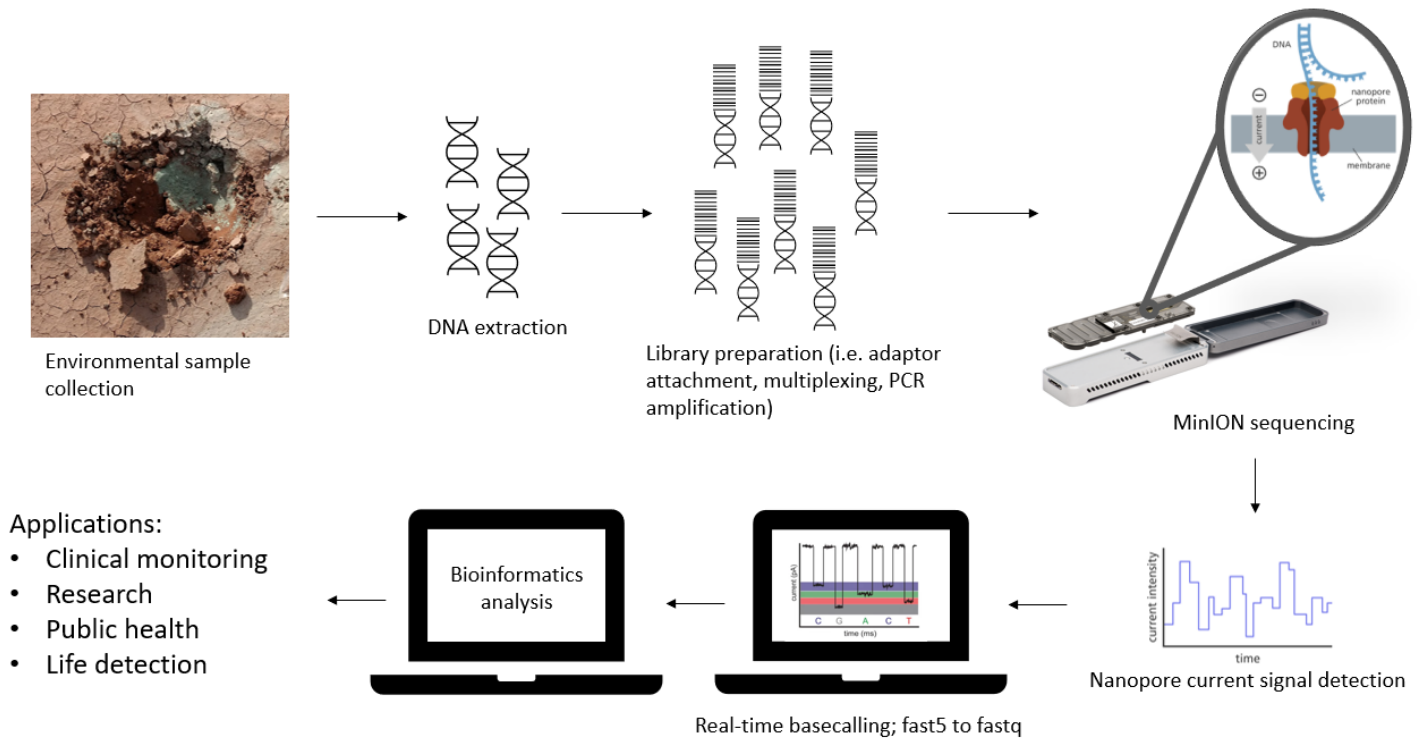


Figure 1.1. Overview of MinION sequencing approach and steps. MinION device and protein images taken from nanoporetech.com.

generation sequencers, which use sequencing by synthesis or sequencing by hybridization and are limited to relatively short read lengths (<500 bp) (Slatko *et al.* 2018). Longer reads simplify contig assembly, genome reconstruction, and resolution of repetitive regions (Goldstein *et al.* 2019). The MinION can also distinguish epigenetic variation and base modifications (e.g. methylation) (Simpson *et al.* 2017; Waters *et al.* 2021). The MinION can generate reads and basecall in real-time, enabling rapid on-site identification of microbial communities (Plesivkova *et al.* 2019).

However, the MinION possesses some potent disadvantages, primarily its high error rate (i.e. miscalled bases, insertions, deletions). The most recent evaluation from the MinION Analysis and Reference Consortium (MARC), an independent group of users assessing MinION error rates and protocols, reported that the error rate for MinION simplex (i.e. single strand) sequencing was

up to 14.5% and up to 7.5% for duplex (i.e. double strand) sequencing (Jain *et al.* 2017), although ONT has updated some of their chemistries since this report was released. ONT states that its current raw read accuracy is >98.3% for simplex sequencing and >99.3% for duplex sequencing. For comparison, Illumina sequencing has an error rate of <0.1% (Manley *et al.* 2016). The MinION's high error rate complicates microbial community characterization in natural metagenomes and low biomass environments, but it can be reduced with the addition of short second-generation sequencing data (e.g. Illumina) to produce highly-accurate consensus sequences (De Maio *et al.* 2019). The MinION also has a minimum DNA input of 1 – 5 ng (with the SQK-RPB004 Rapid PCR Barcoding kit), which corresponds to a biomass of $\sim 10^6$ cells/g (Dolezel *et al.* 2003; Raes *et al.* 2007), roughly threefold higher than that present in Mars analogue environments (Goordial *et al.* 2016a; Niederberger *et al.* 2010).

Datasets consisting of MinION and Illumina (i.e. hybrid datasets) can produce more accurate and more contiguous sequences than either constituent dataset alone, including for single microbial genomes (De Maio *et al.* 2019; Gan *et al.* 2019; Schmidt *et al.* 2017; Shin *et al.* 2019; Tan *et al.* 2018; Wick *et al.* 2017), high biomass metagenomes (Overholt *et al.* 2020; Stewart *et al.* 2019), and the human genome (Jain *et al.* 2018). Metagenome-assembled genome (MAG) generation is also simplified with hybrid datasets; short Illumina reads enable high accuracy across contigs and long MinION reads facilitate greater contiguity (De Maio *et al.* 2019). Indeed, hybrid assemblies have produced higher quality MAGs from natural environments like aquifers and gut microbiomes (Bertrand *et al.* 2019; Overholt *et al.* 2020), although this approach has not been tested in low biomass extreme or analogue environments. Genome reconstruction from metagenomes enables elucidation of individual microbes without pure cultures, an important factor to study the limits of life and how microbes influence their habitats in extreme environments,

where microbial biomass is low, transient, and recalcitrant to culture. Hybrid assembly with MinION sequencing could be used to improve this process and reveal detailed microbial metabolisms and survival strategies in extreme and analogue environments.

1.4.2 MinION utilization in remote field work and space science

The MinION's ability to produce sequencing data in real-time, combined with its small size and portability, make it ideal in clinical and remote field work applications where quick, on-site diagnosis and analysis is necessary (Edwards *et al.* 2016; Stüder *et al.* 2021; Tanaka *et al.* 2019). Real-time genomic surveillance is an important diagnostic tool for identification and monitoring, especially for highly virulent diseases where appropriate control measures can be implemented if sequence data is generated quickly enough (Quick *et al.* 2016). In 2015, the MinION was launched as part of a portable surveillance laboratory for the Ebola virus in Guinea. Identification of Ebola-positive samples was possible within 24 hours of sample acquisition, despite resource limitations and practical difficulties working in remote field sites (Quick *et al.* 2016). In 2016, the ZiBRA (Zika in Brazil Real-time Analysis) project was launched to improve monitoring and assessing the genetic diversity of the Zika virus in Brazil (Faria *et al.* 2016; Quick *et al.* 2017). In-field sequencing in a mobile laboratory across five Brazilian states produced fragmentary, but still identifiable, Zika genomes (Faria *et al.* 2016). When refined with a multiplexed tiling PCR protocol, the resulting consensus sequences of clinical Zika virus samples covered >97% of the Zika virus genome (Quick *et al.* 2017).

The MinION has also been used to identify microbial communities in remote, extreme environments where the microbial communities can be ephemeral and logistical risks can

introduce contamination (Edwards *et al.* 2020; Wight *et al.* 2020). MinION sequencing was performed *in situ* in the high Arctic and the Antarctic Dry Valleys (Goordial *et al.* 2017; Johnson *et al.* 2017). Canadian high Arctic permafrost sequences were also linked to microbes from in-field cultivation and colourimetric assays, forming a multi-pronged approach for life detection (Goordial *et al.* 2017). In-field sequencing of glacial cryoconites in Svalbard reliably characterized the microbial community present with both shotgun metagenomics and 16S rRNA gene sequencing. The resulting preprint of initial results was released within 23 days of sample collection, which is within the order of doubling time for bacterial community members, yielding a microbial community description within its generation time (Edwards *et al.* 2019; Edwards *et al.* 2016).

Crew health and contamination control monitoring aboard the International Space Station (ISS) are traditionally limited to culture-dependent methods (e.g. colony forming units (CFU) counts). Culture-dependent methods require time for cultivation and exclude non-culturable members of the spacecraft environment; however, in 2017, the MinION became the first sequencer to operate in space as part of the Biomolecule Sequencer Project and identified *Staphylococcus* spp. *in situ* on the ISS (Burton *et al.* 2020). When in-flight sequencing and *de novo* assembly of lambda bacteriophage, *Escherichia coli*, and *Mus musculus* were benchmarked against terrestrial sequencing and assembly of the same organisms, no significant difference in quality existed between the two datasets (Castro-Wallace *et al.* 2017). The MinION is robust enough to withstand launch and descent vibrations, and its nanopores can function successfully in microgravity. This proof-of-concept demonstrates the potential for MinION sequencing to be used as a tool for crew health diagnosis, contamination monitoring, and extant life detection; these abilities are contrary to other DNA detection methods, such as nucleic acid dyes and fluorometry. While the MinION

typically requires room temperature or higher for operation, it has been used successfully in cold ambient temperatures (Johnson *et al.* 2017) and there exists precedent for temperature-controlled space mission experiments (e.g. the *Viking* biological experiments) (Klein 1977; Klein 1978a; Klein 1978b; Levin and Straat 2016). For life detection missions, the MinION could also be used to identify non-DNA-based life; it has been shown to detect non-standard bases in nucleic acid chains (i.e. inosine) and produce a reliable ionic current signature for identification (Carr *et al.* 2017), demonstrating its ability to detect life in an agnostic manner (i.e. without presupposing underlying biochemistry) (Johnson *et al.* 2018). The MinION's promise as a tool in remote field applications and space missions require more testing to prove functionality in diverse Mars and icy moons analogue environments.

1.5 Mars and icy worlds analogue environments

Analogue environments on Earth that approximate the physical, chemical, and morphological conditions on extraterrestrial bodies are useful for testing mission logistics, instruments, and approximating putative extraterrestrial biology and adaptations. Mars and icy worlds analogue environments should present similar environmental conditions such as freezing temperatures, high salt, strong UV radiation, low precipitation, and geomorphology indicating past fluvial activity (Table 1.3) (Ellery *et al.* 2002; Thiel *et al.* 2011). The following environments mimic Martian and icy world environmental conditions and are strong candidates for evaluating life detection with the MinION and investigating their microbial community composition.

Table 1.3. Terrestrial environments that can act as analogues for Mars and the icy moons.

Location	Example environments	Environmental analogue characteristics	MinION sequencing used <i>in situ</i>?	Reference
McMurdo Dry Valleys, Antarctica	Permafrost, cryptoendoliths, ice-wedge polygon terrain, glaciers, cryoconites	Hyper aridity, freezing temperatures, limited nutrient input, high solar radiation	Yes	(Archer <i>et al.</i> 2017; De Los Ríos <i>et al.</i> 2014; Goordial <i>et al.</i> 2016b; Johnson <i>et al.</i> 2017; Mezzasoma <i>et al.</i> 2022)
Atacama Desert, Chile	Desert terrain, cryptoendoliths, hypoliths	Hyper aridity, freezing temperatures, limited nutrient input, high solar radiation, salt basins	Yes	(Glass <i>et al.</i> 2018; Sánchez-García <i>et al.</i> 2018; Wierzchos <i>et al.</i> 2013; Wierzchos <i>et al.</i> 2015)
Río Tinto, Spain	Sulfide deposits	Highly oxidizing	No	(Edwards <i>et al.</i> 2007; Sánchez-García <i>et al.</i> 2020)
Axel Heiberg Island, Canada	Permafrost, cryptoendoliths, ice-wedge polygon terrain, glaciers, cold salt springs, sea ice, cryoconites	Aridity, freezing temperatures, limited nutrient input, high solar radiation, saline acidic brines	Yes	(Goordial <i>et al.</i> 2017; Macey <i>et al.</i> 2020; Magnuson <i>et al.</i> 2020; Niederberger <i>et al.</i> 2010)
Hanksville, UT, USA	Inverted paleochannels, desert terrain	Aridity, geomorphology	No	(Clarke and Stoker 2011; Cloutis <i>et al.</i> 2017; Martins <i>et al.</i> 2011)
Svalbard, Greenland	Volcanic terrain, hot springs, glaciers, cryoconites	Freezing temperatures, geomorphology	Yes	(Edwards <i>et al.</i> 2011; Hodson <i>et al.</i> 2010)
Sub-ice lakes	Antarctica (Lake Vostok, Lake Vida); Canadian high Arctic (Devon Island subglacial ice cap lake)	Extreme isolation, hypersalinity	No	(Bulat <i>et al.</i> 2011; Doran <i>et al.</i> 2003; Murray <i>et al.</i> 2012; Rutishauser <i>et al.</i> 2018)
Subsurface cave systems	Lava tubes in Hawaii, New Mexico, California	Geomorphology, geochemistry	No	(Northup <i>et al.</i> 2011; O'Connor <i>et al.</i> 2021)

1.5.1 Hanksville inverted paleochannels

Inverted paleochannels are the result of inverted relief, in which a fluvial system is more resistant to erosion over time than its surrounding areas. Because of the higher permeability sediments in a fluvial channel, water flow leads to channel cementation. As the channel dries out, the neighbouring floodplains are eroded away faster than the channel itself, resulting in a dried out, raised ridge (Stoker *et al.* 2011; Williams *et al.* 2007; Williams *et al.* 2009). Sinuous ridges are elongated ridge features on the Martian surface that strongly resemble inverted paleochannels, dating from the Noachian to the Amazonian periods (Balme *et al.* 2020; Davis *et al.* 2016). While they may have formed from non-fluvial processes (e.g. wrinkle ridges), sinuous ridges represent a widespread aqueous history of Mars and are present globally, particularly in the northern upland region of Arabia Terra (Balme *et al.* 2020; Davis *et al.* 2016). A prominent sinuous ridge in this region is Aram Dorsum, a former candidate landing site for ExoMars' *Rosalind Franklin* rover (Balme *et al.* 2020).

A number of inverted paleochannels are located near Hanksville, UT, USA (Figure 1.2) and this site was selected for CanMars 2016, a simulation Mars sample return mission led jointly by the Canadian Space Agency and Western University (Osinski *et al.* 2018) based on its Martian analogue features. The Hanksville paleochannels are located ~7.8 km NW of Hanksville in a cold, arid desert, with an average annual temperature of 11.9 °C and 144 mm of precipitation (Martins *et al.* 2011). This area can experience daily temperature fluctuations of ~20 °C and months without any precipitation (Godfrey *et al.* 2008). Shaped by wind and fluvial erosion, the Hanksville paleochannels resemble sinuous ridges and Martian gullies (Godfrey 1997; Malin and Edgett 2000; Martins *et al.* 2011). As well as geomorphology, the mineralogy of the Hanksville paleochannels

also bears some resemblance to Mars, containing sulfates (e.g. gypsum), carbonates, and clays (Martins *et al.* 2011).

Knowledge of the microbiology of this site is relatively limited, but the adjacent Mars Desert Research Station (MDRS) is dominated by Bacteria, as shown by a PCR-based detection survey of MDRS (Thiel *et al.* 2011). A 16S and 18S rRNA gene survey of MDRS revealed high bacterial and moderate eukaryotic diversity, with low archaeal diversity (Direito *et al.* 2011). Actinobacteria, Proteobacteria, Bacteroidetes, and Gemmatimonadetes were dominant community members, and eukaryotes were represented by fungi (Blastocladiomycota, Zygomycota), green algae (Chlorophyta), bacterivorous flagellates (*Heteromita globosa*), and other protozoans (e.g. ciliophores) (Direito *et al.* 2011). Several putative extremophilic taxa were also present detected



Figure 1.2. Hanksville inverted paleochannel site. View from *Jotunheim*, a prominent inverted paleochannel in the area.

Bacteria, Archaea, and Eukarya, including radioresistant, thermophilic, psychrophilic, and halophilic taxa (Direito *et al.* 2011; Thiel *et al.* 2011). The presence of these microorganisms signifies the analogue potential of the neighbouring Hanksville paleochannels in addition to its geomorphology, geology, and environmental conditions.

1.5.2 Lithobionts and University Valley cryptoendoliths

Rock-dwelling communities of microorganisms (i.e. lithobionts) are common globally, particularly among cold and hot deserts, where rocks offer physical stability (Coleine *et al.* 2021b; Fernández-Martínez *et al.* 2021; Van Goethem *et al.* 2016; Wierzchos *et al.* 2012). Lithobiontic communities can exist on rock surfaces (i.e. epiliths), under rock surfaces (i.e. hypoliths), and within rocks (i.e. endoliths) (Pointing and Belnap 2012). Endolithic habitats offer further stability to microbial communities through thermal buffering, water retention, direct contact with minerals, and protection against UV radiation. Endoliths can be categorized as cryptoendoliths (i.e. inhabiting the porous spaces within the rock and indirectly connected to the surface), chasmoendoliths (i.e. living within cracks and fissures from the rock surface), and euendoliths (i.e. microorganisms able to actively penetrate the rock surface) (Coleine *et al.* 2021b; Fernández-Martínez *et al.* 2021; Wierzchos *et al.* 2012). Endolithic microbes are typically found within sandstone (Archer *et al.* 2017; Goordial *et al.* 2016a), quartz (Khan *et al.* 2011), gypsum and gypsum crusts (Wierzchos *et al.* 2011; Wierzchos *et al.* 2015), halite (Crits-Christoph *et al.* 2016), and granite (Selbmann *et al.* 2017), where the rocks are semi-transparent and porous to allow for the passage of light and nutrients into the rock interior.

Endolithic habitats in Antarctica are a primary niche for microbes, where less than 1% of the continent's surface is ice-free (Coleine *et al.* 2021b; Fernández-Martínez *et al.* 2021). Among these ice-free areas are the McMurdo Dry Valleys, some of the coldest and most arid environments on Earth. University Valley is a particularly cold and dry region of the McMurdo Dry Valleys, with a mean annual air temperature of $-23.4 \pm 8.3^{\circ}\text{C}$, <10 mm of snow precipitation per year, a mean annual relative humidity of $45.5 \pm 14\%$, and an aridity index of <0.05 (Fisher *et al.* 2016; Goordial *et al.* 2016a). University Valley's terrain is primarily dry permafrost overlaying ice-cemented ground, as well as polygonal sand wedges, desert pavement, and sandstone cliffs and valley walls. These features make University Valley a robust contemporary Mars analogue site, especially for northern latitude permafrost at the Phoenix Lander site (68.2188°N , 125.7492°W) (Heldmann *et al.* 2013; McKay *et al.* 2017). As the Martian environment transitioned from warm and wet during the Noachian and Hesperian epochs ($\sim 4.5 - 2.9$ bya) to its current cold and arid Amazonian period (~ 2.9 bya – present), any putative extant life would have retreated into hospitable niches like endoliths, where the rock interior offers protection from the harsh environmental conditions (Wierzchos *et al.* 2012; Ye *et al.* 2021). Cryptoendolithic communities are the most widely distributed endolithic community in the McMurdo Dry Valleys (Zucconi *et al.* 2016) and sandstone cryptoendoliths from University Valley thus represent a compelling analogue site for studying biosignature detection and extremophile characterization.

Light attenuation within cryptoendoliths drives the common banding and visible layers visible in cryptoendolithic rocks (Figure 1.3) (Nienow *et al.* 1988). This stratification also dictates the physical location of community members within the rock; subsurface green bands consist of green algae and/or Cyanobacteria and are often overlain by a black band of lichenized fungi (De Los Ríos *et al.* 2014; Friedmann 1982). The lichenized layer filters out UV radiation, while

photosynthetic green algae and Cyanobacteria inhabit a space of narrow light attenuation that allows photosynthesis and radiation protection (Matthes *et al.* 2001). Cryptoendoliths can be categorized based on their dominant photoautotrophic community: Cyanobacteria-dominated or lichen-dominated. Lichen-dominated fungi are common in sandstone-hosted cryptoendoliths in Antarctica (Friedmann 1982; Zucconi *et al.* 2016). University Valley cryptoendoliths were previously determined to contain viable microbial communities via measurement of their respiration rates of ^{14}C acetate in temperatures as low as $-20\text{ }^{\circ}\text{C}$ (Goordial *et al.* 2016a). This activity is in contrast with the surrounding permafrost, where Goordial *et al.* (2016) detected no radiorespiration activity in the majority (4 out of 7) of the dry and ice- cemented permafrost soil



Figure 1.3. Sandstone from University Valley, Antarctica containing a cryptoendolithic community visible as the green line parallel to the rock surface in the figure and indicated by the red arrow.

samples, and suggesting that extant life in extremely cold, arid conditions is largely restricted to lithic microhabitats. The taxonomy of the University Valley cryptoendoliths was found to be dominated by Bacteria (Acidobacteria) and Fungi (Lecanoromycetes) via 16S/18S rRNA gene sequencing (Goordial *et al.* 2016a), both of which are common taxa in Antarctic cryptoendoliths and desert soils (Coleine *et al.* 2018; Mezzasoma *et al.* 2022; Ortiz *et al.* 2021; Qu *et al.* 2020). Lecanoromycetes is a large class of lichen-forming fungi previously found to dominate the fungal portion of Antarctic cryptoendolith communities (Coleine *et al.* 2018) and Acidobacteria are frequently observed in association with Antarctic lichens, as well (Park *et al.* 2016). A separate 16S/18S rRNA gene sequencing study on University Valley cryptoendoliths found Cyanobacteria were dominant, followed by Proteobacteria (Alphaproteobacteria), Chlorophyta, and some lichen-forming ascomycetes (*Lecidea* sp.) (Archer *et al.* 2017).

Lichen-dominated cryptoendoliths in Antarctica are known to contain a core group of Actinobacteria and Proteobacteria (Coleine *et al.* 2019; Van Goethem *et al.* 2016) and other prominent taxa in McMurdo Dry Valley endolithic communities include *Chroococcidiopsis* sp. and free-living algal species (e.g. *Hemichloris antarctica*) (Archer *et al.* 2017; Büdel *et al.* 2008; Pointing *et al.* 2009). While all three domains of life have been detected in Antarctic cryptoendoliths, the bacterial community tends to be the most diverse, species-rich, and heterogenous (Coleine *et al.* 2021a) and may be responsible for seeding Antarctic surface permafrost populations (Goordial *et al.* 2016a).

1.5.3 Cryoconites and sea ice

The term “cryoconite” refers to the granular dust composed of rock particles, soot, and microbial matter that forms on icy surfaces, particularly glacial ablation zones (Cook *et al.* 2016). Cryoconite holes (also known as “cryoconites”) are the small supra-ice depressions (<1 m across, <0.5 m deep) formed by this windblown material, resulting in a localized increase in the surface ice albedo and producing cylindrical holes containing basal layer of dark sediment overlain with meltwater (Millar *et al.* 2021). Cryoconites can occur on glaciers, sea ice, lake ice, ice sheets, and in alpine environments (Figure 1.4), and are hotspots of microbial diversity in icy environments, providing key functions (e.g. nutrient cycling, carbon fixation, mineral aggregation) (Anesio *et al.* 2017; Edwards *et al.* 2013b; Maccario *et al.* 2015; Weisleitner *et al.* 2019). Cryoconites can be classified according to their granule composition (i.e. organic or inorganic), granule shape/size, and the presence/absence of ice lids (Cook *et al.* 2016). Organic matter (OM) is always a key component of cryoconite material; however, the variation in OM type (i.e. living/dead microbes, microbial exudates, persistent organic pollutants (POPs), other allochthonous and autochthonous OM) (Hodson *et al.* 2010) and abundance as compared with inorganic matter (e.g. mineral fragments of phyllosilicate and quartz) can impact melt and microbial processes within the cryoconites (Edwards *et al.* 2011). Cryoconites may be physically separated from surface and atmospheric exchange by an ice lid, which affects net ecosystem production; it is suggested that cryoconites with an ice lid more than 3 mm thick are net heterotrophic and less than 3 mm thick are net autotrophic (Cook *et al.* 2010; Telling *et al.* 2012).

Due to the extreme environmental conditions on cryoconites (e.g. freezing temperatures, high solar radiation, low nutrient input), cryoconites can act as analogues to icy extraterrestrial



Figure 1.4. Sea ice cryoconites at Allen Bay, NU, Canada.

environments (e.g. Martian polar ice caps, Enceladus, Europa) (Kaczmarek *et al.* 2016; Zawierucha *et al.* 2017). Enceladus and Europa possess subsurface oceans and observed water plume activity. These water plumes are known to contain particulate matter (e.g. silica particles, salts, organics) and the ejection of water plumes upwards could result in deposition of this material onto the icy surface, resulting in cryoconite-like areas of material accumulation. Additionally, Europa's chaos terrain (i.e. warped and enmeshed surface features of raised ridges, cracks, and valleys) indicate some active resurfacing due to water-ice and freeze-out activity, which could also result in the accretion of cryoconite-like material. Endogenous material from the subsurface oceans

is then exposed and accessible for future mission investigations (Nordheim *et al.* 2018; Pappalardo *et al.* 2013; Schmidt *et al.* 2011). Microbes in cryoconites must cope with extreme conditions including freezing temperatures, low nutrient availability, and high solar radiation. As such, these environments contain a high number of extremophiles and polyextremophiles and are ideal environments to investigate the physical limits of life and molecular mechanisms used by microbes to cope with them (Cook *et al.* 2016; Kaczmarek *et al.* 2016; Zawierucha *et al.* 2017).

Cyanobacteria and Proteobacteria are frequently dominant in glacier and alpine cryoconites, which generate high rates of primary production and are structurally supported by filamentous Cyanobacteria (Segawa *et al.* 2017). Heterotrophy-dominated cryoconites also exist and are sustained by allochthonous carbon input (Edwards *et al.* 2016; Edwards *et al.* 2014). As well as better understanding the microbiology of icy worlds analogue environments, studies of sea ice cryoconites in the Canadian high Arctic are necessary to predict how ever-changing sea ice due to climate change will affect the distribution and composition of these increasingly transitory habitats (Edwards *et al.* 2020; Fernández-Gómez *et al.* 2019). Previous studies of cryoconites in the Canadian Arctic have been limited to glacial environments. Canadian high Arctic cryoconites on White Glacier (Axel Heiberg Island), the Devon ice cap (Devon Island), and the Penny ice cap (Baffin Island) are dominated by photoautotrophs as Cyanobacteria and Chlorophyta, as well as containing protists and micro-invertebrates (Mueller *et al.* 2001; Takeuchi *et al.* 2001). This is consistent with reports from other Arctic glacial cryoconites (Edwards *et al.* 2011; Edwards *et al.* 2013a; Edwards *et al.* 2014; Edwards *et al.* 2013c; Millar *et al.* 2021), although detailed genetic studies of Canadian high Arctic cryoconites are lacking. Sea ice in the Canadian high Arctic is known to comprise heterotrophic community members, particularly among first-year sea ice, such as Bacteroidetes (*Flavobacterium*, *Polaribacter*), Alphaproteobacteria (*Roseobacter*, SAR11), and

Gammaproteobacteria (Alonso-Sáez *et al.* 2008; Collins *et al.* 2010; Garneau *et al.* 2016; Yergeau *et al.* 2017). However, the extent to which these taxa overlap with and influence cryoconite communities on sea ice is unknown.

1.6 Extraterrestrial simulation experiments

Experiments simulating extraterrestrial conditions are often performed to investigate life detection strategies and cell and biosignature survival. Searching for life on Mars or the icy worlds requires comprehensive understanding of microbial and biosignature behaviour under the extreme conditions present on these planetary bodies, both individually and collectively. NASA, the European Space Agency (ESA), the Russian State Space Corporation (Roscosmos), and the Japanese Aerospace Exploration Agency (JAXA) have conducted numerous experiments using the extreme conditions present in low Earth orbit (e.g. microgravity, cosmic radiation, freezing temperatures) to explore the potential for lithopanspermia across the Solar System, forward contamination limits, and the likelihood of extant life on the Martian surface (e.g. O/OREOS, EXPOSE, BIOPAN, Tanpopo) (Berger *et al.* 2012; Demets *et al.* 2005; Horneck *et al.* 2010; Kawaguchi *et al.* 2016; Minelli *et al.* 2010; Nicholson *et al.* 2011; Olsson-Francis and Cockell 2010; Rabbow *et al.* 2012). Ground-based simulation facilities also exist, particularly for modelling environmental conditions, investigating microbial survival, testing space mission equipment, and selecting landing sites on Mars (Table 1.4) (Olsson-Francis and Cockell 2010; Sobrado *et al.* 2014).

Table 1.4. List of Mars simulation chambers and their environmental parameters. The first row lists the corresponding environmental conditions on Mars for comparison.

Chamber name	Location	Temperature (°C)	Atmospheric pressure (mbar)	Atmospheric composition	UV source	Reference
Mars	N/A	-123 to +25	8	95% CO ₂ , 2.7% N ₂ , 1.6% Ar, 0.13% H ₂ O, 0.08% CO	Sun	(Horneck <i>et al.</i> 2010; Schuerger 2015)
MARTE	Centro de Astrobiología, Spain	-15	8	>95% CO ₂ , 5% air+H ₂ O	Xenon, negligible deuterium	(Sobrado <i>et al.</i> 2014)
Planetary environmental simulation chamber	Centro de Astrobiología, Spain	-269.15 to 51.85	5x10 ⁻⁹ to 5	95% CO ₂ , 2.7% N ₂ , 1.6% Ar, 0.6% H ₂ O	Deuterium	(Mateo-Martí <i>et al.</i> 2006)
ME/mini-ME	University of Winnipeg, Canada	≥ -125	~5.3	CO ₂	Deuterium	(Cloutis <i>et al.</i> 2007; Craig <i>et al.</i> 2001)
MASC	Vrije Universiteit Amsterdam, Netherlands	-30.15 to -9.85	6 to 10	CO ₂	N/A	(Motamedi <i>et al.</i> 2015)
MESCH	University of Aarhus, Denmark	≥ -140	5 to 10	95% CO ₂ , 3% N ₂ , 1.5% Ar, 0.1% O ₂ , 0.01% CO	Xenon-mercury	(Jensen <i>et al.</i> 2008)
MEC	Shandong University, China	-150 to 200	≥1	CO ₂ , N ₂ , Ar, O ₂	Xenon	(Wu <i>et al.</i> 2021)
MaSimKa	DLR Institute of Planetary Research, Germany	-25.15 to 79.85	2 to 12	95% CO ₂	Halogenide-mercury	(Bauermeister <i>et al.</i> 2010)
Humidity-LAB	DLR Institute of Planetary Research, Germany	-75 to 20	10 to 11	95% CO ₂	N/A	(Vera <i>et al.</i> 2010)
PEACH	Washington University, USA	≥ -100	3 × 10 ⁻² to ambient	CO ₂	Xenon, deuterium	(Sobron and Wang 2012)

1.6.1 Mars simulation chambers

Mars simulation chambers can investigate a range of environmental conditions (e.g. Martian temperature, atmospheric pressure, radiation) and their effects jointly or independently. As such, Martian simulation experiments can be conducted in relatively simple anoxic containers or sophisticated vacuum chambers. Indeed, the first Mars simulation experiments were conducted in anaerobic jars (Fulton 1958; Olsson-Francis and Cockell 2010). Modern Mars chambers are typically constructed of stainless steel, with independently controlled environmental parameters. This independent control allows for finer scale imitation of natural variation in Martian conditions (e.g. diurnal and seasonal fluctuation, solar longitude, elevation, dust shielding).

As Mars possesses minimal atmospheric pressure, vacuum chambers are often used with a circulating gas mix of primarily CO₂ to both mimic the Martian atmosphere and eliminate external ambient air that may leak into the chamber (Kleiman et al. 2013; Mateo-Martí et al. 2006; Olsson-Francis and Cockell 2010). Gas mixtures and their input are monitored, regulated by flow controllers/valves, and measured via mass spectrometry. Liquid nitrogen is frequently used to control internal air temperature as well as surface temperature of the sample holder, circulating within and around the chamber walls and sample tray. Helium can also be used locally to cool sample holders. UV irradiation can be performed with noble gas (e.g. xenon) or deuterium lamps, generally mounted on the chamber exterior and transmitting light through optical bundles or a quartz viewport (Mateo-Martí *et al.* 2006; Olsson-Francis and Cockell 2010; Schuerger *et al.* 2003; Sobrado *et al.* 2014).

1.6.2 Previous experiments in Mars simulation chambers

Mars simulation chambers have been used to investigate the effects of Martian environmental conditions on a wide array of organisms and biomolecules: bacteria and archaea (e.g. spore-formers, extremophiles, model organisms), eukaryotes (e.g. yeast), microbial communities in environmental matrices, and biomolecules (e.g. DNA, pigments) (Table 1.5).

Most Mars exposure experiments have been conducted on pure cultures of bacteria. *Bacillus* spp. (*B. cereus*, *B. megaterium*, *B. mycoides*, *B. pumilus*, *B. subtilis*, and *B. thuringiensis*) are commonly used due to their ability to produce endospores and tolerate harsh conditions. *Bacillus* spores are able to survive limited amounts of time in simulated Mars environments; they are known to lose 99.9% of their viability within the first 5 minutes of exposure (Nicholson *et al.* 2018) and survive up to 180 minutes (Schuerger *et al.* 2003; Schuerger and Nicholson 2006), but shielding provided by *Bacillus* cell monolayers or soil layers <1 mm thick are enough to increase this survival to an equivalent of 115 Martian sols (4 W/m² of UVC irradiation, -10 °C, 0.7 kPa) (Cockell *et al.* 2000; Nicholson *et al.* 2018; Osman *et al.* 2008) and perhaps further. Physical shielding protects against the harsh Martian UV, which is measured within three bands: UVA (400 – 320 nm; ~38 W/m²), UVB (320 – 280 nm; ~8 W/m²), and UVC (280 – 200 nm; ~3 – 4.55 W/m²) (Cockell *et al.* 2000; Schuerger *et al.* 2003). UVC is the shortest wavelength, the most biocidal, and the most damaging to cellular machinery and molecules (Cockell *et al.* 2005; Schuerger *et al.* 2003; Schuerger and Nicholson 2006). Spore structural components, such as acid-soluble spore proteins, coat layers, and dipicolinic acid, as well as photoproduct repair and maintenance of spore core dehydration, are essential for the resistance of *Bacillus* spores to Martian conditions (Cortêsão *et al.* 2019; Moeller *et al.* 2012).

Table 1.5. List of organisms tested in Mars simulation chambers. Low Earth orbit refers to the area of space below an altitude of ~2000 km. All astrobiology and exposure experiments performed in space have occurred in low Earth orbit. Mars simulation conditions refers to ground-based simulation experiments.

Organism/environment tested	Low Earth orbit	Mars simulation conditions	Reference
Bacteria/bacterial spores			
<i>Acidithiobacillus ferrooxidans</i>		x	(Gómez <i>et al.</i> 2010)
<i>Anabaena cylindrica</i>	x	x	(Cockell <i>et al.</i> 2011; Olsson-Francis <i>et al.</i> 2009)
<i>Arthrobacter psychrolactophilus</i>		x	(Johnson <i>et al.</i> 2011)
<i>Bacillus cereus</i>		x	(Hagen <i>et al.</i> 1967)
<i>Bacillus megaterium</i>		x	(Hawrylewicz <i>et al.</i> 1962)
<i>Bacillus mycoides</i>		x	(Imshenetskiĭ <i>et al.</i> 1984)
<i>Bacillus pumilus</i>		x	(Imshenetskiĭ <i>et al.</i> 1984)
<i>Bacillus subtilis</i>	x	x	(Cortêsão <i>et al.</i> 2019; Fajardo-Cavazos <i>et al.</i> 2010; Moeller <i>et al.</i> 2012; Nicholson <i>et al.</i> 2018; Schuerger <i>et al.</i> 2003; Wassmann <i>et al.</i> 2012)
<i>Bacillus thuringiensis</i>	x		(Taylor <i>et al.</i> 2022)
<i>Carnobacterium</i> spp.		x	(Nicholson <i>et al.</i> 2014; Nicholson <i>et al.</i> 2013)
<i>Chroococcidiopsis</i>	x	x	(Baqué <i>et al.</i> 2013; Cockell <i>et al.</i> 2011; Cockell <i>et al.</i> 2005)
<i>Clostridium botulinum</i>		x	(Hawrylewicz <i>et al.</i> 1962)
<i>Clostridium butyricum</i>		x	(Koike <i>et al.</i> 1996)
<i>Clostridium celatum</i>		x	(Koike <i>et al.</i> 1996)
<i>Deinococcus aerius</i>	x		(Kawaguchi <i>et al.</i> 2018)
<i>Deinococcus geothermalis</i>	x	x	(Panitz <i>et al.</i> 2013)
<i>Deinococcus radiodurans</i>	x	x	(de la Vega <i>et al.</i> 2007; Diaz and Schulze-Makuch 2006; Gómez <i>et al.</i> 2010; Kawaguchi <i>et al.</i> 2020)
<i>Escherichia coli</i>	x	x	(Berry <i>et al.</i> 2010; Diaz and Schulze-Makuch 2006; Koike <i>et al.</i> 1996)
<i>Klebsiella pneumoniae</i>		x	(Hawrylewicz <i>et al.</i> 1962)
<i>Leptolyngbya</i>		x	(De Vera <i>et al.</i> 2014a)
<i>Micrococcus luteus</i>	x		(Zhukova and Kondratyev 1965)
<i>Nostoc commune</i>	x		(Cockell <i>et al.</i> 2011; Jänchen <i>et al.</i> 2016)

<i>Nostoc microscopicum</i>		x	(De Vera <i>et al.</i> 2014a)
<i>Photobacterium</i>		x	(Zhukova and Kondratyev 1965)
<i>Psuedomonas aeruginosa</i>	x	x	(Hawrylewicz <i>et al.</i> 1968)
<i>Psychrobacter cryohalolentis</i> K5		x	(Smith <i>et al.</i> 2009)
<i>Salmonella enterica</i>		x	(Roy <i>et al.</i> 2016)
<i>Serratia liquefaciens</i>		x	(Berry <i>et al.</i> 2010; Schuerger <i>et al.</i> 2020)
<i>Staphylococcus aureus</i>		x	(Parfenov and Lukin 1973)
<i>Streptomyces albus</i>		x	(Hawrylewicz <i>et al.</i> 1968)
<i>Synechococcus</i>	x		(Mancinelli 2015; Mancinelli <i>et al.</i> 1998)
Archaea			
<i>Halobacterium noricense</i>		x	(Stan-Lotter <i>et al.</i> 2002)
<i>Halococcus dombrowski</i>		x	(Stan-Lotter <i>et al.</i> 2002)
<i>Halorubrum chaoviator</i>	x		(Johnson <i>et al.</i> 2011; Mancinelli 2015)
<i>Methanobacterium</i>		x	(Johnson <i>et al.</i> 2011; Morozova <i>et al.</i> 2007)
<i>Methanosarcina</i>		x	(Morozova <i>et al.</i> 2007)
Algae, fungi, and yeasts			
<i>Aspergillus niger</i>		x	(Zhukova and Kondratyev 1965)
<i>Aspergillus terreus</i>		x	(Sarantopoulou <i>et al.</i> 2011)
<i>Aspergillus versicolor</i>	x		(Novikova <i>et al.</i> 2015)
<i>Cladosporium herbarum</i>		x	(Sarantopoulou <i>et al.</i> 2014)
<i>Cryomyces antarcticus</i>	x	x	(Onofri <i>et al.</i> 2019; Pacelli <i>et al.</i> 2017)
<i>Penicillium roqueforti</i>	x		(Hotchin <i>et al.</i> 1965)
<i>Rhodotorula mucilaginosa</i>		x	(Zhukova and Kondratyev 1965)
<i>Trebouxia sp.</i>		x	(Sánchez <i>et al.</i> 2014)
<i>Trichophyton terrestre</i>	x		(Taylor <i>et al.</i> 2022)
Lichens			
<i>Aspicillia fruiticulosa</i>	x	x	(Raggio <i>et al.</i> 2011)
<i>Buellia frigida</i>		x	(Meeßen <i>et al.</i> 2015)
<i>Circinaria gyrosa</i>	x	x	(De La Torre Noetzel <i>et al.</i> 2018; Sánchez <i>et al.</i> 2014)
<i>Pleopsidium chlorophanum</i>		x	(de Vera <i>et al.</i> 2014b)
<i>Rhizocarpon geographicum</i>	x	x	(Sánchez <i>et al.</i> 2014)
<i>Xanthoria elegans</i>	x	x	(Brandt <i>et al.</i> 2015; De Vera <i>et al.</i> 2004; Sancho <i>et al.</i> 2007)
<i>Xanthoria parietina</i>		x	(De Vera <i>et al.</i> 2004)

Animals			
<i>Caenorhabditis elegans</i>	x	x	(Higashibata <i>et al.</i> 2006; Johnson <i>et al.</i> 2011)
<i>Milnesium tardigradum</i>	x		(Jönsson <i>et al.</i> 2008)
<i>Mniobia russeola</i>		x	(Jönsson and Wojcik 2017)
<i>Ramazzottius varieornatus</i>		x	(Johnson <i>et al.</i> 2011)
<i>Richtersius coronifer</i>	x	x	(Jönsson <i>et al.</i> 2008; Jönsson and Wojcik 2017)
Viruses			
T7 phage		x	(Taylor <i>et al.</i> 2022)
Natural environmental samples			
Permafrost		x	(Hansen <i>et al.</i> 2009; Morozova <i>et al.</i> 2007)
Cryptoendolithic sandstone		x	(Onofri <i>et al.</i> 2013)
Epilithic limestone	x		(Cockell <i>et al.</i> 2011)

Extremophiles able to tolerate one or more Martian environmental conditions (e.g. psychrophiles, halophiles, desiccation-tolerant microbes) are also frequently tested in Mars chambers. *Psychrobacter cryohalolentis* K5 lost all viability after 8 hours of exposure to Martian conditions (4.55 W/m² of UVC irradiation, 12.5 °C, 7.1 mbar), although the presence of a mineral salt matrix increased its survival one- to threefold (Smith *et al.* 2009). Psychrotolerant *Arthrobacter psychrolactophilus* exhibited a half-life of ~2.5 days in a 40-day Mars chamber exposure, losing 99.9996% of its biomass within 30 days, even when inoculated and exposed within a Mars simulation soil matrix. While cell numbers slightly increased after 30 days, this increase may be due to residual *A. psychrolactophilus* metabolism on accumulated dead cells. Similar expected half-lives within UV-exposed, light, and dark control samples indicate that rather than UV, low water activity, desiccation stress, and small amounts of organic carbon are the most detrimental to *A. psychrolactophilus* survival (Johnson *et al.* 2011).

Halophiles, such as *Halorubrum chaoviator* and *Halobacterium* spp., are often extremely tolerant of high radiation and desiccating conditions, and *H. chaoviator* was found to have a 100%

survival rate under 0.5 mm of simulant soil and 40 days of Martian conditions. Halophilic archaea like *H. chaoviator* and *H. salinarum* have robust DNA repair mechanisms, high intracellular Mn/Fe ratios, and scavenging of reactive oxygen species (ROS) by intracellular halides. These features may be side effects of desiccation resistance due to the hypersaline environments in which halophiles are found, but also enable resistance to radiation and oxidative stress (Johnson *et al.* 2011; Kish *et al.* 2009; Kottemann *et al.* 2005).

Desiccation-tolerant organisms, such as *Chroococcidiopsis* spp., have also been tested in Mars chambers. Cockell *et al.* (2005) found that while *Chroococcidiopsis* cells perished after 30 minutes of Mars-like conditions (UVC, UVB, and UVA flux of 3.73, 8.27, and 37.67 W/m², respectively), its phycobilisomes and esterases were still detectable after 4 hours, and DNA after 8 hours. Conversely, sandstone containing endolithic *Chroococcidiopsis* cells were still viable and growing after 8 hours of exposure (Cockell *et al.* 2005). While the desiccation tolerance of *Chroococcidiopsis* enables efficient DNA repair (Billi *et al.* 2000), a 3-month Mars-like exposure (average UV flux of ~50 W/m²) resulted in total cell death, although biosignature detection (e.g. DNA, carotenoids) was still possible (Baqué *et al.* 2016). *Chroococcidiopsis* cells within biofilms are more tolerant to high UV radiation, likely due to the protection afforded by extracellular polymeric substances (EPS) (Baqué *et al.* 2013).

Radiation-resistant microorganisms are also promising extremophiles for the study of life detection and survival within Mars simulation chambers. As well as surviving extreme radioactivity, *Deinococcus radiodurans* is a polyextremophile and able to tolerate the combined effects of several harsh environmental conditions (e.g. high UV radiation, low pressure, freezing temperature) better than other microbes (e.g. *Escherichia coli*, *Acidithiobacillus ferrooxidans*) (Diaz and Schulze-Makuch 2006; Gómez *et al.* 2010, Horne *et al.* 2022). When exposed to 1 day

of Mars-like conditions, *D. radiodurans* is severely affected, losing up to 99.9% of cellular viability within 1 cm of the surface (although a depth of 5 cm maintains viability at 56%) (Diaz and Schulze-Makuch 2006). While Martian temperature cycles and humidity also influence viability, UV radiation has the most deleterious effect on *D. radiodurans* (de la Vega *et al.* 2007).

Within Mars simulation chambers, eukaryotes exhibit variable survival and responses. Yeasts like *Cryptococcus* sp. showed a 7% survival rate after a 40-day Mars-like exposure (Johnson *et al.* 2011), while filamentous fungi and their conidia may be able to impart more resistance to Mars-like conditions than that present in regular coenocytic cells, surviving a UVC dose of up to 2000 J/m² (Blachowicz *et al.* 2019). Higher eukaryotes like nematodes were unable to survive any exposure to Mars-like conditions, while tardigrades such as *Ramazzottius varieornatus* exhibited a survival rate of at least 70% during a 40-day Mars simulation exposure (Johnson *et al.* 2011). *Cryomyces* spp. have also exhibited strong resistance to Mars-like conditions, particularly UV and osmotic stress tolerance, with some species maintaining viability after 22 days of exposure (Onofri *et al.* 2013).

Within natural communities (e.g. endoliths, lichens), cellular viability is aided by the presence of a natural mineral matrix and protective microbial exudates (e.g. EPS). Cryptoendolithic sandstone communities exhibited positive growth for algal, fungal, and bacterial colonies after exposure to Martian UVC (1000 J/m²) and atmospheric pressure (Onofri *et al.* 2013). Mars analogue soil also protects microbes from Martian environmental conditions. While respiration and substrate utilization decreased under UV exposure, culturable bacteria and genetic diversity in soils rich in iron oxides remained unaffected after 8 Martian sols (Hansen *et al.* 2005). Hansen *et al.* (2009) further found that in natural permafrost communities, 80 Martian sols of exposure resulted in a decrease of the total and viable microbial cells, as well as DNA and amino

acid concentration, but that 2 cm of permafrost dust was enough to effectively shield the community from the deleterious surface conditions (Hansen *et al.* 2009). Permafrost microbial communities may be naturally resistant to Mars-like conditions; 90% of methanogens from Siberian permafrost were found to survive 22 days of Mars-like exposure, while 99.7% of non-permafrost methanogens were killed under the same conditions (Morozova *et al.* 2007). Vacuum and UV exposure to lichen samples resulted in 50% viability retention; ascospores of *Xanthoria elegans* demonstrated the highest survival of lichens tested, and lichens in general are well-protected by their pigments and outer gelatinous structure (De Vera *et al.* 2004). *Circinaria gyrosa* can also survive Mars-like conditions but loses photosynthetic ability after 30 days of exposure (De La Torre Noetzel *et al.* 2018). Conversely, *Pleopsidium chlorophanum* may retain its photosynthetic capabilities after simulated Mars exposure (de Vera *et al.* 2014b).

Biomolecules (e.g. DNA, pigments, amino acids) may be more resistant to Martian exposure than living cells (Hansen *et al.* 2009) and were detectable after simulated Mars exposure (Baqué *et al.* 2016; Blachowicz *et al.* 2019); however, naked DNA from *Bacillus* spores showed pyrimidine dimer and photoproduct formation when exposed to Mars-like conditions (Nicholson *et al.* 2018). As well as being strongly biocidal, UVC radiation is the most detrimental Martian environmental condition to DNA, inducing cyclobutane pyrimidine dimer (CPD) formation (i.e. thymine-thymine, thymine-cytosine, cytosine-thymine, cytosine-cytosine), photoproduct formation (i.e. 6-4 pyrimidine-pyrimidone and 6-4 pyrimidine-pyrimidonine), Dewar isomers, strand breaks, base modifications, and DNA-DNA/DNA-protein crosslinks (Douki 2013; Friedberg *et al.* 2006; Nicholson *et al.* 2018; Taylor and Cohrs 1987). These side effects can interfere with downstream detection techniques like PCR and sequencing (Fajardo-Cavazos *et al.* 2010; Sikorsky *et al.* 2004). Additionally, UV radiation induces cellular apoptosis, which can

cause DNA fragmentation as the cell breaks apart (Dwyer *et al.* 2012; Erental *et al.* 2014; Takada *et al.* 2017). While the MinION can operate in microgravity and on low biomass samples containing high amounts of environmental inhibitors (Carr *et al.* 2020; Goordial *et al.* 2017), it is currently unknown if it is able to detect DNA from samples exposed to Mars-like conditions and if the myriad of destructive effects from UVC radiation (e.g. pyrimidine dimer formation, DNA fragmentation) will prevent effective DNA detection and sequencing. This knowledge will be crucial to determining the MinION's efficacy as a tool for life detection in missions targeting Mars and the icy moons Europa and Enceladus.

1.7 Conclusion

There has not been a mission focused on searching for extant life in our Solar System since the launch of the Viking mission in August 1975. In that time, we have learned about promising areas for habitability in our Solar System besides Earth; organic molecules and liquid water exist on Mars, and the icy moons Europa and Enceladus possess liquid water oceans containing particulate matter (Eigenbrode *et al.* 2018; Nimmo and Pappalardo 2016; Spencer *et al.* 2006; Szopa *et al.* 2020). Robust instrumentation such as the MinION can operate in extreme environments on Earth and effectively detect DNA, but there exists a gap in knowledge regarding the MinION's ability to detect DNA from Mars analogue samples and reconstruct individual microbial genomes to illuminate putative extraterrestrial survival strategies, metabolisms, and lifestyles. This work aims to bridge that gap and provide valuable knowledge on the efficacy of DNA as a biosignature and the MinION as a tool for life detection and genome reconstruction. In Chapter 2, I demonstrate the MinION's ability to detect DNA from a Mars analogue environment

(including putative lower limits of detection) and complement results from other instruments used in space missions. In Chapter 3, I show that the MinION can detect DNA from samples exposed to Mars-like environmental conditions to further establish its utility for extant life detection. In Chapter 4, I generated genome bins from an icy moons analogue environment to show the MinION's efficacy as a tool for detailed genome studies in extreme environments.

Connecting text

To evaluate the MinION's efficacy as a tool for life detection, it must be tested in a variety of robust Mars analogue environments, both alone and in conjunction with other established space mission instruments. The following chapter presents a proof-of-concept utilization of the MinION for direct life detection in the Hanksville paleochannels and links the MinION-generated sequences to data from X-ray diffraction, reflectance spectroscopy, Raman spectroscopy, and Life Detector Chip (LDChip) microarray immunoassay analyses to contextualize the taxonomy and metabolisms present. I also compared the MinION metagenome to Illumina 16S rRNA gene sequences to better describe the microbial diversity present and evaluate the MinION's accuracy. Additionally, this work presents the first determination of the MinION's putative lower detection limit for DNA.

This manuscript appears in:

Maggiore, C., Stromberg, J., Blanco, Y., Goordial, J., Cloutis, E., García-Villadangos, M., ... & Whyte, L. (2020). The limits, capabilities, and potential for life detection with MinION sequencing in a paleochannel Mars analog. *Astrobiology*, 20(3), 375-393. DOI: 10.1089/ast.2018.1964

**Chapter 2. The limits, capabilities, and potential for life detection with MinION sequencing
in a paleochannel Mars analogue**

Catherine Maggiori¹, Jessica Stromberg², Yolanda Blanco³, Jacqueline Goordial^{1,4}, Edward Cloutis⁵, Miriam García-Villadangos³, Victor Parro³, Lyle Whyte¹

¹Department of Natural Resource Sciences, Faculty of Agricultural and Environmental Sciences, McGill University, Ste. Anne-de-Bellevue, Quebec, Canada

²CSIRO Mineral Resources Flagship, 26 Dick Perry Avenue, WA 6151, Australia

³Department of Molecular Evolution, Centro de Astrobiología (INTA-CSIC), Torrejón de Ardoz, Madrid, Spain

⁴Bigelow Laboratory for Ocean Sciences, East Boothbay, Maine, United States

⁵Department of Geography, Faculty of Science, University of Winnipeg, Winnipeg, Manitoba, Canada

2.1 Abstract

No instrument capable of direct life detection has been included on a mission payload to Mars since NASA's Viking missions in the 1970s. This prevents us from discovering if life is or ever was present on Mars. DNA is an ideal target biosignature since it is unambiguous, non-specific, and readily detectable with nanopore sequencing. Here, we present a proof-of-concept utilization of the Oxford Nanopore Technologies (ONT) MinION sequencer for direct life detection and show how it can complement results from established space mission instruments. We used nanopore sequencing data from the MinION to detect and characterize the microbial life in a set of paleochannels near Hanksville, Utah, USA, with supporting data from X-ray diffraction, reflectance spectroscopy, Raman spectroscopy, and Life Detector Chip (LDChip) microarray immunoassay analyses. These paleochannels are analogues to Martian sinuous ridges. The MinION-generated metagenomes reveal a rich microbial community dominated by Bacteria and containing radioresistant, psychrophilic, and halophilic taxa. With spectral data and LDChip immunoassays, these metagenomes were linked to the surrounding Mars analogue environment and potential metabolisms (e.g. methane production and perchlorate reduction). This shows a high degree of synergy between these techniques for detecting and characterizing biosignatures. We also resolved a prospective lower limit of ~ 0.001 ng of DNA required for successful sequencing. This work represents the first determination of the MinION's DNA detection limits beyond ONT recommendations and the first whole metagenome analysis of a sinuous ridge analogue.

2.2 Introduction

The search for biosignatures is increasingly important in Mars exploration missions and will be a primary objective for the upcoming ExoMars 2020 and Mars 2020 missions (McLennan *et al.* 2012; Mustard *et al.* 2013a; Mustard *et al.* 2013b; Summons *et al.* 2014). In order to test strategies, techniques, logistics, and instruments, terrestrial analogue sites are used to approximate field operations and further understand the corresponding extraterrestrial body's environment, geology, and potential for life and biosignature preservation (Thiel *et al.* 2011). Hanksville, Utah, USA is situated near a number of diverse Mars analogues, including segmented and inverted anastomosing paleochannels exhumed from the Late Jurassic Brushy Basin Member of the Morrison Formation (Clarke and Stoker 2011; Ehrenfreund *et al.* 2011; Williams *et al.* 2007). Like other inverted fluvial channels, the Hanksville paleochannels have resulted from relief inversion, in which materials in topographic lows are more resistant to erosion than their surroundings (Clarke and Stoker 2011; Williams *et al.* 2007; Williams *et al.* 2009). Because fluvial channels are comprised of higher-permeability sediments than their floodplain surroundings, the water flow can lead to cementation of the channels. Cemented fluvial channels can then be exhumed by denudation of the surrounding landscape, resulting in inversion of the former topography (Clarke and Stoker 2011; Williams *et al.* 2009). The Hanksville paleochannels were exhumed in this way, and the sedimentary sandstone of the channels is capped with erosion-resistant coarse sandstones and fine-grained conglomerates (Williams *et al.* 2007; Williams *et al.* 2009). This capping protects the underlying clay floodplains and preserves the fluvial sediments, as well as sedimentary structures and biosignatures (Clarke and Stoker 2011; Williams *et al.* 2007). The Hanksville paleochannels are strong geomorphological analogues to sinuous ridges on Mars, which is a non-

specific term for elongated ridge structures on the Martian surface. They may have formed from inverted stream channels but could also result from other, non-hydrological processes (e.g. wrinkle ridges) (Williams *et al.* 2013; Williams *et al.* 2009).

Dating from the Noachian Period to the Amazonian Period on Mars, sinuous ridges represent compelling evidence for a history of prolific water flow (Balme *et al.* 2015; Clarke and Stoker 2011; Davis *et al.* 2016). They are distributed globally, but are particularly abundant in Arabia Terra, the northernmost region of Mars' heavily cratered southern highlands (Clarke and Stoker 2011; Davis *et al.* 2016; Williams *et al.* 2009). One prominent sinuous ridge in this area is Aram Dorsum, a former candidate landing site for ExoMars 2020 (downselected in March 2017). In November 2016, the Hanksville paleochannels were chosen for CanMars 2016, a simulation Mars sample return mission led jointly by the Canadian Space Agency and Western University (Osinski *et al.* 2018). Mars sample return will take its first steps with the Mars 2020 rover, which will identify and cache organic samples and water-formed samples for potential return to Earth in the 2030s (Beegle *et al.* 2015; Mustard *et al.* 2013a; Mustard *et al.* 2013b; Summons *et al.* 2014).

The National Research Council (USA) and the Mars 2020 Science Definition Team both state that the determination if life is or ever was present on Mars is the prime focus of the 2013 – 2022 decade (Mustard *et al.* 2013b; NRC 2012). Yet neither ExoMars 2020 nor Mars 2020 contain instrumentation capable of detecting definitive biosignatures, which are substances, objects, or patterns that could not form via abiotic processes (Hays *et al.* 2017; Mustard *et al.* 2013b; Sephton 2018). Nucleic acids, including DNA, are strong definitive biosignatures given the virtual impossibility of their generation in the absence of life (Mustard *et al.* 2013b; Neveu *et al.* 2018). In missions focusing on Mars, DNA is an especially good target. There is some evidence for the exchange of possible microbe-carrying rocks between Earth and Mars during the Late Heavy

Bombardment period ~ 4 billion years ago, when both planets shared a warm and wet environment capable of harbouring life (Mileikowsky *et al.* 2000). Overall geological and chemical similarities between Earth and Mars indicate that any potential Martian life could share fundamental biochemistry with terrestrial life because the emergence of inorganic-based biology would require conditions and chemistries vastly different from the two rocky planets (e.g. gas giants and icy moons) (Mustard *et al.* 2013b). There is also a widespread occurrence of organic molecules in interstellar space (Meinert *et al.* 2016; Pace 2001) and putative hydrogen-rich aliphatics have recently been detected in Mars' Gale Crater (Eigenbrode *et al.* 2018). While it is certainly not definite that life on Mars (or anywhere else in our solar system) would share its biochemical phenotype with Earth, we should include the capability to detect these features on Mars exploration missions. We must search for what we know before we can rule out its impossibility. This is especially true with increasing activity in both the private and public space sectors that could compromise future life detection and science activities on Mars (Fairén *et al.* 2017; Musk 2017; Spry *et al.* 2018).

As well as detecting DNA, life detection instrumentation should have the capacity for miniaturization and low power requirements to ease deployment on a rover or lander vehicle. It should also have proven functionality in terrestrial analogue environments (Ellery *et al.* 2002). The Oxford Nanopore Technologies' (ONT) MinION is a promising candidate for life detection based on these requirements. The MinION is a miniaturized device designed to sequence DNA, RNA, and potentially proteins (Goordial *et al.* 2017; Leggett and Clark 2017; Loman and Watson 2015). The MinION uses nanopore technology to generate sequences (Leggett and Clark 2017; Loman and Watson 2015). It is portable and can operate in difficult environmental conditions, including the high Arctic, Antarctic, tropical rainforests, and the microgravity of the International Space

Station (Castro-Wallace *et al.* 2017; Edwards *et al.* 2016; Goordial *et al.* 2017; John *et al.* 2016; Johnson *et al.* 2017; Menegon *et al.* 2017). Indeed, the MinION was the first sequencer to operate in space as part of the Biomolecule Sequencer project in 2016 (Castro-Wallace *et al.* 2017; John *et al.* 2016), making it a promising candidate for direct life detection in space missions. Its small size would make it easier and cheaper to develop than larger payloads, it can function in a controlled environment like the heated interior chamber of a rover, and it can directly detect unambiguous signs of life through nucleic acid sequencing (Carr *et al.* 2017; Goordial *et al.* 2017). This would enable the best selection of samples for future caching and potential return to Earth (Goordial *et al.* 2017). If DNA is detected on a mission, the ability of the MinION to generate sequences in real time also means that contamination from terrestrial microorganisms can be quickly ruled out. However, ONT requires a minimum input of 400 ng of DNA without PCR amplification and 1 ng of DNA with PCR amplification for MinION sequencing. The low biomass present in many Mars analogues, like high elevation University Valley permafrost (10^3 cells/g) (Goordial *et al.* 2016a) and Lost Hammer Spring sediment (10^5 cells/g) (Niederberger *et al.* 2010), corresponds to just $\sim 0.01 - 1$ ng of DNA based on an average bacterial genome size of $2 - 5$ Mbp and $\sim 2.5 - 5$ fg of DNA per genome (Dolezal *et al.* 2003; Raes *et al.* 2007; Goordial *et al.* 2017), meaning that DNA detection limits of MinION sequencing need to be explored beyond ONT recommendations.

We tested the life detection capability of the MinION with samples from a high fidelity analogue environment, the Hanksville paleochannels. We determined DNA detection limits using a high biomass endolith sample and generated a metagenomic profile of this site with MinION sequences. Simultaneous analyses with an X-ray diffractometer, micro-reflectance spectrometer, and micro-Raman spectrometer and protein detection with the LDChip (Life Detector Chip) (Parro

et al. 2005) were also performed to complement MinION results and to establish baseline data for a paleochannel environment. These instruments were chosen because they are analogues to current and future payload instruments. An X-ray diffractometer forms the core of the Curiosity rover's CheMin instrument, a micro-reflectance spectrometer acts as an approximation for ExoMars 2020's Mars Multispectral Imager for Subsurface Studies (Ma_MISS), and a micro-Raman spectrometer approximates ExoMars 2020's Raman Laser Spectrometer (RLS) (Rull *et al.* 2017) and Mars 2020's SuperCam and SHERLOC (Scanning Habitable Environments with Raman and Luminescence for Organics and Chemicals). The LDChip approximates the Life Marker Chip (LMC), a former Pasteur payload candidate for ExoMars 2020. These instruments characterize other biosignatures (e.g. isotopes, organics, and polymeric biomarkers), contextualize the environment and geologic setting, and help reveal metabolic potential of the microbial community.

2.3 Materials and Methods

2.3.1 Sample site and collection

The study site is located approximately 7.8 km NW of Hanksville, Utah, USA (38.41709915, -110.78539335; Figure 2.1). It is part of the Colorado Plateau and contains a diverse array of early Jurassic to late Cretaceous-aged evaporitic and fluvial sediments. The geology of the site is dominated by quartz, calcite, and gypsum, and has been shaped by fluvial and aeolian processes (Martins *et al.* 2011; Stoker *et al.* 2011). It is an arid desert with an average annual temperature of 11.9 °C and 144 mm of precipitation (Martins *et al.* 2011). Samples were collected to represent a range of geomorphology and biomasses (e.g. desiccated regolith, high biomass

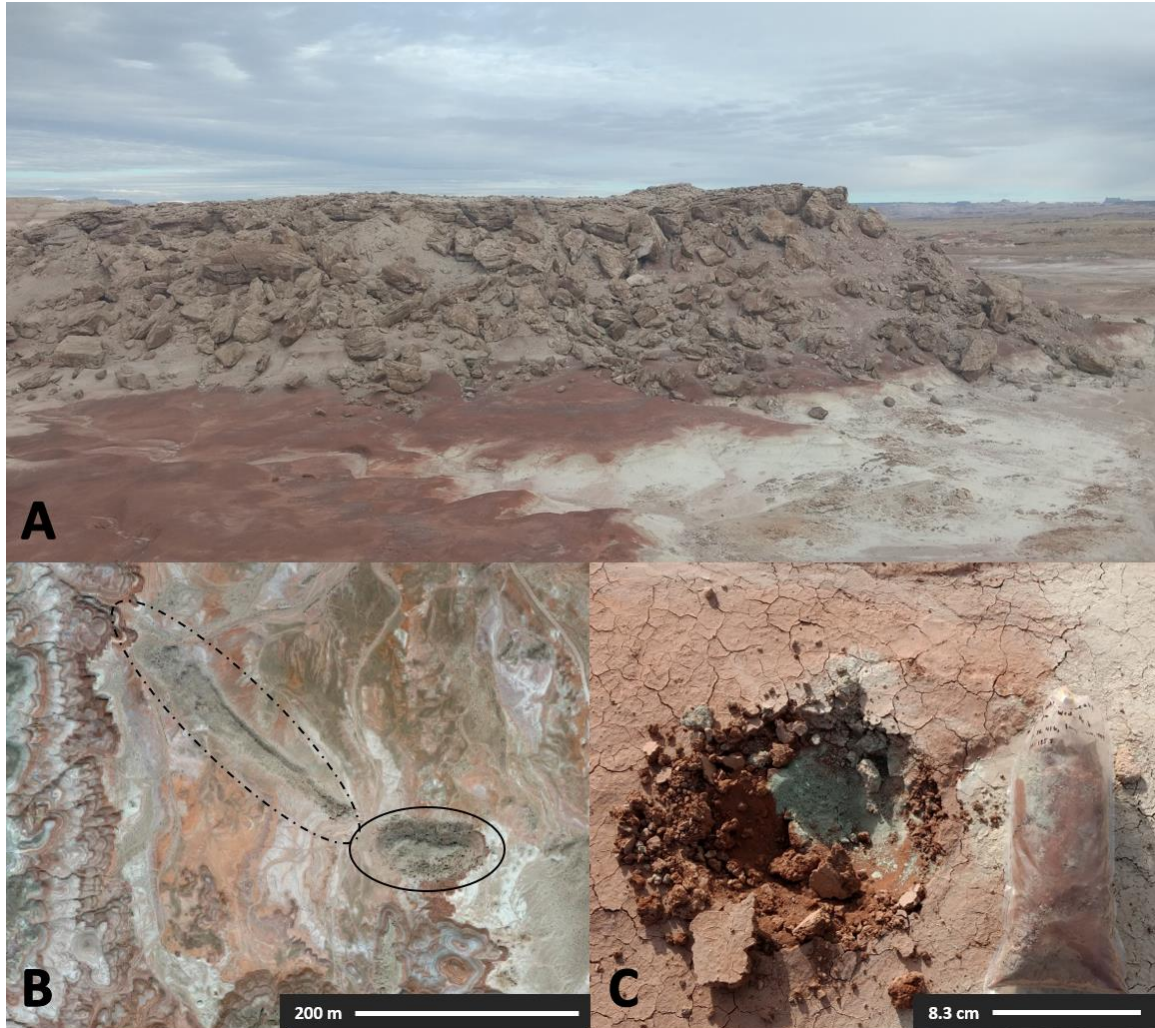


Figure 2.1. Hanksville paleochannel site and samples. **(A)** Side view of Jotunheim (38.41709915, -110.78539335), an inverted river channel. **(B)** Aerial view of the study site. Two main inverted channels are circled; Jotunheim is circled in the black, solid line. **(C)** Regolith sample S2 *in situ* during collection. Surface regolith is dark red and visibly desiccated, and covers a layer of light green sand.

endoliths). Regolith was aseptically collected with a hand shovel and harder rocks were broken off of larger concretions with a rock hammer. All collection tools were sterilized with 70 % ethanol and a lighter. Latex gloves were worn during collection and samples were loaded into sterile Whirl Pak plastic bags. Samples were transported from the Utah site to Montreal, Quebec, Canada at ~ 5 °C and subsequently stored at -30 °C while waiting for analysis at McGill University (MinION

sequencing), the University of Winnipeg (X-ray diffraction, reflectance spectroscopy, Raman spectroscopy), and the Centro de Astrobiología (INTA-CSIC) (LDChip immunoassays).

2.3.2 DNA extraction and MinION sequencing

DNA was extracted from all samples with the PowerLyzer PowerSoil DNA Isolation Kit (Mo Bio Laboratories, Inc., Carlsbad, CA) according to the manufacturer's protocol and eluted in 50 µl of nuclease-free water. Extractions were stored at -20 °C until sequencing. Extractions were prepared for 1D single strand sequencing using the Rapid Low Input by PCR Barcoding kit (SQK-RLB001) and all samples were sequenced on 1 R9.5 FLO-MIN107 flow cell during 1 run (Table 2.1).

DNA detection limits were established using endolith sample E4, since it had the highest percent of sequences classified in the Joint Genome Institute's Integrated Microbial Genomes and Microbiomes Expert Review (JGI IMG/M ER) system (Markowitz *et al.* 2011) and the second highest number of sequences produced (Table 2.2). In order to determine if the MinION could distinguish false positives from true positives, a run containing no DNA (3 µl of sterile nuclease-free water) was also sequenced using the same method (SQK-RLB001 preparation) on an R9.5 flow cell. The detection limit trial samples were prepared for sequencing using the Rapid PCR Barcoding kit (SQK-RPB004), since the Rapid Low Input by PCR Barcoding kit (SQK-RLB001) was discontinued soon after our metagenome analyses. Each trial was sequenced on a separate R9.4 FLO-MIN106 flow cell; R9.5 chemistry was no longer recommended for 1D single strand sequencing when we conducted our detection limit trials.

All sequences were basecalled with MinKNOW v1.7.7 and underwent the following downstream processing: basecalled sequences were demultiplexed and trimmed using Porechop version 0.2.3 (<https://github.com/rrwick/Porechop>) with parameters “--barcode_threshold 60” and “--barcode_diff 1.” Demultiplexed sequences were corrected and assembled with Canu version 1.7 +75 (Koren *et al.* 2017) with parameters “corOutCoverage=10000,” “corMhapSensitivity=high,” “correctedErrorRate=0.16,” and an assumed genome size of 4.7 Mbp (Raes *et al.* 2007). These sequences were then uploaded to JGI IMG/M ER (Markowitz *et al.* 2011) for annotation. All datasets are public, and the JGI IMG/M ER submission IDs are included in Table 2.1 for the shotgun metagenome and in Table 2.2 for the detection limit sequences. A bubble plot of the whole shotgun metagenome was constructed using the following script: <https://github.com/alex-bagnoud/OTU-table-to-bubble-plot.git>.

We also performed 16S rRNA gene sequencing with an Illumina MiSeq according to the protocol described in Kozich *et al.* (2013). All sequences were classified using the mothur software package (http://www.mothur.org/wiki/MiSeq_SOP) and the SILVA v132 reference files. Sequence data is publicly available on NCBI with the following BioProject accession number: PRJNA544288. OTU tables and taxonomy classification were used to construct bubble plots with the following script: <https://github.com/alex-bagnoud/OTU-table-to-bubble-plot.git>. Principal coordinates analysis (PCoA), PERMANOVA values, and PHRED quality score plots were constructed in CLC Genomics Workbench v12.0 (<https://www.qiagenbioinformatics.com/>).

2.3.3 Powder X-ray diffraction (XRD)

X-ray diffraction (XRD) data was acquired in continuous scans from 5 to 80° 2 θ on a Bruker D8 Advance with a DAVINCI automated powder diffractometer from crushed aliquots of sample. It uses a Bragg-Brentano goniometer with a theta-theta system. The setup was equipped with a 2.5° incident Soller slit, 1.0 mm divergence slit, a 2.0 mm scatter slit, a 0.6 mm receiving slit, and a curved secondary graphite monochromator. Diffracted X-rays were collected by a scintillation counter at increments of 0.02° and an integration time of 1 second per step. The line focus Co X-ray tube was operated at 40 kV and 40 mA, using a take-off angle of 6°. Diffraction patterns were interpreted using Bruker Diffracsuite EVA software and the International Center for Diffraction Data Powder Diffraction File (ICDD-PDF-2) database.

2.3.4 Reflectance Spectroscopy (UV-VIS-NIR, 350-2500 nm)

Spectra of regolith samples were collected in a powdered and whole rock aliquot, and multiple spots were analyzed on the endolith-bearing samples (both fresh and weathered rock, and endolith surfaces). Long wave ultraviolet, visible and near-infrared (350-2500 nm) reflectance spectra were measured with an Analytical Spectral Devices FieldSpec Pro HR spectrometer (ASD). This instrument has a spectral resolution between 2 and 7 nm (internally resampled by the instrument to 1 nm). Spectra were collected at a viewing geometry of $i = 30^\circ$ and $e = 0^\circ$ with incident light being provided by an in-house 150 W quartz-tungsten-halogen collimated light source. Samples were measured relative to a Spectralon® 100 % diffuse reflectance standard and corrected for minor (< 2 %) irregularities in its absolute reflectance. We acquired and averaged

200 spectra of the dark current, standard, and sample to provide sufficient signal-to-noise for subsequent interpretation.

2.3.5 Raman Spectroscopy (532 nm)

Raman spectra were collected from multiple spots on both whole rock and powdered (< 45 μ m) samples (same as the reflectance spectra) using a B&W Tek i-Raman-532-S instrument in the Raman shift range of 175-4000 cm^{-1} . This was done with a spectral resolution of $\sim 4 \text{ cm}^{-1}$ at 614 nm with a 532 nm excitation energy provided by a $\sim 50 \text{ mW}$ solid state diode laser. Raman-scattered light was detected by a GlacierTM T, a high spectral resolution (0.08 nm) thermoelectrically cooled (14 $^{\circ}\text{C}$) CCD detector. The automatic integration time function (which increases integration time incrementally, until the response is close to saturation) was used, yielding an optimal signal-to-noise ratio (SNR). Measurements for each sample were made by first acquiring a dark current spectrum, followed by measurement of the sample. Both measurements were made using an identical viewing geometry, integration time, and number of averaged spectra. Raman-shift calibration was monitored through regular measurements of a polystyrene standard. The RUFF database (<http://rruff.info/>) was used for peak identification (Downs 2006).

2.3.6 LDChip (Life Detector Chip) Biomolecule Detection

The LDChip (Life Detector Chip) is the core of the SOLID (Signs of Life Detector) instrument (Parro *et al.* 2011) and consists of an antibody microarray composed of about 200 polyclonal antibodies (purified IgG fraction) designed to search for microbial molecular

biomarkers for environmental and space applications (Rivas *et al.* 2008). The LDChip contains antibodies to: i) prokaryotic strains to cover the most abundant phylogenetic phyla and groups; ii) proteins and peptides from key metabolic processes operating in extreme and “normal” environments (e.g. nitrogen fixation, sulfate reduction/oxidation, iron reduction/oxidation, methanogenesis); iii) universal microbial markers like peptidoglycan; and iv) crude extracts from extreme environments (Parro *et al.* 2011; Rivas *et al.* 2008). The targets for the antibodies of this study are described in (Sánchez-García *et al.* 2018b) (personal communication). For this work, LDChip microarrays were constructed, processed, and analyzed as detailed described in Blanco *et al.* (2015, 2017). Briefly, samples (IgG fraction of each antibody) were printed in a triplicate spot-pattern on the surface of epoxy-activated glass slides, fluorescently labeled, titrated, and used in a mixture that consisted of 181 antibodies to reveal immunoreactions. 0.5 g of each sample were resuspended into 2 mL of TBSTRR buffer (0.4 M Tris-HCl pH 8, 0.3 M NaCl, 0.1 % Tween 20) and used as a multianalyte-containing sample for fluorescent sandwich microarray immunoassays (FSMI). LDChip images were analyzed and quantified by GenePix Pro Software (Molecular Devices, CA, USA). The final fluorescence intensity (F) was quantified as described previously (Blanco *et al.* 2012; Rivas *et al.* 2011). An additional cut-off threshold, which was the interval of F with an accumulated frequency higher than 80 %, was applied to minimize the probability of false positives. Results were finally represented as a color-patterned heatmap for a better visualization, normalizing output F attending to number of antibodies per taxonomic/metabolic group and to total microarray fluorescence values (He *et al.* 2007).

2.4 Results

2.4.1 MinION sequencing produced diverse metagenomes from the Hanksville paleochannels

DNA was extracted from all samples and sequenced with the MinION (Table 2.1). The highest input was 19.5 ng from sample R2 and the lowest was 0.667 ng from sample S2. With the exceptions of samples E1, S3, and R2, total reads produced generally increased with input DNA, while average sequence length was between 2598 bp and 3571 bp for all samples. After adaptor trimming and correction with Porechop and Canu, the total number of reads decreased sharply as a result of Canu's error correction, removal of noisy sequences, and replacement with consensus sequences. The number of hits classified by JGI IMG/M ER was very low (0.72 % – 9.15 %) (Table 2.1). This is not uncommon for nanopore sequencing, which can have classification rates ranging from 15 % (Edwards *et al.* 2017) single strand 1D sequencing and up to 98 % (Brown *et al.* 2017) for double strand for 1D² sequencing. This may be partially due to high error rates in MinION basecalling (Jain *et al.* 2017) and is likely exacerbated in natural microbial consortia. Additionally, metagenomic datasets tend to have low taxon classification in general due to incomplete databases and higher numbers of unclassifiable sequences, as opposed to amplicon sequencing datasets (Tessler *et al.* 2017).

The Hanksville paleochannel metagenomes contain rich microbial communities, with members from all three domains of life (Bacteria, Archaea, and Eukarya), as well as viruses (Figure 2.2). The samples contain a wide variety of Bacteria, with samples E1 and R1 each containing

Table 2.1. Input DNA and MinION sequence details from the Hanksville paleochannel samples. Also included are the number of correct reads by Canu, the percent of reads classified by JGI IMG/M ER, and the JGI IMG/M ER submission ID.

Sample type	Sample name	Input DNA (ng)	Total reads	Avg. sequence length (bp)	Corrected reads	% of hits classified	JGI Submission ID
Endolith	E1	5.07	1971	2939	589	2.54	184799
Endolith	E2	4.5	4026	3056	1683	2.61	184800
Endolith	E3	4.71	11 943	3372	8261	7.96	185540
Endolith	E4	4.04	9885	3571	6643	9.15	185543
Endolith	E5	4.475	9189	3513	6317	8.43	185546
Regolith	S1	0.756	2446	2598	868	2.64	185544
Regolith	S2	0.667	3580	3293	1519	0.96	185545
Regolith	S3	9	3352	3021	1434	1.22	185548
Rock	R1	3.03	4702	2884	2654	6.77	185547
Rock	R2	19.5	1594	2920	369	0.72	185559
Rock	R3	3.975	8461	3310	4560	4.46	185550

genes from 21 distinct bacterial phyla. Proteobacteria, Actinobacteria, Cyanobacteria, and Bacteroidetes were most prominent phyla encountered. Proteobacteria and Actinobacteria were detected in all 11 samples, and in large proportions ($\geq 10\%$) in 7 and 3 samples, respectively. Three endolith samples (E3, E4, and E5) were strongly dominated by Cyanobacteria ($\geq 76\%$), followed by Bacteroidetes and Proteobacteria. Nostocales was the most prominent cyanobacterial order present. Among the sediment and rock samples, Actinobacteria, Bacteroidetes, and Proteobacteria were the dominant taxa, save sample R3, which had Cyanobacteria as a chief phylum (38%). This sample had also had Nostocales as its most abundant cyanobacterial order. R3 had no visible endoliths and instead was covered by a dark oxidized coating (likely desert varnish). Desert varnish has been observed at the Viking and Pathfinder landing sites on Mars (Guinness *et al.* 1997; McCauley *et al.* 1979), and while the method of desert varnish formation remains unclear, it is postulated to involve microbial mediation and deposition of manganese-rich

films (Dorn and Oberlander 1981). Archaea were present in small proportions (~ 1 %) in 7 out of 11 samples as Euryarchaeota and Thaumarchaeota. Among the bacterial and archaeal genes detected are several extremophiles capable of surviving Mars-like conditions, further enforcing the analogue potential of this site beyond geomorphology. These extremophiles include UV-resistant and halophilic Halobacteria, methanogens Methanobacteria and Methanomicrobia, desiccation-tolerant *Chroococidiopsis*, and 25 distinct genomes of the polyextremophilic phylum Deinococcus-Thermus (Direito *et al.* 2011). Also present in the paleochannel metagenomes is a diverse range of eukaryotes, including fungi as Ascomycota, algae as Streptophyta and Chlorophyta, and unclassified Eukarya (mainly algal protists and choanoflagellates).

2.4.2 Illumina 16S rRNA gene sequencing revealed a rich bacterial community in the Hanksville paleochannels

Given the large proportion of bacteria detected in the MinION sequencing data, we performed 16S rRNA gene sequencing to better illuminate the bacterial diversity present and provide a comparison to the MinION results. This comparison can be seen in Figure 2.3. Sequencing the 16S rRNA gene content of the 11 samples yielded 2 478 778 reads of mean length 253 bp. 1435 OTUs were generated after clustering at 97 % similarity. The most abundant phyla detected among these OTUs were Actinobacteria, Cyanobacteria, Proteobacteria, Deinococcus-Thermus, and Chloroflexi (Figure 2.3A). and these were detected in all samples. In particular, Actinobacteria comprised ≥ 5 % of OTUs in all samples. Like the MinION results, three of the endolith samples were strongly dominated by Cyanobacteria (particularly Nostocales) (≥ 44 %) but were samples E1, E2, and E4 (rather than E3, E4, and E5). Unlike the MinION data, E3 and

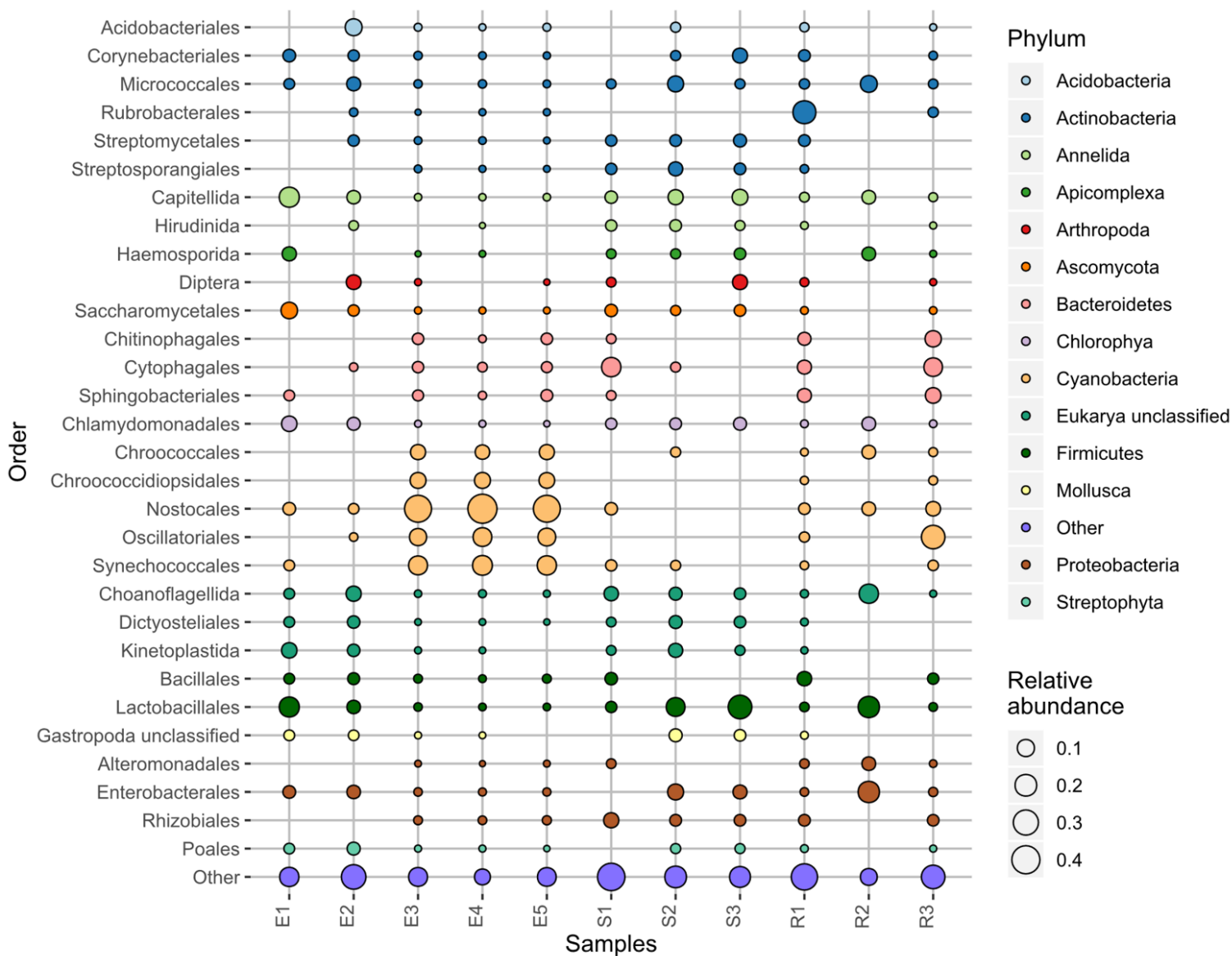


Figure 2.2. Metagenomes of the Hanksville paleochannel samples generated by MinION sequencing. All three domains of life are detected, as well as viruses. Samples E1, E2, E3, E4, and E5 are endoliths. Samples S1, S2, and S3 are regolith. Samples R1, R2, and R3 are non-endolith rocks.

E5 contained higher proportions of Actinobacteria and Deinococcus-Thermus (mostly Deinococcales) ($\geq 13\%$) instead of Cyanobacteria. Sediment and rock samples were dominated by Actinobacteria, Proteobacteria, and Chloroflexi. The endolith, sediment, and rock samples showed some differences in taxonomy, which was visualized with a weighted UniFrac principal

coordinates analysis (PCoA) of the 16S data (PERMANOVA: pseudo-f statistic = 2.89990; p-value = 0.01905) (Anderson and Walsh 2013) (Figure 2.4). The endoliths appear to cluster solely with other endolith samples (E1, E2, and E4 vs. E3 and E5), demonstrating the closer phylogenetic relationship within the endolith samples.

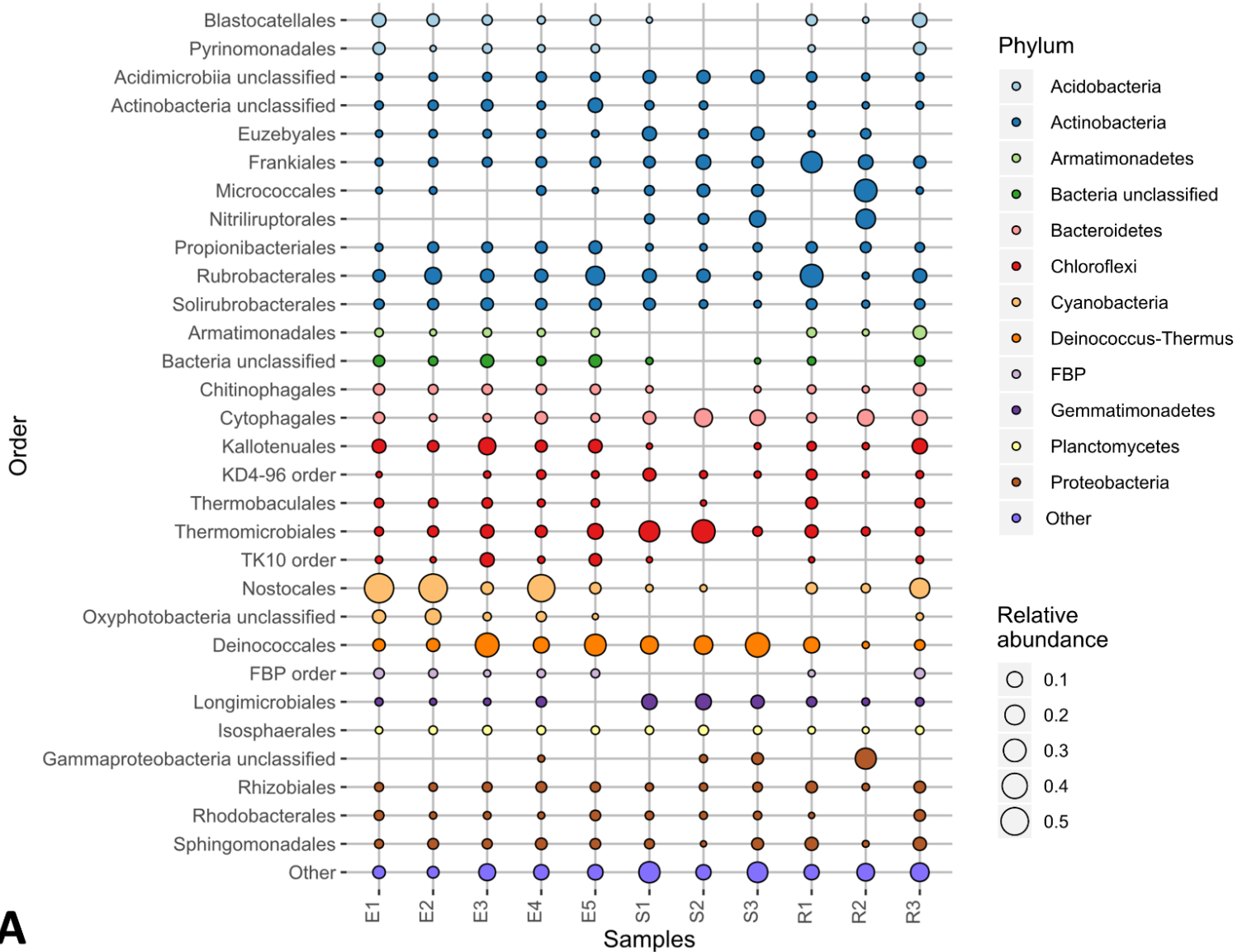


Figure 2.3. (A) Bacterial 16S rRNA community profile of the Hanksville paleochannels generated by Illumina MiSeq sequencing.

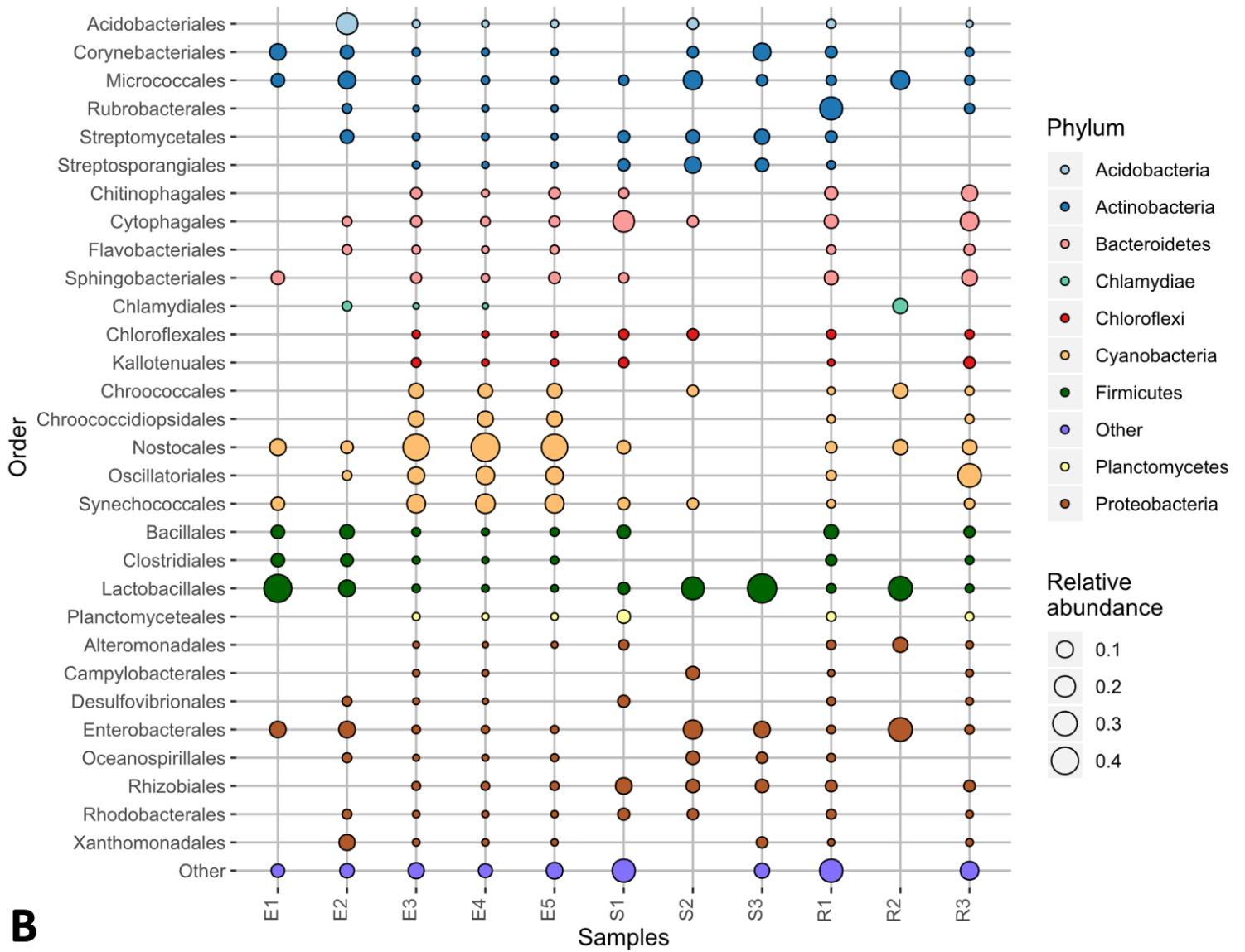


Figure 2.3. (B) Bacterial content of the whole shotgun metagenome from MinION sequencing of the Hanksville paleochannels.

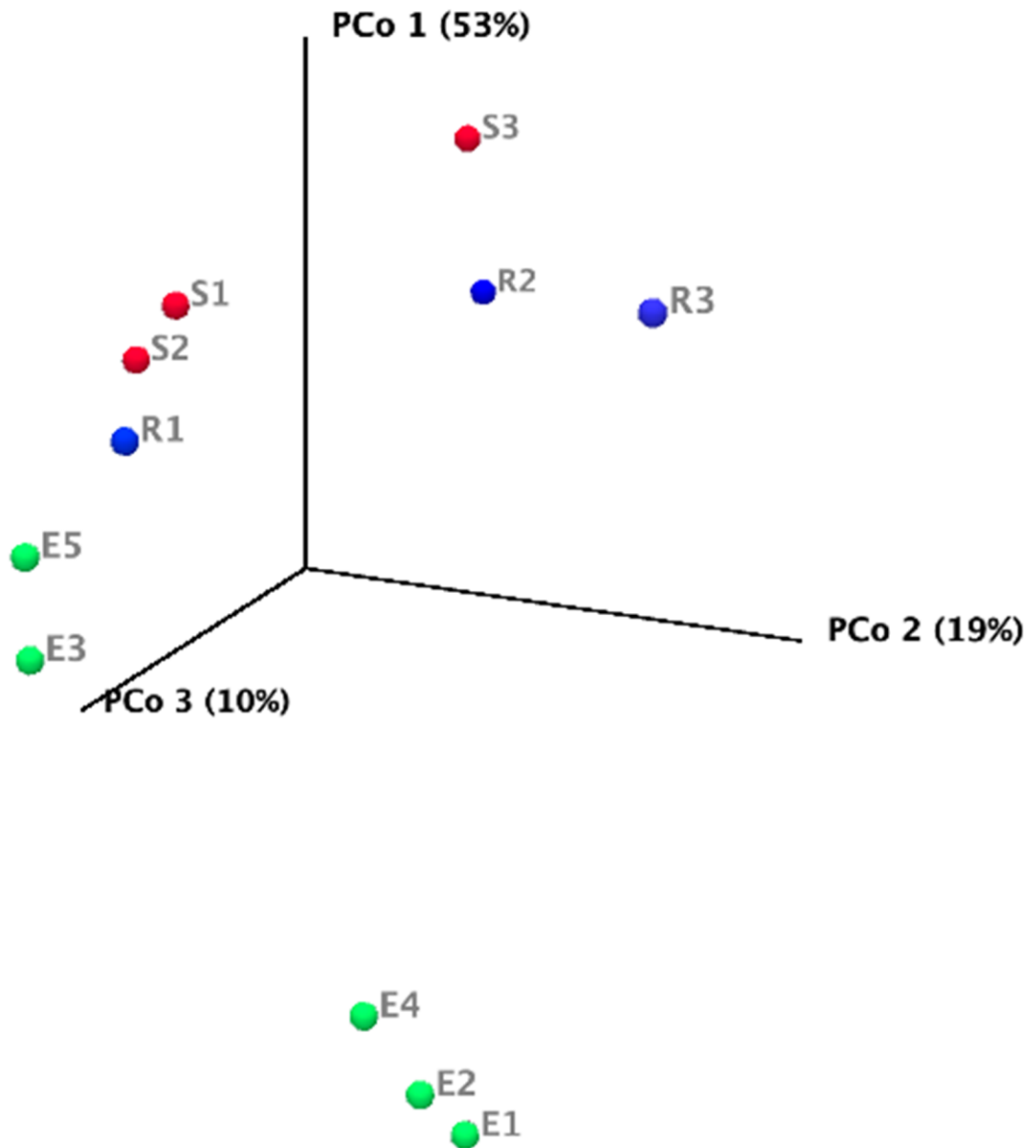


Figure 2.4. Weighted UniFrac principal coordinates analysis (PCoA) of the 16S rRNA sequencing data of the Hanksville paleochannels. Samples are coloured by type: endoliths in green (E1, E2, E3, E4, and E5), sediment in red (S1, S2, and S3), and non-endolith rocks in blue (R1, R2, and R3). The variation between samples is expressed as percentages along each axis.

2.4.3 Determination of putative DNA detection limits for MinION sequencing

We used high quality DNA from endolith sample E4 to determine prospective DNA detection limits of MinION sequencing (Table 2.2; Figure 2.5). We began our detection limit trials at 0.110 ng of DNA, a tenth of the minimum recommended input from ONT. Sequencing 0.110 ng of DNA from E4 yielded 253 188 total reads, nearly 26 times more than when 4.04 ng of DNA from this sample was sequenced. This is likely due to the use of R9.4 FLO-MIN106 flow cells rather than R9.5 FLO-MIN107 flow cells. R9.5 chemistry was initially recommended during our metagenome sequencing but has since been advised for only 1D² double strand sequencing by ONT (1D single strand sequencing was employed in this study). We subsequently tested 0.0408 ng, 0.0106 ng, and 0.00106 ng of DNA. Total read number dropped with input concentration, as expected, and the metagenomes produced during these trials are relatively similar (Figure 2.5). Cyanobacteria are the dominant phylum, followed by Proteobacteria and Bacteroidetes. Other phyla become more prominent as input DNA decreases and Cyanobacteria are completely undetected in the final 0.00106 ng trial. We also determined if the MinION would produce a false

Table 2.2. DNA detection limit trial details with endolith sample E4. Also included are the number of correct reads by Canu, the percent of reads classified by JGI IMG/M ER, and the JGI IMG/M ER submission ID.

Sample	Input DNA (ng)	Total reads	Corrected reads	% of hits classified	JGI Submission ID
Endolith E4	0.110	253 188	109 064	31.24	190088
	0.0408	192 959	65 445	5.89	195531
	0.0106	64 300	21 582	1.56	195532
	0.00106	1448	513	2.14	195533
No DNA (3 µl nuclease-free water)	0	121	55	0	190089

positive with no DNA present. Sequencing nuclease-free water containing no DNA produced 121 reads, likely as a result of barcode adapter dimers and PCR amplification of these dimers. None of these reads were classified by JGI IMG/M ER. We also examined the quality score distribution of this run, as compared to the other DNA inputs in the detection limit trials (Supplementary Figure 2.1). PHRED score is a common metric of sequence quality (Manley *et al.* 2016) and decreases strongly with DNA input in our study, with a seemingly random distribution in our run containing

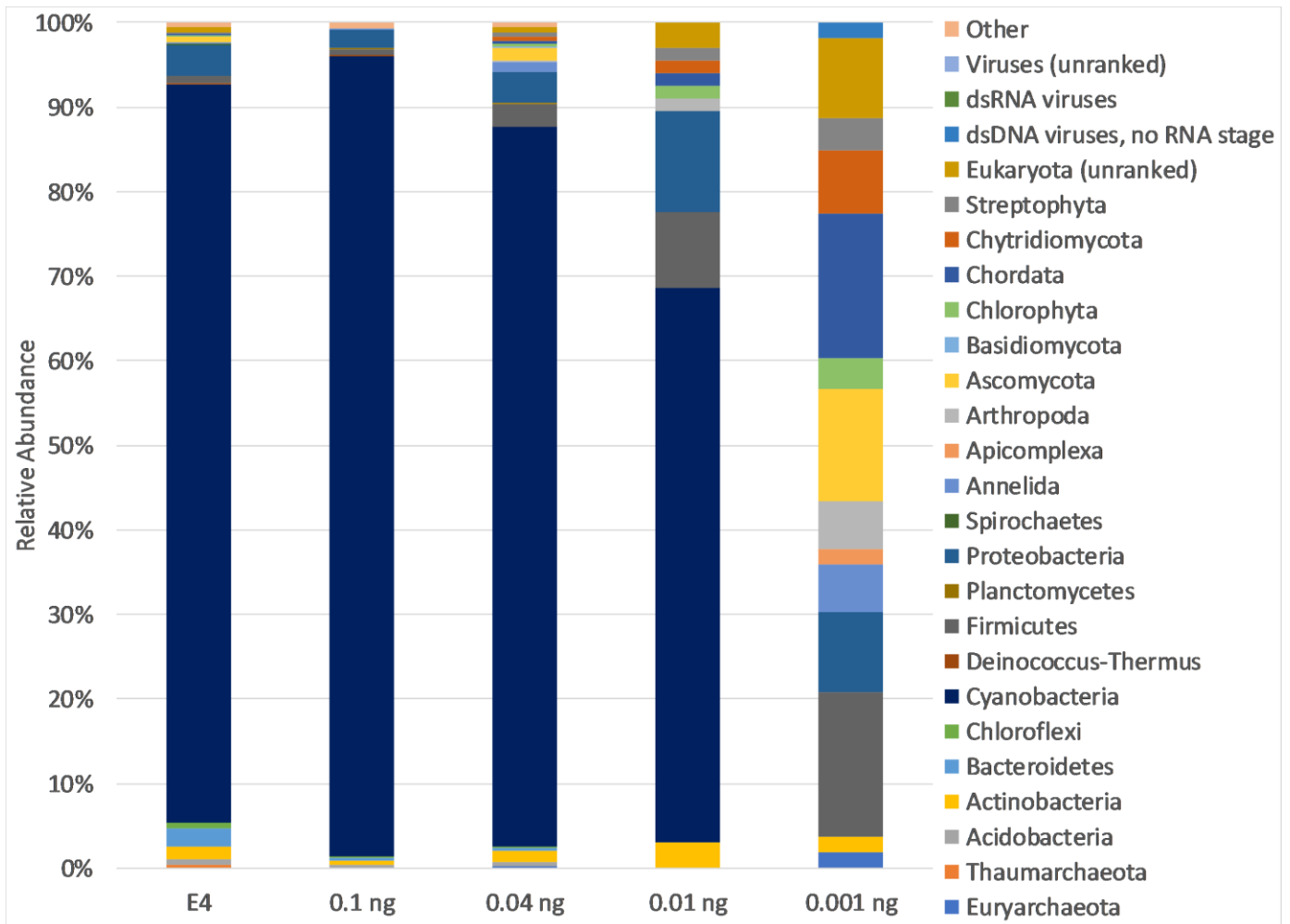


Figure 2.5. Detection limit trials with endolith sample E4 at the phyla level. The first column “E4” is the same data as presented in Figure 2. Taxonomy and abundance change with input DNA, and the final 0.001 ng trial bears little resemblance to E4’s original community composition.

no DNA. Low sequence number, lack of classification, and random quality score distributions are therefore strongly indicative of a run in which no environmental DNA is present.

2.4.4 Powder X-ray Diffraction (XRD) revealed a quartz-rich environment

The X-ray diffraction patterns of the Hanksville paleochannel samples are dominated by quartz (Supplementary Table 2.1). Many samples also contain minor chemical sedimentary minerals (gypsum and calcite) and a phyllosilicate component identified in most cases as montmorillonite. The diffraction patterns for endolith samples E2, E3, and E4 contain only quartz, while endoliths E1 and E5 also exhibit traces of calcite and albite (possible Ca-rich), respectively. Regolith samples S1 and S2 display similar mineralogy, with minor of albite (Ca-rich) and montmorillonite. Regolith S3 is more heterogenous and contains calcite, gypsum, albite (Ca-rich), and montmorillonite. The non-endolithic rock samples R1, R2, and R3 are diverse; R2 is composed of minor of magnesian calcite, carbonate-fluorapatite, and nontronite. R1 contains montmorillonite, gypsum, and apatite-(CaCl), while R3 has a minor calcite component.

2.4.5 Reflectance spectra show hydrated minerals and some organic features

The reflectance spectra of all samples are dominated by absorption features characteristic of hydrated mineral phases (Figure 2.6). Prominent absorption features include overtones and combinations of H₂O and OH⁻ stretches and bends occurring at ~ 1400 nm (OH⁻), ~ 1900 nm (H₂O and OH⁻), and a combination of vibrational stretching and bending of Al₂OH at ~ 2220 nm. The shape and position of the main ~ 1400, ~ 1900, ~ 2200 nm (Al-OH), and 2350 nm (Mg-OH)

features in the samples provide insights into the hydrated and sheet silicate phases present. The presence of a ~ 1400 nm and ~ 1900 nm band indicates that both OH⁻ and molecular water are

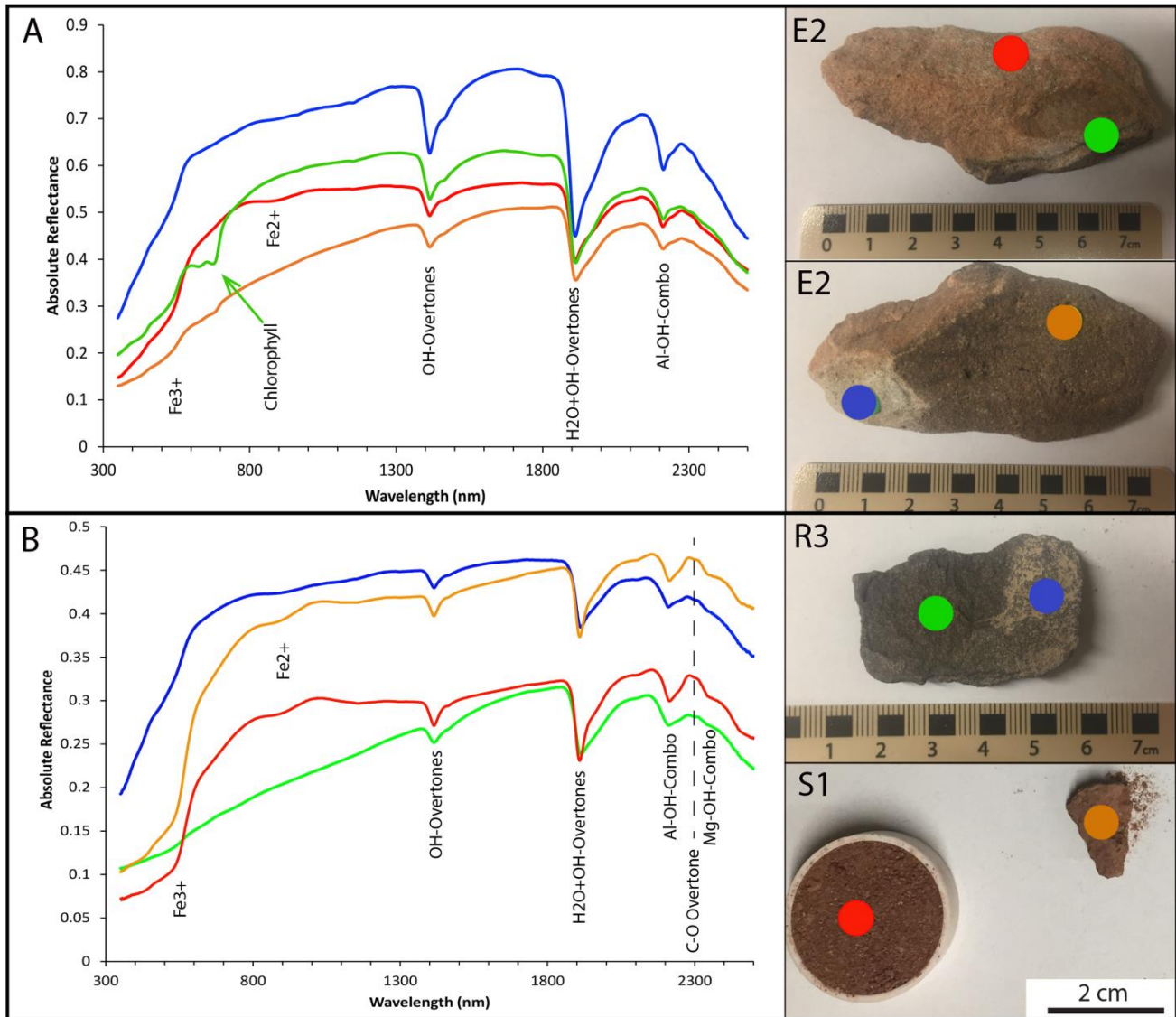


Figure 2.6. Reflectance spectra of representative samples from the Hanksville paleochannels with major absorption features labelled. **(A)** Endolith-bearing samples have a prominent feature at 670 nm indicative of chlorophyll. The dark surface of the sample also shows a minor feature at 670 nm which may indicate desiccated endolithic communities. **(B)** Spectra of non-endolith bearing samples varies as a reflection of mineralogy. The red color of regolith sample S1 is reflected in the strong Fe absorptions in the VNIR region of the spectrum, and also shows evidence for carbonate bearing phases.

present in the samples (Cloutis *et al.* 2006). The position, shape and depth of these water features and the ~ 2200 nm (band center at ~ 2212 nm) feature indicates that the bulk of the samples have spectra characteristic of montmorillonite (Bishop *et al.* 2008; Clark *et al.* 1990). The weak feature observed in multiple samples at ~ 2300 nm is a C-O feature due to the second overtone of a CO₂ asymmetrical stretch and is indicative of carbonate minerals (Figure 2.6B) (Clark *et al.* 1990). This position is indicative of carbonate chemistry and in these samples supports the presence of calcite. Absorption features of Fe-bearing oxyhydroxyides such as goethite at ~ 500 nm, ~ 900 nm, and ~ 1150 nm are also evident, as is the characteristic drop in reflectance below ~ 1000 nm due to charge transfers in Fe-bearing minerals (Crowley *et al.* 2003).

Organic features are also present, primarily in samples containing visible endoliths (E1, E2, E3, E4, and E5). These samples exhibit a characteristic absorption band at 670 nm, a sharp increase in reflectance (“chlorophyll bump” or “green peak”) preceding this feature, and an overall drop in reflectance below ~ 800 nm (“red edge”) that are all diagnostic of chlorophyll a (Rhind *et al.* 2014; Stromberg *et al.* 2014). A small peak at ~ 400 nm can be attributed to the presence of porphyrins, resulting either from the degradation of chlorophylls or as a component of various cytochromes (Berg *et al.* 2014). A broad band at ~ 465 nm can be indicative of either carotenoids (Berg *et al.* 2014) or NADPH (Ammor 2007). A generic C-H overtone at ~ 1750 nm is also present, but N-bearing molecules can also affect absorption features in this region (Berg *et al.* 2014).

2.4.6 Prominent bands of chlorophyll and quartz are observed in the Raman spectra

The samples exhibit a large number of distinct Raman peaks at an excitation wavelength of 532 nm (Figure 2.7), which was chosen to optimize biomolecule detection and mimic that of

the Raman Laser Spectrometer (RLS) on ExoMars 2020 (Edwards *et al.* 2012; Rull *et al.* 2017). Prominent peaks associated with the mineralogy of the site are observed at $\sim 470 \text{ cm}^{-1}$ (quartz) and $\sim 1006 \text{ cm}^{-1}$ (gypsum) (Edwards *et al.* 2007). The non-endolith samples are dominated by background iron fluorescence, a common artifact in Fe-containing samples and a 532 nm source.

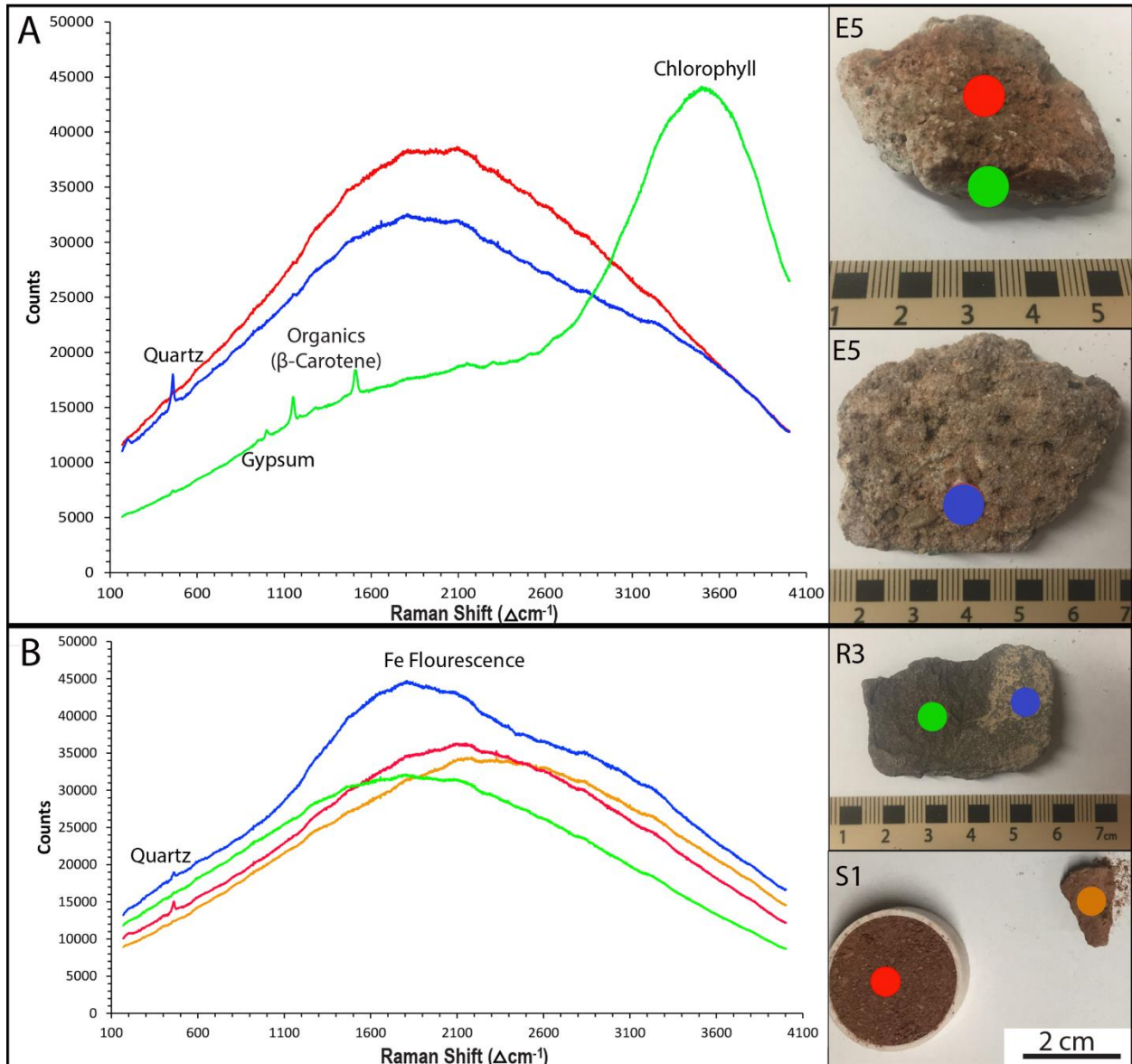


Figure 2.7. Raman spectra of representative samples from the Hanksville paleochannels with major features labelled. **(A)** Endolith-bearing samples have spectral features consistent with the presence of chlorophyll and other organic compounds. **(B)** The Raman spectra of non-endolith bearing samples are dominated by a broad Fe fluorescence feature.

Other noticeable features include a small peak at $\sim 930 \text{ cm}^{-1}$, which is attributable to C-COO^- stretching vibrations (Kim *et al.* 1987) or the presence of perchlorate (Jones *et al.* 1961; Ruan *et al.* 2006). Asymmetric stretching vibrations from CO_2 are presented as a small band at $\sim 2340 \text{ cm}^{-1}$ (Feng *et al.* 2004; Sandford and Allamandola 1990). A peak at $\sim 1655 \text{ cm}^{-1}$ is indicative of the presence of organics and represents the amide I band in classical Raman spectroscopy. This band is the result of asymmetric C=O stretching vibrations and α -helical secondary structure in proteins (Maiti *et al.* 2004; Thomas *et al.* 1987).

The endolith-bearing samples also contain numerous features indicative of the presence of organic matter. A broad spectral feature at $\sim 3530 \text{ cm}^{-1}$ signifies the presence of chlorophyll in these samples (Rhind *et al.* 2014). Peaks at $\sim 1155 \text{ cm}^{-1}$ and $\sim 1520 \text{ cm}^{-1}$ are the result of C-C and C=C stretching vibrations, respectively, in various carotenoids, including β -carotene (Edwards *et al.* 2005; Ellery *et al.* 2002; Rhind *et al.* 2014), bacteriorhodopsin (Jehlička *et al.* 2013), bacterioruberin (Marshall *et al.* 2006), astaxanthin (Kaczor and Baranska 2011), and lutein (Edwards *et al.* 2007). Additionally, while the $\sim 470 \text{ cm}^{-1}$ band is characteristic of quartz, this feature can also indicate the presence of parietin, a secondary UV-protectant pigment. Edwards *et al.* (2005) noted that the $\sim 470 \text{ cm}^{-1}$ feature only appeared in samples from known parietin-containing environments and attributed its cause to parietin rather than quartz.

2.4.7 LDChip immunoassays detected a wide variety of potential metabolisms and taxa

Positive signals corresponding to antibodies against numerous bacterial, archaeal, and viral organisms were detected by the LDChip (Figures 2.8 and 2.9). The strongest immunoassay signals corresponded to biomarkers associated to Actinobacteria (*Streptomyces*), Cyanobacteria

(*Aphanizomenon*, *Chroococidiopsis*), iron-sulfur bacteria from *Acidithiobacillia* (*Acidithiobacillus*), Nitrospirae (*Leptospirillum*), and crude environmental extracts from the Río Tinto that are rich in iron and sulfur. Proteins relating to common microbial functions (e.g. chaperones HscA2 and HtpG) were readily detected, as well as more specialized functions, such as nitrogen metabolism (e.g. NifD and nitrate reductase) and hydric stress (e.g. DhnA). The LDChip also detected proteins related to perchlorate reduction in samples E1, E2, S1, and S3. Archaeal markers associated with halophiles (*Haloferax*) and methanogens (*Methanobacterium*) were detected in samples E3, and E4, S1, S2, S3, and R1, respectively.

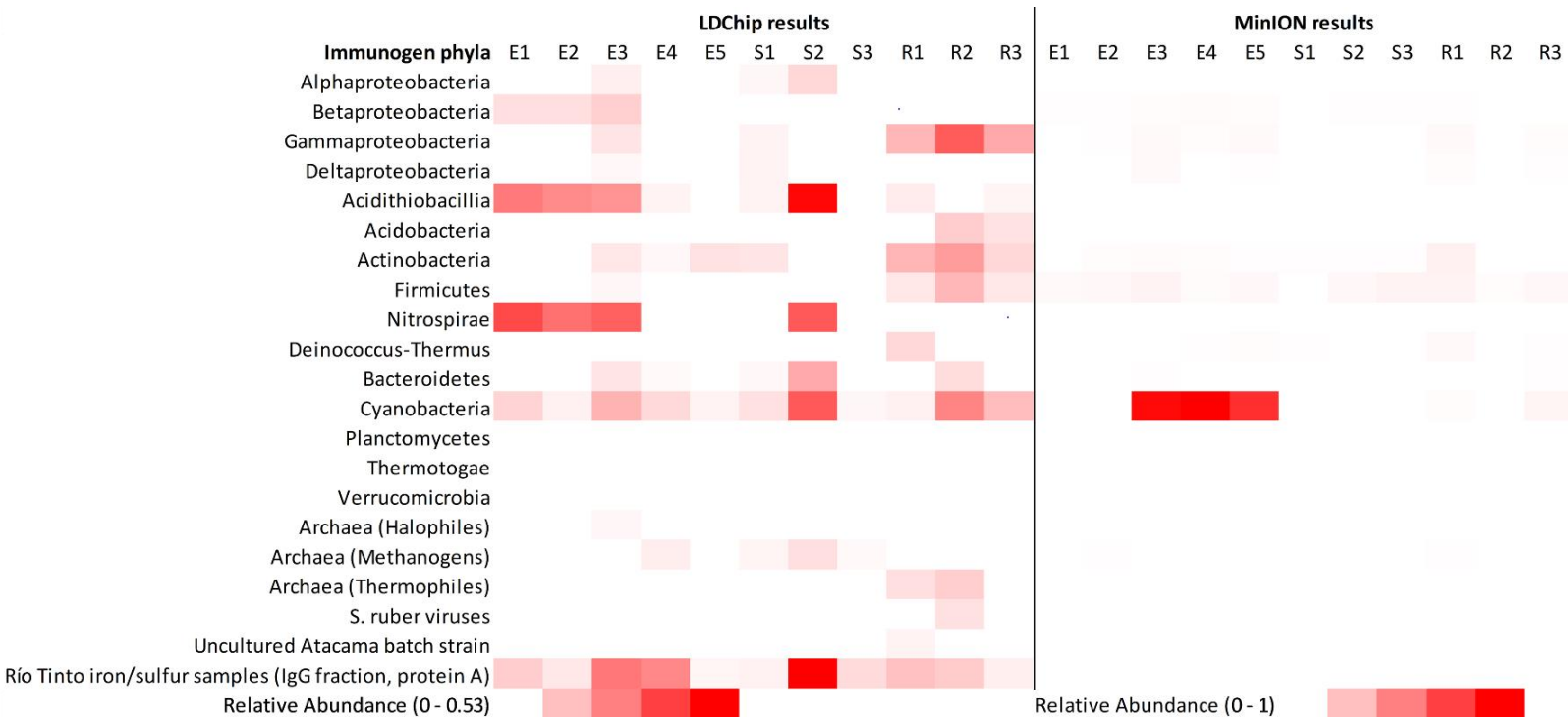


Figure 2.8. Heat map comparing positive LDChip and MinION results at the phylum level. Relative abundance, which represents the value of signal intensity corresponding to each positive antibody within the category with regards to the other categories and to the total signal intensity in the sample, was plotted in a scale from white (negative results) to red (maximum). The maximum value was 0.53 for LDChip results. Total number of MinION sequences corresponding to the listed antibodies were counted and are presented on a scale from 0 – 1.

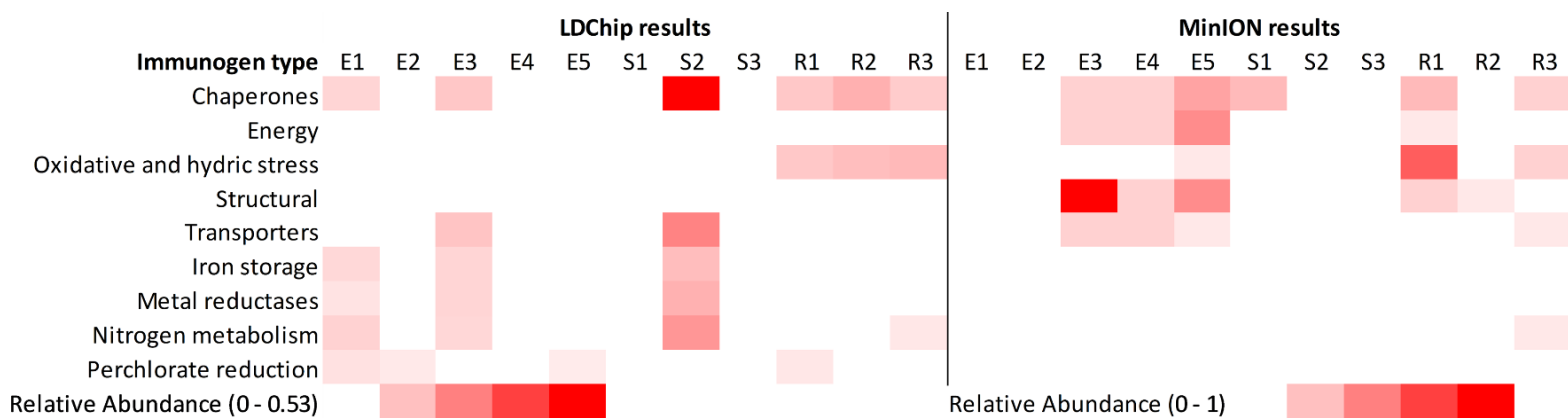


Figure 2.9. Heat map comparing positive LDChip and MinION results for specific protein detection. Relative abundance, which represents the value of signal intensity corresponding to each positive antibody within the category with regards to the other categories and to the total signal intensity in the sample, was plotted in a scale from white (negative results) to red (maximum). The maximum value was 0.53 for LDChip results. Total number of MinION sequences corresponding to the listed antibodies were counted and are presented on a scale from 0 – 1.

2.5 Discussion

2.5.1 MinION metagenomes complement and support XRD data, reflectance spectra, Raman spectra, and LDChip immunoassays

Here we have shown that the MinION is capable of detecting a wide variety of microorganisms from all three domains of life, as well as viruses (Figure 2.2). Our results are consistent with a previous study by Direito *et al.* (2011), who conducted a 16S rRNA survey of the Mars Desert Research Station (MDRS) soil, an area adjacent to the Hanksville paleochannels. Direito *et al.* (2011) found overall high diversity in the bacterial and eukaryal populations of this area, and low archaeal diversity. Bacteria dominated the total microbial content in our study, as well as in a PCR-based detection survey of the MDRS (Thiel *et al.* 2011). Strangely, we also detected *Mollusca*, *Cnidaria*, and *Porifera*. These organisms are not common laboratory

contaminants, but *Mollusca* were present in the Direito *et al.* (2011) study where MinION sequencing was not used. Direito *et al.* (2011) noted the presence of a hill consisting of fossil oyster shells in this area, signifying the marine history of this environment and indicating that these sequences are potentially naturally occurring.

Direct comparison of the bacterial taxa detected in both Illumina and MinION sequencing shows some overlap (Figure 2.3). In particular, Acidobacteria, Actinobacteria, Bacteroidetes, Chloroflexi, Cyanobacteria, Planctomycetes, and Proteobacteria were detected in proportions > 15 % for all reads in both runs. While shotgun metagenome datasets often reveal more diversity and more rare taxa in an environment (Poretsky *et al.* 2014; Ranjan *et al.* 2016), our 16S amplicons revealed more diversity in the Hanksville paleochannels than our shotgun MinION data. Specifically, the candidate phylum FBP was detected in 7 of our 11 samples in the amplicon dataset but was completely absent in our MinION data. FBP is closely related to Armatimonadetes (Lee *et al.* 2013) and is a common member of extreme environmental consortia (Tahon *et al.* 2018). Gemmatimonadetes was also a significant component of our 16S dataset (mainly Longimicrobiales) but was detected only as small amounts of Gemmatimonadales in E3 and E5 in our shotgun dataset. This discrepancy was also observed by Tessler *et al.* (2017), who found that < 50 % of phyla detected in 16S amplicon datasets were also found in shotgun datasets. Conversely, nearly all phyla detected in their shotgun metagenomes were also picked up in their amplicon data. Inherent differences between these techniques can account for these differences, namely reduced database size for shotgun metagenomes and a higher proportion of reads mapped to unknown taxa in shotgun datasets (Tessler *et al.* 2017). Our study introduces additional challenges that can contribute to the lower diversity observed in our shotgun data: low read output

and the MinION's inherently high error rate of $\sim 7.5\% - 14.5\%$ (Jain *et al.* 2017). As a comparison, Illumina sequencing has an error rate of $< 0.1\%$ (Manley *et al.* 2016).

The LDChip and MinION revealed somewhat different microbial profiles, both phylogenetically and metabolically (Figures 2.8 and 2.9). While both sets of data detected Cyanobacteria, Proteobacteria, Bacteroidetes, and Firmicutes, differences arose at subphyla levels. The intrinsic differences in each technique can account for these variations. The groups detected by the LDChip can be very broad, while MinION sequencing is inherently specific to a certain gene or taxa. While the LDChip's polyclonal antibodies are raised to detect certain proteins and peptides, they might be also recognizing similar epitopes in other proteins or closely related taxa (Parro *et al.* 2011). Additionally, the specific microorganism may have been present but not had the gene in question sequenced by the MinION. The LDChip can also detect dead microbial polymers (e.g. proteins and EPS) even when neither cells nor DNA are present. This indicates the powerful complementarity of both techniques to detect a wide variety of microorganisms and different types of definitive biosignatures in an environment (proteins and nucleic acids).

XRD results (Supplementary Table 2.1), reflectance spectra (Figure 2.6), and Raman spectra (Figure 2.7) provide geological context for our MinION data and characterize the surrounding environment. LDChip results (Figures 2.8 and 2.9) also supplement the MinION sequences through more targeted detection of specific molecular markers. Table 2.3 shows the complementary relationship between these methods. The Hanksville paleochannel environment is quartz-rich, as all samples presented quartz as their major mineral detected by XRD. Quartz has been shown to support cyanobacterial desert communities in previous studies (Lacap *et al.* 2011; Schlesinger *et al.* 2003; Warren-Rhodes *et al.* 2006). This corroborates the dominance of Cyanobacteria in samples E3, E4, E5, and R3 in the MinION metagenomes, as well as the presence

Table 2.3. Relationship between MinION sequences, XRD data, reflectance spectra, Raman spectra, and LDChip immunoassays. A feature is presented in the left column, and its presence, potential presence as microbial taxa, or resulting trait in the corresponding techniques is noted. ND = not detected.

Feature	Technique				
	XRD	Reflectance	Raman	MinION	LDChip
Quartz	Major	ND	470 cm ⁻¹ peak	Cyanobacteria	Cyanobacteria
Calcite	Minor	ND	ND	Cyanobacteria, SRBs, <i>Bacillus</i> , sulfate system/sulfate-sulfur system transport genes, sulfur metabolism	Cyanobacteria, <i>Bacillus</i> , SRBs
Gypsum	Minor	ND	1006 cm ⁻¹ peak	Cyanobacteria, Halobacteria, SRBs, sulfate system/sulfate-sulfur system transport genes, sulfur metabolism	Cyanobacteria, <i>Haloferax</i> , SRBs
Iron	ND	Fe-bearing oxyhydroxides (~ 500 nm, ~ 900 nm, ~ 1150 nm), Fe-bearing mineral charge transfers (> ~ 1000 nm)	Background Fe fluorescence	Heme oxygenase	Iron reductase, iron/sulfur environmental samples from Río Tinto
Perchlorate	ND	ND	~ 930 cm ⁻¹	ND	Perchlorate reductase
Chlorophyll	ND	670 nm, chlorophyll bump, red edge, porphyrins at ~ 400 nm	~ 3530 cm ⁻¹	Cyanobacteria, chlorophyll photosystem I and II genes, protochlorophyllide reductase, protoporphyrin IX cyclase	Cyanobacteria
Carotenoids	ND	ND	ND	Cyanobacteria, β-carotene ketolase and hydroxylase	Cyanobacteria
Nitrogen metabolism	ND	ND	ND	NifU, NirS	NifD1, nitrate reductase
Methane metabolism	ND	ND	ND	Methanobacteria, Methanomicrobia	<i>Methanobacterium</i>

of Cyanobacteria in all samples in both the MinION and LDChip data. Raman spectra also revealed quartz as a $\sim 470 \text{ cm}^{-1}$ peak. Calcite was present as a minor mineral in the XRD spectra, and is known to be commonly precipitated by many types of environmental bacteria (Boquet *et al.* 1973; Castanier *et al.* 1999), including sulfate-reducing bacteria (SRBs) (Van Lith *et al.* 2003) and various species of *Bacillus* (Boquet *et al.* 1973). *Bacillus* were detected in our MinION sequences, as were SRBs from Desulfobacterales and Desulfovibrionales. The presence of SRBs was further indicated by genes involved in sulfate transport, sulfate-sulfur assimilation, and sulfur and sulfate metabolism (e.g. sulfate transport system permease and sulfate adenylyltransferase). The LDChip also detected *Bacillus* and SRBs among the Firmicutes, Deltaproteobacteria, and positive results for antibodies raised against crude environmental extracts from the Río Tinto that are rich in iron and sulfur. Gypsum was in the samples, as indicated by XRD spectra and a Raman peak at $\sim 1006 \text{ cm}^{-1}$ and gypsum itself a source of sulfate. It therefore could host the same SRBs and their associated protein groups. Gypsum is also conducive to the presence of archaeal and cyanobacterial halophiles (Jehlicka and Oren 2013; Oren *et al.* 2009; Ziolkowski *et al.* 2013), supporting the detection of various Cyanobacteria and Halobacteria by the MinION and LDChip. Iron was detected as Fe-bearing oxyhydroxides in the reflectance spectra and as background fluorescence in the Raman spectra. Iron is crucial for most bacterial metabolisms (Frawley and Fang 2014), and Fe-oxyhydroxides are associated with both iron-oxidizing bacteria (Emerson *et al.* 1999) and iron-reducing bacteria (Luef *et al.* 2013). The LDChip exhibited positive results for antibodies raised against crude environmental extracts rich in iron and sulfur from the Río Tinto in all samples. Heme oxygenase was detected in our MinION data, as well. Perchlorate may have been responsible for the $\sim 930 \text{ cm}^{-1}$ feature in non-endolith Raman spectra and perchlorate reductase was detected by the LDChip. Perchlorate comprises 0.5 – 1 % of mid-latitude Martian

surface soils (Glavin *et al.* 2013; Hecht *et al.* 2009), and perchlorate reduction genes indicate the presence of microorganisms that can tolerate perchlorate-rich soils and that could serve as models for Martian life. Perchlorate can also be used as a terminal electron acceptor during anaerobic growth for perchlorate-reducing bacteria (Coates *et al.* 1999).

We also detected numerous signatures for biological pigments and other metabolisms. In the reflectance spectra, chlorophyll is presented as a characteristic absorption band at 670 nm, its preceding “chlorophyll bump”, and its trailing “red edge” (Rhind *et al.* 2014; Stromberg *et al.* 2014). Porphyrins are denoted by a small peak at ~ 400 nm (Berg *et al.* 2014; Giovannetti 2012), and a broad band at ~ 465 nm can be indicative of carotenoids (Berg *et al.* 2014). Raman spectra also contain a strong chlorophyll feature at ~ 3530 cm^{-1} , and peaks at ~ 1155 cm^{-1} and ~ 1520 cm^{-1} indicate the presence of various carotenoids, including β -carotene (Edwards *et al.* 2005; Ellery *et al.* 2002; Rhind *et al.* 2014), bacteriorhodopsin (Jehlička *et al.* 2013), bacterioruberin (Marshall *et al.* 2006), astaxanthin (Kaczor and Baranska 2011), and lutein (Edwards *et al.* 2007). Parietin may also be denoted by a band at ~ 470 cm^{-1} (Edwards *et al.* 2005). The presence of microbial pigments is supported by both MinION and LDChip results, which detected Cyanobacteria in all samples. Specifically, genes encoding chlorophyll’s photosystem I and II, protochlorophyllide reductase, β -carotene ketolase and hydroxylase, and protoporphyrin IX cyclase were detected by the MinION. The LDChip indicated the presence of nitrogen metabolizing microorganisms, as did some MinION sequences, but they differed on the specific gene or protein. The LDChip detected NifD1 and nitrate reductase, while the MinION detected NifU and NirS. Together, the LDChip and the MinION were able to detect a wider variety of genes involved in the nitrogen cycle than either alone. The same is true for methanogenic microorganisms. *Methanobacterium* was detected by the LDChip, while *Methanosarcina*, *Methanotherix*, *Methanolacinia*, and *Methanosarcinales*

were detected by the MinION. Through this combination of multiple techniques, we have characterized this paleochannel environment as rich in quartz, calcite, and gypsum and able to host a wide variety of microorganisms, including numerous Cyanobacteria and SRBs. We can also infer these microbes' potential metabolisms, which includes nitrogen cycling, sulfur cycling, methane production, and perchlorate reduction.

2.5.2 Putative MinION DNA detection limits and suitability for life detection

DNA is an ideal target in the search for life since it is unambiguous, non-specific, and readily detectable with nanopore sequencing. Past meteoritic exchange between Earth and Mars (Mileikowsky *et al.* 2000), as well as the abundance of carbon molecules in our Solar System (Pace 2001) indicates a plausibility of organic-based biochemistry for potential Martian life (Mustard *et al.* 2013b). However, an extremely important criterion for life detection in sample return and other space exploration missions is the ability to detect low biomass, such as that present in various Mars analogue environments. We have successfully shown that the MinION can detect DNA as low as ~ 0.001 ng and that it will not produce a false positive when no DNA is present. This is further enforced by Pontefract *et al.* (2018), who showed that the MinION will not produce sequencing artifacts or noise signals that could be mistaken positive results. Producing sequencing data in real-time is also a strong asset. Chiefly, it would enable the best selection of samples to cache for potential future return to Earth (e.g. those containing DNA or other nucleic acids) (Goordial *et al.* 2017). While the MinION's high error rate (~ 7.5 % – 14.5 %) (Jain *et al.* 2017) and low classification rate (Edwards *et al.* 2016) can be problematic, a well-curated genetic database of clean room contaminants would enable the quick and efficient identification of contamination on

missions. Our comparison between Illumina 16S amplicon data and MinION shotgun metagenome data has shown that the MinION is able to reliably detect common lineages in an environment. Despite the possibility of shared heritage between terrestrial and potential Martian organisms (Carr *et al.* 2017; Mileikowsky *et al.* 2000), the divergence between them would likely have occurred ~ 4 billion years ago and any Martian DNA would map outside of modern branches on the tree of life (Fairén *et al.* 2017). Therefore, any potential Martian life would be an independent lineage and unable to be classified. The MinION has been shown to sequence inosine in nucleic acid chains (Carr *et al.* 2017), demonstrating its ability to detect non-standard DNA and indicating its potential to detect a wider variety of charged chains. This indicates its potential for life detection on non-Earth like worlds, such as the gas giants and icy moons (e.g. Enceladus and Europa) (Mustard *et al.* 2013b). In fact, a solid state (i.e. non-degradable) nanopore sequencer for detection of organic linear polymers is currently being developed by NASA's Concepts for Ocean worlds Life Detection Technology program (Bywaters *et al.* 2017).

While low input preparations for MinION sequencing (such as that employed here) require a PCR step for amplification and adapter attachment, the primers used are non-specific, and instead are attached to nucleic acid strands via transposase mediation. This greatly reduces the inherent bias present in PCR and renders the overall protocol non-specific for certain genes or organisms. However, this introduces the need for a thermocycler in MinION-based life detection. PCR is possible in space and is able to be miniaturized for deployment, as shown by the successful use of the miniPCR system aboard the ISS during the Biomolecule Sequencing project (John *et al.* 2016), but it is one more instrument that needs to be automated and added to the sequencing process.

Our putative lower limit for sequencing is ~0.001 ng of DNA, which corresponds to 100 cells/g (Dolezel *et al.* 2003; Raes *et al.* 2007), a biomass common in Mars analogue environments

(Goordial *et al.* 2016a; Niederberger *et al.* 2010). This is based on an average bacterial genome size of 2 – 5 Mbp and ~ 2.5 – 5 fg of DNA per genome (Dolezal *et al.* 2003; Raes *et al.* 2007; Goordial *et al.* 2017). However, this assumes 100 % extraction efficiency, which is unlikely. The lower limit of DNA detection in a mission will be strongly dependent on the extraction method and must be chosen to optimize efficiency, as well as automation and miniaturization. Sequencing preparation will also need to be automated and miniaturized before deployment. This could be accomplished with the SOLID-SPU (Signs of Life Detector Sample Preparation Unit) (Parro *et al.* 2011) for DNA extraction and the VolTRAX device by ONT for sequencing preparation. Both instruments require relatively little human intervention but would still require a microfluidics system to connect the components. We are exploring these options presently.

The techniques we have employed here form a powerful suite capable of biosignature detection and environmental characterization. The MinION was able to directly detect unambiguous biosignatures in all sample types (endolith, regolith, rock) from this paleochannel site analogous to Martian sinuous ridges. There are prominent organic and water-related features in the XRD data, reflectance spectra, and Raman spectra, though by themselves these biosignatures are not conclusive and an abiotic origin cannot be precluded. Features indicating pigments are present but only in samples containing high biomass endoliths. The LDChip detected signals corresponding only to the antibodies present on the chip and this introduces a strong bias towards very specific protein groups and species. However, when these techniques are combined with the MinION, which can detect and sequence DNA from a wide variety of microorganisms in many types of samples and in very small amounts, the potential for biosignature identification and characterization is greatly increased.

2.6 Conclusion

We present this work as a proof-of-concept that MinION sequencing is a promising candidate for direct life detection in future space exploration missions. It can detect DNA down to ~ 0.001 ng (and potentially lower). The MinION is small, portable, low cost, and can successfully detect life in many analogue environments, including the Hanksville paleochannels. Dominated by Bacteria, the taxa detected here were able to be linked to the surrounding environment with XRD data, reflectance spectroscopy, Raman spectroscopy, and LDChip immunoassays. We can infer the presence of Cyanobacteria and SRBs based on these complementary analyses. Nanopore technology is synergistic with these techniques and together they provide a thorough characterization of this environment and its biosignatures. Although development of the MinION as a standalone instrument offers significant challenges (e.g. automated nucleic acid extraction and sample preparation), it represents a positive future for a direct life detection payload.

2.7 References

- Ammor M. S. (2007) Recent advances in the use of intrinsic fluorescence for bacterial identification and characterization. *Journal of fluorescence*, 17: 455-459.
- Anderson M. J., and Walsh D. C. (2013) PERMANOVA, ANOSIM, and the Mantel test in the face of heterogeneous dispersions: what null hypothesis are you testing? *Ecological monographs*, 83: 557-574.
- Balme M., Grindrod P., Sefton-Nash E., Davis J., Gupta S., Fawdon P., Sidiropoulos P., Yershov V., and Muller J.-P. (2015) Aram Dorsum: A Noachian Inverted Fluvial Channel System and Candidate Exomars 2018 Rover Landing Site. Lunar and Planetary Science Conference.
- Beegle L., Bhartia R., White M., DeFlores L., Abbey W., Wu Y.-H., Cameron B., Moore J., Fries M., and Burton A. (2015) SHERLOC: Scanning habitable environments with Raman & luminescence for organics & chemicals. Aerospace Conference, 2015 IEEE. IEEE.
- Berg B., Ronholm J., Applin D., Mann P., Izawa M., Cloutis E., and Whyte L. (2014) Spectral features of biogenic calcium carbonates and implications for astrobiology. *International Journal of Astrobiology*, 13: 353-365.
- Bishop J. L., Dobreá E. Z. N., McKeown N. K., Parente M., Ehlmann B. L., Michalski J. R., Milliken R. E., Poulet F., Swayze G. A., and Mustard J. F. (2008) Phyllosilicate diversity and past aqueous activity revealed at Mawrth Vallis, Mars. *Science*, 321: 830-833.
- Blanco Y., Prieto-Ballesteros O., Gómez M. J., Moreno-Paz M., García-Villadangos M., Rodríguez-Manfredi J. A., Cruz-Gil P., Sánchez-Román M., Rivas L. A., and Parro V. (2012) Prokaryotic communities and operating metabolisms in the surface and the permafrost of Deception Island (Antarctica). *Environmental microbiology*, 14: 2495-2510.
- Boquet E., Boronat A., and Ramos-Cormenzana A. (1973) Production of calcite (calcium carbonate) crystals by soil bacteria is a general phenomenon. *Nature*, 246: 527.
- Brown B. L., Watson M., Minot S. S., Rivera M. C., and Franklin R. B. (2017) MinION™ nanopore sequencing of environmental metagenomes: a synthetic approach. *GigaScience*, 6: 1-10.
- Bywaters K., Schmidt H., Vercootere W., Deamer D., Hawkins A., Quinn R., Burton A., and Mckay C. (2017) Development of Solid-State Nanopore Technology for Life Detection.
- Carr C. E., Mojarro A., Hachey J., Saboda K., Tani J., Bhattaru S. A., Smith A., Pontefract A., Zuber M. T., and Doebler R. (2017) Towards in situ sequencing for life detection. Aerospace Conference, 2017 IEEE. IEEE.
- Castanier S., Le Métayer-Levrel G., and Perthuisot J.-P. (1999) Ca-carbonates precipitation and limestone genesis—the microbiogeologist point of view. *Sedimentary geology*, 126: 9-23.
- Castro-Wallace S. L., Chiu C. Y., John K. K., Stahl S. E., Rubins K. H., McIntyre A. B., Dworkin J. P., Lupisella M. L., Smith D. J., and Botkin D. J. (2017) Nanopore DNA sequencing and genome assembly on the International Space Station. *Scientific reports*, 7: 18022.
- Clark R. N., King T. V., Klejwa M., Swayze G. A., and Vergo N. (1990) High spectral resolution reflectance spectroscopy of minerals. *Journal of Geophysical Research: Solid Earth*, 95: 12653-12680.

- Clarke J. D., and Stoker C. R. (2011) Concretions in exhumed and inverted channels near Hanksville Utah: implications for Mars. *International Journal of Astrobiology*, 10: 161-175.
- Cloutis E. A., Hawthorne F. C., Mertzman S. A., Krenn K., Craig M. A., Marcino D., Methot M., Strong J., Mustard J. F., and Blaney D. L. (2006) Detection and discrimination of sulfate minerals using reflectance spectroscopy. *Icarus*, 184: 121-157.
- Coates J. D., Michaelidou U., Bruce R. A., O'Connor S. M., Crespi J. N., and Achenbach L. A. (1999) Ubiquity and diversity of dissimilatory (per) chlorate-reducing bacteria. *Applied and Environmental Microbiology*, 65: 5234-5241.
- Crowley J., Williams D., Hammarstrom J., Piatak N., Chou I.-M., and Mars J. (2003) Spectral reflectance properties (0.4–2.5 μm) of secondary Fe-oxide, Fe-hydroxide, and Fe-sulphate-hydrate minerals associated with sulphide-bearing mine wastes. *Geochemistry: Exploration, Environment, Analysis*, 3: 219-228.
- Davis J., Balme M., Grindrod P., Williams R., and Gupta S. (2016) Extensive Noachian fluvial systems in Arabia Terra: Implications for early Martian climate. *Geology*, 44: 847-850.
- Direito S. O., Ehrenfreund P., Marees A., Staats M., Foing B., and Röling W. F. (2011) A wide variety of putative extremophiles and large beta-diversity at the Mars Desert Research Station (Utah). *International Journal of Astrobiology*, 10: 191-207.
- Dolezel J., Bartos J., Voglmayr H., and Greilhuber J. (2003) Nuclear DNA content and genome size of trout and human. *Cytometry. Part A: the journal of the International Society for Analytical Cytology*, 51: 127.
- Dorn R. I., and Oberlander T. M. (1981) Microbial origin of desert varnish. *Science*, 213: 1245-1247.
- Downs R. (2006) The RRUFF Project: an integrated study of the chemistry, crystallography, Raman and infrared spectroscopy of minerals. Program and Abstracts of the 19th General Meeting of the International Mineralogical Association in Kobe, Japan, 2006.
- Edwards A., Debonnaire A. R., Sattler B., Mur L. A., and Hodson A. J. (2016) Extreme metagenomics using nanopore DNA sequencing: a field report from Svalbard, 78 N. *bioRxiv*: 073965.
- Edwards A., Soares A., Rassner S., Green P., Felix J., and Mitchell A. (2017) Deep Sequencing: Intra-terrestrial metagenomics illustrates the potential of off-grid Nanopore DNA sequencing. *bioRxiv*: 133413.
- Edwards H. G., Hutchinson I., and Ingley R. (2012) The ExoMars Raman spectrometer and the identification of biogeological spectroscopic signatures using a flight-like prototype. *Analytical and bioanalytical chemistry*, 404: 1723-1731.
- Edwards H. G., Vandenabeele P., Jorge-Villar S. E., Carter E. A., Perez F. R., and Hargreaves M. D. (2007) The Rio Tinto Mars analogue site: an extremophilic Raman spectroscopic study. *Spectrochimica Acta Part A: Molecular and Biomolecular Spectroscopy*, 68: 1133-1137.
- Edwards H. G., Villar S. E. J., Parnell J., Cockell C. S., and Lee P. (2005) Raman spectroscopic analysis of cyanobacterial gypsum halotrophs and relevance for sulfate deposits on Mars. *Analyst*, 130: 917-923.
- Ehrenfreund P., Röling W., Thiel C., Quinn R., Sephton M., Stoker C., Kotler J., Direito S., Martins Z., and Orzechowska G. (2011) Astrobiology and habitability studies in preparation for future Mars missions: trends from investigating minerals, organics and biota. *International Journal of Astrobiology*, 10: 239-253.

- Eigenbrode J. L., Summons R. E., Steele A., Freissinet C., Millan M., Navarro-González R., Sutter B., McAdam A. C., Franz H. B., and Glavin D. P. (2018) Organic matter preserved in 3-billion-year-old mudstones at Gale crater, Mars. *Science*, 360: 1096-1101.
- Ellery A., Kolb C., Lammer H., Parnell J., Edwards H., Richter L., Patel M., Romstedt J., Dickensheets D., and Steele A. (2002) Astrobiological instrumentation for Mars—the only way is down. *International Journal of Astrobiology*, 1: 365-380.
- Emerson D., Weiss J. V., and Megonigal J. P. (1999) Iron-oxidizing bacteria are associated with ferric hydroxide precipitates (Fe-plaque) on the roots of wetland plants. *Applied and Environmental Microbiology*, 65: 2758-2761.
- Fairén A. G., Parro V., Schulze-Makuch D., and Whyte L. (2017) Searching for life on Mars before it is too late. *Astrobiology*, 17: 962-970.
- Feng X., Matranga C., Vidic R., and Borguet E. (2004) A vibrational spectroscopic study of the fate of oxygen-containing functional groups and trapped CO₂ in single-walled carbon nanotubes during thermal treatment. *The Journal of Physical Chemistry B*, 108: 19949-19954.
- Frawley E. R., and Fang F. C. (2014) The ins and outs of bacterial iron metabolism. *Molecular microbiology*, 93: 609-616.
- Giovannetti R. (2012) The use of Spectrophotometry UV-Vis for the Study of Porphyrins. In: *Macro To Nano Spectroscopy*, InTech.
- Glavin D. P., Freissinet C., Miller K. E., Eigenbrode J. L., Brunner A. E., Buch A., Sutter B., Archer P. D., Atreya S. K., and Brinckerhoff W. B. (2013) Evidence for perchlorates and the origin of chlorinated hydrocarbons detected by SAM at the Rocknest aeolian deposit in Gale Crater. *Journal of Geophysical Research: Planets*, 118: 1955-1973.
- Goordial J., Altshuler I., Hindson K., Chan-Yam K., Marcoléfas E., and Whyte L. (2017) In situ field sequencing and life detection in remote (79° 26' N) Canadian High Arctic permafrost ice wedge microbial communities. *Frontiers in microbiology*, 8: 2594.
- Goordial J., Davila A., Lacelle D., Pollard W., Marinova M. M., Greer C. W., DiRuggiero J., McKay C. P., and Whyte L. G. (2016) Nearing the cold-arid limits of microbial life in permafrost of an upper dry valley, Antarctica. *The ISME journal*, 10: 1613.
- Guinness E. A., Arvidson R. E., Clark I. H., and Shepard M. K. (1997) Optical scattering properties of terrestrial varnished basalts compared with rocks and soils at the Viking Lander sites. *Journal of Geophysical Research: Planets*, 102: 28687-28703.
- Hays L. E., Graham H. V., Des Marais D. J., Hausrath E. M., Horgan B., McCollom T. M., Parenteau M. N., Potter-McIntyre S. L., Williams A. J., and Lynch K. L. (2017) Biosignature preservation and detection in Mars analog environments. *Astrobiology*, 17: 363-400.
- He Z., Gentry T. J., Schadt C. W., Wu L., Liebich J., Chong S. C., Huang Z., Wu W., Gu B., and Jardine P. (2007) GeoChip: a comprehensive microarray for investigating biogeochemical, ecological and environmental processes. *The ISME journal*, 1: 67.
- Hecht M., Kounaves S., Quinn R., West S., Young S., Ming D., Catling D., Clark B., Boynton W., and Hoffman J. (2009) Detection of perchlorate and the soluble chemistry of martian soil at the Phoenix lander site. *Science*, 325: 64-67.
- Jain M., Tyson J. R., Loose M., Ip C. L., Eccles D. A., O'Grady J., Malla S., Leggett R. M., Wallerman O., and Jansen H. J. (2017) MinION Analysis and Reference Consortium: Phase 2 data release and analysis of R9.0 chemistry. *F1000Research*, 6.

- Jehlička J., Edwards H., and Oren A. (2013) Bacterioruberin and salinixanthin carotenoids of extremely halophilic Archaea and Bacteria: a Raman spectroscopic study. *Spectrochimica Acta Part A: Molecular and Biomolecular Spectroscopy*, 106: 99-103.
- Jehlicka J., and Oren A. (2013) Raman spectroscopy in halophile research. *Frontiers in microbiology*, 4: 380.
- John K., Botkin D., Burton A., Castro-Wallace S., Chaput J., Dworkin J., Lehman N., Lupisella M., Mason C., and Smith D. (2016) The Biomolecule Sequencer Project: Nanopore sequencing as a dual-use tool for crew health and astrobiology investigations.
- Johnson S. S., Zaikova E., Goerlitz D. S., Bai Y., and Tighe S. W. (2017) Real-Time DNA Sequencing in the Antarctic Dry Valleys Using the Oxford Nanopore Sequencer. *Journal of Biomolecular Techniques: JBT*, 28: 2.
- Jones M. M., Jones E. A., Harmon D. F., and Semmes R. T. (1961) A search for perchlorate complexes. Raman spectra of perchlorate solutions. *Journal of the American Chemical Society*, 83: 2038-2042.
- Kaczor A., and Baranska M. (2011) Structural changes of carotenoid astaxanthin in a single algal cell monitored in situ by Raman spectroscopy. *Analytical chemistry*, 83: 7763-7770.
- Kim S. K., Kim M. S., and Suh S. W. (1987) Surface-enhanced Raman scattering (SERS) of aromatic amino acids and their glycyl dipeptides in silver sol. *Journal of Raman spectroscopy*, 18: 171-175.
- Koren S., Walenz B. P., Berlin K., Miller J. R., Bergman N. H., and Phillippy A. M. (2017) Canu: scalable and accurate long-read assembly via adaptive k-mer weighting and repeat separation. *Genome research*, 27: 722-736.
- Kozich J. J., Westcott S. L., Baxter N. T., Highlander S. K., and Schloss P. D. (2013) Development of a dual-index sequencing strategy and curation pipeline for analyzing amplicon sequence data on the MiSeq Illumina sequencing platform. *Applied and environmental microbiology: AEM*. 01043-13.
- Lacap D. C., Warren-Rhodes K. A., McKay C. P., and Pointing S. B. (2011) Cyanobacteria and chloroflexi-dominated hypolithic colonization of quartz at the hyper-arid core of the Atacama Desert, Chile. *Extremophiles*, 15: 31-38.
- Lee K. C.-Y., Herbold C., Dunfield P. F., Morgan X. C., McDonald I. R., and Stott M. B. (2013) Phylogenetic delineation of the novel phylum Armatimonadetes (former candidate division OP10) and definition of two novel candidate divisions. *Appl. Environ. Microbiol.*, 79: 2484-2487.
- Leggett R. M., and Clark M. D. (2017) A world of opportunities with nanopore sequencing. *Journal of Experimental Botany*.
- Loman N. J., and Watson M. (2015) Successful test launch for nanopore sequencing. *Nature methods*, 12: 303-304.
- Luef B., Fakra S. C., Csencsits R., Wrighton K. C., Williams K. H., Wilkins M. J., Downing K. H., Long P. E., Comolli L. R., and Banfield J. F. (2013) Iron-reducing bacteria accumulate ferric oxyhydroxide nanoparticle aggregates that may support planktonic growth. *The ISME journal*, 7: 338.
- Maiti N. C., Apetri M. M., Zagorski M. G., Carey P. R., and Anderson V. E. (2004) Raman spectroscopic characterization of secondary structure in natively unfolded proteins: α -synuclein. *Journal of the American Chemical Society*, 126: 2399-2408.
- Manley L. J., Ma D., and Levine S. S. (2016) Monitoring error rates in Illumina sequencing. *Journal of biomolecular techniques: JBT*, 27: 125.

- Markowitz V. M., Chen I.-M. A., Palaniappan K., Chu K., Szeto E., Grechkin Y., Ratner A., Jacob B., Huang J., and Williams P. (2011) IMG: the integrated microbial genomes database and comparative analysis system. *Nucleic acids research*, 40: D115-D122.
- Marshall C. P., Carter E. A., Leuko S., and Javaux E. J. (2006) Vibrational spectroscopy of extant and fossil microbes: relevance for the astrobiological exploration of Mars. *Vibrational Spectroscopy*, 41: 182-189.
- Martins Z., Sephton M., Foing B., and Ehrenfreund P. (2011) Extraction of amino acids from soils close to the Mars Desert Research Station (MDRS), Utah. *International Journal of Astrobiology*, 10: 231-238.
- McCauley J., Breed C., El-Baz F., Whitney M., Grolier M., and Ward A. (1979) Pitted and fluted rocks in the Western Desert of Egypt: Viking comparisons. *Journal of Geophysical Research: Solid Earth*, 84: 8222-8232.
- McLennan S., Sephton M., Beaty D., Hecht M., Pepin B., Leya I., Jones J., Weiss B., Race M., and Rummel J. (2012) Planning for Mars returned sample science: final report of the MSR End-to-End International Science Analysis Group (E2E-iSAG). *Astrobiology*, 12: 175-230.
- Meinert C., Myrgorodska I., De Marcellus P., Buhse T., Nahon L., Hoffmann S. V., d'Hendecourt L. L. S., and Meierhenrich U. J. (2016) Ribose and related sugars from ultraviolet irradiation of interstellar ice analogs. *Science*, 352: 208-212.
- Menegon M., Cantaloni C., Rodriguez-Prieto A., Centomo C., Abdelfattah A., Rossato M., Bernardi M., Xumerle L., Loader S., and Delledonne M. (2017) On site DNA barcoding by nanopore sequencing. *PloS one*, 12: e0184741.
- Mileikowsky C., Cucinotta F. A., Wilson J. W., Gladman B., Horneck G., Lindegren L., Melosh J., Rickman H., Valtonen M., and Zheng J. (2000) Natural transfer of viable microbes in space: 1. From Mars to Earth and Earth to Mars. *Icarus*, 145: 391-427.
- Musk E. (2017) Making humans a multi-planetary species. *New Space*, 5: 46-61.
- Mustard J., Adler M., Allwood A., Bass D., Beaty D., and Bell J. (2013a) Appendices to the Report of the Mars 2020 Science Definition Team. *Mars Exploration Program Analysis Group*: 154.
- Mustard J., Adler M., Allwood A., Bass D., Beaty D., Bell J., Brinckerhoff W., Carr M., Des Marais D., and Brake B. (2013b) Report of the mars 2020 science definition team. *Mars Explor. Progr. Anal. Gr*: 155-205.
- Neveu M., Hays L. E., Voytek M. A., New M. H., and Schulte M. D. (2018) The Ladder of Life Detection. *Astrobiology*.
- Niederberger T. D., Perreault N. N., Tille S., Lollar B. S., Lacrampe-Couloume G., Andersen D., Greer C. W., Pollard W., and Whyte L. G. (2010) Microbial characterization of a subzero, hypersaline methane seep in the Canadian High Arctic. *The ISME journal*, 4: 1326.
- NRC. (2012) Vision and voyages for planetary science in the decade 2013-2022. National Academies Press.
- Oren A., Sørensen K. B., Canfield D. E., Teske A. P., Ionescu D., Lipski A., and Altendorf K. (2009) Microbial communities and processes within a hypersaline gypsum crust in a saltern evaporation pond (Eilat, Israel). *Hydrobiologia*, 626: 15-26.
- Osinski G. R., Battler M., Caudill C. M., Francis R., Haltigin T., Hipkin V. J., Kerrigan M., Pilles E., Pontefract A., and Tornabene L. L. (2018) The CanMars Mars Sample Return analogue mission. *Planetary and Space Science*, (in press).
- Pace N. R. (2001) The universal nature of biochemistry. *Proceedings of the National Academy of Sciences*, 98: 805-808.

- Parro V., de Diego-Castilla G., Rodríguez-Manfredi J. A., Rivas L. A., Blanco-López Y., Sebastián E., Romeral J., Compostizo C., Herrero P. L., and García-Marín A. (2011) SOLID3: a multiplex antibody microarray-based optical sensor instrument for in situ life detection in planetary exploration. *Astrobiology*, 11: 15-28.
- Parro V., Rodríguez-Manfredi J., Briones C., Compostizo C., Herrero P., Vez E., Sebastián E., Moreno-Paz M., García-Villadangos M., and Fernández-Calvo P. (2005) Instrument development to search for biomarkers on Mars: terrestrial acidophile, iron-powered chemolithoautotrophic communities as model systems. *Planetary and Space Science*, 53: 729-737.
- Pontefract A., Hachey J., Zuber M. T., Ruvkun G., and Carr C. E. (2018) Sequencing Nothing: Exploring Failure Modes of Nanopore Sensing and Implications for Life Detection. *Life Sciences in Space Research*.
- Poretzky R., Rodríguez-R L. M., Luo C., Tsementzi D., and Konstantinidis K. T. (2014) Strengths and limitations of 16S rRNA gene amplicon sequencing in revealing temporal microbial community dynamics. *PloS one*, 9: e93827.
- Raes J., Korbel J. O., Lercher M. J., Von Mering C., and Bork P. (2007) Prediction of effective genome size in metagenomic samples. *Genome biology*, 8: R10.
- Ranjan R., Rani A., Metwally A., McGee H. S., and Perkins D. L. (2016) Analysis of the microbiome: Advantages of whole genome shotgun versus 16S amplicon sequencing. *Biochemical and biophysical research communications*, 469: 967-977.
- Rhind T., Ronholm J., Berg B., Mann P., Applin D., Stromberg J., Sharma R., Whyte L., and Cloutis E. (2014) Gypsum-hosted endolithic communities of the Lake St. Martin impact structure, Manitoba, Canada: spectroscopic detectability and implications for Mars. *International Journal of Astrobiology*, 13: 366-377.
- Rivas L. A., Aguirre J., Blanco Y., González-Toril E., and Parro V. (2011) Graph-based deconvolution analysis of multiplex sandwich microarray immunoassays: applications for environmental monitoring. *Environmental microbiology*, 13: 1421-1432.
- Rivas L. A., García-Villadangos M., Moreno-Paz M., Cruz-Gil P., Gómez-Elvira J., and Parro V. (2008) A 200-antibody microarray biochip for environmental monitoring: searching for universal microbial biomarkers through immunoprofiling. *Analytical chemistry*, 80: 7970-7979.
- Ruan C., Wang W., and Gu B. (2006) Surface-enhanced Raman scattering for perchlorate detection using cystamine-modified gold nanoparticles. *Analytica chimica acta*, 567: 114-120.
- Rull F., Maurice S., Hutchinson I., Moral A., Perez C., Diaz C., Colombo M., Belenguer T., Lopez-Reyes G., and Sansano A. (2017) The Raman Laser Spectrometer for the ExoMars Rover Mission to Mars. *Astrobiology*, 17: 627-654.
- Sánchez-García L., Fernández M., García-Villadangos M., Blanco Y., Cady S., Hinman N., Bowden M., Pointing S., Lee K., Warren-Rhodes K. and others. (2018) Microbial biomarker transition in high altitude sinter mounds from El Tatio (Chile) through different stages of hydrothermal activity. *Frontiers in microbiology*, (under review).
- Sandford S., and Allamandola L. (1990) The physical and infrared spectral properties of CO₂ in astrophysical ice analogs. *The Astrophysical Journal*, 355: 357-372.
- Schlesinger W. H., Phippen J. S., Wallenstein M. D., Hofmockel K. S., Klepeis D. M., and Mahall B. E. (2003) Community composition and photosynthesis by photoautotrophs under quartz pebbles, southern Mojave Desert. *Ecology*, 84: 3222-3231.

- Sephton M. A. (2018) Selecting Mars samples to return to Earth. *Astronomy & Geophysics*, 59: 1.36-1.38.
- Spry J. A., Race M., Kminek G., Siegel B., and Conley C. (2018) Planetary Protection Knowledge Gaps for Future Mars Human Missions: Stepwise Progress in Identifying and Integrating Science and Technology Needs. 48th International Conference on Environmental Systems.
- Stoker C. R., Clarke J., Direito S. O., Blake D., Martin K. R., Zavaleta J., and Foing B. (2011) Mineralogical, chemical, organic and microbial properties of subsurface soil cores from Mars Desert Research Station (Utah, USA): Phyllosilicate and sulfate analogues to Mars mission landing sites. *International Journal of Astrobiology*, 10: 269-289.
- Stromberg J., Applin D., Cloutis E., Rice M., Berard G., and Mann P. (2014) The persistence of a chlorophyll spectral biosignature from Martian evaporite and spring analogues under Mars-like conditions. *International Journal of Astrobiology*, 13: 203-223.
- Summons R., Sessions A., Allwood A., Barton H., Beaty D., Blakkolb B., Canham J., Clark B., Dworkin J., and Lin Y. (2014) Planning considerations related to the organic contamination of Martian samples and implications for the Mars 2020 rover. *Astrobiology*, 14: 969-1027.
- Tahon G., Tytgat B., Lebbe L., Carlier A., and Willems A. (2018) *Abditibacterium utsteinense* sp. nov., the first cultivated member of candidate phylum FBP, isolated from ice-free Antarctic soil samples. *Systematic and applied microbiology*, 41: 279-290.
- Tessler M., Neumann J. S., Afshinnekoo E., Pineda M., Hersch R., Velho L. F. M., Segovia B. T., Lansac-Toha F. A., Lemke M., and DeSalle R. (2017) Large-scale differences in microbial biodiversity discovery between 16S amplicon and shotgun sequencing. *Scientific reports*, 7: 6589.
- Thiel C. S., Ehrenfreund P., Foing B., Pletser V., and Ullrich O. (2011) PCR-based analysis of microbial communities during the EuroGeoMars campaign at Mars Desert Research Station, Utah. *International Journal of Astrobiology*, 10: 177-190.
- Thomas G. J., Prescott B., and Urry D. W. (1987) Raman amide bands of type-II β -turns in cyclo-(VPGVG)₃ and poly-(VPGVG), and implications for protein secondary-structure analysis. *Biopolymers*, 26: 921-934.
- Van Lith Y., Warthmann R., Vasconcelos C., and Mckenzie J. A. (2003) Sulphate-reducing bacteria induce low-temperature Ca-dolomite and high Mg-calcite formation. *Geobiology*, 1: 71-79.
- Warren-Rhodes K. A., Rhodes K. L., Pointing S. B., Ewing S. A., Lacap D. C., Gomez-Silva B., Amundson R., Friedmann E. I., and McKay C. P. (2006) Hypolithic cyanobacteria, dry limit of photosynthesis, and microbial ecology in the hyperarid Atacama Desert. *Microbial ecology*, 52: 389-398.
- Williams R. M., Chidsey Jr T. C., and Eby D. E. (2007) Exhumed paleochannels in central Utah—Analog for raised curvilinear features on Mars.
- Williams R. M., Irwin III R. P., Burr D. M., Harrison T., and McClelland P. (2013) Variability in Martian sinuous ridge form: Case study of Aeolis Serpens in the Aeolis Dorsa, Mars, and insight from the Mirackina paleoriver, South Australia. *Icarus*, 225: 308-324.
- Williams R. M., Irwin R. P., and Zimbelman J. R. (2009) Evaluation of paleohydrologic models for terrestrial inverted channels: Implications for application to martian sinuous ridges. *Geomorphology*, 107: 300-315.
- Ziolkowski L., Mykytczuk N., Omelon C., Johnson H., Whyte L., and Slater G. (2013) Arctic gypsum endoliths: a biogeochemical characterization of a viable and active microbial community.

Connecting text

Chapter 2 of this work presents evidence of the MinION's ability to detect DNA from Mars analogue samples; however, it remains unknown if the MinION can detect DNA from analogue samples exposed to Mars-like conditions, which will be a crucial factor in determining its suitability for future life detection missions. The following chapter describes DNA detection with MinION sequencing in University Valley cryptoendoliths that have been exposed to a Mars simulation chamber (i.e. Mars-like temperature, pressure, atmospheric composition, UV radiation), as well as cell membrane-derived lipid and protein detection. In addition, a supplemental UVC exposure was also performed; as UVC is the most biocidal and destructive Martian environmental element to DNA, I performed MinION sequencing on the cryptoendolith samples after extended and more powerful UVC exposure to ascertain how long DNA remains detectable with the MinION.

**Chapter 3. Biosignature detection and MinION sequencing of Antarctic cryptoendoliths
after exposure to Mars simulation conditions**

Catherine Maggiori^{1*}, Miguel Angel Fernández-Martínez^{1,2}, Louis-Jacques Bourdages¹, Laura Sánchez-García³, Mercedes Moreno-Paz³, Jesús Sobrado³, Daniel Carrizo³, Álvaro Vicente-Retortillo³, Jacqueline Goordial⁴, Lyle G. Whyte¹

¹Department of Natural Resource Sciences, Faculty of Agricultural and Environmental Sciences, McGill University, Ste. Anne-de-Bellevue, Quebec, Canada

²Department of Ecology, Universidad Autónoma de Madrid, Ciudad Universitaria de Cantoblanco, 28049 Madrid, Spain

³Department of Molecular Evolution, Centro de Astrobiología (INTA-CSIC), Torrejón de Ardoz, Madrid, Spain

⁴School of Environmental Sciences, University of Guelph, Guelph, Ontario, Canada

3.1 Abstract

In the search for life in our Solar System, Mars remains a promising target based on its proximity and similarity to Earth. When Mars transitioned from a warmer, wetter climate to its current dry and freezing conditions, any putative extant life probably retreated into habitable refugia like the interior of rocks; terrestrial cryptoendolithic microorganisms (i.e. those inhabiting rock interiors) thus represent compelling modern day Mars analogues, particularly those from the hyperarid McMurdo Dry Valleys in Antarctica. As DNA is a strong definitive biosignature given the virtual impossibility of its generation in the absence of life, we investigated DNA detection with MinION sequencing in Antarctic cryptoendoliths after a ~58-sol exposure in MARTE, a Mars environmental chamber, in conjunction with protein and lipid detection. The MARTE exposure resulted in changes in community composition and DNA, proteins, and cell membrane-derived lipids remained detectable after this exposure. Of the multitude of extreme environmental conditions on Mars, UV radiation (specifically UVC) is the most destructive to both cells and DNA. As such, we further investigated if a UVC exposure corresponding to ~278 Martian years would impede DNA detection via MinION sequencing. The MinION was able to successfully detect and sequence DNA after this UVC radiation exposure, suggesting its utility for life detection in future astrobiology missions.

3.2 Introduction

As a hyperarid polar desert, the McMurdo Dry Valleys are some of the coldest and driest environments on Earth. University Valley is in the stable upland zone of the McMurdo Dry Valleys in the Quartermain Mountain Range of Victoria Land, Antarctica. University Valley experiences mean annual air temperatures of $-23.4 \pm 8.3^{\circ}\text{C}$ and presents extremely limited precipitation only as snow (e.g. <10 mm per year, with a mean annual relative humidity of $45.5 \pm 14\%$, an aridity index of <0.05 , and an estimated 74 h of bulk water above the ice table per year) (Fisher *et al.* 2016; Goordial *et al.* 2016a; Wierzchos *et al.* 2012). While it is chiefly dominated by ice-cemented ground overlain with dry permafrost (Heldmann *et al.* 2013), it also exhibits some variable ground cover (e.g. polygonal sand wedges, sandstone boulders, desert pavement, cryptoendolithic rocks). This arid permafrost and ice-cemented ground make University Valley a strong modern-day Mars analogue, particularly for northern latitudes like the Phoenix landing site (68.2188°N , 125.7492°W) (Heldmann *et al.* 2013; McKay *et al.* 2017).

If life ever arose on Mars, it likely would have occurred when Mars had a warmer and wetter climate, c. 2 – 4 billion years ago (Dong *et al.* 2007; Fairén 2010; Leask and Ehlmann 2022; McKay *et al.* 2017). As large bodies of liquid water progressively disappeared from the Martian surface, putative life could have retreated into hospitable niches, firstly those with smaller or temporary water bodies (Fernández-Martínez *et al.* 2021; Lezcano *et al.* 2019) and subsequently underground (e.g. lava tubes, caves, subglacial lakes) or within surface rocks (e.g. cryptoendoliths) (de Vera *et al.* 2014; McKay *et al.* 1992; O'Connor *et al.* 2021; Orosei *et al.* 2018). This latter strategy of cryptoendolithic colonization (i.e. rock-dwelling microorganisms living within the natural pore spaces of rocks) (Wierzchos *et al.* 2012) is widespread in a diverse range of extreme

environments, including the McMurdo Dry Valleys (Goordial *et al.* 2016a; McKay *et al.* 2017; Wierzchos *et al.* 2012), Antarctic nunataks (Fernández-Martínez *et al.* 2021), the Atacama Desert (Wierzchos *et al.* 2011; Wierzchos *et al.* 2013; Wierzchos *et al.* 2015), geothermal hot springs (Walker *et al.* 2005), and deep subsurface environments (Jørgensen and Zhao 2016; Lee *et al.* 2015). The rock interior offers microorganisms thermal buffering, moisture, nutrient retention, and protection from UV radiation, freezing temperatures, and freeze-thaw events (Wierzchos *et al.* 2012; Ye *et al.* 2021). Thus, rock colonization acts as an effective survival strategy in extreme environments and the interior of rocks is also a favourable environment for the preservation of biosignatures. As putative life on the Martian surface would have withdrawn into habitable refugia as the planet transitioned to its current inhospitable state, cryptoendoliths in extreme environments on Earth can act as a model for potential biosignature preservation and detection methods for future Mars exploratory missions focused on detecting extant life.

Biosignatures exist across a broad spectrum of signs and/or substances that indicate the presence or past presence of life, including both definitive (e.g. nucleic acids, proteins, cell membrane-derived lipids) and more ambiguous phenomena (e.g. atmospheric gases and temporal variability) (Hays *et al.* 2017; Neveu *et al.* 2018; Schwieterman *et al.* 2018). Proteins and cell membrane-derived lipids (e.g. fatty acids) can be detected with immunoassays (e.g. the Life Marker Chip, a previous payload candidate for the *Rosalind Franklin* rover, and the Life Detector Chip aka LDChip, an antibody immunoassay for microbial biomarker detection) (Martins 2011; Parro *et al.* 2011; Parro *et al.* 2008; Rivas *et al.* 2008; Sims *et al.* 2012) and gas chromatography-mass spectroscopy (GC-MS). GC-MS has been included on mission payloads previously (e.g. the *Viking* biological experiments, SAM on *Curiosity*) (Klein 1977; Millan *et al.* 2016). There have been numerous expeditions to Mars with the explicit goal of searching for biosignatures, including

the *Viking* missions (which remains the only space mission experiments performed to search for extant life) (Klein 1977; Levin and Straat 2016), the Mars Science Laboratory and *Curiosity* rover, the Mars 2020 *Perseverance* rover, and the upcoming (but now delayed) ExoMars *Rosalind Franklin* rover (Eigenbrode *et al.* 2018; Mustard *et al.* 2013b; Vago *et al.* 2017). The latter missions are searching instead for organic molecules and signs of ancient life (Eigenbrode *et al.* 2018; Maurice *et al.* 2021; Rull *et al.* 2017), rather than signs of microbial metabolism and extant microbial life (Klein 1978a; Levin and Straat 2016). However, organic molecules (e.g. thiophenes, aromatic and aliphatic hydrocarbons) are not conclusive signs of life and may arise without biology (Eigenbrode *et al.* 2018). To this end, detecting unambiguous biosignatures, such as DNA, proteins, and cell membrane-derived lipids, that strongly signify the presence of extant or recently extinct life in this environment will be of utmost importance (McKay *et al.* 1992; Mustard *et al.* 2013b). Detecting these biosignatures on Mars will be challenging, as they would be subjected to further deleterious environmental conditions, including strong UV and ionizing radiation, freezing temperatures, desiccation, and oxidation. Radiation is the most detrimental of these effects on both cells and biomolecules (Hansen *et al.* 2009; Schuerger 2015; Ye *et al.* 2021), particularly the UVC band of UV radiation (Schuerger *et al.* 2003).

Like proteins and cell membrane-derived lipids, DNA is an unambiguous biosignature that cannot be generated without the presence of life (Neveu *et al.* 2018). As defined by NASA: “Life is a self-sustaining chemical system capable of Darwinian evolution” (Council 2019); substances that enable Darwinism, like DNA, are thus powerful biosignatures (Benner 2017). However, instrumentation targeted towards detecting DNA has never been included on a mission payload. DNA can be detected with nanopore sequencing via the Oxford Nanopore Technologies’ (ONT) MinION, a portable, low mass biomolecule sequencer with low energy requirements. The MinION

was previously used on the International Space Station as part of the Biomolecule Sequencing Project (John *et al.* 2016) and has also been used to detect DNA from low biomass Mars analogue samples, demonstrating its promise as a candidate for future biosignature detection missions (Goordial *et al.* 2017 ; Maggiori *et al.* 2020). However, the MinION has yet to be tested on samples that have experienced the harshness of a Mars-like environment.

In this study, we tested the detectability of DNA, proteins, and lipids in cryptoendoliths from University Valley when exposed to Mars-like conditions using MARTE, a vacuum simulation chamber developed at the Centro de Astrobiología (INTA-CSIC) capable of mimicking Martian temperature, pressure, UV radiation, and atmospheric composition (Sobrado *et al.* 2014). Biosignature detection was performed using MinION sequencing, LDChip immunoassays, and GC-MS after a MARTE exposure of ~58 Martian days (sols) based on the UVC dose. Additionally, as UV radiation is the most deleterious effect on DNA and to better characterize the viability of MinION sequencing on DNA detection on Mars analogue samples that have experienced Mars-like UV radiation, we further exposed University Valley cryptoendoliths to a UVC chamber for a duration of ~278 Martian years.

3.3 Methods

3.3.1 Sample site and collection

University Valley (~1.5 km long by 500 m wide) is a small hanging valley located in a precipitation shadow of the Transantarctic Mountains, ~450 m above the floor of nearby Beacon



Figure 3.1. Study and sampling site in the McMurdo Dry Valleys, Antarctica. The light blue box frames University Valley, while the red star marks the sampling location. Inset displays the continent of Antarctica.

Valley, and 1600 – 1800 m above sea level (Lacelle *et al.* 2011) (Figure 3.1). Cryptoendolith samples were acquired as described in Goordial *et al.* (2016). For the exposures, fragments of rock from this University Valley site showing colonization were selected. Briefly, cryptoendoliths were collected from University Valley’s North-West valley wall (77.51745°S, 160.41356°E) with an ethanol-sterilized rock hammer and placed into sterile Whirlpak bags. Samples were kept frozen and shipped to McGill University and stored at –20 °C in a cryochamber until processing, with the exception of ~48 h when a mechanical malfunction compromised the temperature maintenance of the cryochamber that resulted in temperatures up to 30 °C measured by the sensor within the chamber. While the samples were frozen, the warmer temperatures could have affected the

biomass and community composition of the University Valley cryptoendoliths; however, the native microbial consortia are likely adapted to freeze-thaw cycles (Chan-Yam *et al.* 2019). A previous study by Lanoil *et al.* (2009) showed that Antarctic permafrost exposed to above-freezing temperatures (up to 25 °C for 40 hours followed by 4 °C for 15 months) may have experienced a maximum of 4.1 doublings and become enriched in certain phylotypes suited to the 4 °C environment (Lanoil *et al.* 2009). This finding indicates that cell growth and consortia skew towards certain taxa in the present study was minimal. We believe that the overarching goals of this work (i.e. evaluation of the MinION as a DNA detection tool and examination of the change in biosignatures after exposure to Mars-like conditions) remain unaffected by this brief period of above-zero temperatures.

3.3.2 Mars chamber (MARTE) exposure

We used MARTE, a Mars environmental simulation chamber, at the Centro de Astrobiología (CAB) to mimic Martian surface conditions (i.e. temperature, pressure, atmospheric composition, UV radiation). MARTE was previously used for testing electromechanical instruments for space missions in analogue conditions (Sobrado *et al.* 2014). Table 3.1 lists the MARTE chamber specifications and the corresponding Martian environmental conditions.

University Valley cryptoendoliths were placed into MARTE for a 96-hour total exposure (Figure 3.2). Subsamples were removed at the following time points: 24 hours (sample T1_M), 72 hours (sample T2_M), and 96 hours (sample T3_M). This information, as well as the corresponding sols based on UVC dose and DNA content as determined by the Qubit 3.0 Fluorometer from Invitrogen with the dsDNA HS Assay Kit (Q32854), is detailed in Table 3.2. A “time zero” sample

Table 3.1. Environmental conditions in MARTE and on Mars.

	MARTE	Mars
Temperature (°C)	-15	-123 to +25 (Horneck 2000)
Atmospheric pressure (mbar)	8	8 (Sobrado <i>et al.</i> 2014)
Atmospheric composition	>95% CO ₂ , 5% air+H ₂ O	95% CO ₂ , 2.7% N ₂ , 1.6% Ar, 0.13% H ₂ O, 0.08% CO (Sobrado <i>et al.</i> 2014)
UV source	Xenon, negligible deuterium	Sun
UV radiation (nm)	225 – 395	200 – 400 (Schuerger <i>et al.</i> 2003)

(T_{0M}) was kept frozen at -25 °C outside the chamber. A completely sterilized sandstone rock sample (NC_M) was kept within the chamber for the duration of the exposure and used as a negative control; this sterilized sample served as a proxy for possible exogenous contamination during the manipulation of the rest of the samples. NC_M was initially dried at 105°C, followed by ignition in a muffle furnace for 2 hours at 360 °C (Nelson and Sommers 1996). The MARTE exposure subjected samples T1_M, T2_M, and T3_M to the following conditions: chamber interior temperature of -15 °C (taking <1 hour to from ambient temperature to reach -15 °C), atmospheric pressure of 8 mbar with an atmospheric composition of >95% CO₂ (remaining <5% comprised of air and water), and Xenon UV exposure of UVA (320-395 nm): 1.46 W/m², UVB (265-322 nm): 0.33 W/m², and UVC (225-280 nm): 0.25 W/m² (Table 3.3). MARTE’s deuterium source was also applied from day 2 of the exposure onward; however, the deuterium lamp lost its emissivity at 160 nm and its remaining radiation was negligible. We have thus chosen to focus our UV dose calculations and estimations solely on the Xenon source emissions.

UV doses were calculated using COMIMART (COMplutense and MICHigan MARS Radiative Transfer model) (Vicente-Retortillo *et al.* 2015). COMIMART calculates the solar

irradiation in several bands (UV to NIR) on the surface of Mars. Using the Phoenix lander site (68.2188°N, 125.7492°W), an assumed opacity of 0.42 (the average opacity measured during the

Table 3.2. Exposure time and DNA content in the MARTE samples.

Sample	Exposure time (days)	Equivalent exposure time based on UVC (sols)	DNA content (ng/μl)
T0 _M	0	0	2.04
T1 _M	1	14.4	1.59
T2 _M	2	28.8	7.70
T3 _M	4	57.6	11.5



Figure 3.2. The MARTE vacuum chamber. Clockwise from left: MARTE exterior; interior and sample holder from MARTE's viewport containing University Valley cryptoendoliths; side view of University Valley cryptoendoliths in the MARTE sample holder.

Table 3.3. UV irradiation and doses for MARTE from the Xenon source emissions.

UV band	Range (nm)	Irradiation (W/m²)	Irradiation dose per 24 hours (MJ/m²)
UVA	320-395	1.46	0.126144
UVB	265-322	0.33	0.028512
UVC	225-280	0.25	0.0216

Phoenix mission), and solar longitude values between 0° and 359° (where 0° corresponds to the Martian spring equinox, 90° corresponds to the Martian northern summer solstice, 180° corresponds to the Martian autumn equinox, and 270° corresponds to the northern winter solstice); this range corresponds to a Martian year. We determined the range of irradiation doses on the surface of Mars, inside of MARTE, and their equivalents in Martian sols (Table 3.4).

3.3.3 UVC chamber construction and exposure

The UVC chamber was custom built at McGill University. Two Philips 13 W TUV 2-pin germicidal twin tube CFL bulbs were connected within a modified McMaster-Carr 13.5” x 10” x 5.5” plastic protective storage case with foam using two Leviton Gx23-2 base 2-pin fluorescent lampholders and a Philips Advance Magnetic Ballast 13W Plug-in CFL. Power was controlled using a 2-position Rocker switch and the chamber was sealed with Dow Corning potting silicone. UVC output was monitored with a General Tools & Instruments UV512C Digital UVC Meter. Triplicate samples of University Valley cryptoendoliths together with two negative controls per sample type (one covered inside of the UVC chamber; one sterilized in the same manner as NC_M and uncovered inside of the UVC chamber) were placed in a grid-like formation within the chamber (Figure 3.3) which itself was situated in an incubator held at –20 °C and ambient air pressure. The chamber conditions are detailed in Table 3.5.

Table 3.4. Irradiation doses at the Phoenix lander site on Mars based on the UVA, UVB, and UVC irradiation and the equivalent time in sols of MARTE exposure at various solar longitudes (Ls). These values assume an opacity of 0.42 and are calculated using the COMMIMART model. “Equivalent in sols (MARTE)” refers to the equivalent of 1 terrestrial day based on the UVA, UVB, or UVC dose.

	UVA	UVB	UVC
Ls 0 (Mars) (MJ/m ²)	0.191	0.06	0.01
Equivalent in sols (MARTE)	0.66	0.48	1.71
Ls 90 (Mars) (MJ/m ²)	0.69	0.22	0.05
Equivalent in sols (MARTE)	0.18	0.13	0.44
Ls 180 (Mars) (MJ/m ²)	0.22	0.07	0.01
Equivalent in sols (MARTE)	0.59	0.42	1.52
Ls 323 (Mars) (MJ/m ²)	0.22	0.005	0.0015
Equivalent in sols (MARTE)	0.099	4.32	14.4

Samples were removed at the following time points: 14 days (sample T1_{UV}), 28 days (sample T2_{UV}), 42 days (sample T3_{UV}), and 56 days (sample T4_{UV}). Two negative controls were included: an unsterilized, covered control and a sterilized, uncovered control. Table 3.6 details the time exposed, corresponding sols, and DNA content of these samples as determined by the Qubit 3.0 Fluorometer from Invitrogen with the dsDNA HS Assay Kit (Q32854). Sample T0_{UV} was unexposed, kept frozen at -25 °C, and represents time zero. UVC doses and corresponding sols were calculated using the COMIMART radiation model at the Phoenix lander site, as described in the previous section and in Supplementary Table 3.1 (Vicente-Retortillo *et al.* 2015).

Table 3.5. UVC chamber and Mars conditions.

	Total area (cm²)	Number of bulbs at 254 nm (UVC)	UV output per bulb (W)	Total UV output (W)	Average UVC flux (W/m²)
UVC chamber	372.22	2	13	52	~4 – 70
Mars	N/A	N/A	N/A	N/A	~0.9 – 1.2



Figure 3.3. Custom UVC chamber containing University Valley cryptoendoliths. Unsterilized, covered negative control is circled in red. Sterilized and uncovered negative control is circled in blue.

Table 3.6. UVC chamber exposure time and DNA content. Equivalent exposure time is based on COMMIMART at Ls 323 and the irradiance average produced by the UVC chamber, which is assuming that the irradiance values produced correspond to the entire UVC range and with the typical shape of the Martian solar spectrum.

Sample	Exposure time (days)	Equivalent exposure time based on UVC dose (sols/ Martian years)	DNA content (ng/μl)
T0 _{UV}	0	0/0	0.586
			0.236
			0.315
T1 _{UV}	14	25 301/ 37.8	1.64
			0.248
			1.89
T2 _{UV}	28	55 580/ 83.1	0.0820
			0.289
			Below limit of detection
T3 _{UV}	42	109 939/ 164.4	0.063
			Below limit of detection
			Below limit of detection
T4 _{UV}	56	185 636/ 277.6	0.0535
			0.0499
			Below limit of detection

3.3.4 DNA extraction and MinION sequencing

After the 4-day MARTE exposure and the 56-day UV chamber exposure, DNA was extracted from all samples using the Qiagen DNeasy PowerLyzer PowerSoil DNA kit (Cat No./ID: 12855-50) according to the manufacturer's protocol, save that the elution step was performed in four subsequent stages using 50 μL nuclease-free water: each time point was split into four subsamples for extraction and each subsample eluate was used as the elution liquid for the following subsample extraction in order to maximize DNA yield. Extractions were prepared for sequencing using the Rapid PCR Barcoding kit (SQK-RPB004) and sequenced with a MinION

Mk1b device on an R9.4 FLO-MIN106 flow cell. MARTE sequences were basecalled with MinKNOW version 1.7.7 and trimmed using Porechop version 0.2.4 (<https://github.com/rrwick/Porechop>). UVC chamber sequences were basecalled and trimmed with MinKNOW version 22.05.5. This updated version of MinKNOW contained trimming parameters; Porechop was not needed.

MARTE sequences were corrected, trimmed, and assembled using Canu version 2.1.1 (Koren *et al.* 2017) and the following parameters: “stopOnLowCoverage=1,” “correctedErrorRate=0.16,” and “genomeSize=5.0M.” Sequences were polished using nanopolish version 0.13.2 and default parameters (Loman *et al.* 2015). Mapping and indexing were performed with minimap2 version 2.17 (Li 2018) and samtools version 1.11 (Li *et al.* 2009), respectively. Polished contigs were then uploaded to JGI IMG/M ER (Markowitz *et al.* 2011) for annotation. UVC chamber sequences were too few in number for Canu correction and assembly, and as such were annotated with Kaiju version 1.8.2 (Menzel *et al.* 2016).

3.3.5 Life Detector Chip (LDChip) biomolecule detection

We analyzed the samples with the LDChip to search for potential biomarkers. The LDChip is the core of the SOLID (Signs of Life Detector) instrument which encompasses 200 polyclonal antibodies raised against microbial cells (bacteria and archaea), extracellular polymeric substances (EPS), spores, and proteins involved in oxidative stress and the main microbial metabolic processes (Rivas *et al.* 2008; Sánchez-García *et al.* 2018a; Sánchez-García *et al.* 2020). A total of two 0.5 g replicates of each sample were suspended in 2 ml of TBSTRR extraction buffer (0.4 M Tris-HCl pH 8, 0.3 M NaCl, 0.1% Tween 20), vortexed and sonicated in a hand-held ultrasonic

homogenizer UP200Ht (Hielscher Ultrasound Technology) to extract the organic matter. Three cycles of sonication were applied to each sample, and the liquid extracts were filtered to reduce coarse material with a 20 μm pore size diameter. Aliquots of 50 μl were analyzed by a fluorescent Sandwich Microarray Immunoassay (FSMI) as previously described (Blanco *et al.*, 2015). Briefly, filtrates were incubated for 1 hour at room temperature (RT), washed three times, and finally, a fluorescent mixture of the 200 antibodies, was incubated at RT for 1 h. After a final wash step, the arrays were scanned and analyzed with the Gene pix pro 7.0 software (Molecular Devices LLC, CA, USA). The fluorescence intensity of each positive antigen-antibody pair was calculated and considered positive only when its value was at least 2.5 times over the background level and a signal-to-noise ratio (SNR) higher than 3 (Blanco *et al.* 2012; Rivas *et al.* 2011). Positive fluorescence values that T0_M and T3_M had in common were statistically analyzed with a T-test. This statistical test was performed on added values per antibody category and visualized on boxplots, both carried out in R computing language (Team 2013).

3.3.6 Lipid extraction and analysis

Lyophilized and ground subsamples (7.5 g) of T0_M and T3_M were extracted with ultrasound sonication (3 x 15 minutes) using a 3:1 (v/v) mixture of dichloromethane (DCM) and methanol (MeOH) to obtain a total lipid extract (TLE). Prior to extraction, tetracosane-D₅₀, myristic acid-D₂₇ and 2-hexadecanol were added as internal standards.

The clean, concentrated, and desulfurized TLE (Sánchez-García *et al.* 2018a) was hydrolyzed overnight with KOH (6% MeOH) at room temperature (Grimalt *et al.* 1992). *n*-Hexane and HCl (37%) were then used to separate the neutral and acidic (liberated carboxylic groups)

fractions from the hydrolyzed extract (Sánchez-García *et al.* 2020). Further separation of the neutral fraction into non-polar (hydrocarbons) and polar (alkanols and sterols) was done according to Sánchez-García *et al.* 2020b. Prior to analysis, the acidic fraction was transesterified with BF₃ in MeOH to produce fatty acid methyl esters (FAMES) and the polar fraction trimethylsilylated (N,O-bis [tri- methylsilyl] trifluoroacetamide [BSTFA]) to analyze the resulting trimethyl silyl alkanols as in (Sánchez-García *et al.* 2020).

All fractions were analyzed using gas chromatography-mass spectrometry (GC–MS) using a 6850 GC System coupled to a 5975C VL MSD Triple-Axis detector (Agilent Technologies, Santa Clara, CA, USA) that operated in conditions described in Sánchez-García *et al.* 2018. Compound identification was based on retention time and mass spectra comparison with reference materials and the NIST mass spectral database. Quantification was performed with the use of external calibration curves of *n*-alkanes (C₁₀ to C₄₀), FAMES (C₆ to C₂₄) and *n*-alkanols (C₁₄, C₁₈ and C₂₂), all supplied by Sigma-Aldrich (Madrid, Spain). Recovery of the internal standards was measured to average $72 \pm 18\%$.

3.4 Results

3.4.1 DNA remained detectable and sequenceable after exposure in MARTE and in the UVC chamber

Based on the UVC dose, 1 day in MARTE corresponds to between 0.44 and 14.4 Martian sols (Table 3.4). The UVC irradiation inside of MARTE most closely resembled irradiation at the Phoenix lander site in winter, specifically Ls 323 (Table 3.3). At a solar longitude of 323°, our 4-

day exposure can be assumed to simulate an equivalent of 57.6 Martian days; we have thus chosen to discuss our results based on this calculation.

DNA was still detectable from the University Valley cryptoendolith community during and after exposure in MARTE. The DNA content from T0_M (2.04 ng/μl) to T3_M (11.5 ng/μl) varied, exhibiting no clear pattern or linear decrease with exposure (Table 3.2). MinION sequencing of the University Valley cryptoendoliths before and after exposure revealed a community dominated by algae as Chlorophyta (Chlamydomonadales, Trebouxiophyceae) and Cyanobacteria (Synechococcales, Nostocales) (Figure 3.4). Proteobacteria as Hyphomicrobiales and Burkholderiales are the next most prominent taxa present.

To supplement the MARTE exposure and further examine the MinION's ability to detect DNA in Mars analogue samples after exposure to extreme Mars-like conditions, we exposed the University Valley cryptoendoliths samples to a UVC chamber at -20 °C for 56 days. This exposure corresponded to ~278 Martian years based on the UVC dose (Table 3.6). Like the exposure in MARTE, DNA remained detectable and sequenceable after the UVC exposure. DNA concentration appeared to decrease overall from T0_{UV} (0.236 – 0.586 ng/μl) to T4_{UV} (0.0499 – 0.0535 ng/μl), although a slight increase from T0_{UV} to T1_{UV} (0.248 – 1.89 ng/μl) was observed (Table 3.6).

The microbial community at T0_{UV} contained primarily Ascomycota (Helotiales, Eurotiales, and Umbilicariales), followed by Acidobacteria and Proteobacteria (Hyphomicrobiales, Burkholderiales) (Figure 3.5). Over the course of the UVC chamber exposure, the University Valley cryptoendolith community changed, with decreases in Ascomycota and increases in Proteobacteria, Cyanobacteria (Nostocales, Oscillatoriales), and Actinobacteria (Propionibacteriales).

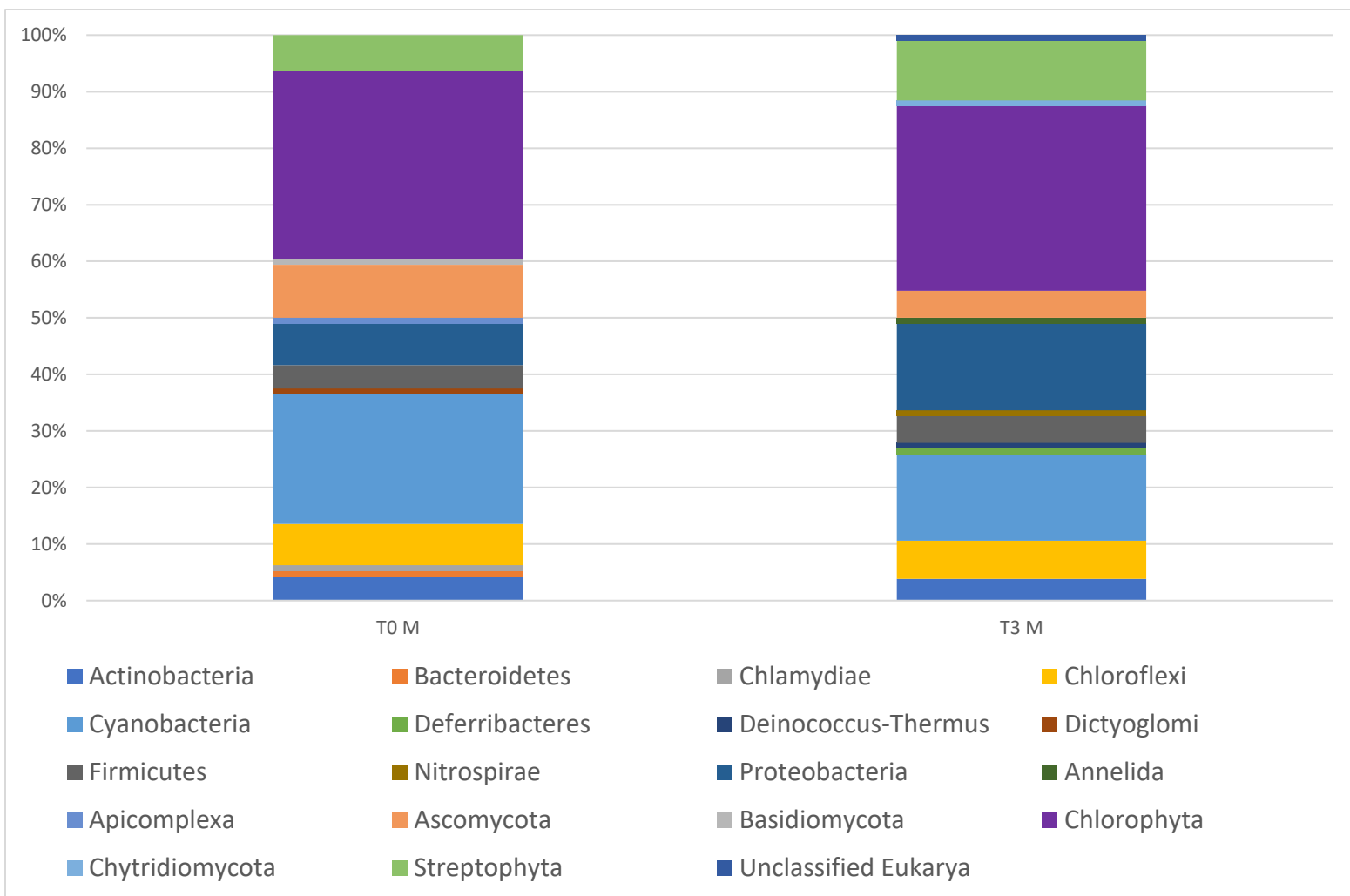


Figure 3.4. Community composition at the phylum level of the University Valley cryptoendoliths at T0_M and T3_M (MARTE samples) as revealed by MinION sequencing.

3.4.2 Protein profile changes in MARTE as revealed by LDChip immunoassays

The LDChip revealed immuno-detection of several microbial markers corresponding to different taxa and metabolisms, and MARTE exposure to the University Valley cryptoendoliths altered their protein content and profile in several ways (Figure 3.6). In terms of taxonomy, the

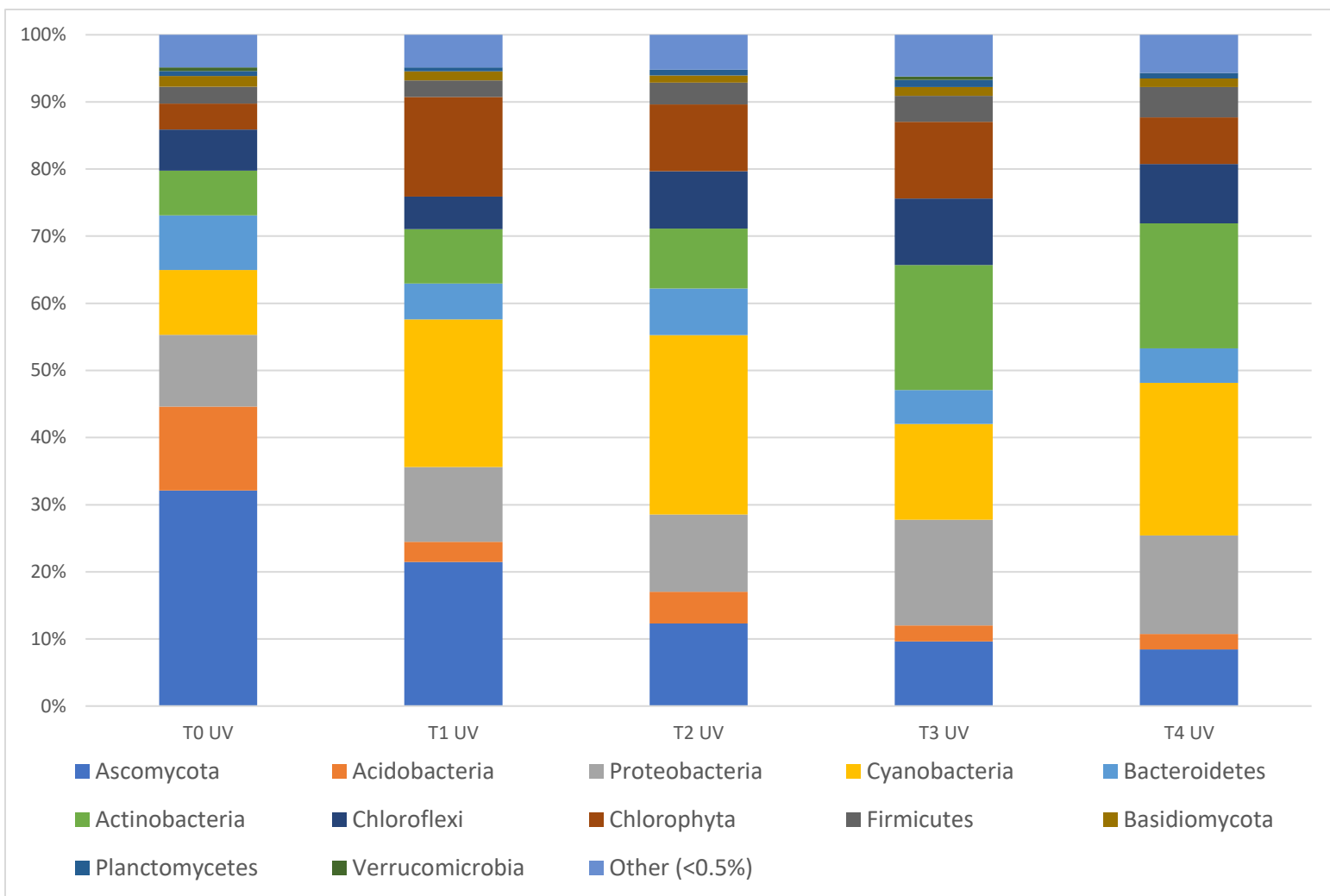


Figure 3.5. Community composition at the phylum level of the University Valley cryptoendoliths (UVC chamber samples) at T_{0UV}, T_{1UV}, T_{2UV}, T_{3UV}, and T_{4UV} as revealed by MinION sequencing.

cryptoendolith community at T_{0M} was dominated (>50%) by Proteobacteria, chiefly as Gammaproteobacteria. Betaproteobacteria and Cyanobacteria as Cyanophyceae were secondarily present. After exposure, statistically significant changes in taxonomy occurred; Alphaproteobacteria, Deltaproteobacteria, and Firmicutes (Clostridia) decreased in the

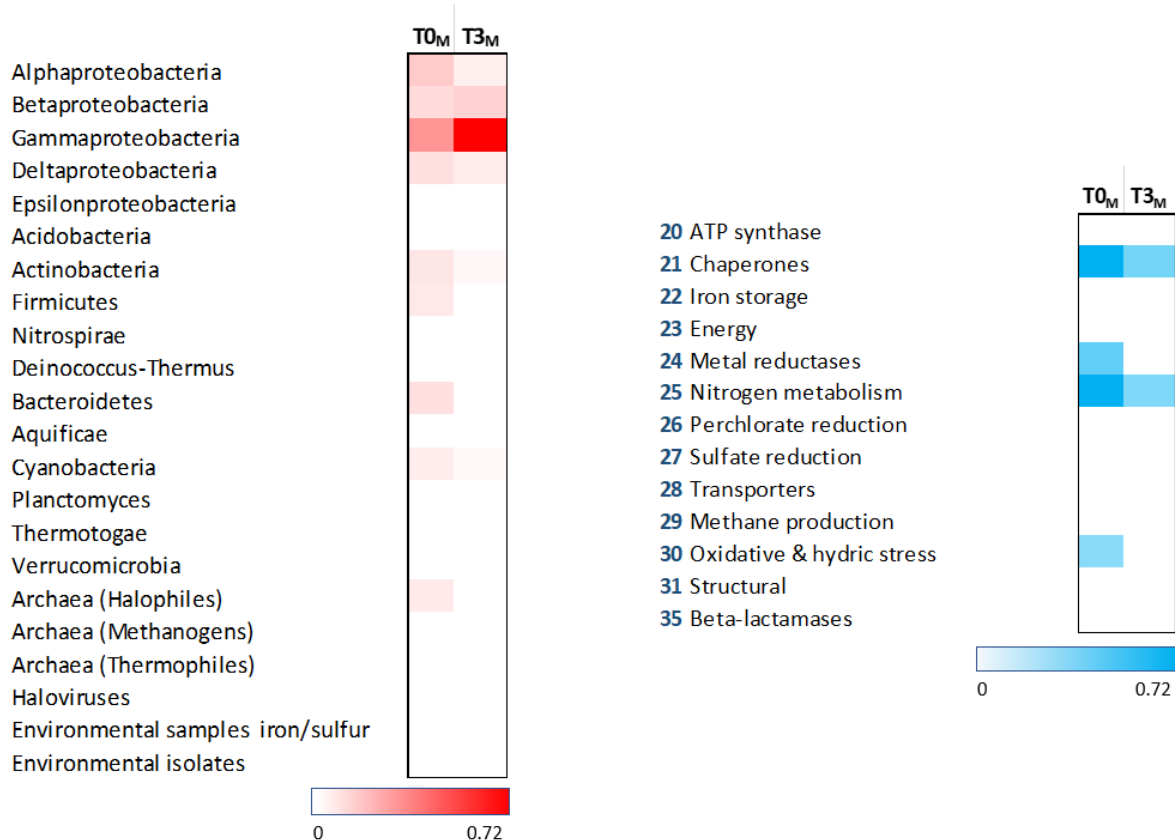


Figure 3.6. LDChip-generated heat map displaying the protein content and microbial diversity of T0_M and T3_M from the University Valley cryptoendoliths. The colour intensity corresponds to the relative fluorescence intensity.

cryptoendolith community. Conversely, Betaproteobacteria (*Polaromonas* and *Dechloromonas*) and Gammaaproteobacteria (*Acidithiobacillus* and *Halothiobacillus*) increased after exposure (Figure 4.6 and Supplementary Figure 3.1). The metabolic profile of the samples was also altered. Chaperone proteins and nitrogen fixation proteins decreased from T0_M – T3_M while metal reductases disappeared entirely after MARTE exposure.

3.4.3 MARTE exposure altered the lipid content of the University Valley cryptoendoliths

Post-exposure in MARTE, there was an overall increase in the cell membrane-derived compounds (i.e. lipid biomarkers) from T0_M to T3_M, with a few exceptions (Figure 3.7). Low molecular weight (LMW) unsaturated alkanes (C_{17:1}, C_{18:1} and C_{19:1}; Figure 3.7b) likely related to Cyanobacteria (Coates *et al.* 2014), high molecular weight (HMW) alkanols (\geq C₂₈; Figure 3.7e), some unknown methylated alkanes (Figure 3.7b) or alkanols (Figure 3.7f), and some compounds from the polar fraction (desmosterol or alkenones; Figure 3.7f) decreased after exposure to MARTE. Otherwise, most compounds in the three polarity fractions increased after radiation. The overall increase in most lipids after exposure may be due to cell degradation and release of cell membrane components (i.e. lipids). In general, linear and saturated fatty acids (i.e. *n*-fatty acids) were greater in abundance in both T0_M and T3_M than the homologous *n*-alkanes and *n*-alkanols (Figure 3.7c vs. 3.7a and 3.7e).

Overall, in the University Valley cryptoendoliths there was a prevailing presence of eukaryotic lipid biomarkers, such as HMW linear and saturated compounds (i.e. >20 carbons; Figure 3.7a, 3.7c and 3.7e). These compounds are often associated with higher plants (e.g. *n*-C₂₅ and *n*-C₂₇ alkanes; *n*-C₂₆ and *n*-C₂₈ fatty acids; and *n*-C₂₉ alkanol) (Eglinton and Hamilton 1967; Hedges and Prahl 1993; Otto *et al.* 2005), sterols also derived from plants or algae (campesterol or β -sitosterol) (Martin-Creuzburg and Merkel 2016; Volkman 1986) or from animal (i.e. crustacean) sources (desmosterol) (Meyers 1997) (Figure 3.7f). In addition, the peak of phytol (Figure 3.7f), the esterifying alcohol of cyanobacterial and green-plant chlorophylls (Didyk *et al.* 1978), revealed abundance of phototrophs, either eukaryotic or prokaryotic. In the acidic fraction,

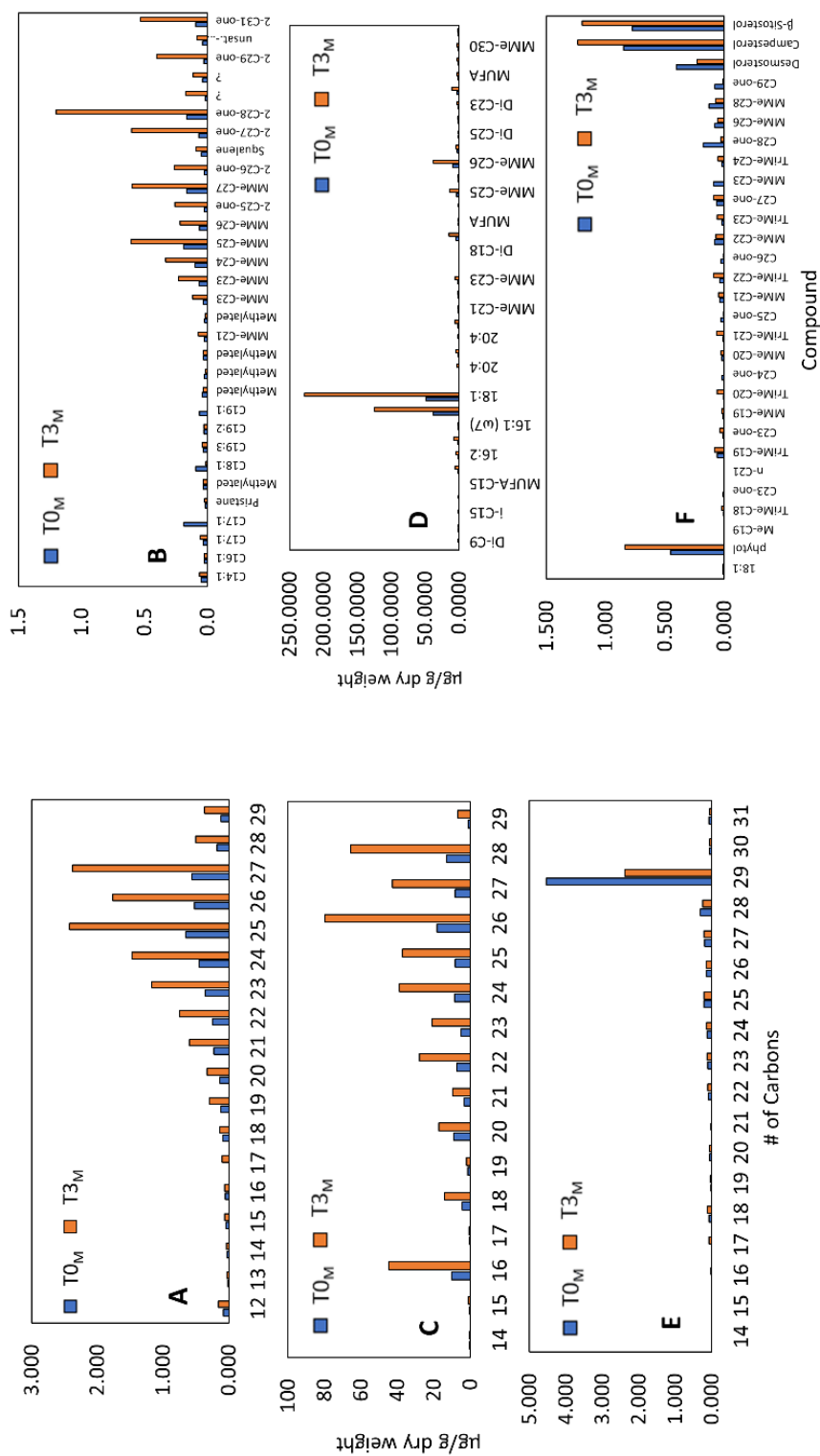


Figure 3.7. Molecular lipid profile of the University Valley cryptoendoliths at T_{0M} and T_{3M}. From top left: A) *n*-alkanes; B) other apolar compounds; C) *n*-fatty acids; D) other acids; E) *n*-alkanols; F) other polar compounds. In a, c, and e, simple numbers in the x-axis refer to the number of carbons in the chain. In b, d, and f, unsaturated compounds are represented as C_x:_y, where x stands for the total number of carbons and y the number of unsaturations (i.e. double bonds). Mme-C_x and TriMe-C_x refer to compounds of x carbons with one or three methyl groups, respectively, and “methylated” to unknown compounds with one or more methyl groups. In b, 2-C_x-one stands for 2-alkenones of x carbons; “unsat.” For an unknown unsaturated compound; and “?” for an unidentified hydrocarbon. In d, MUFA refers to monounsaturated fatty acids and Di-C_x dicarboxylic acid of x carbons.

there was also a high relative abundance of hexadecenoic acid (C₁₆), ubiquitous in prokaryotic and eukaryotic sources (Harwood 2012).

3.5 Discussion

3.5.1 Changes in DNA content post-MARTE and UVC chamber exposure

Over the course of the MARTE exposure, the DNA content in the University Valley cryptoendoliths changed, but exhibited no clear pattern over time (Table 3.2). This variation may be the result of the natural heterogeneity present in cryptoendolith samples (Mergelov *et al.* 2018; Wierzchos *et al.* 2015). DNA was successfully detected and able to be sequenced after the ~58 sol exposure in MARTE indicating that the MinION can be used to detect DNA on samples exposed to short-term Martian environmental conditions. Of the myriad extreme, destructive environmental effects on Mars (e.g. freezing temperatures, limited water and nutrient availability), UV radiation, particularly UVC (200 – 280 nm), is the most detrimental to cellular survival (Cockell *et al.* 2005; Johnson *et al.* 2011; Schuerger *et al.* 2003; Schuerger and Nicholson 2006). UVC exposure causes extensive cellular machinery and biomolecule damage, as well as effecting DNA directly via the formation of pyrimidine dimer and photoproducts, strand breaks, and base modifications (Douki 2013; Friedberg *et al.* 2006; Nicholson *et al.* 2018). As such, we exposed University Valley cryptoendolith samples to a UVC exposure corresponding to ~278 Martian years to further evaluate the MinION's performance at DNA detection in Mars-like conditions.

The DNA content of the University Valley cryptoendoliths after UVC exposure overall decreased, although with a slight increase from T_{0UV} to T_{1UV} (Table 3.6). Like the DNA

concentration from the MARTE incubation (T_{0M} to T_{3M}), this discrepancy may be accounted for by the natural variation in cryptoendolith biomass (Mergelov *et al.* 2018; Wierzchos *et al.* 2015). The initial taxonomy at T_{0UV} was dominated by Ascomycota (Helotiales, Eurotiales, and Umbilicariales), Acidobacteria and Proteobacteria (Hyphomicrobiales, Burkholderiales) (Figure 3.5). This classification differs from T_{0M} , in which Chlorophyta (Chlamydomonadales, Trebouxiophyceae) and Cyanobacteria (Synechococcales, Nostocales) were dominant (Figure 3.4). As exposure time in the UVC chamber progressed, the microbial community was altered, growing to favour Proteobacteria (Hyphomicrobiales, Burkholderiales), Cyanobacteria (Nostocales, Oscillatoriales), and Actinobacteria (Propionibacteriales) over Ascomycota and Acidobacteria. The difference between the taxonomy of the MARTE and UVC-exposed samples may be due to a combination of different classification pipelines (JGI IMG/M ER vs. Kaiju), as well as the previously mentioned natural variation within cryptoendolithic samples (Mergelov *et al.* 2018; Wierzchos *et al.* 2015). Additionally, samples from the UVC incubation (T_{0UV} to T_{4UV}) were sequenced in triplicate, while MARTE incubation samples were sequenced as technical replicates; this difference may also account for the differences in taxonomy between incubations, and in combination with the MinION's inherently high error rate, may not be perfectly representative of the cryptoendolithic community present. However, in conjunction with results from the LDChip and cell membrane-derived lipid analyses (discussed below), as well as comparison with previous reports of the University Valley cryptoendolithic community (Goordial *et al.* 2016a; Mergelov *et al.* 2018; Wierzchos *et al.* 2015), we believe that our interpretations are broadly accurate and our overall goal of DNA detection after Mars environmental exposure has been achieved.

Of the taxa detected by MinION sequencing after MARTE and UVC chamber exposure, Nostocales in particular are known to survive well under simulated Mars conditions, with *Nostoc* sp. exhibiting a survival rate of 72% under a Mars-like stratosphere environment (Ye *et al.* 2021). UV acts as the primary deleterious effect on the survival of most microbes under Mars environmental conditions (Cockell *et al.* 2005) and has been previously shown to impede the detection of cyanobacterial DNA (from *Chroococcidiopsis* sp. CCME 029) (Baqué *et al.* 2016). A 383-sol exposure of Mars-like UV (~50 W/m²) on *Chroococcidiopsis* sp. CCME 029 precluded PCR detection of DNA, but when *Chroococcidiopsis* cells were combined with Mars simulant soil, PCR fingerprints were observed. These results are further supported by experiments on *Bacillus* spp.; Fajardo-Cavazos *et al.* (2010) found that ~90% of *Bacillus* DNA molecules exposed were inactivated and unable to act as effective templates for qPCR after 60 minutes of exposure to Martian pressure, atmospheric composition, and 4.1 W/m² of UVC irradiation (Fajardo-Cavazos *et al.* 2010). A separate experiment on *Bacillus* spores found that 99.9% of viability was lost within the first 5 minutes of exposure, but when shielding was provided by *Bacillus* cell monolayers or soil layers <1 mm thick, cellular survival was found to increase to an equivalent of 115 Martian sols (4 W/m² of UVC irradiation, -10 °C, 0.7 kPa) (Nicholson *et al.* 2018). Natural environmental matrices are known to protect their communities from the deleterious effects of Mars-like surface conditions and enhance biosignature detectability (Hansen *et al.* 2009; Onofri *et al.* 2013). These results are consistent with what we observed in the present work; the natural environmental matrix of the University Valley cryptoendolithic rock provided effective shielding and likely enabled DNA detection and sequencing after ~278 years of Mars-like UVC. The MinION sequencing protocol used in this work also required a nonspecific PCR step, further demonstrating that the exposure did not prevent DNA from being used as an effective PCR template. Future investigations

will need to repeat these experiments for longer durations to determine exactly how long DNA detection with the MinION is possible after exposure to Mars-like environmental conditions and UVC radiation.

3.5.2 Protein and lipid biomolecule changes during the MARTE exposure

Statistically significant changes in the microbial and metabolic protein profile were observed via the LDChip; specifically, Alphaproteobacteria, Deltaproteobacteria, and Clostridia (Firmicutes) decreased while Betaproteobacteria (*Polaromonas* and *Dechloromonas*) and Gammaproteobacteria (*Acidithiobacillus* and *Halothiobacillus*) signals strongly increased after exposure (Figure 3.6; Supplementary Figure 3.1). Chaperone proteins, nitrogen fixation proteins (NifD, NifH, NifS), and metal reductases decreased with MARTE exposure. This pattern indicates a decrease in metabolic functionality over the course of the exposure as the extreme Mars-like conditions inhibit survival and viability of the community (Cockell *et al.* 2005; Diaz and Schulze-Makuch 2006; Ye *et al.* 2021). The increase of *Acidithiobacillus* and *Halothiobacillus* may signify a greater tolerance of Martian conditions than other community members, which may be a side effect of their halotolerance; halophiles and halotolerant microbes typically have robust DNA repair mechanisms, high Mn/Fe ratios for general stress protection, and their intracellular halides can act as scavengers for reactive oxygen species (ROS) (Johnson *et al.* 2011; Kish *et al.* 2009; Kottemann *et al.* 2005; Santos *et al.* 2019), all of which may contribute not only to desiccation resistance in salty environments but also radiation resistance and oxidative stress tolerance. Indeed, species of *Acidithiobacillus* have been previously shown to survive short-term exposure to Martian conditions when protected by <5 mm of regolith or rock (Gómez *et al.* 2010).

Lipid changes over the exposure involved an overall increase of biomarkers (*n*-alkanes, *n*-fatty acids, phytosterols, branched and unsaturated alkanes and fatty acids) likely signifying the destruction of cellular membranes and further release of free lipid chains, which are the lipid compounds targeted by the extraction protocol applied here. While the signal of some cyanobacterial (C_{17:1}, C_{18:1}, C_{19:1}), algal (2-alkenones), or animal (desmosterol) biomarkers decreased, most biomarker signals, specifically those assigned to phototrophs (i.e. phytol, HMW *n*-alkanes and *n*-fatty acids, phytosterols, or unsaturated fatty acids) increased after MARTE exposure. Thus, the lipid results reflect a greater survival of photoautotrophic remnants.

The photoautotrophs detected by the LDChip in the University Valley cryptoendoliths are known to survive and retain some viability under Mars-like conditions. Specifically, Cyanobacteria such as *Nostoc* sp. have a relatively low (28%) death rate in Mars-like conditions (Ye *et al.* 2021). *Chroococcidiopsis* spp. die within 30 minutes of exposure to Martian environmental conditions (UVC, UVB, and UVA flux of 3.73, 8.27, and 37.67 W/m², respectively), but survival and viability is increased up to 8 hours when protected by a sandstone matrix (Cockell *et al.* 2005) and biosignatures from *Chroococcidiopsis* (e.g. DNA, carotenoids) remained detectable after a 3-month exposure (average UV flux of ~50 W/m²) (Baqué *et al.* 2016). The desiccation tolerance of *Nostoc* and *Chroococcidiopsis* enables strong radiation tolerance through sub-cellular structure stability and the ability to readily enter metabolic dormancy, and this resistance may account for the detection of *Nostoc* and *Chroococcidiopsis* in the University Valley cryptoendoliths via the LDChip before and after MARTE exposure (Mosca *et al.* 2019; Potts 1999).

3.5.3 The University Valley cryptoendolith community may be dominated by photoautotrophs

DNA, proteins, and lipids were all detectable pre- and post-MARTE exposure in the University Valley cryptoendolith communities, and these biosignatures revealed a community that may be dominated by photoautotrophs. In T0_M and T3_M, Cyanobacteria and Chlorophyta comprise >50% and ~47% of the microbial community based on MinION sequencing, respectively (Figure 3.4). Conversely, the LDChip detected higher amounts of Proteobacteria (Alphaproteobacteria, Betaproteobacteria, and Gammaproteobacteria) than photoautotrophs (Figure 4.6). The prevalence of HMW linear and saturated compounds in the lipid profile of T0_M and T3_M signifies the presence of eukaryotes as higher plants or algae (Eglinton and Hamilton 1967; Hedges and Prahl 1993; Volkman *et al.* 1998), further supporting the dominance of photoautotrophs in this community (Figure 3.7). Algae are indicated in the lipid profile via the presence of monomethyl-HMW alkanes and 2-alkanones and Cyanobacteria via the presence of monounsaturated LMW alkanes, pristane, mono- and diunsaturated C18 acids (Ahlgren *et al.* 1992; Cranwell 1978; Dijkman *et al.* 2010; Parenteau *et al.* 2014; Volkman *et al.* 1980), all of which increased post-exposure. Phytol and phytosterols were also present, potentially from photoautotrophs as higher plants or algae (Didyk *et al.* 1978; Luo *et al.* 2019; Meyers 1997; Vega-García *et al.* 2021; Volkman *et al.* 1998). Vegetation in Antarctica is scarce and is mostly distributed in moist habitats and in Maritime Antarctica (Cabrerizo *et al.* 2016; Carrizo *et al.* 2019; Vega-García *et al.* 2021; Velázquez *et al.* 2013). Yet, the presence of plant-derived lipids (mosses or vascular plant remnants) from a period in Antarctica when the climate was warmer and vegetation more abundant (e.g., Mid-Miocene or Eocene) has been documented in the McMurdo Ice Shelf (Lezcano *et al.* 2022). Plant lipids

degrade minimally and can be preserved over geological time periods (Brocks *et al.* 2003), even more so if favoured by preservation strategies (e.g. xeropreservation or protective organic-mineral interactions (Sánchez-García *et al.* 2018a; Wilhelm *et al.* 2017).

The taxonomy of University Valley cryptoendoliths was previously found to be dominated by heterotrophic bacteria and fungi (Acidobacteria and Lecanoromycetes, respectively) (Goordial *et al.* 2016a). Cryptoendoliths are often categorized based on whether their photoautotrophic community is Cyanobacteria- or lichen-dominated. Lichen-dominated cryptoendoliths are common in Antarctic sandstone (Friedmann 1982; Zucconi *et al.* 2016); however, another 16S/18S rRNA survey of University Valley cryptoendoliths found Cyanobacteria as the prevalent community members, followed by Proteobacteria and lichenizing fungi (Archer *et al.* 2017). Our initial taxonomy of the University Valley cryptoendoliths varied between T0_M and T0_{UV}, with T0_M containing primarily photoautotrophs (Chlorophyta and Cyanobacteria) and T0_{UV} containing Ascomycota, Acidobacteria, and Proteobacteria, probably because of natural variation of the sample (Mergelov *et al.* 2018; Wierzchos *et al.* 2015). The orders of Ascomycota present (Helotiales and Umbilicariales) in T0_{UV} are lichenizing fungi (Larson 1983; Suija *et al.* 2015), suggesting that the University Valley cryptoendoliths can vary between Cyanobacteria- and lichen-dominated depending on the localized area of sampling.

3.5.4 Implications for extant life detection with MinION sequencing

Like proteins and cell membrane-derived lipids, DNA is an unambiguous sign of extant or recently extinct life. Extant life has not been a target for missions to Mars since the Viking biological experiments in the 1970s, the results of which remain controversial (Levin and Straat

2016; Navarro-González *et al.* 2010). Activity in both public and private space sectors is increasing, with some goals aiming for human explorers on Mars by 2040 (Linck *et al.* 2019; Musk 2017); microbial contamination with the arrival of humans on Mars would deleteriously effect our ability to detect and characterize native Martian life (Fairén *et al.* 2017; Rummel and Conley 2018; Spry *et al.* 2018). Adding DNA as a target biosignature and the MinION as a detection instrument to future Mars missions would enable extant life detection on Mars as well as identify forward contamination of terrestrial microorganisms. The ability to detect extant life on Mars would also contribute to further environmental characterization and contextualization of the Viking results (Banfield *et al.* 2021).

The MinION has previously been shown to operate in microgravity and *in situ* in extreme Mars analogue environments (Goordial *et al.* 2017; John *et al.* 2016; Johnson *et al.* 2017); however, this is the first work showing its functionality at detecting life in samples exposed to robust Mars-like conditions. Targets for sample collection on Mars should include those likely to preserve biosignatures and/or harbour extant life, such as lava tubes, subglacial lakes, or within rocks (de Vera *et al.* 2014; McKay *et al.* 1992; O'Connor *et al.* 2021; Orosei *et al.* 2018). DNA has a half-life of ~500 years, persisting in cold environments on the order of millions of years (Kaplan 2012; van der Valk *et al.* 2021), although this timeline would vary under the combined extreme pressures on the Martian surface. DNA was previously shown to be detectable via PCR after Mars-like exposure even when cells lose their colony-forming capabilities (Baqué *et al.* 2016), demonstrating that cells do not need to maintain viability for DNA to be detectable.

In the present work, the MinION could detect DNA from cryptoendolithic samples after ~58 sols of exposure to combined Martian environmental conditions in MARTE (i.e. Martian temperature, pressure, atmospheric composition, UV radiation) and after ~278 Martian years of

exposure to strong UVC radiation at $-20\text{ }^{\circ}\text{C}$ in the UVC chamber (although this exposure only involved UVC radiation and a polyextreme exposure may produce different timescales for DNA detection). These are not geological time scales and instead represent extant life detection. Our results therefore suggest that the MinION could detect extant or recently extinct life on Mars from naturally and quite recently exhumed samples (e.g. young Martian craters) (Quantin *et al.* 2016) or from target samples collected during missions (e.g. rocks harbouring cryptoendoliths, rock cores from Mars 2020 and the future *Rosalind Franklin* rover) (De Sanctis *et al.* 2017; Mangold *et al.* 2021). Additionally, the generation of sequences in real-time from the MinION would enable quick, reliable identification of samples for future caching (Goordial *et al.* 2017), as well as contamination monitoring to prevent potential forward contamination of the Martian biosphere by missions arriving there in subsequent decades (Fairén *et al.* 2017).

While there may exist shared ancestry between any putative Martian life and terrestrial organisms via lithopanspermia (Mileikowsky *et al.* 2000), the divergence would have occurred ~ 4 billion years ago, ensuring that Martian life would exist on a distant branch of the tree of life (Fairén *et al.* 2010), separate from modern terrestrial organisms and preventing any mistaken identity with common contaminants. Indeed, the MinION is also able to detect non-standard bases in nucleic acid chains, indicating its potential for agnostic life detection (i.e. biomolecule detection without presupposing biochemistry) (Carr *et al.* 2017; Johnson *et al.* 2018).

The MinION requires further development to reach a suitable technology readiness level (TRL) for planetary exploration missions, including integration of DNA extraction protocols, automated sequencing preparation, and the use of non-biological nanopores to prevent degradation during travel (Maggiore *et al.* 2020). Additionally, exact lower limits for detection in Mars simulation conditions and the exact effects of UVC radiation (e.g. DNA crosslinks and pyrimidine

dimers) on DNA detection with the MinION need to be constrained. However, this work shows that DNA is detectable from cryptoendoliths with MinION sequencing after up to ~278 Martian years of exposure to Mars-like conditions and demonstrates the MinION's potential viability in future extant life detection missions.

3.6 Conclusion

This study examines DNA, protein, and lipid detection in Mars analogue samples after a ~58-sol exposure to a Mars simulation chamber (MARTE), as well as DNA detection with MinION sequencing after strong UVC exposure for ~278 Martian years. MARTE exposure did not prevent successful DNA, protein, or lipid detection and resulted in changes in community composition (e.g. increase in some halotolerant community members). Lipid changes also signified the destruction of cellular membranes and the potential xeropreservation of plant lipids in the University Valley cryptoendoliths. Likewise, UVC exposure did not preclude DNA detection via MinION sequencing, suggesting that the MinION could be a promising tool for extant life detection on Mars for recently exhumed samples, as well as supporting biosignature detection results from protein immunoassays and gas chromatography-mass spectroscopy.

3.7 References

- Ahlgren G., Gustafsson I. B., and Boberg M. (1992) FATTY ACID CONTENT AND CHEMICAL COMPOSITION OF FRESHWATER MICROALGAE 1. *Journal of phycology*, 28: 37-50.
- Archer S. D., de los Ríos A., Lee K. C., Niederberger T. S., Cary S. C., Coyne K. J., Douglas S., Lacap-Bugler D. C., and Pointing S. B. (2017) Endolithic microbial diversity in sandstone and granite from the McMurdo Dry Valleys, Antarctica. *Polar Biology*, 40: 997-1006.
- Banfield D., Stern J., Davila A., Johnson S. S., Brain D., Wordsworth R., Horgan B., Williams R. M., Niles P., and Rucker M. (2021) Summary of the Mars Science Goals, Objectives, Investigations, and Priorities. *Bulletin of the American Astronomical Society*, 53: 142.
- Baqué M., Verseux C., Böttger U., Rabbow E., de Vera J.-P. P., and Billi D. (2016) Preservation of biomarkers from cyanobacteria mixed with Marslike regolith under simulated Martian atmosphere and UV flux. *Origins of Life and Evolution of Biospheres*, 46: 289-310.
- Benner S. A. (2017) Detecting Darwinism from molecules in the Enceladus plumes, Jupiter's moons, and other planetary water lagoons. *Astrobiology*, 17: 840-851.
- Blanco Y., Prieto-Ballesteros O., Gómez M. J., Moreno-Paz M., García-Villadangos M., Rodríguez-Manfredi J. A., Cruz-Gil P., Sánchez-Román M., Rivas L. A., and Parro V. (2012) Prokaryotic communities and operating metabolisms in the surface and the permafrost of Deception Island (Antarctica). *Environmental microbiology*, 14: 2495-2510.
- Brocks J. J., Buick R., Logan G. A., and Summons R. E. (2003) Composition and syngeneity of molecular fossils from the 2.78 to 2.45 billion-year-old Mount Bruce Supergroup, Pilbara Craton, Western Australia. *Geochimica et Cosmochimica Acta*, 67: 4289-4319.
- Cabrerizo A., Tejado P., Dachs J., and Benayas J. (2016) Anthropogenic and biogenic hydrocarbons in soils and vegetation from the South Shetland Islands (Antarctica). *Science of the Total Environment*, 569: 1500-1509.
- Carr C. E., Mojarro A., Hachey J., Saboda K., Tani J., Bhattaru S. A., Smith A., Pontefract A., Zuber M. T., and Doeblner R. (2017) Towards in situ sequencing for life detection. Aerospace Conference, 2017 IEEE. IEEE.
- Carrizo D., Sánchez-García L., Menes R. J., and García-Rodríguez F. (2019) Discriminating sources and preservation of organic matter in surface sediments from five Antarctic lakes in the Fildes Peninsula (King George Island) by lipid biomarkers and compound-specific isotopic analysis. *Science of The Total Environment*, 672: 657-668.
- Chan-Yam K., Goordial J., Greer C., Davila A., McKay C. P., and Whyte L. G. (2019) Microbial activity and habitability of an Antarctic dry valley water track. *Astrobiology*, 19: 757-770.
- Coates R. C., Podell S., Korobeynikov A., Lapidus A., Pevzner P., Sherman D. H., Allen E. E., Gerwick L., and Gerwick W. H. (2014) Characterization of cyanobacterial hydrocarbon composition and distribution of biosynthetic pathways. *PLOS one*, 9: e85140.
- Cockell C. S., Schuenger A. C., Billi D., Friedmann E. I., and Panitz C. (2005) Effects of a simulated martian UV flux on the cyanobacterium, *Chroococcidiopsis* sp. 029. *Astrobiology*, 5: 127-140.

- Council N. R. (2019) The limits of organic life in planetary systems. The national academy of press.
- Cranwell P. (1978) Extractable and bound lipid components in a freshwater sediment. *Geochimica et Cosmochimica Acta*, 42: 1523-1532.
- De Sanctis M. C., Altieri F., Ammannito E., Biondi D., De Angelis S., Meini M., Mondello G., Novi S., Paolinetti R., and Soldani M. (2017) Ma_MISS on ExoMars: mineralogical characterization of the martian subsurface. *Astrobiology*, 17: 612-620.
- de Vera J.-P., Schulze-Makuch D., Khan A., Lorek A., Koncz A., Möhlmann D., and Spohn T. (2014) Adaptation of an Antarctic lichen to Martian niche conditions can occur within 34 days. *Planetary and Space Science*, 98: 182-190.
- Diaz B., and Schulze-Makuch D. (2006) Microbial survival rates of *Escherichia coli* and *Deinococcus radiodurans* under low temperature, low pressure, and UV-irradiation conditions, and their relevance to possible martian life. *Astrobiology*, 6: 332-347.
- Didyk B., Simoneit B., Brassell S. t., and Eglinton G. (1978) Organic geochemical indicators of palaeoenvironmental conditions of sedimentation. *Nature*, 272: 216-222.
- Dijkman N. A., Boschker H. T., Stal L. J., and Kromkamp J. C. (2010) Composition and heterogeneity of the microbial community in a coastal microbial mat as revealed by the analysis of pigments and phospholipid-derived fatty acids. *Journal of Sea Research*, 63: 62-70.
- Dong H., Rech J. A., Jiang H., Sun H., and Buck B. J. (2007) Endolithic cyanobacteria in soil gypsum: Occurrences in Atacama (Chile), Mojave (United States), and Al-Jafr Basin (Jordan) Deserts. *Journal of Geophysical Research: Biogeosciences*, 112.
- Douki T. (2013) The variety of UV-induced pyrimidine dimeric photoproducts in DNA as shown by chromatographic quantification methods. *Photochemical & Photobiological Sciences*, 12: 1286-1302.
- Eglinton G., and Hamilton R. J. (1967) Leaf Epicuticular Waxes: The waxy outer surfaces of most plants display a wide diversity of fine structure and chemical constituents. *science*, 156: 1322-1335.
- Eigenbrode J. L., Summons R. E., Steele A., Freissinet C., Millan M., Navarro-González R., Sutter B., McAdam A. C., Franz H. B., and Glavin D. P. (2018) Organic matter preserved in 3-billion-year-old mudstones at Gale crater, Mars. *Science*, 360: 1096-1101.
- Fairén A. G. (2010) A cold and wet Mars. *Icarus*, 208: 165-175.
- Fairén A. G., Davila A. F., Lim D., Bramall N., Bonaccorsi R., Zavaleta J., Uceda E. R., Stoker C., Wierzchos J., and Dohm J. M. (2010) Astrobiology through the ages of Mars: the study of terrestrial analogues to understand the habitability of Mars. *Astrobiology*, 10: 821-843.
- Fairén A. G., Parro V., Schulze-Makuch D., and Whyte L. (2017) Searching for life on Mars before it is too late. *Astrobiology*, 17: 962-970.
- Fajardo-Cavazos P., Schuerger A. C., and Nicholson W. L. (2010) Exposure of DNA and *Bacillus subtilis* spores to simulated martian environments: use of quantitative PCR (qPCR) to measure inactivation rates of DNA to function as a template molecule. *Astrobiology*, 10: 403-411.
- Fernández-Martínez M. Á., García-Villadangos M., Paz M. M., Gangloff V., Carrizo D., Blanco Y., González Herrero S., Sánchez-García L., Prieto-Ballesteros O., and Altshuler I. (2021) Geomicrobiological heterogeneity of lithic habitats in the extreme environment of Antarctic Nunataks: A potential early Mars analog. *Frontiers in Microbiology*, 12: 1568.

- Fisher D. A., Lacelle D., Pollard W., Davila A., and McKay C. P. (2016) Ground surface temperature and humidity, ground temperature cycles and the ice table depths in University Valley, McMurdo Dry Valleys of Antarctica. *Journal of Geophysical Research: Earth Surface*, 121: 2069-2084.
- Friedberg E. C., Aguilera A., Gellert M., Hanawalt P. C., Hays J. B., Lehmann A. R., Lindahl T., Lowndes N., Sarasin A., and Wood R. D. (2006) DNA repair: from molecular mechanism to human disease. *DNA repair*, 5: 986-996.
- Friedmann E. I. (1982) Endolithic microorganisms in the Antarctic cold desert. *Science*, 215: 1045-1053.
- Gómez F., Mateo-Martí E., Prieto-Ballesteros O., Martín-Gago J., and Amils R. (2010) Protection of chemolithoautotrophic bacteria exposed to simulated Mars environmental conditions. *Icarus*, 209: 482-487.
- Goordial J., Altshuler I., Hindson K., Chan-Yam K., Marcoléfas E., and Whyte L. (2017) In situ field sequencing and life detection in remote (79° 26' N) Canadian High Arctic permafrost ice wedge microbial communities. *Frontiers in microbiology*, 8: 2594.
- Goordial J., Davila A., Lacelle D., Pollard W., Marinova M. M., Greer C. W., DiRuggiero J., McKay C. P., and Whyte L. G. (2016) Nearing the cold-arid limits of microbial life in permafrost of an upper dry valley, Antarctica. *The ISME journal*, 10: 1613.
- Grimalt J. O., de Wit R., Teixidor P., and Albaigés J. (1992) Lipid biogeochemistry of Phormidium and Microcoleus mats. *Organic Geochemistry*, 19: 509-530.
- Hansen A. A., Jensen L. L., Kristoffersen T., Mikkelsen K., Merrison J., Finster K. W., and Lomstein B. A. (2009) Effects of long-term simulated martian conditions on a freeze-dried and homogenized bacterial permafrost community. *Astrobiology*, 9: 229-240.
- Harwood J. (2012) Lipids in plants and microbes. Springer Science & Business Media.
- Hays L. E., Graham H. V., Des Marais D. J., Hausrath E. M., Horgan B., McCollom T. M., Parenteau M. N., Potter-McIntyre S. L., Williams A. J., and Lynch K. L. (2017) Biosignature preservation and detection in Mars analog environments. *Astrobiology*, 17: 363-400.
- Hedges J. I., and Prahl F. G. (1993) Early diagenesis: consequences for applications of molecular biomarkers. In: *Organic geochemistry*, Springer, pp 237-253.
- Heldmann J., Pollard W., McKay C., Marinova M., Davila A., Williams K., Lacelle D., and Andersen D. (2013) The high elevation Dry Valleys in Antarctica as analog sites for subsurface ice on Mars. *Planetary and Space Science*, 85: 53-58.
- Horneck G. (2000) The microbial world and the case for Mars. *Planetary and Space Science*, 48: 1053-1063.
- John K., Botkin D., Burton A., Castro-Wallace S., Chaput J., Dworkin J., Lehman N., Lupisella M., Mason C., and Smith D. (2016) The Biomolecule Sequencer Project: Nanopore sequencing as a dual-use tool for crew health and astrobiology investigations.
- Johnson A. P., Pratt L. M., Vishnivetskaya T., Pfiffner S., Bryan R. A., Dadachova E., Whyte L., Radtke K., Chan E., and Tronick S. (2011) Extended survival of several organisms and amino acids under simulated martian surface conditions. *Icarus*, 211: 1162-1178.
- Johnson S. S., Anslyn E. V., Graham H. V., Mahaffy P. R., and Ellington A. D. (2018) Fingerprinting non-terran biosignatures. *Astrobiology*, 18: 915-922.
- Johnson S. S., Zaikova E., Goerlitz D. S., Bai Y., and Tighe S. W. (2017) Real-Time DNA Sequencing in the Antarctic Dry Valleys Using the Oxford Nanopore Sequencer. *Journal of Biomolecular Techniques: JBT*, 28: 2.

- Jørgensen S. L., and Zhao R. (2016) Microbial inventory of deeply buried oceanic crust from a young ridge flank. *Frontiers in microbiology*, 7: 820.
- Kaplan M. (2012) DNA has a 521-year half-life [at 13.1 C]: genetic material can't be recovered from dinosaurs—but it lasts longer than thought. *Nature News*, 10.
- Kish A., Kirkali G., Robinson C., Rosenblatt R., Jaruga P., Dizdaroglu M., and DiRuggiero J. (2009) Salt shield: intracellular salts provide cellular protection against ionizing radiation in the halophilic archaeon, *Halobacterium salinarum* NRC-1. *Environmental microbiology*, 11: 1066-1078.
- Klein H. P. (1977) The Viking biological investigation: general aspects. *Journal of Geophysical Research*, 82: 4677-4680.
- Klein H. P. (1978) The Viking biological experiments on Mars. *Icarus*, 34: 666-674.
- Koren S., Walenz B. P., Berlin K., Miller J. R., Bergman N. H., and Phillippy A. M. (2017) Canu: scalable and accurate long-read assembly via adaptive k-mer weighting and repeat separation. *Genome research*, 27: 722-736.
- Kottemann M., Kish A., Iloanusi C., Bjork S., and DiRuggiero J. (2005) Physiological responses of the halophilic archaeon *Halobacterium* sp. strain NRC1 to desiccation and gamma irradiation. *Extremophiles*, 9: 219-227.
- Lacelle D., Davila A. F., Pollard W. H., Andersen D., Heldmann J., Marinova M., and McKay C. P. (2011) Stability of massive ground ice bodies in University Valley, McMurdo Dry Valleys of Antarctica: Using stable O–H isotope as tracers of sublimation in hyper-arid regions. *Earth and Planetary Science Letters*, 301: 403-411.
- Lanoil B., Skidmore M., Priscu J. C., Han S., Foo W., Vogel S. W., Tulaczyk S., and Engelhardt H. (2009) Bacteria beneath the West Antarctic ice sheet. *Environmental Microbiology*, 11: 609-615.
- Larson D. (1983) The pattern of production within individual Umbilicaria lichen thalli. *New Phytologist*, 94: 409-419.
- Leask E. K., and Ehlmann B. L. (2022) Evidence for deposition of chloride on Mars from small-volume surface water events into the Late Hesperian-Early Amazonian. *AGU Advances*, 3: e2021AV000534.
- Lee M. D., Walworth N. G., Sylvan J. B., Edwards K. J., and Orcutt B. N. (2015) Microbial communities on seafloor basalts at Dorado Outcrop reflect level of alteration and highlight global lithic clades. *Frontiers in microbiology*, 6: 1470.
- Levin G. V., and Straat P. A. (2016) The case for extant life on Mars and its possible detection by the Viking labeled release experiment. *Astrobiology*, 16: 798-810.
- Lezcano M. Á., Moreno-Paz M., Carrizo D., Prieto-Ballesteros O., Fernández-Martínez M. Á., Sánchez-García L., Blanco Y., Puente-Sánchez F., de Diego-Castilla G., and García-Villadangos M. (2019) Biomarker profiling of microbial mats in the geothermal band of Cerro Caliente, Deception Island (Antarctica): life at the edge of heat and cold. *Astrobiology*, 19: 1490-1504.
- Lezcano M. Á., Sanchez-Garcia L., Quesada A., Carrizo D., Fernández-Martínez M. Á., Cavalcante-Silva E., and Parro V. (2022) Comprehensive metabolic and taxonomic reconstruction of an ancient microbial mat from the McMurdo Ice Shelf (Antarctica) by integrating genetic, metaproteomics and lipid biomarker analyses. *Frontiers in Microbiology*: 1225.
- Li H. (2018) Minimap2: pairwise alignment for nucleotide sequences. *Bioinformatics*, 34: 3094-3100.

- Li H., Handsaker B., Wysoker A., Fennell T., Ruan J., Homer N., Marth G., Abecasis G., and Durbin R. (2009) The sequence alignment/map format and SAMtools. *Bioinformatics*, 25: 2078-2079.
- Linck E., Crane K. W., Zuckerman B. L., Corbin B. A., Myers R. M., Williams S. R., Carioscia S. A., Garcia R., and Lal B. (2019) Evaluation of a Human Mission to Mars by 2033. JSTOR.
- Loman N. J., Quick J., and Simpson J. T. (2015) A complete bacterial genome assembled de novo using only nanopore sequencing data. *Nature methods*, 12: 733-735.
- Luo G., Yang H., Algeo T. J., Hallmann C., and Xie S. (2019) Lipid biomarkers for the reconstruction of deep-time environmental conditions. *Earth-Science Reviews*, 189: 99-124.
- Maggiore C., Stromberg J., Blanco Y., Goordial J., Cloutis E., García-Villadangos M., Parro V., and Whyte L. (2020) The Limits, Capabilities, and Potential for Life Detection with MinION Sequencing in a Paleochannel Mars Analog. *Astrobiology*, 20: 375-393.
- Mangold N., Gupta S., Gasnault O., Dromart G., Tarnas J., Sholes S., Horgan B., Quantin-Nataf C., Brown A., and Le Mouélic S. (2021) Perseverance rover reveals an ancient delta-lake system and flood deposits at Jezero crater, Mars. *Science*, 374: 711-717.
- Markowitz V. M., Chen I.-M. A., Palaniappan K., Chu K., Szeto E., Grechkin Y., Ratner A., Jacob B., Huang J., and Williams P. (2011) IMG: the integrated microbial genomes database and comparative analysis system. *Nucleic acids research*, 40: D115-D122.
- Martin-Creuzburg D., and Merkel P. (2016) Sterols of freshwater microalgae: potential implications for zooplankton nutrition. *Journal of Plankton Research*, 38: 865-877.
- Martins Z. (2011) In situ biomarkers and the Life Marker Chip. *Astronomy & Geophysics*, 52: 1.34-1.35.
- Maurice S., Wiens R. C., Bernardi P., Caïs P., Robinson S., Nelson T., Gasnault O., Reess J.-M., Deleuze M., and Rull F. (2021) The SuperCam instrument suite on the Mars 2020 rover: Science objectives and Mast-Unit description. *Space Science Reviews*, 217: 1-108.
- McKay C. P., Andersen D., and Davila A. (2017) Antarctic environments as models of planetary habitats: University Valley as a model for modern Mars and Lake Untersee as a model for Enceladus and ancient Mars. *The Polar Journal*, 7: 303-318.
- McKay C. P., Friedman E. I., Wharton R. A., and Davies W. L. (1992) History of water on Mars: a biological perspective. *Advances in Space Research*, 12: 231-238.
- Menzel P., Ng K. L., and Krogh A. (2016) Fast and sensitive taxonomic classification for metagenomics with Kaiju. *Nature communications*, 7: 1-9.
- Mergelov N., Mueller C. W., Prater I., Shorkunov I., Dolgikh A., Zazovskaya E., Shishkov V., Krupskaya V., Abrosimov K., and Cherkinsky A. (2018) Alteration of rocks by endolithic organisms is one of the pathways for the beginning of soils on Earth. *Scientific Reports*, 8: 1-15.
- Meyers P. A. (1997) Organic geochemical proxies of paleoceanographic, paleolimnologic, and paleoclimatic processes. *Organic geochemistry*, 27: 213-250.
- Mileikowsky C., Cucinotta F. A., Wilson J. W., Gladman B., Horneck G., Lindegren L., Melosh J., Rickman H., Valtonen M., and Zheng J. (2000) Natural transfer of viable microbes in space: 1. From Mars to Earth and Earth to Mars. *Icarus*, 145: 391-427.
- Millan M., Szopa C., Buch A., Coll P., Glavin D. P., Freissinet C., Navarro-González R., François P., Coscia D., and Bonnet J.-Y. (2016) In situ analysis of martian regolith with the SAM experiment during the first mars year of the MSL mission: Identification of

- organic molecules by gas chromatography from laboratory measurements. *Planetary and Space Science*, 129: 88-102.
- Mosca C., Rothschild L. J., Napoli A., Ferré F., Pietrosanto M., Fagliarone C., Baqué M., Rabbow E., Rettberg P., and Billi D. (2019) Over-expression of UV-damage DNA repair genes and ribonucleic acid persistence contribute to the resilience of dried biofilms of the desert cyanobacterium *Chroococcidiopsis* exposed to Mars-like UV flux and long-term desiccation. *Frontiers in Microbiology*, 10: 2312.
- Musk E. (2017) Making humans a multi-planetary species. *New Space*, 5: 46-61.
- Mustard J., Adler M., Allwood A., Bass D., Beaty D., Bell J., Brinckerhoff W., Carr M., Des Marais D., and Brake B. (2013) Report of the mars 2020 science definition team. *Mars Explor. Progr. Anal. Gr.* 155-205.
- Navarro-González R., Vargas E., de La Rosa J., Raga A. C., and McKay C. P. (2010) Reanalysis of the Viking results suggests perchlorate and organics at midlatitudes on Mars. *Journal of Geophysical Research: Planets*, 115.
- Nelson D. W., and Sommers L. E. (1996) Total carbon, organic carbon, and organic matter. *Methods of soil analysis: Part 3 Chemical methods*, 5: 961-1010.
- Neveu M., Hays L. E., Voytek M. A., New M. H., and Schulte M. D. (2018) The Ladder of Life Detection. *Astrobiology*.
- Nicholson W. L., Schuerger A. C., and Douki T. (2018) The photochemistry of unprotected DNA and DNA inside *Bacillus subtilis* spores exposed to simulated Martian surface conditions of atmospheric composition, temperature, pressure, and solar radiation. *Astrobiology*, 18: 393-402.
- O'Connor B. R., Fernández-Martínez M. Á., Léveillé R. J., and Whyte L. G. (2021) Taxonomic characterization and microbial activity determination of cold-adapted microbial communities in lava tube ice caves from Lava Beds National Monument, a high-fidelity Mars analogue environment. *Astrobiology*, 21: 613-627.
- Onofri S., Barreca D., Selbmann L., Isola D., Rabbow E., Horneck G., De Vera J., Hatton J., and Zucconi L. (2013) Resistance of Antarctic black fungi and cryptoendolithic communities to simulated space and Martian conditions. *Studies in Mycology*, 75: 115-170.
- Orosei R., Lauro S., Pettinelli E., Cicchetti A., Coradini M., Cosciotti B., Di Paolo F., Flamini E., Mattei E., and Pajola M. (2018) Radar evidence of subglacial liquid water on Mars. *Science*, 361: 490-493.
- Otto A., Simoneit B. R., and Rember W. C. (2005) Conifer and angiosperm biomarkers in clay sediments and fossil plants from the Miocene Clarkia Formation, Idaho, USA. *Organic Geochemistry*, 36: 907-922.
- Parenteau M. N., Jahnke L. L., Farmer J. D., and Cady S. L. (2014) Production and early preservation of lipid biomarkers in iron hot springs. *Astrobiology*, 14: 502-521.
- Parro V., de Diego-Castilla G., Rodríguez-Manfredi J. A., Rivas L. A., Blanco-López Y., Sebastián E., Romeral J., Compostizo C., Herrero P. L., and García-Marín A. (2011) SOLID3: a multiplex antibody microarray-based optical sensor instrument for in situ life detection in planetary exploration. *Astrobiology*, 11: 15-28.
- Parro V., Rivas L. A., and Gómez-Elvira J. (2008) Protein microarrays-based strategies for life detection in astrobiology. *Space science reviews*, 135: 293-311.
- Potts M. (1999) Mechanisms of desiccation tolerance in cyanobacteria. *European Journal of Phycology*, 34: 319-328.

- Quantin C., Popova O., Hartmann W. K., and Werner S. C. (2016) Young Martian crater Gratteri and its secondary craters. *Journal of Geophysical Research: Planets*, 121: 1118-1140.
- Rivas L. A., Aguirre J., Blanco Y., González-Toril E., and Parro V. (2011) Graph-based deconvolution analysis of multiplex sandwich microarray immunoassays: applications for environmental monitoring. *Environmental microbiology*, 13: 1421-1432.
- Rivas L. A., García-Villadangos M., Moreno-Paz M., Cruz-Gil P., Gómez-Elvira J., and Parro V. (2008) A 200-antibody microarray biochip for environmental monitoring: searching for universal microbial biomarkers through immunoprofiling. *Analytical chemistry*, 80: 7970-7979.
- Rull F., Maurice S., Hutchinson I., Moral A., Perez C., Diaz C., Colombo M., Belenguer T., Lopez-Reyes G., and Sansano A. (2017) The Raman Laser Spectrometer for the ExoMars Rover Mission to Mars. *Astrobiology*, 17: 627-654.
- Rummel J. D., and Conley C. A. (2018) Inadvertently finding Earth contamination on Mars should not be a priority for anyone. *Astrobiology*, 18: 108-115.
- Sánchez-García L., Aeppli C., Parro V., Fernández-Remolar D., García-Villadangos M., Chong-Diaz G., Blanco Y., and Carrizo D. (2018) Molecular biomarkers in the subsurface of the Salar Grande (Atacama, Chile) evaporitic deposits. *Biogeochemistry*, 140: 31-52.
- Sánchez-García L., Carrizo D., Molina A., Muñoz-Iglesias V., Lezcano M. Á., Fernández-Sampedro M., Parro V., and Prieto-Ballesteros O. (2020) Fingerprinting molecular and isotopic biosignatures on different hydrothermal scenarios of Iceland, an acidic and sulfur-rich Mars analog. *Scientific reports*, 10: 1-13.
- Santos S. P., Yang Y., Rosa M. T., Rodrigues M. A., La Tour D., Bouthier C., Sommer S., Teixeira M., Carrondo M. A., and Cloetens P. (2019) The interplay between Mn and Fe in *Deinococcus radiodurans* triggers cellular protection during paraquat-induced oxidative stress. *Scientific reports*, 9: 1-12.
- Schuenger A. (2015) Ultraviolet irradiation on the surface of Mars: Implications for EVA activities during future human missions. *Planetary Protection Knowledge Gaps for Human Extraterrestrial Missions*, 1845: 1011.
- Schuenger A. C., Mancinelli R. L., Kern R. G., Rothschild L. J., and McKay C. P. (2003) Survival of endospores of *Bacillus subtilis* on spacecraft surfaces under simulated martian environments:: implications for the forward contamination of Mars. *Icarus*, 165: 253-276.
- Schuenger A. C., and Nicholson W. L. (2006) Interactive effects of hypobaria, low temperature, and CO₂ atmospheres inhibit the growth of mesophilic *Bacillus* spp. under simulated martian conditions. *Icarus*, 185: 143-152.
- Schwieterman E. W., Kiang N. Y., Parenteau M. N., Harman C. E., DasSarma S., Fisher T. M., Arney G. N., Hartnett H. E., Reinhard C. T., and Olson S. L. (2018) Exoplanet biosignatures: a review of remotely detectable signs of life. *Astrobiology*, 18: 663-708.
- Sims M. R., Cullen D. C., Rix C. S., Buckley A., Derveni M., Evans D., García-Con L. M., Rhodes A., Rato C. C., and Stefinovic M. (2012) Development status of the life marker chip instrument for ExoMars. *Planetary and Space Science*, 72: 129-137.
- Sobrado J. M., Martín-Soler J., and Martín-Gago J. A. (2014) Mimicking Mars: A vacuum simulation chamber for testing environmental instrumentation for Mars exploration. *Review of Scientific Instruments*, 85: 035111.
- Spry J. A., Race M., Kminek G., Siegel B., and Conley C. (2018) Planetary Protection Knowledge Gaps for Future Mars Human Missions: Stepwise Progress in Identifying and

- Integrating Science and Technology Needs. 48th International Conference on Environmental Systems.
- Suija A., Ertz D., Lawrey J. D., and Diederich P. (2015) Multiple origin of the lichenicolous life habit in Helotiales, based on nuclear ribosomal sequences. *Fungal Diversity*, 70: 55-72.
- Team R. C. (2013) R: A language and environment for statistical computing.
- Vago J. L., Westall F., Coates A. J., Jaumann R., Korablev O., Ciarletti V., Mitrofanov I., Josset J.-L., De Sanctis M. C., and Bibring J.-P. (2017) Habitability on early Mars and the search for biosignatures with the ExoMars Rover. *Astrobiology*, 17: 471-510.
- van der Valk T., Pečnerová P., Díez-del-Molino D., Bergström A., Oppenheimer J., Hartmann S., Xenikoudakis G., Thomas J. A., Dehasque M., and Sağlıcan E. (2021) Million-year-old DNA sheds light on the genomic history of mammoths. *Nature*, 591: 265-269.
- Vega-García S., Sánchez-García L., Prieto-Ballesteros O., and Carrizo D. (2021) Molecular and isotopic biogeochemistry on recently-formed soils on King George Island (Maritime Antarctica) after glacier retreat upon warming climate. *Science of the Total Environment*, 755: 142662.
- Velázquez D., Lezcano M. Á., Frias A., and Quesada A. (2013) Ecological relationships and stoichiometry within a Maritime Antarctic watershed. *Antarctic Science*, 25: 191-197.
- Vicente-Retortillo Á., Valero F., Vázquez L., and Martínez G. M. (2015) A model to calculate solar radiation fluxes on the Martian surface. *Journal of Space Weather and Space Climate*, 5: A33.
- Volkman J., Johns R., Gillan F., Perry G., and Bavor Jr H. (1980) Microbial lipids of an intertidal sediment—I. Fatty acids and hydrocarbons. *Geochimica et Cosmochimica Acta*, 44: 1133-1143.
- Volkman J. K. (1986) A review of sterol markers for marine and terrigenous organic matter. *Organic geochemistry*, 9: 83-99.
- Volkman J. K., Barrett S. M., Blackburn S. I., Mansour M. P., Sikes E. L., and Gelin F. (1998) Microalgal biomarkers: a review of recent research developments. *Organic Geochemistry*, 29: 1163-1179.
- Walker J. J., Spear J. R., and Pace N. R. (2005) Geobiology of a microbial endolithic community in the Yellowstone geothermal environment. *Nature*, 434: 1011-1014.
- Wierzchos J., Cámara B., de Los Ríos A., Davila A., Sánchez Almazo I., Artieda O., Wierzchos K., Gomez-Silva B., McKay C., and Ascaso C. (2011) Microbial colonization of Calcium sulfate crusts in the hyperarid core of the Atacama Desert: implications for the search for life on Mars. *Geobiology*, 9: 44-60.
- Wierzchos J., Davila A. F., Artieda O., Cámara-Gallego B., de los Ríos A., Neilson K. H., Valea S., García-González M. T., and Ascaso C. (2013) Ignimbrite as a substrate for endolithic life in the hyper-arid Atacama Desert: implications for the search for life on Mars. *Icarus*, 224: 334-346.
- Wierzchos J., DiRuggiero J., Vítek P., Artieda O., Souza-Egipsy V., Skaloud P., Tisza M., Davila A. F., Vílchez C., and Garbayo I. (2015) Adaptation strategies of endolithic chlorophototrophs to survive the hyperarid and extreme solar radiation environment of the Atacama Desert. *Frontiers in microbiology*, 6: 934.
- Wierzchos J., Ríos A. d. I., and Ascaso C. (2012) Microorganisms in desert rocks: the edge of life on Earth.
- Wilhelm M. B., Davila A. F., Eigenbrode J. L., Parenteau M. N., Jahnke L. L., Liu X.-L., Summons R. E., Wray J. J., Stamos B. N., and O'Reilly S. S. (2017) Xeropreservation of

- functionalized lipid biomarkers in hyperarid soils in the Atacama Desert. *Organic geochemistry*, 103: 97-104.
- Ye T., Wang B., Li C., Bian P., Chen L., and Wang G. (2021) Exposure of cyanobacterium *Nostoc* sp. to the Mars-like stratosphere environment. *Journal of Photochemistry and Photobiology B: Biology*, 224: 112307.
- Zucconi L., Onofri S., Cecchini C., Isola D., Ripa C., Fenice M., Madonna S., Reboleiro-Rivas P., and Selbmann L. (2016) Mapping the lithic colonization at the boundaries of life in Northern Victoria Land, Antarctica. *Polar Biology*, 39: 91-102.

Connecting text

In the preceding chapters, I established that the MinION can be used to detect DNA on Mars analogue samples and samples exposed to Mars-like environmental conditions. As the MinION can produce long, repeat-spanning reads, it could also be an effective tool for genome reconstruction from metagenomes, enabling the study individual genomes without pure cultures. However, the ability of the MinION to resolve genomes from extreme analogue environments is largely undetermined. To facilitate better understanding of individual microbes in analogue environments, we used a combination short- and long-read (i.e. hybrid) for contig assembly and genome binning. Using samples from sea ice cryoconites in the Canadian high Arctic, hybrid assembly produced more complete and more contiguous metagenome-assembled genomes (MAGs) than either constituent technology alone. A putatively novel MAG was also produced and is discussed in depth.

This manuscript appears in:

Maggiore, C., Raymond-Bouchard, I., Brennan, L., Touchette, D., & Whyte, L. (2021). MinION sequencing from sea ice cryoconites leads to de novo genome reconstruction from metagenomes. *Scientific Reports*, 11(1), 1-16. DOI: <https://doi.org/10.1038/s41598-021-00026-x>

Chapter 4. MinION sequencing from sea ice cryoconites leads to *de novo* genome reconstruction from metagenomes

Catherine Maggiori¹, Isabelle Raymond-Bouchard¹, Laura Brennan¹, David Touchette¹, Lyle Whyte¹

¹Department of Natural Resource Sciences, Faculty of Agricultural and Environmental Sciences, McGill University, Ste. Anne-de-Bellevue, Quebec, Canada

4.1 Abstract

Genome reconstruction from metagenomes enables detailed study of individual community members, their metabolisms, and their survival strategies. Obtaining high quality metagenome-assembled genomes (MAGs) is particularly valuable in extreme environments like sea ice cryoconites, where the native consortia are recalcitrant to culture and strong astrobiology analogues. We evaluated three separate approaches for MAG generation from Allen Bay, Nunavut sea ice cryoconites – HiSeq-only, MinION-only, and hybrid (HiSeq + MinION) – where field MinION sequencing yielded a reliable metagenome. The hybrid assembly produced longer contigs, more coding sequences, and more total MAGs, revealing a microbial community dominated by Bacteroidetes. The hybrid MAGs also had the highest completeness, lowest contamination, and highest N50. A putatively novel species of *Octadecabacter* is among the hybrid MAGs produced, containing the genus's only known instances of genomic potential for nitrate reduction, denitrification, sulfate reduction, and fermentation. This study shows that the inclusion of MinION reads in traditional short read datasets leads to higher quality metagenomes and MAGs for more accurate descriptions of novel microorganisms in this extreme, transient habitat and has produced the first hybrid MAGs from an extreme environment.

4.2 Introduction

Cryoconites are small holes (<1 m in diameter, <0.5 m deep) on icy surfaces containing water and wind-blown particles (Cook *et al.* 2016; Edwards *et al.* 2014). They form when organic and inorganic materials are deposited and melt small pockets on the ice, forming a basal level of dark sediment overlain with meltwater and providing a refuge for microorganisms. Cryoconites occur in Arctic, Antarctic, and alpine regions on glaciers, ice sheets, sea ice, and lake ice (Anesio *et al.* 2017; Cook *et al.* 2016; Edwards *et al.* 2013b; Weisleitner *et al.* 2019). They are hotspots of microbial diversity in icy environments, containing a wide variety of taxa (e.g. Cyanobacteria, heterotrophic bacteria, protists, algae, micro-invertebrates) (Mueller *et al.* 2001) and provide key functions in icy ecosystems (e.g. carbon fixation, mineral aggregation, nutrient cycling, pollutant degradation) (Cook *et al.* 2016; Maccario *et al.* 2015). However, regional and global interaction scales of cryoconites are not well-understood (Edwards *et al.* 2014), particularly for cryoconites on sea ice and in the Canadian Arctic Archipelago. Characterizing the microbial community in cryoconite holes will increase our comprehension of life in cold environments, for which a unified picture is severely lacking (Edwards *et al.* 2020), and offer predictions on how changing sea ice will affect these communities, their distribution, and the surrounding ecosystem. For example, as the scope of brine in the central Arctic Ocean (CAO) expands with climate change, it is expected that freshwater and brackish Actinobacteria, Betaproteobacteria and Flavobacteriia will increase in number and range across the CAO (Fernández-Gómez *et al.* 2019). Consequences of this expansion could be increased photoheterotrophy, increased use of dissolved organic matter (DOM), and increased infection numbers of ice-associated fish by *Flavobacterium* and *Polaribacter* in the water column (Fernández-Gómez *et al.* 2019).

Field investigations of remote locations like sea ice benefit our understanding of the microbial interactions in these fragile and increasingly transient environments (Edwards *et al.* 2020). Field sequencing reduces logistical risks including contamination or sample loss during transport, optimizes the capture of specific communities in space and time (Wight *et al.* 2020), and can be performed with the Oxford Nanopore Technologies' (ONT) MinION sequencer, a miniaturized device designed to sequence DNA, RNA, and potentially proteins (Goordial *et al.* 2017; Leggett and Clark 2017; Loman and Watson 2015). The MinION also generates sequences in real-time, enabling rapid identification of community members for further targeted analyses in the field (e.g. determining if metabolic genes present are active via *in situ* respiration). It is low cost, has low energy requirements, and can sequence samples containing environmental inhibitors and low biomass (Carr *et al.* 2017; Goordial *et al.* 2017). The MinION has been successfully used in extreme environments, generating sequences from Svalbard, Axel Heiberg Island, Antarctica, and the International Space Station (Castro-Wallace *et al.* 2017; Edwards *et al.* 2016; Goordial *et al.* 2017; Johnson *et al.* 2017), and the MinION is being explored as a tool for direct life detection in astrobiology studies. DNA is an unambiguous biosignature and the MinION has potential to be adapted and utilized for *in situ* life detection (Carr *et al.* 2020; Goordial *et al.* 2017; Maggiori *et al.* 2020; Sutton *et al.* 2019). Testing the MinION in a variety of Mars analogue environments further establishes its utility in this context. Cryoconites are analogues to icy extraterrestrial environments (e.g. Martian polar ice caps, Enceladus, Europa) given their extreme environmental conditions (e.g. freezing temperatures, low nutrient input, high solar radiation) (Kaczmarek *et al.* 2016; Zawierucha *et al.* 2017). In particular, the icy moon Europa is a promising target in the search for biosignatures based on its possession of chaos regions: geologically young surface regions where active resurfacing may be ongoing, potentially depositing endogenous material onto

the icy surface in a manner similar to cryoconite formation, where it remains exposed and accessible for future mission investigations (e.g. Europa Lander concept mission) (Nordheim *et al.* 2018; Pappalardo *et al.* 2013). The microorganisms inhabiting cryoconite holes can therefore act as promising models for astrobiology (Kaczmarek *et al.* 2016; Zawierucha *et al.* 2017) and detailed studies of their genomes beyond initial biosignature detection with the MinION can yield valuable insights into survival strategies, lifestyles, and potential biosignatures in icy extraterrestrial analogues.

A strong benefit of single-molecule sequencers like the MinION is their ability to produce genome-sized contigs and long reads that span repetitive regions (Goldstein *et al.* 2019; Jain *et al.* 2018). Assembly, genome reconstruction, and characterizing structural variations become easier with longer, more contiguous reads, but nanopore sequencing exhibits significantly higher error rates than second-generation sequencing platforms (e.g. ~7.5 – 14.5% for MinION sequencing (Jain *et al.* 2017), <0.1% for Illumina sequencing (Manley *et al.* 2016)), although these error rates are continually being improved. Short Illumina reads have the opposite problem: highly accurate sequencing in non-repetitive regions, but low contiguity across assemblies (Jain *et al.* 2018). The two types of sequencing can be combined and assembled together to produce a hybrid dataset; long MinION reads provide contiguity and repeat resolution, while short reads facilitate local base pair accuracy (De Maio *et al.* 2019). Hybrid assemblies have produced more accurate and more contiguous genomes than either constituent dataset alone, including for bacterial isolates (e.g. plastic and repetitive genomes of *Enterobacteriaceae* (De Maio *et al.* 2019), plasmid-rich *Klebsiella pneumoniae* (Wick *et al.* 2017), GC-variable strains (Goldstein *et al.* 2019) and eukaryotic organisms (e.g. wild tomato *Solanum pennellii* (Schmidt *et al.* 2017), winged Antarctic

midge *Parochlus steinenii* (Shin *et al.* 2019), clownfish *Amphiprion ocellaris* (Tan *et al.* 2018), blacklip abalone *Haliotis rubra* (Gan *et al.* 2019)).

Reconstructing genomes from metagenomes – metagenome-assembled genomes (MAGs) or genome bins – is more complex than single genome reconstruction due to the greater diversity of genomes present and the introduction of intergenomic repeats i.e. similar repetitive regions from different genomes (Somerville *et al.* 2019). Hybrid assemblies produce metagenome datasets with more accurate community representation and more contiguous MAGs in both mock bacterial communities (Nicholls *et al.* 2019; Sevim *et al.* 2019) and natural consortia (e.g. gut microbiomes (Bertrand *et al.* 2019), aquifers (Overholt *et al.* 2020), wastewater (Brown *et al.* 2021)). However, this approach has yet to be tested in a low biomass, extreme, and remote sample site, where the reconstruction of individual community members would provide a robust understanding of their survival strategies and contributions to the local ecosystem (Overholt *et al.* 2020).

In this study, we collected material from cryoconite holes on sea ice in Allen Bay, Nunavut in the Canadian high Arctic (Figure 4.1) and performed field sequencing with the MinION. DNA extractions and sequencing runs were performed in the field in order to test the performance and robustness of portable extraction devices in tandem with the MinION in an extreme sea ice environment (Raymond-Bouchard *et al.* 2021). The MinION reads were later assembled with Illumina (HiSeq) reads to produce a hybrid metagenome and hybrid MAGs. We compared these hybrid datasets to HiSeq-only and MinION-only metagenomes and MAGs to evaluate their contiguity and accuracy (e.g. MAG completeness, contamination, N50). This comparison will determine if hybrid assembly is a viable approach for studying low biomass, extreme, and progressively more transient environments and produce the first hybrid MAGs from an extreme environment.

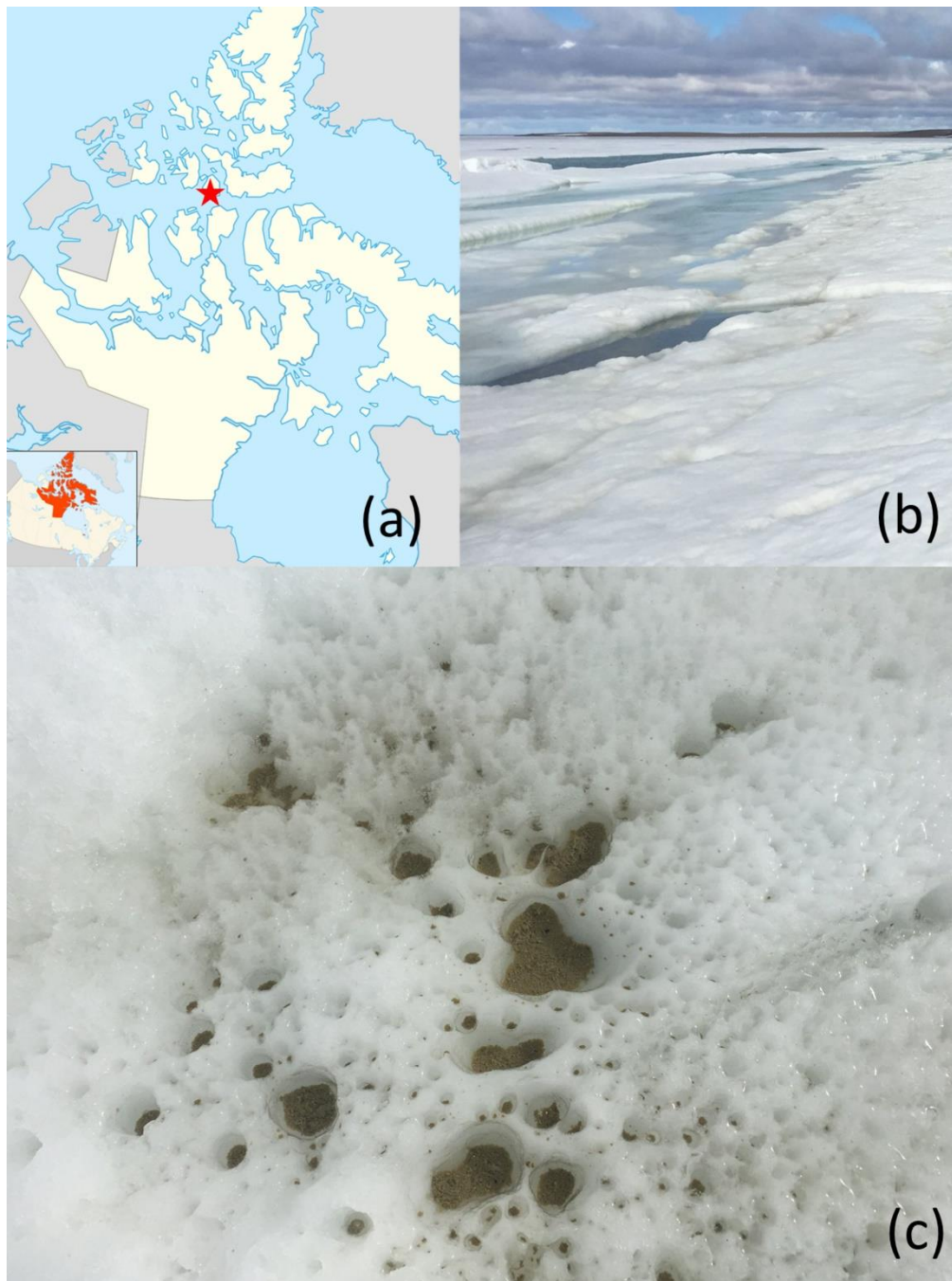


Figure 4.1. Allen Bay sea ice location and cryoconites. (a) Sampling location in the Canadian high Arctic (latitude: 74.44707; longitude: -95.0348). Map generated by Google maps version 10.86.1 (<https://www.google.com/maps/place/Resolute,+NU/@76.3182414,-114.8698166,4z/data=!4m5!3m4!1s0x51dc1af3fbf4579b:0x986b529216b123b6!8m2!3d74.697299!4d-94.8297289>). (b) Ground view of the Allen Bay sea ice. Photo taken on site by David Touchette. (c) Aerial view of the cryoconite sampling location. Photo taken on site by Isabelle Raymond-Bouchard.

4.3 Results

4.3.1 Geochemistry of the Allen Bay sea ice collection site

Physico-chemical parameters of the Allen Bay sea ice collection site were measured *in situ* in July 2018 (Table 4.1). The pH of the cryoconite meltwater was recorded as 7.96, with a salinity of 0.13 ppt. Total dissolved solids and dissolved oxygen were recorded as 0.173 g/L and 12.90 mg/L (91.7%), respectively. Oxidation reduction potential (ORP) was -114.4 mV, indicating a reducing environment in the meltwater (Lipson *et al.* 2010). Total organic carbon (TOC) was determined to be 112.75 ppm and ammoniacal nitrogen was measured at 1.81 ppm in neighbouring cryoconite meltwater.

Table 4.1. Physico-chemical characteristics of the Allen Bay sea ice cryoconite collection site.

pH	Temperature (°C)	Salinity (ppt)	Total dissolved solids (g/L)	Dissolved oxygen (%; mg/L)	Oxidation reduction potential (ORP) (mV)	Total organic carbon (TOC) (ppm)	NH₄-N (ppm)
7.96	1.33	0.13	0.173	91.7; 12.90	-114.4	112.75	1.81

4.3.2 The Allen Bay sea ice cryoconite metagenome is dominated by *Bacteroidetes*

Three assembly methods were tested in this study and used to evaluate the cryoconite metagenomes and resulting metagenome-assembled genomes (MAGs): HiSeq sequencing with metaSPAdes assembly, hybrid assembly with metaSPAdes and combined HiSeq+MinION datasets, and MinION sequencing with Canu assembly (Table 4.2). HiSeq sequencing produced

22.9 Gbp of data, ~19x more than that with MinION sequencing (1.2 Gbp). Despite having a ~1/19 fraction of the raw data produced by the HiSeq-only assembly, the MinION-only dataset had the longest average contig length and the highest proportion of ultra-long (>50 000 bp) contigs in its dataset. The addition of MinION data in the hybrid dataset likewise increased the average contig length, number of ultra-long contigs (> 50 000 bp), number of coding sequences classified by JGI IMG/M ER, and total MAGs produced with respect to the HiSeq-only assembly. These improvements are detailed in Table 4.3 and Supplementary Figure 4.1.

The 3 metagenomes (HiSeq, hybrid, and MinION) differ in proportion and breakdown of taxa due to the differences in their constituent sequencing technologies (Jain *et al.* 2018; Jain *et al.* 2017; Manley *et al.* 2016). MinION field sequencing produced a metagenome chiefly dominated (>90%) by Bacteroidetes as Flavobacteriales (*Flavobacterium* sp. ALD4, *Flavobacterium* sp. ACAM 123, *Flavobacterium frigoris*, and *Flavobacterium gillisiae*) (Figure 4.2). Like many

Table 4.2. Sequencing information for each assembly method (HiSeq with metaSPAdes, hybrid with metaSPAdes and combined HiSeq/MinION datasets, MinION with Canu).

Assembly type	Sequencing data (Gbp)	Number of contigs	Average contig length (bp)	Number of contigs >50 000 bp	Number of coding sequences classified by JGI	Total number of genes present	MAGs produced
HiSeq	22.9	2 197 534	1067	20	378 987	382 480	37
Hybrid	N/A	2 159 929	1163	48	397 048	400 814	44
MinION	1.2	3741	6734	36	48 475	49 539	4

Table 4.3. MAGs produced with HiSeq and hybrid assembly with >50% completeness and <10% contamination. MAG parameters were determined with CheckM. Metaerg taxonomy is determined via predicted ORFs that inherited their taxonomy from GTDB. Taxonomy is determined to the species level if coding sequences align to one species >50%.

Assembly type	MAG ID	Genome size (bp)	Longest contig (bp)	Mean contig length (bp)	N50	Completeness (%)	Contamination (%)	Closest Metaerg GTDB-based taxonomy
HiSeq	HiSeq_31	3 218 255	51 014	7926	9977	90.6	1.7	<i>Octadecabacter arcticus</i>
	HiSeq_14	3 193 410	34 424	5592	7860	80.2	3.4	<i>Polaromonas</i> sp. JS666
	HiSeq_32	2 854 964	29 037	6781	3796	77.3	0.6	<i>Pseudomonas</i> sp.
	HiSeq_30	1 577 574	14 969	4612	5723	52.1	1.7	<i>Nonlabens marinus</i>
	HiSeq_8	1 930 594	28 420	5274	4775	51.7	3.4	<i>Flavobacterium</i> sp.
	HiSeq_19	1 677 201	32 650	5392	5599	51.3	1.7	<i>Nonlabens</i> sp.
Hybrid	Hybrid_5	3 275 525	122 374	14 557	19 997	90.9	0.6	<i>Octadecabacter arcticus</i>
	Hybrid_20	3 024 995	47 365	9166	11 848	84.2	1.0	<i>Pseudomonas</i> sp.
	Hybrid_35	3 189 002	54 478	8032	10 334	79.5	1.4	<i>Polaromonas</i> sp. JS666
	Hybrid_12	1 885 346	36 215	7141	11 449	64.0	1.6	<i>Nonlabens marinus</i>
	Hybrid_27	1 821 856	32 650	6093	19 324	56.3	0.6	<i>Nonlabens</i> sp.
	Hybrid_21	2 613 398	43 486	8799	6309	50.8	0.8	<i>Flavobacterium</i> sp.

Flavobacterium spp., *F.* sp. ALD4., *F.* sp. ACAM 123, *F. frigoris*, and *F. gillisiae* are aquatic bacterial heterotrophs and are common in polar environments (e.g. Arctic sea ice, Antarctic saline lake water, and Antarctic microbial mats) (Kirchman 2002; McCammon and Bowman 2000; Van Trappen *et al.* 2004). The metabolic pathways present in the MinION metagenome indicate largely aerobic metabolisms via oxidative phosphorylation, glycolysis, the tricarboxylic acid (TCA) cycle,

the Enter-Doudoroff pathway, and glyoxylate shunt. Some fermentative and anaerobic terminal electron acceptor pathways are also present (e.g. full pathways for dissimilatory nitrate reduction, assimilatory nitrate reduction, and assimilatory sulfate reduction), as well as partial carbon fixation pathways via the reductive TCA cycle.

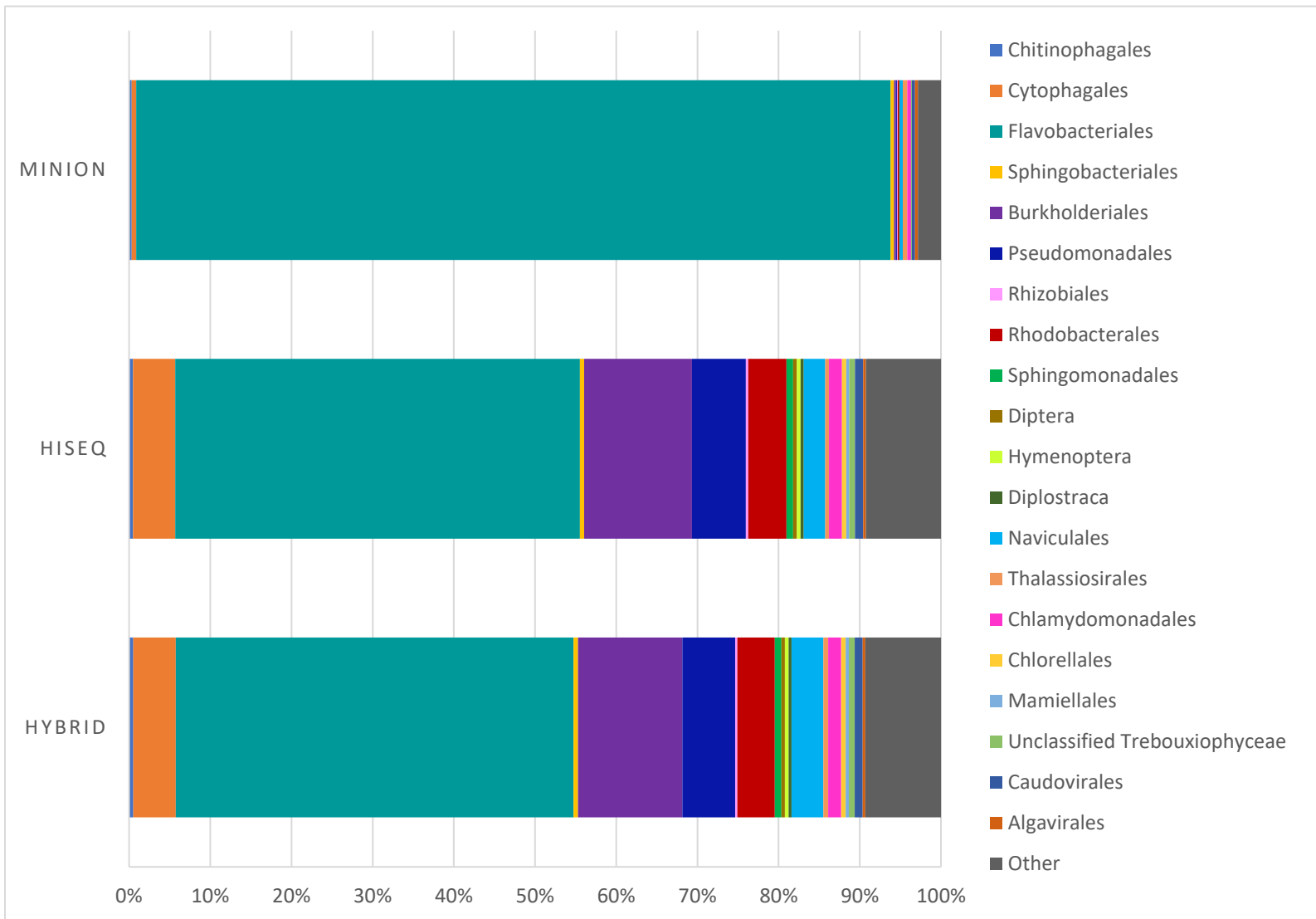


Figure 4.2. Community composition from metagenomes of the Allen Bay sea ice. The HiSeq-only metagenome, hybrid metagenome, and MinION-only metagenome are presented.

Similarly, the HiSeq and hybrid metagenomes largely contain Bacteroidetes (~55% in the HiSeq and hybrid datasets, >90% in the MinION dataset) as Flavobacteriales (*Flavobacterium* spp.) (Figure 4.2) and aerobic heterotrophic metabolic pathways (e.g. oxidative phosphorylation, the TCA cycle, the Enter-Doudoroff pathway, glyoxylate shunt). Secondly present in the HiSeq and hybrid metagenomes are Proteobacteria as Burkholderiales (*Polaromonas* spp.), Pseudomonadales (*Pseudomonas* spp. and *Psychrobacter* spp.), and Rhodobacterales (*Loktanella salsilacus* and *Octadecabacter* spp.). Eukarya are also present as green algae (Chlorophyta), diatoms (Bacillariophyta), and arthropods (Diptera, Diplostraca), as well as small amounts of viruses (Caudovirales, Algavirales) and Archaea in all three assembly methods. Caudovirales are bacteriophages while Algavirales prey on eukaryotic algae (Van Etten *et al.* 2002). Archaeal sequences are primarily Euryarchaeota as Methanomicrobia and Halobacteria. The HiSeq and hybrid metagenomes differ slightly in the proportions of taxa present (e.g. Bacteroidetes present as ~55.9% and 56.7% in the hybrid and HiSeq metagenomes, respectively; Proteobacteria present as ~26% and ~27% in the hybrid and HiSeq metagenomes, respectively), but possess all of the same taxa at the phylum level, except for Candidatus Gracilibacteria, detected exclusively in the hybrid and MinION metagenomes. Gracilibacteria are an uncultured lineage previously detected in deep-sea sediment and microbial mats (Ley *et al.* 2006) with limited metabolisms and an opal stop codon encoding for glycine (Rinke *et al.* 2013).

4.3.3 Metagenome-assembled genome (MAG) properties from HiSeq, hybrid, and MinION assemblies

37 and 44 MAGs were produced from the HiSeq and hybrid assemblies, respectively. Neither method produced bins with unique taxonomic assignments. Table 4.3 presents the details of bins with at least 50% completeness and less than 10% contamination as determined by CheckM. These details are plotted in Supplementary Figure 4.1. One high-quality (i.e. >90% complete, <5% contaminated, presence of the 23S, 16S, and 5S rRNA genes and at least 18 tRNAs) (Bowers *et al.* 2017) and five medium-quality bins (i.e. \geq 50% complete, <5% contaminated) (Bowers *et al.* 2017; Overholt *et al.* 2020) were produced from the hybrid method. Six medium-quality bins were obtained from the HiSeq method. Similar taxonomies for the high- and medium-quality bins were produced with each method as identified with GTDB (One *Octadecabacter* MAG, one *Polaromonas* MAG, one *Pseudomonas* MAG, two *Nonlabens* MAGs, and one *Flavobacterium* MAG), albeit with differing completeness, contamination, and genome dimensions. When directly comparing MAGs with the same taxonomy, in nearly all cases the hybrid MAGs had higher completeness, N50 values, mean contig length, longest contig, and lower contamination; the only exception is Hybrid_35 with a completeness of 79.5%, slightly lower than HiSeq_14's completeness of 80.2%. The hybrid MAGs also have larger genomes, likewise with the exception of Hybrid_35 and HiSeq_14. The taxonomies produced strongly reflect the dominance of Flavobacteriales (*Flavobacterium* sp. and *Nonlabens* spp.), Burkholderiales (*Polaromonas* sp000751355), Pseudomonadales (*Pseudomonas* sp.), and Rhodobacterales (*Octadecabacter arcticus*) in the metagenomes. Full sets of rRNA (i.e. 5S, 23S, and 16S) were

present in 4 MAGs: one hybrid MAG (Hybrid_5) and three MinION MAGs (MinION_3, MinION_RD_2, MinION_RD_3).

Genome binning was attempted for the MinION-only datasets; however, the resulting MAGs were of high contamination and medium-to-low completeness, even after short-read polishing and frameshift correction (Supplementary Table 4.1). Only one MinION MAG could be assigned taxa below Bacteria (*Flavobacterium* sp.); however, this MAG's contamination was so high (93.9%) as to make this designation irrelevant. Nevertheless, the MinION metagenome clearly represented the taxa present in the HiSeq and hybrid MAGs (*Octadecabacter*, *Polaromonas*, *Pseudomonas*, and *Flavobacterium*).

As MinION reads are known to be of poorer quality than Illumina-produced sequences (e.g. more insertion-deletions) (Jain *et al.* 2017), we assessed if the addition of MinION sequences significantly affected the contig and individual MAG quality of the hybrid dataset as compared with the HiSeq dataset via the number of indels present. Higher indel rates can introduce premature stop codons and result in truncated ORFs, which can be seen in gene prediction tools: the ratio between the length of predicted proteins and their best matches will be <1 if there are many indels present in the dataset (Stewart *et al.* 2019). Plots of frequency vs. query length:hit length for each assembly method, as well the highest quality HiSeq and hybrid MAGs, are presented in Figure 4.3. The hybrid plots do not differ significantly from the HiSeq plots and both show that the majority of the contigs present have a query length:hit length ratio of ~ 1 ; the query length (our sequence) and the length of its best match (hit length) are generally the same, indicating that the effect of indels in the hybrid and HiSeq datasets is minimal. This trend is further reflected in the highest quality hybrid and HiSeq MAGs (Hybrid_5 and HiSeq_31, respectively). When the MinION metagenome was polished with the HiSeq reads (i.e. the MinION_RD metagenome), the

query length:hit length of the contigs increased to ~ 1 . These ratios indicate that while indels still impact the quality and accuracy of MinION sequences, this effect is strongly diminished when paired with HiSeq assembly (i.e. hybrid metagenome and Hybrid_5) or HiSeq polishing (i.e. MinION_RD metagenome).

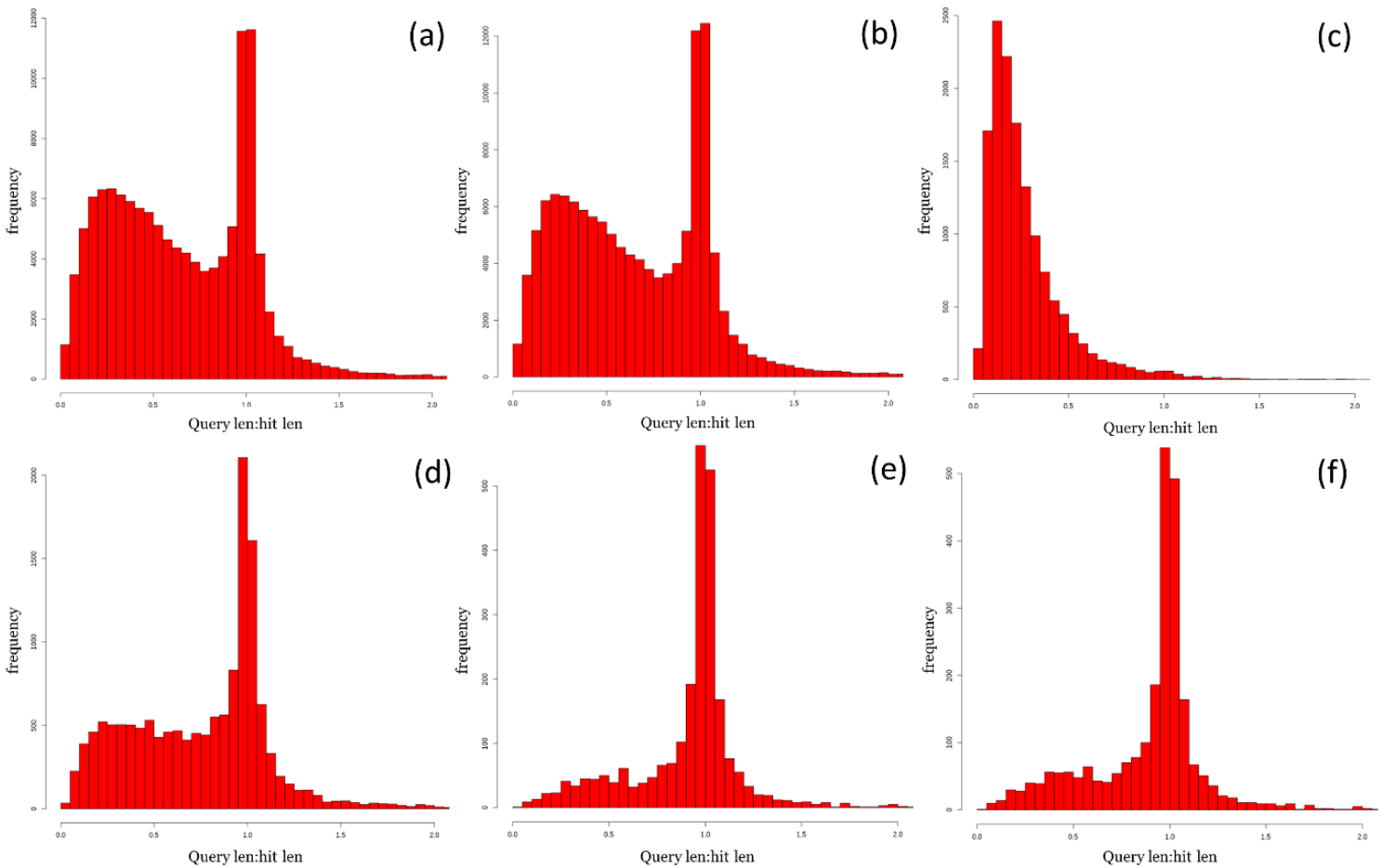


Figure 4.3. IDEEL plots of frequency (y-axis) vs. query length:hit length (x-axis) for: (a) hybrid metagenome; (b) HiSeq metagenome; (c) MinION metagenome; (d) polished MinION metagenome (MinION_RD); (e) Hybrid_5 MAG; (f) HiSeq_31 MAG. Query length:hit length is the ratio between the contig and its best match in the UniProt TREMBL database. If the contig contains few indels, this ratio will be ~ 1 .

4.3.4 Hybrid_5: A potential novel species of *Octadecabacter*

We recovered one high-quality and five medium-quality bins (Bowers *et al.* 2017; Overholt *et al.* 2020) from the hybrid assembly method and six medium-quality bins (Bowers *et al.* 2017) from the HiSeq assembly method (Table 4.3). The most complete and least contaminated bins belonged to *Octadecabacter* (Hybrid_5, HiSeq_31), *Pseudomonas* (Hybrid_20), and *Polaromonas* (HiSeq_14). *Pseudomonas* and *Polaromonas* are familiar taxa in polar environments (e.g. active layer permafrost, sea ice, seawater) (Lin *et al.* 2017; Margesin *et al.* 2012; Mattes *et al.* 2008), and our MAGs matched closely with *Pseudomonas fluorescens* (Hybrid_20) and *Polaromonas* sp. JS666 (HiSeq_14), although both MAGs lack a 16S gene. Hybrid_20 is a non-photosynthetic heterotroph capable of nitrate reduction and denitrification, consistent with the metabolic properties of *Pseudomonas fluorescens* and other polar pseudomonads (Ghiglione *et al.* 2002; Lin *et al.* 2017). HiSeq_14 is a non-photosynthetic heterotroph capable of sulfur oxidation and nitrate reduction, in line with its closest match *Polaromonas* sp. JS666 and other Arctic *Polaromonas* strains (Margesin *et al.* 2012; Mattes *et al.* 2008). We have thus chosen to focus our analyses on the *Octadecabacter* MAG Hybrid_5, as the survival strategies and detailed metabolic characteristics of this genus are not as well-described as both *Pseudomonas* and *Polaromonas*. Additionally, Hybrid_5 exhibits unique features as compared with other members of *Octadecabacter* and some genomic features lacking in HiSeq_31, including a 16S gene.

Hybrid_5 has the highest completeness (90.9%) and lowest contamination (0.6%) of all MAGs produced in any assembly method (Table 4.3). It has a genome size of 3.27 Mbp, a mean contig length of 14.5 kbp, an N50 of 19.9 kbp, and was identified as belonging to the *Octadecabacter* genus by both GTDB and MiGA. The genus *Octadecabacter* is typified by

Octadecabacter arcticus and *Octadecabacter antarcticus*, marine psychrophiles with a bipolar distribution and rich in octadecanoic acid (Gosink *et al.* 1997; Vollmers *et al.* 2013). One complete 16S rRNA gene was found in Hybrid_5 aligning to *O. arcticus* with 98% identity. When mapped to the *O. arcticus* genome, Hybrid_5 and its HiSeq counterpart HiSeq_31 show a reduced genome size, although Hybrid_5 traverses slightly more of the *O. arcticus* genome (Figure 4.4). *O. arcticus* has a genome size of 5.2 Mbp (Vollmers *et al.* 2013), while Hybrid_5 and HiSeq_31 have genome sizes of 3.28 and 3.22 Mbp, respectively. This reduced size is likely due to the incompleteness of draft MAGs (Chen *et al.* 2020). The average nucleotide identity (ANI) of Hybrid_5 was calculated at 93.51% with *O. arcticus*, below the threshold of 95% similarity for identical species, indicating that Hybrid_5 represents a potential novel species in the *Octadecabacter* genus.

Like *O. arcticus*, Hybrid_5 possesses genes encoding a complete tricarboxylic acid (TCA) cycle, Embden-Meyerhof glycolysis, oxidative phosphorylation, and the acetyl-CoA pathway (Figure 4.5). A full Entner-Doudoroff pathway and glyoxylate shunt are also present, cycles that typically act as alternatives to glycolysis and the citric acid cycle, respectively (Ahn *et al.* 2016; DangThu *et al.* 2020). The glyoxylate shunt may also allow Hybrid_5 to accumulate C4 compounds alongside the TCA cycle (Schneider *et al.* 2012). Hybrid_5 may be motile as it encodes for several flagellum production genes, including flagellar biosynthesis genes *flhAB* and *fliPQR*, basal body rod genes *flgCFG*, and motor switch genes *fliN* and *fliY* (Liu and Ochman 2007). Features indicating potential anaerobic metabolic capabilities are also present, including full lactic acid and ethanol fermentation pathways, an incomplete Calvin-Benson-Bassham (CBB) cycle (glyceraldehyde-3P to ribulose-5P), an incomplete reductive TCA cycle (S-malate to citrate), and a complete acetyl-CoA pathway for potential carbon fixation and acetyl-CoA generation (Oelgeschläger and Rother 2008). While Hybrid_5 possesses a full pyruvate dehydrogenase

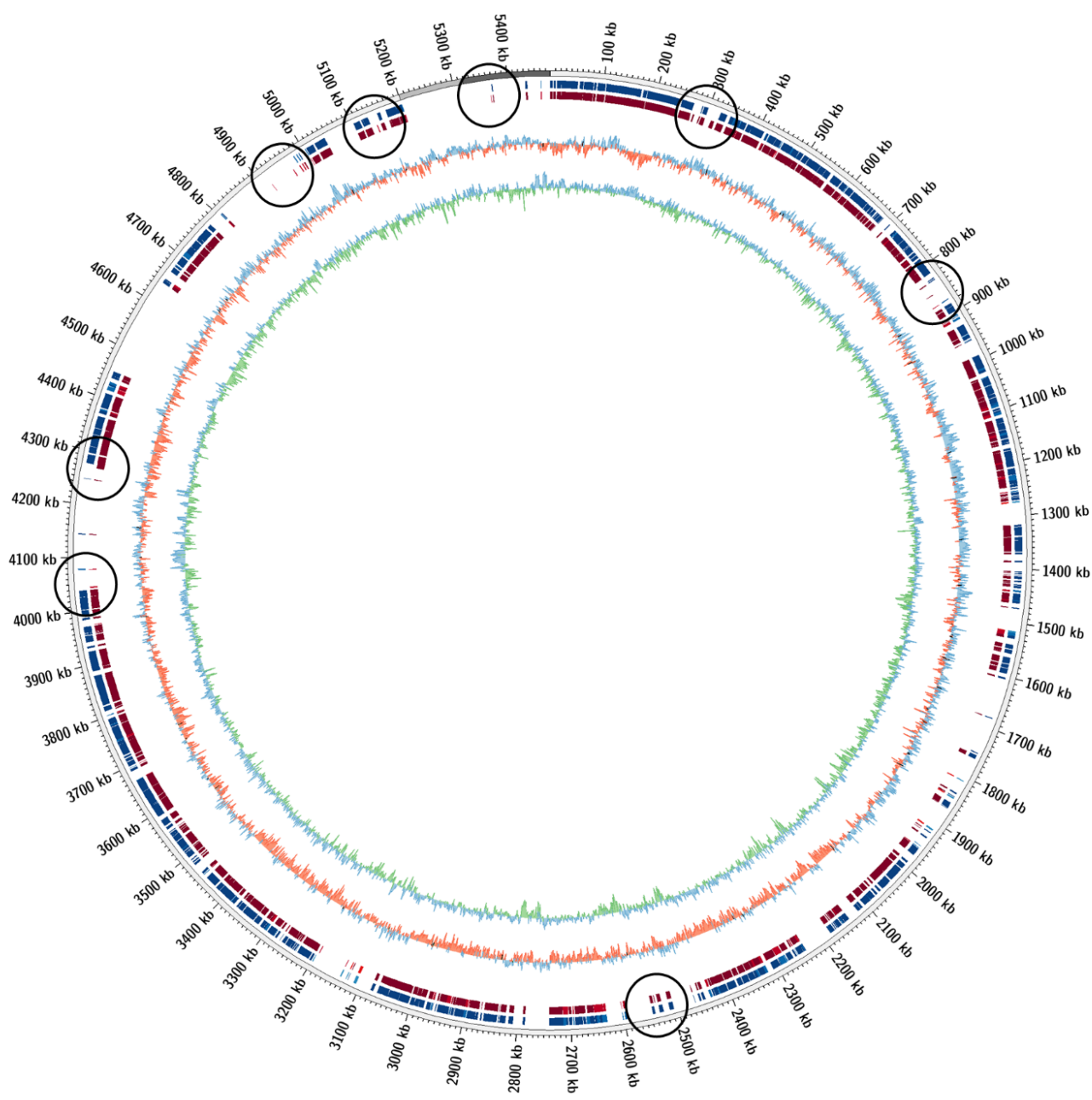


Figure 4.4. mummer2circo alignment of Hybrid_5 (red) and HiSeq_31 (blue) to the *Octadecabacter arcticus* genome (grey). Center plots are GC skew (blue/red) and GC content/variation (blue/green). Areas where Hybrid_5 covers more of the *O. Arcticus* genome are circled in black.

complex [EC 1.2.4.1; EC 2.3.1.12; EC 1.8.1.4] for pyruvate oxidation under aerobic conditions, its genome also has pyruvate:ferredoxin oxidoreductase [EC 1.7.2.1] for anaerobic oxidation of pyruvate (Hutcherson *et al.* 2017).

Hybrid_5 encodes a complete assimilatory sulfate reduction pathway (sulfate adenylyltransferase, *sat* and *cysND* [EC:2.7.7.4]; adenylylsulfate kinase, *cysC* [EC:2.7.1.25]; phosphoadenosine phosphosulfate reductase, *cysH* [EC:1.8.4.8]; sulfite reductase (NADPH), *cysJI* [EC:1.8.1.2] and sulfite reductase (ferredoxin), *sir* [EC:1.8.7.1]) and a partial dissimilatory sulfate reduction pathway (sulfate adenylyltransferase, *sat* [EC:2.7.7.4]; adenylylsulfate reductase, *aprAB* [EC:1.8.99.2]). Hybrid_5 also contains genes for full pathways of dissimilatory nitrate reduction (nitrate reductase, *narGHI* [EC:1.7.5.1] and *napAB* [EC:1.9.6.1]; nitrite reductase, *nirBD* [EC:1.7.1.15]), assimilatory nitrate reduction (ferredoxin-nitrate reductase, *narB* [EC:1.7.7.2] and *nasAB* [EC:1.7.99.-]; ferredoxin-nitrite reductase, *nirA* [EC:1.7.1.1]) and denitrification (nitrate reductase, *narGHI* [EC:1.7.5.1] and *napAB* [EC:1.9.6.1]; NO-forming nitrite reductase, *nirK* [EC:1.7.2.1]; nitric oxide reductase, *norBC* [EC:1.7.2.5]; nitrous oxide reductase, *nosZ* [EC:1.7.2.4]). Nitrite oxidoreductase, *nxrAB* (EC:1.7.99.-), is present but Hybrid_5 lacks a complete nitrification pathway. *nar*, *nap*, and *nas* nitrate reductases are all encoded by Hybrid_5; Nap is located in the periplasmic membrane for dissipation of reducing power, Nar is a respiratory transmembrane protein that generates a proton motive force for ATP production, and Nas biosynthesizes N products in the cytoplasm (Kuypers *et al.* 2018; Moreno-Vivián *et al.* 1999), signifying that Hybrid_5 is able to use nitrate for redox balancing, as a terminal electron acceptor, and as a nitrogen source (Moreno-Vivián *et al.* 1999).

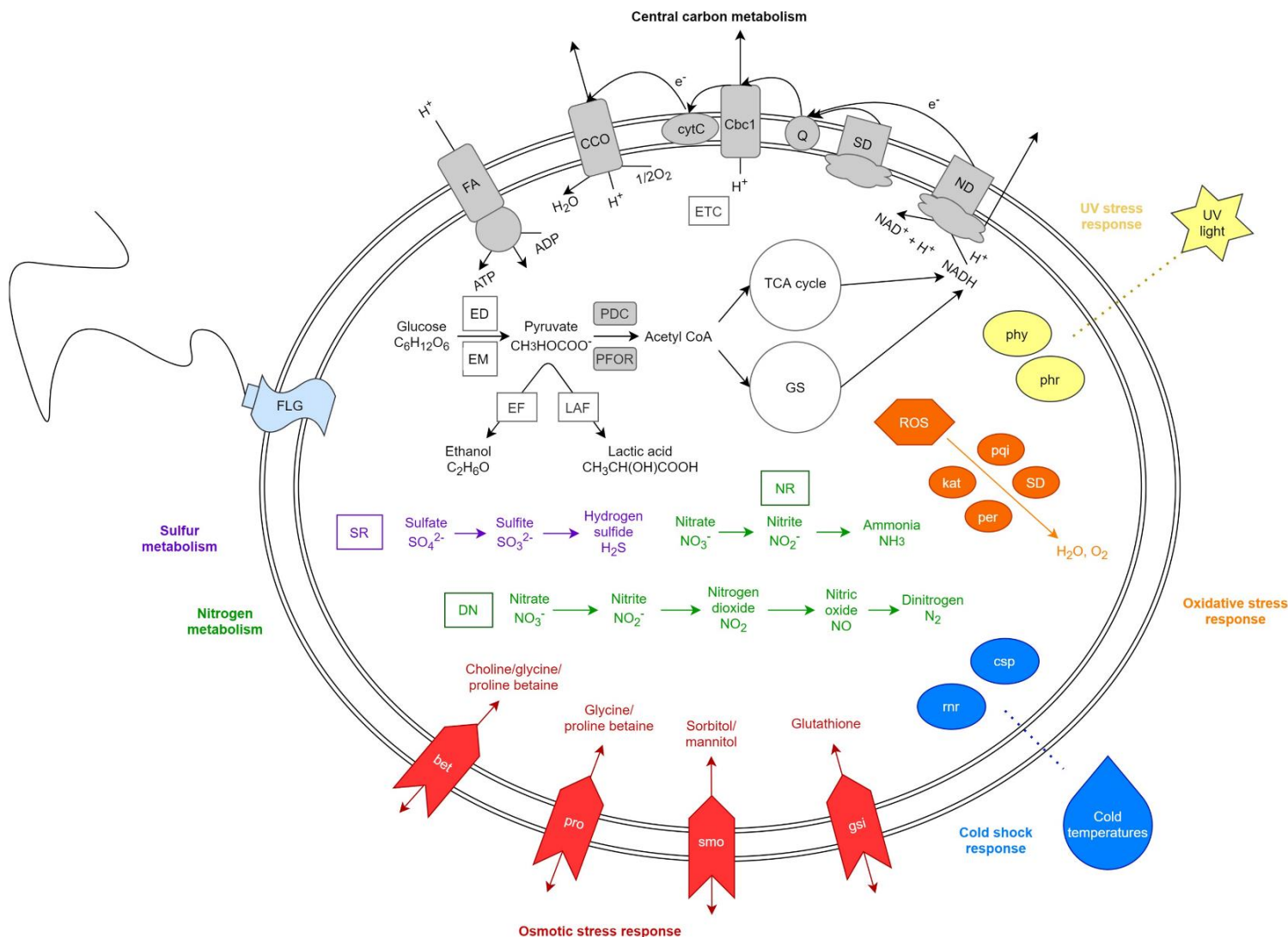


Figure 4.5. Model of Hybrid_5 cellular systems based on genomic data. Central carbon, nitrogen, and sulfur metabolisms are present, as well as stress response genes and pathways. Central carbon metabolism: Cbc1 = cytochrome bc1 complex; CCO = cytochrome c oxidase, cbb3-type; cytC = cytochrome C; ED = Entner-Doudoroff pathway; EF = ethanol fermentation; EM = Embden-Meyerhof glycolysis; ETC = electron transport chain; FA = F-type ATPase; Q = ubiquinone/quinone pool; GS = glyoxylate shunt; LAF = lactic acid fermentation; ND = NADH dehydrogenase; PDC = pyruvate dehydrogenase complex; PFOR = pyruvate:ferredoxin oxidoreductase; SD = succinate dehydrogenase; TCA = tricarboxylic acid. Nitrogen metabolism: DN = denitrification; NR = nitrate reduction. Sulfur metabolism: SR = sulfur reduction. Cold shock response: csp = cold shock protein; rnr = cold shock-induced ribonuclease R. Osmotic stress response: bet = glycine/choline/proline betaine transporters; gsi = glutathione transporters; pro = glycine/proline betaine transporters; smo = sorbitol/mannitol transporters. Oxidative stress response: kat = catalase-peroxidase; per = peroxidase; pqi = paraquat-inducible protein A; ROS = reactive oxygen species; SD = superoxide dismutase; UV stress response: phr = photolyase; phy = phytoene synthase. FLG = flagellar biosynthesis genes.

Many stress response and cold adaptation genes are present in Hybrid_5 (Supplementary Table 4.2), including general stress response (SOS-response transcriptional regulation), as well as more specialized genetic responses to extreme environments. Allen Bay experiences 24-hour light from the months of May to August (Canada 2020) which, coupled with the high albedo on sea ice, suggests that cryoconite consortia in this region must cope with deleterious UV radiation during these months (Hatam *et al.* 2014; Maccario *et al.* 2015). Hybrid_5 contains genes for carotenoid production (phytoene synthase) and photolyase *phrB* for DNA repair caused specifically by UV damage (Edwards *et al.* 2020; Goordial *et al.* 2016b; Raymond-Bouchard *et al.* 2018). Nutrient deprivation and rapid fluctuations are also common in sea ice and cryoconite environments (De Maayer *et al.* 2014; Maccario *et al.* 2015), and Hybrid_5 appears to endure these difficulties with *pho* genes and glycerol-3-phosphate O-acyltransferase (Goordial *et al.* 2016b; Raymond-Bouchard *et al.* 2018).

Cold temperatures such as those encountered in Allen Bay (1.33 °C; Table 4.1) require specialized genome-level adaptations, a number of which are present in Hybrid_5. These include cold shock proteins (*csp*), which bind to DNA and RNA to regulate transcription and translation at low temperatures (Bakermans *et al.* 2011), as well as molecular chaperones (e.g. *dnaJ*, *dnaK*, *hslO*) and chaperonins (e.g. *groES*, *groEL*) that ensure proper folding of cellular macromolecules (Edwards *et al.* 2020; Goordial *et al.* 2016b; Varin *et al.* 2012). Maintaining enzymatic rates for replication, transcription, and translation becomes more difficult at cold temperatures, and Hybrid_5 possesses several genes to counteract this reduced efficiency, such as recombination factors (e.g. *recA*, *recR*), DNA repair proteins (e.g. *recN*, *radA*), transcription termination factors (e.g. *rho*, *nusA*), and translation initiation factors (e.g. IF-1, IF-2) (Raymond-Bouchard *et al.* 2018; Varin *et al.* 2012). Proper protein folding is maintained in Hybrid_5 by peptidyl-prolyl cis-trans

isomerase and *tig* (Edwards *et al.* 2020). Membrane fluidity is negatively impacted at cold temperatures, and Hybrid_5 appears to compensate for this effect with several membrane, peptidoglycan, and polysaccharide capsule alteration and production genes including peptidoglycan synthesis genes *murABCDEFGF*, fatty acid elongation genes *fabBFGH*, and exopolysaccharide biosynthesis gene *epsC* (Barreteau *et al.* 2008; Goordial *et al.* 2016b; Magnuson *et al.* 2020; Raymond-Bouchard *et al.* 2018).

Osmotic and oxidative stress are also prevalent in cold environments due to increased environmental salinity and reactive oxygen species (ROS). The genomic adaptations present in Hybrid_5 to cope with rapid changes in environmental solute concentrations include several compatible solute (e.g. proline, glycine betaine, choline, carnitine, mannitol, sorbitol, glutamate) synthesis and transport genes, and transmembrane channel proteins (e.g. *kdpD*, NhaA family Na⁺:H⁺ antiporter) (Goordial *et al.* 2016b; Krulwich *et al.* 2009; Raymond-Bouchard *et al.* 2018). Hybrid_5 also possesses a number of antioxidant defenses against oxidative stress, such as superoxide dismutase, glutathione synthesis and transport genes (e.g. *gshB*, *gsiABC*), peroxiredoxin, and catalase-peroxidase (Goordial *et al.* 2016b; Raymond-Bouchard *et al.* 2018; Varin *et al.* 2012).

4.4 Discussion

The addition of MinION sequences to the HiSeq dataset resulted in a hybrid assembly superior to either of its constituent datasets. This is substantiated by the increase in contig length and classified coding sequences in the hybrid assembly, as well as the higher contig length, higher N50, higher completeness, and lower contamination in the hybrid MAGs. The increase of N50

increase in the hybrid MAGs indicates higher assembly contiguity than in the HiSeq dataset (Overholt *et al.* 2020; Sevim *et al.* 2019). This is further supported by the general higher completeness of the hybrid MAGs and the higher number of classified coding sequences in the hybrid assembly, despite having fewer contigs than the HiSeq assembly. The hybrid assembly also had the greatest number of MAGs produced, indicating that the addition of even a small amount of MinION data (i.e. 1.2 Gbp and 22.9 Gbp of MinION and HiSeq data, respectively) increases output as well as quality. In terms of financial cost, a “starter pack” from ONT includes a MinION Mk1b device, a flow cell, and a sequencing kit for \$1000 USD. One lane on a HiSeq 4000 typically costs ~\$2000 – 2500 USD, roughly double the price of the MinION starter park, and does not include the capacity to perform multiple runs in-house (although it produces sequences with ~100x fewer errors).

One hybrid MAG (Hybrid_5) and three MinION MAGs (MinION_3, MinION_RD_2, MinION_RD_3) had full complements of ribosomal RNA (i.e. 5S, 23S, and 16S genes). Ribosomal RNA is notoriously difficult to recover from binning programs (Alneberg *et al.* 2018) but remains an important marker for microbial ecology community analyses, particularly the 16S rRNA gene (Case *et al.* 2007). The ability of nanopore sequencing to resolve repetitive regions, like 16S rRNA (Somerville *et al.* 2019; Stewart *et al.* 2019), likely contributed to the recovery of ribosomal RNA in MAGs containing MinION sequences and can allow for greater elucidation of SSU phylogeny than possible with HiSeq-only MAGs. It is likely that with a larger nanopore dataset (e.g. metagenomes from high biomass environments, datasets generated by PromethION or multiple MinION sequencing runs), the benefits of adding long reads to short read datasets would be strengthened further. Indeed, it is possible to produce even genome-length contigs with nanopore sequencing (Bian *et al.* 2020; Jain *et al.* 2018; Loman *et al.* 2015), although these are

typically from single isolates in culture or higher biomass environments than those used in this study.

All three assembly methods tested agreed in their general summary of dominant taxa present in the Allen Bay sea ice (i.e. Bacteroidetes, followed by Proteobacteria). The differences between the MinION and hybrid/HiSeq datasets further support the benefit of additional lab-based sequencing after initial field sequencing with the MinION. Given the improved average contig length and number of coding sequences classified by JGI IMG/M ER in the hybrid assembly, we have based our discussion of the microbial community on this dataset. The hybrid assembly also contains a slightly more diverse metagenome than the HiSeq, likely due to the addition of MinION long reads increasing classification. For example, the phylum Candidatus Gracilibacteria, an uncultured lineage with limited metabolisms (Ley *et al.* 2006), was detected exclusively in the hybrid and MinION metagenomes, and the hybrid dataset contained more unique genes in a higher abundance than the HiSeq dataset, demonstrating the value and utility of hybrid assembly for characterizing extreme astrobiology analogue environments. Studies of Canadian Arctic cryoconites are typically limited to glacial environments; to the best of our knowledge, the present study is the first to examine cryoconite microbial communities on sea ice in the Canadian Arctic.

The Allen Bay sea ice cryoconites are primarily comprised of Bacteria as Bacteroidetes (Flavobacteriales) and Proteobacteria (Burkholderiales, Pseudomonadales, and Rhodobacterales) (Figure 4.2). Low amounts of Archaea were detected in our cryoconite metagenome, which may be due to the summer sampling time; archaeal abundances are known to increase in sea ice during winter (Collins *et al.* 2010). This relatively low sequence diversity is common in sea ice and cryoconite communities, which often contain a few central taxa but exhibit high spatial and temporal variability between sites (Maccario *et al.* 2015). These prevalent taxa in our metagenome

are ubiquitous in polar environments and are consistent with previous reports. Sea ice communities in the Canadian Arctic are frequently dominated by Bacteroidetes (*Flavobacterium*, *Polaribacter*), Alphaproteobacteria (SAR11, *Roseobacter*), and Gammaproteobacteria (*Moritella*) (Alonso-Sáez *et al.* 2008; Collins *et al.* 2010; Garneau *et al.* 2016; Yergeau *et al.* 2017), although their abundance and activity vary seasonally.

Cyanobacteria and Proteobacteria often dominate in glacial and alpine cryoconites and these environments are strongly associated with high rates of primary production (Edwards *et al.* 2014). However, some glacial and alpine cryoconite environments can contain predominantly heterotrophic bacteria (e.g. Alphaproteobacteria, Betaproteobacteria, Bacteroidetes) (Edwards *et al.* 2013a; Edwards *et al.* 2014; Edwards *et al.* 2013b). Indeed, at lower latitudes and on smaller glaciers, heterotrophic dominance may be the norm, supported by allochthonous input of carbon (Edwards *et al.* 2016). Arctic cryoconites frequently contain high abundances of Proteobacteria (Alphaproteobacteria), Bacteroidetes, and Cyanobacteria, as well as eukaryotic algae, protists, and fungi (Edwards *et al.* 2011; Edwards *et al.* 2013a; Edwards *et al.* 2014; Edwards *et al.* 2013c; Mueller *et al.* 2001). Heterotrophic bacteria are abundant in sea ice, particularly first-year sea ice (e.g. Alphaproteobacteria, Gammaproteobacteria, Flavobacteria) (Yergeau *et al.* 2017), supporting the abundance of Bacteroidetes (Flavobacteria) and Betaproteobacteria (Burkholderiales) in our Allen Bay sea ice cryoconites.

The physico-chemical data of the Allen Bay sea ice cryoconites are presented in Table 4.1. The cryoconite water was cold (1.33 °C) and somewhat salty (0.13 ppt), with a pH of 7.96. While the average salinity of Arctic seawater is ~32.5 – 35 ppt (Brogi *et al.* 2018; Brown *et al.* 2015), the salinity of nearby Resolute Bay's under-ice seawater has been previously reported as 0.2 ppt (Brown *et al.* 2015), a value consistent with the low salinity of 0.13 ppt noted here. The

ammoniacal nitrogen present is higher than other Canadian Arctic sites (Martin *et al.* 2010); like organic carbon, $\text{NH}_4\text{-N}$ could also be being actively discharged from the surrounding sea ice or produced by the nitrate-reducing bacteria present. The dissolved oxygen of 12.90 mg/L is similar to other cryoconites (Bagshaw *et al.* 2011; Hodson *et al.* 2010) and is high enough to support an aerobic community. Despite the low number of autotrophic community members, the oxygen content in the Allen Bay sea ice cryoconites is likely maintained with atmospheric exchange (Falkner *et al.* 2005). However, this contrasts with the negative oxidation-reduction potential (Lipson *et al.* 2010) that indicates a reducing environment. Based on the microbial community and DO value, it is possible that the ORP probe was malfunctioning and the reported value is inaccurate.

The low amount of total organic carbon (TOC) present in our cryoconites (112.75 ppm) indicates an overall oligotrophic environment (Singh *et al.* 2014). The TOC in the Allen Bay cryoconites is higher than reported values from seawater of nearby sites on Cornwallis Island (~0.8037 ppm) (Yergeau *et al.* 2017), but lower than other Arctic cryoconites (>10 000 ppm) (Kaštovská *et al.* 2005; Singh *et al.* 2014). Our TOC values are more similar to those reported for Cornwallis Island sea ice (~5 – 217 ppm) (Garneau *et al.* 2016; Yergeau *et al.* 2017), indicating that the carbon is likely exuded from the sea ice (Edwards *et al.* 2020). This low content of autotrophic taxa suggests that our cryoconites do not produce significant quantities of either autochthonous organic carbon or O_2 . While cryoconites can be defined as occurring solely on glaciers, containing filamentous Cyanobacteria as a crucial structural component and a dominance of autotrophic community members (Cook *et al.* 2016; Segawa *et al.* 2017), cryoconites have been previously described in non-glacial habitats and the microbial community of our samples is consistent with heterotrophic cryoconite communities (Edwards *et al.* 2016). Instead of being

produced by filamentous Cyanobacteria, the particulate organic carbon in the Allen Bay sea ice cryoconites is likely provided by periodic allochthonous carbon input (Edwards *et al.* 2013b) and organic exudation from the surrounding sea ice (Edwards *et al.* 2020). The size of the Allen Bay sea ice cryoconites (<3 cm) is also consistent with other cryoconites (Edwards *et al.* 2014), rather than larger supraglacial or sea ice melt pools/ponds (Trivedi *et al.* 2018; Xu *et al.* 2020).

The most complete and contiguous MAG produced from any assembly method was Hybrid_5 (Table 4.3). Hybrid_5 also possesses more unique genes and more genes with higher copy numbers than its HiSeq counterpart, HiSeq_31, demonstrating the value of hybrid assembly in detailed studies of microbial ecology. Hybrid_5 was identified as a member of *Octadecabacter* by both GTDB and MiGA, with an average nucleotide identity (ANI) of 93.51% with *Octadecabacter arcticus*, implying that Hybrid_5 is a potential novel species in the marine psychrophilic *Octadecabacter* genus. The prevalence of *Octadecabacter* in marine environments suggests that Hybrid_5 is not a native cryoconite microorganism and entered this environment via the seawater.

Hybrid_5 contains genes consistent with an aerobic/microaerophilic and heterotrophic lifestyle (Figure 4.5). *O. arcticus* shares these features, with the exception of the glyoxylate cycle; lacking isocitrate lyase [EC 4.1.3.1], *O. arcticus* instead uses the ethylmalonyl-CoA pathway as an alternative carbon metabolism (Schneider *et al.* 2012). The Hybrid_5 genome includes pathways for complete assimilatory sulfate reduction, assimilatory nitrate reduction, dissimilatory nitrate reduction, and denitrification, indicating that it can use sulfate or nitrate as a terminal electron acceptor. While denitrification is generally an anaerobic process, the presence of periplasmic *napAB* is a signpost of aerobic denitrification capabilities in many Proteobacteria, and suggests that Hybrid_5 is able to co-respire oxygen and nitrate (Ji *et al.* 2015). Co-respiration of oxygen

and nitrate is common in areas with rapidly fluctuating concentrations of oxygen, such as variable water flow within cryoconite holes (Marchant *et al.* 2017).

Unlike Hybrid_5, *O. arcticus* possesses few anaerobic features in its genome. It lacks full fermentative pathways, sulfate reduction pathways, and nitrate reduction pathways. While *O. antarcticus* and *O. temperatus* are known to reduce nitrite only (via nitrite reductase, *nirBD* [EC:1.7.1.15]) (Vollmers *et al.* 2013) and *O. sp. SW4* possesses a complete dissimilatory nitrate reduction pathway (nitrate reductase, *narGHI* [EC:1.7.5.1] and nitrite reductase, *nirBD* [EC:1.7.1.15]) (Parks *et al.* 2018), no other species of *Octadecabacter* contains genes for full assimilatory nitrate reduction, denitrification, assimilatory sulfate reduction, lactic acid fermentation, or ethanol fermentation. The presence of these anaerobic features in the Hybrid_5 genome indicates the likelihood that it is a novel species of *Octadecabacter* that functions as a facultative aerobe in its environment (Simon *et al.* 2009). Hybrid_5 further differs from *O. arcticus* in its lack of xanthorhodopsin and gas vesicle formation genes, suggesting it does not use light-driven proton pumping as a source of energy production and is not buoyant in the cryoconite meltwater (Vollmers *et al.* 2013). Hybrid_5 encodes for flagellar biosynthesis and may move via its flagella. However, although both *O. arcticus* and *O. antarcticus* possess flagellar gene clusters, they are non-motile and exact flagellar function remains to be explained (Gosink *et al.* 1997; Vollmers *et al.* 2013).

Cryoconite holes expose their native microbes to numerous external stressors (Cook *et al.* 2016; Maccario *et al.* 2015) and Hybrid_5 has a plethora of ways to cope with these extreme conditions (Supplementary Table 4.2), such as osmotic shock, reactive oxygen species (ROS), and freezing temperatures. The stress tolerance mechanisms of *Octadecabacter* species are largely unknown and the methods used by Hybrid_5 can elucidate these functions in this widespread polar

marine genus. Hybrid_5 synthesizes and transports several compatible solutes, the accumulation of which prevents water loss without disrupting cellular function and reduces the intracellular freezing point (Casanueva *et al.* 2010). In opposition, *O. arcticus* lacks an osmosensitive K⁺ channel histidine kinase and sorbitol/mannitol transport system proteins, and synthesizes ectoine as an osmolyte (Vollmers *et al.* 2013). As gas solubility increases at cold temperatures, so too does the concentration of ROS, necessitating that Hybrid_5 produce antioxidants to prevent cellular damage including superoxide dismutase, glutathione synthesis and transport genes, peroxiredoxin, and catalase-peroxidase (Goordial *et al.* 2016b; Raymond-Bouchard *et al.* 2018; Varin *et al.* 2012), features it shares with *O. arcticus*.

Hybrid_5 also possesses adaptations within its central carbon metabolism that can contribute to oxidative stress tolerance. The glyoxylate shunt is up-regulated under oxidative stress, as it lacks the TCA cycle's decarboxylation steps that produce NADH (Ahn *et al.* 2016; Van Acker and Coenye 2017), and glucose 6-phosphate dehydrogenase (*G6PD/zwf*) in the Entner-Doudoroff pathway converts NADP⁺ to NADPH to protect cells from oxidative stress (DangThu *et al.* 2020). The pyruvate dehydrogenases *aceE* and *aceF* are involved in both oxidative and cold stress responses (Varin *et al.* 2012). Cold temperatures reduce transcriptional and translational enzymatic activity, protein folding rates, and membrane fluidity (Goordial *et al.* 2016b; Raymond-Bouchard *et al.* 2018), and Hybrid_5 differs from HiSeq_31, the corresponding HiSeq-only MAG, in that its genome contains more of these protective features against cold temperatures and stresses. HiSeq_31 appears to lack *murB*, a transcription-repair coupling factor (superfamily II helicase), catalase peroxidase, an Na⁺:H⁺ antiporter, and peroxidase, as well as fewer gene copies of cold shock protein, *cspA*.

The increase in quality generated by the addition of MinION sequences to HiSeq datasets also demonstrates the utility of hybrid assembly in astrobiology and biosignature detection studies; post-initial DNA detection with the MinION, sample return and lab sequencing increase the information yielded to better characterize the natural consortia in extreme environments and elucidate further ways to detect them based on their genomes. MinION sequencing has strong potential for biosignature detection in future robotic and human planetary science missions based on its very small size/mass, minimal power requirements, and ability to produce reliable sequences from extreme environments (Castro-Wallace *et al.* 2017; Goordial *et al.* 2017; Maggiori *et al.* 2020). Nucleic acids are complex organic polymers that can only be produced by living systems, thereby providing an unequivocal biosignature; coupled with a reliable database, the MinION could readily determine if DNA/RNA sequences produced are terrestrial contaminants (Fairén *et al.* 2017), enabling a measure of protection against forward contamination in space missions and theoretically straightforward determination of non-terrestrial sequences (i.e. an unclassifiable, independent lineage). In this study, we have demonstrated the ability of the MinION to produce reliable metagenomes real-time in an extreme analogue environment, the Allen Bay sea ice cryoconites, which brings considerably more value than presence/absence DNA detection or single gene recognition (e.g. 16S); it allows for deeper exploration of phylogeny, as well as functional and metabolic potential. Analyses from samples returned to the laboratory can then be used to improve the characterization of the site's microbiology, as performed here with HiSeq sequencing and hybrid assembly, and inform on future studies for both biosignature detection and environmental microbiology of extreme environments.

Although considerable challenges remain in developing this technology for robotic space missions (e.g. automation of nucleic acid extraction and sequencing preparation, development of

non-degrading solid state nanopores) (Maggiore *et al.* 2020), the MinION's proven functionality in microgravity and space conditions (Carr *et al.* 2020; Castro-Wallace *et al.* 2017; John *et al.* 2016; Sutton *et al.* 2019) indicate its suitability for future life detection missions. While we have shown that MinION sequences can be used to supplement and improve HiSeq data to produce superior MAGs (Overholt *et al.* 2020), we have also demonstrated that the high sequencing error rate inherent in MinION technology currently precludes obtaining high-quality MinION-only MAGs. Significantly reducing the error rate through technology improvements (Jain *et al.* 2017) and/or metagenome-specific assembly and polishing pipelines will be crucial to bringing the MinION to a more robust technology readiness level (TRL) applicable to planetary science. The ideal MinION/nanopore sequencing technology would incorporate solid state nanopores to negate protein stability/degradation due to long flight times and radiation, be capable of detecting and sequencing very low concentrations of nucleic acids (DNA, RNA, xDNA), and generate low-error rate metagenomes and MAGs.

4.5 Conclusion

The present study combines short, accurate HiSeq reads with long, error-prone MinION sequences to produce more contiguous and more correct hybrid metagenomes and MAGs than either constituent dataset alone. MinION sequences generated in the Canadian high Arctic yielded a metagenome generally representative of the microbial community (>50% Bacteroidetes), as well as taxa and metabolisms not detected by traditional short read sequencing (e.g. *Candidatus Gracilibacteria*). When used to supplement HiSeq sequencing data, the resulting hybrid metagenomes contained longer contigs and more classified coding sequences, and the hybrid

MAGs had longer contigs, higher N50, higher completeness, and lower contamination than the HiSeq-only dataset. The increase in quality of the hybrid dataset is despite relatively low data output from the MinION and logistical restrictions of field sequencing. Additionally, none of the shortcomings of MinION sequencing were readily evident in the hybrid datasets (e.g. indel presence). We have also described a potential novel species of *Octadecabacter* (Hybrid_5) that conspicuously differs from its closest relative, *O. arcticus*, in its metabolic potential, possessing pathways for full nitrate reduction, denitrification, sulfate reduction, lactic acid fermentation, and ethanol fermentation pathways. Hybrid_5 likely functions as a facultative aerobe in its environment and the Allen Bay sea ice cryoconite habitat is largely based on aerobic heterotrophy. This knowledge expands our knowledge of genome reconstruction with hybrid assembly in samples from extreme environments.

4.6 Methods

4.6.1 Sample site and collection

Samples were collected from Allen Bay sea ice (latitude: 74.44707; longitude: -95.0348) near Resolute, Nunavut, Canada in the Canadian Arctic Archipelago on July 12, 2018 (Figure 4.1). Allen Bay is located in a polar tundra; the area remains ice-covered for ~10 months per year (Brown *et al.* 2015), experiencing an average annual temperature of -15.7 °C and precipitation of 161.2 mm (Canada 2020). Samples were collected aseptically directly on the sea ice from holes <3 cm in diameter and all collection tools were sterilized with 70% ethanol. Latex gloves were worn during collection and samples were loaded into sterile falcon tubes. Samples were then

transported from the collection site to the Polar Continental Shelf Program facility (PCSP) at the Martin Bergmann Complex in Resolute for immediate DNA extraction and MinION sequencing. Remaining samples were later transported to Montreal, Quebec, Canada at $-5\text{ }^{\circ}\text{C}$ and subsequently stored at $-25\text{ }^{\circ}\text{C}$ prior to analysis at McGill University (geochemical analyses) and Genome Quebec (HiSeq sequencing). DNA extraction was performed differently for MinION and Illumina sequencing and is described for each technique below.

4.6.2 Geochemical Analyses

Dissolved oxygen, salinity, conductivity, total dissolved solids, barometric pressure, pH, and temperature were measured *in situ* with a YSI Pro2030 Field Dissolved Oxygen/Conductivity Meter (Cat No./ID:14-660-204). Nearby cryoconite samples were later analyzed for total organic carbon (TOC) and ammoniacal nitrogen ($\text{NH}_4\text{-N}$) at McGill University. TOC was measured by the ultra-violet /persulfate oxidation method on a Sievers Innovox TOC analyzer (General Electric Power and Water, Water and Process Technologies, Boulder, Colorado, USA). $\text{NH}_4\text{-N}$ concentrations were determined spectrophotometrically using the modified indophenol blue method53 at 650 nm on a microplate reader (μ Quant, BioTek Instruments, Winooski, Vermont, USA).

4.6.3 DNA extraction and MinION sequencing

In order to maximize differential coverage for binning(Albertsen *et al.* 2013), we performed multiple DNA extractions and MinION sequencing runs near Allen Bay at

PCSP(Raymond-Bouchard *et al.* 2021). Extraction details are described in Supplementary Table 4.3. Cell lysis was performed using the SuperFastPrep-2 (MP Biomedicals), a handheld cell homogenizer. With 0.25 – 0.5 g of sample, we used Solution C1 from the Qiagen DNeasy Powerlyzer PowerSoil DNA kit (Cat No./ID: 12855-50) as well as either the Lysing Matrix A beads from MP Biomedicals (Cat No./ID: 116910050) or the PowerSoil beads supplied with the DNeasy kit for 45 seconds at the power setting of 25 for initial extraction. Following initial beating, one extract (Crude) was filtered with a 0.45 µm filter to remove large debris and treated no further. Two other extracts (C3FullM and VolTRAX) underwent the purification steps outlined in the DNeasy protocol (steps #5 – 19) and eluted in 50 µl of nuclease-free water. The final sample (C3Claremont) was extracted with the Claremont SimplePrep X1, an automated DNA extraction and purification system (Cat No./ID: 08.104.01), according to manufacturer's instructions using low inhibitor cartridges (Cat No./ID: 08.440.01) and 0.3 – 0.5 g of sample.

Four MinION sequencing runs were with these extracts as described in Supplementary Table 4.3. Three of the extracts (Crude, C3FullM, and C3Claremont) were prepared for sequencing using the Rapid PCR Barcoding kit (SQK-RPB004) and sequenced on separate R9.4 FLO-MIN106 flow cells with a MinION Mk1b device. One purified extract (VolTRAX) was prepared for sequencing with the VolTRAX sequencing kit (VSK-VSK002) and VolTRAX V2 device. It was subsequently sequenced on a R9.4 FLO-MIN106 flow cell with a MinION Mk1b device. All sequences were basecalled with MinKNOW version 1.7.7 and trimmed using Porechop version 0.2.3 (<https://github.com/rrwick/Porechop>).

4.6.4 DNA extraction and HiSeq sequencing

For HiSeq sequencing, a total of 10 extractions were performed in the laboratory at McGill University and pooled to maximize differential coverage for binning (Albertsen *et al.* 2013). These extractions are described in Supplementary Table 4.4. Cryoconite 1 was extracted as follows: a crude extraction with the SuperFastPrep-2 (C1Crude), a full extraction with the SuperFastPrep-2 and the purification steps outlined in the DNeasy protocol (steps #5 – 19) (C1FullM), and a full and purified extraction with the DNeasy kit according to the manufacturer's instructions (C1Full). Cryoconite 2 was extracted as follows: a full extraction with the SuperFastPrep-2 and the purification steps outlined in the DNeasy protocol (steps #5 – 19) (C2FullM), and two full and purified extractions with the DNeasy kit according to the manufacturer's instructions (C2Full1 and C2Full2). Cryoconite 3 was extracted as follows: a full extraction with the SuperFastPrep-2 and the purification steps outlined in the DNeasy protocol (steps #5 – 19) (C3FullM), two full and purified extractions with the DNeasy kit according to the manufacturer's instructions (C3Full1 and C3Full2), and an extraction with the Claremont SimplePrep X1 (C3Claremont). The SuperFastPrep-2 and Claremont extractions were used as described for MinION sequencing in the previous section.

Samples were prepared for sequencing using the Nextera XT DNA Library Preparation Kit (Cat No./ID: FC-131-1096) and sequenced at Genome Quebec (Montreal, Canada) with an Illumina HiSeq 4000 (paired end 100 bp). All sequences were quality filtered with FastQC and trimmed with trimmomatic version 0.36.

4.6.5 Contig assembly and binning

To assess the value of adding MinION-generated data to traditional contig assembly and genome binning from metagenome methods, we performed three types of assembly and binning: HiSeq, hybrid, and MinION. HiSeq assembly and binning used contigs generated only from HiSeq sequencing. For HiSeq assembly, trimmed and quality filtered sequences were assembled into contigs with metaSPAdes version 3.13.0, a pipeline of the SPAdes assembler using default parameters. Contigs less than 500 bp were discarded and the total assembly length was 261 582 792 bp.

For HiSeq binning, Minimap2 version 2.13 (Li 2018) and Samtools version 1.9 (Li *et al.* 2009) were used for mapping and sorting, respectively. Metabat version 2.12.1 (Kang *et al.* 2015) was used to bin the assembled, mapped, and sorted contigs, followed by contamination reduction and completeness improvement with refinem version 0.0.25 (Parks *et al.* 2017). Final bin statistics were determined with CheckM version 1.0.13 (Parks *et al.* 2015).

Hybrid assembly and binning used sequences from both HiSeq and MinION metagenomes, assembled together into hybrid contigs. For hybrid assembly, trimmed and quality filtered sequences from the HiSeq 4000 sequencer were assembled with the trimmed MinION sequences using the hybrid option of metaSPAdes version 3.13.0 (e.g. default parameters and inclusion of the MinION dataset with the “--nanopore” flag). Contigs less than 500 bp were discarded and the total assembly length was 276 349 668 bp.

For hybrid binning, Minimap2 version 2.13 (Li 2018) and Samtools version 1.9 (Li *et al.* 2009) were used for mapping and sorting, respectively. Metabat version 2.12.1 (Kang *et al.* 2015) was used to bin the assembled, mapped, and sorted contigs, followed by contamination reduction

and completeness improvement with refinem version 0.0.25 (Parks *et al.* 2017). Final bin statistics were determined with CheckM version 1.0.13 (Parks *et al.* 2015).

MinION assembly and binning used contigs generated only from MinION sequencing. For MinION assembly, sequences were corrected and assembled with Canu version 1.8 (Koren *et al.* 2017) with parameters “corOutCoverage=10000,” “corMinCoverage=0,” “corMhapSensitivity=high,” and an assumed genome size of 4.25 Mbp, followed by polishing for consensus sequence improvement with Nanopolish version 0.12.0 (Loman *et al.* 2015) and default parameters. Contigs less than 989 bp were discarded and the total assembly length was 25 193 561 bp.

For MinION binning, additional polishing using the HiSeq short reads with three rounds of Racon version 1.4.11 (Vaser *et al.* 2017) was also performed, as well as frameshift error correction with DIAMOND version 0.9.25 (Buchfink *et al.* 2015) and MEGAN-ization to produce a final fasta file of the MinION contigs with MEGAN-lr (Huson *et al.* 2007). Contigs with coverage significantly different from the mean were manually removed from select MinION bins in order to improve completeness and decrease contamination. Minimap2 version 2.13 (Li 2018) and Samtools version 1.9 (Li *et al.* 2009) were used for mapping and sorting, respectively. Metabat version 2.12.1 (Kang *et al.* 2015) was used to bin the assembled, mapped, and sorted contigs, followed by contamination reduction and completeness improvement with refinem version 0.0.25 (Parks *et al.* 2017). Final bin statistics were determined with CheckM version 1.0.13 (Parks *et al.* 2015).

Metagenomic contigs from all three datasets (HiSeq, hybrid, MinION) were uploaded to JGI IMG/M ER (Markowitz *et al.* 2011) for annotation. Bins from all three datasets (HiSeq, hybrid, MinION) were annotated with both RAST (Aziz *et al.* 2008) and MetaErg (Dong and Strous 2019),

with taxonomy determination based on the Genome Taxonomy Database (GTDB) (Parks *et al.* 2018), and uploaded to the Microbial Genomes Atlas Online (MiGA) (Rodriguez-R *et al.* 2018) for average nucleotide identity (ANI) determination. IDEEL (Stewart *et al.* 2019) was also used to test for ORF interruptions in the contig sets and the completed MAGS using the UniProt TREMBL database (Consortium 2019). Mummer2circos (<https://github.com/metagenlab/mummer2circos>) was used to plot hybrid and HiSeq MAGs against their closest taxonomic relative. Metagenome and MAG data are available in JGI (analysis project IDs Ga0450655, Ga0450656, Ga0450657) and GenBank (BioProject accession number PRJNA673486).

4.7 References

- Ahlgren G., Gustafsson I. B., and Boberg M. (1992) FATTY ACID CONTENT AND CHEMICAL COMPOSITION OF FRESHWATER MICROALGAE 1. *Journal of phycology*, 28: 37-50.
- Ahn S., Jung J., Jang I.-A., Madsen E. L., and Park W. (2016) Role of glyoxylate shunt in oxidative stress response. *Journal of Biological Chemistry*, 291: 11928-11938.
- Albertsen M., Hugenholtz P., Skarshewski A., Nielsen K. L., Tyson G. W., and Nielsen P. H. (2013) Genome sequences of rare, uncultured bacteria obtained by differential coverage binning of multiple metagenomes. *Nature biotechnology*, 31: 533-538.
- Alneberg J., Karlsson C. M., Divne A.-M., Bergin C., Homa F., Lindh M. V., Hugerth L. W., Ettema T. J., Bertilsson S., and Andersson A. F. (2018) Genomes from uncultivated prokaryotes: a comparison of metagenome-assembled and single-amplified genomes. *Microbiome*, 6: 173.
- Alonso-Sáez L., Sánchez O., Gasol J. M., Balagué V., and Pedrós-Alio C. (2008) Winter-to-summer changes in the composition and single-cell activity of near-surface Arctic prokaryotes. *Environmental Microbiology*, 10: 2444-2454.
- Ammor M. S. (2007) Recent advances in the use of intrinsic fluorescence for bacterial identification and characterization. *Journal of fluorescence*, 17: 455-459.
- Anderson M. J., and Walsh D. C. (2013) PERMANOVA, ANOSIM, and the Mantel test in the face of heterogeneous dispersions: what null hypothesis are you testing? *Ecological monographs*, 83: 557-574.
- Anesio A. M., Lutz S., Christmas N. A., and Benning L. G. (2017) The microbiome of glaciers and ice sheets. *npj Biofilms and Microbiomes*, 3: 1-11.
- Archer S. D., de los Ríos A., Lee K. C., Niederberger T. S., Cary S. C., Coyne K. J., Douglas S., Lacap-Bugler D. C., and Pointing S. B. (2017) Endolithic microbial diversity in sandstone and granite from the McMurdo Dry Valleys, Antarctica. *Polar Biology*, 40: 997-1006.
- Aziz R. K., Bartels D., Best A. A., DeJongh M., Disz T., Edwards R. A., Formsma K., Gerdes S., Glass E. M., and Kubal M. (2008) The RAST Server: rapid annotations using subsystems technology. *BMC genomics*, 9: 1-15.
- Bagshaw E., Tranter M., Wadham J., Fountain A., and Mowlem M. (2011) High-resolution monitoring reveals dissolved oxygen dynamics in an Antarctic cryoconite hole. *Hydrological Processes*, 25: 2868-2877.
- Bakermans C., Bergholz P. W., Rodrigues D. F., Vishnivetskaya T. A., Ayala-del-Río H. L., and Tiedje J. M. (2011) Genomic and expression analyses of cold-adapted microorganisms. *Polar microbiology: life in a deep freeze*: 126-155.
- Balme M., Grindrod P., Sefton-Nash E., Davis J., Gupta S., Fawdon P., Sidiropoulos P., Yershov V., and Muller J.-P. (2015) Aram Dorsum: A Noachian Inverted Fluvial Channel System and Candidate Exomars 2018 Rover Landing Site. Lunar and Planetary Science Conference.
- Banfield D., Stern J., Davila A., Johnson S. S., Brain D., Wordsworth R., Horgan B., Williams R. M., Niles P., and Rucker M. (2021) Summary of the Mars Science Goals, Objectives, Investigations, and Priorities. *Bulletin of the American Astronomical Society*, 53: 142.

- Baqué M., Verseux C., Böttger U., Rabbow E., de Vera J.-P. P., and Billi D. (2016) Preservation of biomarkers from cyanobacteria mixed with Marslike regolith under simulated Martian atmosphere and UV flux. *Origins of Life and Evolution of Biospheres*, 46: 289-310.
- Barreteau H., Kovač A., Boniface A., Sova M., Gobec S., and Blanot D. (2008) Cytoplasmic steps of peptidoglycan biosynthesis. *FEMS microbiology reviews*, 32: 168-207.
- Beegle L., Bhartia R., White M., DeFlores L., Abbey W., Wu Y.-H., Cameron B., Moore J., Fries M., and Burton A. (2015) SHERLOC: Scanning habitable environments with Raman & luminescence for organics & chemicals. Aerospace Conference, 2015 IEEE. IEEE.
- Benner S. A. (2017) Detecting Darwinism from molecules in the Enceladus plumes, Jupiter's moons, and other planetary water lagoons. *Astrobiology*, 17: 840-851.
- Berg B., Ronholm J., Applin D., Mann P., Izawa M., Cloutis E., and Whyte L. (2014) Spectral features of biogenic calcium carbonates and implications for astrobiology. *International Journal of Astrobiology*, 13: 353-365.
- Bertrand D., Shaw J., Kalathiyappan M., Ng A. H. Q., Kumar M. S., Li C., Dvornicic M., Soldo J. P., Koh J. Y., and Tong C. (2019) Hybrid metagenomic assembly enables high-resolution analysis of resistance determinants and mobile elements in human microbiomes. *Nature biotechnology*, 37: 937-944.
- Bian L., Li F., Ge J., Wang P., Chang Q., Zhang S., Li J., Liu C., Liu K., and Liu X. (2020) Chromosome-level genome assembly of the greenfin horse-faced filefish (*Thamnaconus septentrionalis*) using Oxford Nanopore PromethION sequencing and Hi-C technology. *Molecular ecology resources*, 20: 1069-1079.
- Bishop J. L., Dobrea E. Z. N., McKeown N. K., Parente M., Ehlmann B. L., Michalski J. R., Milliken R. E., Poulet F., Swayze G. A., and Mustard J. F. (2008) Phyllosilicate diversity and past aqueous activity revealed at Mawrth Vallis, Mars. *Science*, 321: 830-833.
- Blanco Y., Prieto-Ballesteros O., Gómez M. J., Moreno-Paz M., García-Villadangos M., Rodríguez-Manfredi J. A., Cruz-Gil P., Sánchez-Román M., Rivas L. A., and Parro V. (2012) Prokaryotic communities and operating metabolisms in the surface and the permafrost of Deception Island (Antarctica). *Environmental microbiology*, 14: 2495-2510.
- Boquet E., Boronat A., and Ramos-Cormenzana A. (1973) Production of calcite (calcium carbonate) crystals by soil bacteria is a general phenomenon. *Nature*, 246: 527.
- Bowers R. M., Kyrpides N. C., Stepanauskas R., Harmon-Smith M., Doud D., Reddy T., Schulz F., Jarett J., Rivers A. R., and Elie-Fadrosh E. A. (2017) Minimum information about a single amplified genome (MISAG) and a metagenome-assembled genome (MIMAG) of bacteria and archaea. *Nature biotechnology*, 35: 725-731.
- Brocks J. J., Buick R., Logan G. A., and Summons R. E. (2003) Composition and syngeneity of molecular fossils from the 2.78 to 2.45 billion-year-old Mount Bruce Supergroup, Pilbara Craton, Western Australia. *Geochimica et Cosmochimica Acta*, 67: 4289-4319.
- Broggi S. R., Ha S.-Y., Kim K., Derrien M., Lee Y. K., and Hur J. (2018) Optical and molecular characterization of dissolved organic matter (DOM) in the Arctic ice core and the underlying seawater (Cambridge Bay, Canada): Implication for increased autochthonous DOM during ice melting. *Science of The Total Environment*, 627: 802-811.
- Brown B. L., Watson M., Minot S. S., Rivera M. C., and Franklin R. B. (2017) MinION™ nanopore sequencing of environmental metagenomes: a synthetic approach. *GigaScience*, 6: 1-10.

- Brown C. L., Keenum I. M., Dai D., Zhang L., Vikesland P. J., and Pruden A. (2021) Critical evaluation of short, long, and hybrid assembly for contextual analysis of antibiotic resistance genes in complex environmental metagenomes. *Scientific reports*, 11: 1-12.
- Brown K. A., Miller L. A., Mundy C. J., Papakyriakou T., Francois R., Gosselin M., Carnat G., Swystun K., and Tortell P. D. (2015) Inorganic carbon system dynamics in landfast Arctic sea ice during the early-melt period. *Journal of Geophysical Research: Oceans*, 120: 3542-3566.
- Buchfink B., Xie C., and Huson D. H. (2015) Fast and sensitive protein alignment using DIAMOND. *Nature methods*, 12: 59-60.
- Bywaters K., Schmidt H., Vercoutere W., Deamer D., Hawkins A., Quinn R., Burton A., and McKay C. (2017) Development of Solid-State Nanopore Technology for Life Detection.
- Cabrerizo A., Tejedó P., Dachs J., and Benayas J. (2016) Anthropogenic and biogenic hydrocarbons in soils and vegetation from the South Shetland Islands (Antarctica). *Science of the Total Environment*, 569: 1500-1509.
- Canada E. (2020) Canadian Climate Normals 1981-2010 Station Data.
- Carr C. E., Bryan N. C., Saboda K. N., Bhattaru S. A., Ruvkun G., and Zuber M. T. (2020) Nanopore sequencing at Mars, Europa, and microgravity conditions. *npj Microgravity*, 6: 1-6.
- Carr C. E., Mojarro A., Hachey J., Saboda K., Tani J., Bhattaru S. A., Smith A., Pontefract A., Zuber M. T., and Doebler R. (2017) Towards in situ sequencing for life detection. Aerospace Conference, 2017 IEEE. IEEE.
- Carrizo D., Sánchez-García L., Menes R. J., and García-Rodríguez F. (2019) Discriminating sources and preservation of organic matter in surface sediments from five Antarctic lakes in the Fildes Peninsula (King George Island) by lipid biomarkers and compound-specific isotopic analysis. *Science of The Total Environment*, 672: 657-668.
- Casanueva A., Tuffin M., Cary C., and Cowan D. A. (2010) Molecular adaptations to psychrophily: the impact of 'omic' technologies. *Trends in microbiology*, 18: 374-381.
- Case R. J., Boucher Y., Dahllöf I., Holmström C., Doolittle W. F., and Kjelleberg S. (2007) Use of 16S rRNA and rpoB genes as molecular markers for microbial ecology studies. *Applied and environmental microbiology*, 73: 278-288.
- Castanier S., Le Métayer-Levrel G., and Perthuisot J.-P. (1999) Ca-carbonates precipitation and limestone genesis—the microbiogeologist point of view. *Sedimentary geology*, 126: 9-23.
- Castro-Wallace S. L., Chiu C. Y., John K. K., Stahl S. E., Rubins K. H., McIntyre A. B., Dworkin J. P., Lupisella M. L., Smith D. J., and Botkin D. J. (2017) Nanopore DNA sequencing and genome assembly on the International Space Station. *Scientific reports*, 7: 18022.
- Chan-Yam K., Goordial J., Greer C., Davila A., McKay C. P., and Whyte L. G. (2019) Microbial activity and habitability of an Antarctic dry valley water track. *Astrobiology*, 19: 757-770.
- Chen L.-X., Anantharaman K., Shaiber A., Eren A. M., and Banfield J. F. (2020) Accurate and complete genomes from metagenomes. *Genome research*, 30: 315-333.
- Clark R. N., King T. V., Klejwa M., Swayze G. A., and Vergo N. (1990) High spectral resolution reflectance spectroscopy of minerals. *Journal of Geophysical Research: Solid Earth*, 95: 12653-12680.

- Clarke J. D., and Stoker C. R. (2011) Concretions in exhumed and inverted channels near Hanksville Utah: implications for Mars. *International Journal of Astrobiology*, 10: 161-175.
- Cloutis E. A., Hawthorne F. C., Mertzman S. A., Krenn K., Craig M. A., Marcino D., Methot M., Strong J., Mustard J. F., and Blaney D. L. (2006) Detection and discrimination of sulfate minerals using reflectance spectroscopy. *Icarus*, 184: 121-157.
- Coates J. D., Michaelidou U., Bruce R. A., O'Connor S. M., Crespi J. N., and Achenbach L. A. (1999) Ubiquity and diversity of dissimilatory (per) chlorate-reducing bacteria. *Applied and Environmental Microbiology*, 65: 5234-5241.
- Coates R. C., Podell S., Korobeynikov A., Lapidus A., Pevzner P., Sherman D. H., Allen E. E., Gerwick L., and Gerwick W. H. (2014) Characterization of cyanobacterial hydrocarbon composition and distribution of biosynthetic pathways. *PLOS one*, 9: e85140.
- Cockell C. S., Schuerger A. C., Billi D., Friedmann E. I., and Panitz C. (2005) Effects of a simulated martian UV flux on the cyanobacterium, *Chroococcidiopsis* sp. 029. *Astrobiology*, 5: 127-140.
- Collins R. E., Rocap G., and Deming J. W. (2010) Persistence of bacterial and archaeal communities in sea ice through an Arctic winter. *Environmental microbiology*, 12: 1828-1841.
- Consortium U. (2019) UniProt: a worldwide hub of protein knowledge. *Nucleic acids research*, 47: D506-D515.
- Cook J., Edwards A., Takeuchi N., and Irvine-Fynn T. (2016) Cryoconite: the dark biological secret of the cryosphere. *Progress in Physical Geography*, 40: 66-111.
- Council N. R. (2019) The limits of organic life in planetary systems. The national academy of press.
- Cranwell P. (1978) Extractable and bound lipid components in a freshwater sediment. *Geochimica et Cosmochimica Acta*, 42: 1523-1532.
- Crowley J., Williams D., Hammarstrom J., Piatak N., Chou I.-M., and Mars J. (2003) Spectral reflectance properties (0.4–2.5 μm) of secondary Fe-oxide, Fe-hydroxide, and Fe-sulphate-hydrate minerals associated with sulphide-bearing mine wastes. *Geochemistry: Exploration, Environment, Analysis*, 3: 219-228.
- DangThu Q., Jang S. H., and Lee C. (2020) Biochemical comparison of two glucose 6-phosphate dehydrogenase isozymes from a cold-adapted *Pseudomonas mandelii*. *Extremophiles: life under extreme conditions*.
- Davis J., Balme M., Grindrod P., Williams R., and Gupta S. (2016) Extensive Noachian fluvial systems in Arabia Terra: Implications for early Martian climate. *Geology*, 44: 847-850.
- De Maayer P., Anderson D., Cary C., and Cowan D. A. (2014) Some like it cold: understanding the survival strategies of psychrophiles. *EMBO reports*, 15: 508-517.
- De Maio N., Shaw L. P., Hubbard A., George S., Sanderson N. D., Swann J., Wick R., AbuOun M., Stubberfield E., and Hoosdally S. J. (2019) Comparison of long-read sequencing technologies in the hybrid assembly of complex bacterial genomes. *Microbial genomics*, 5.
- De Sanctis M. C., Altieri F., Ammannito E., Biondi D., De Angelis S., Meini M., Mondello G., Novi S., Paolinetti R., and Soldani M. (2017) Ma_MISS on ExoMars: mineralogical characterization of the martian subsurface. *Astrobiology*, 17: 612-620.

- de Vera J.-P., Schulze-Makuch D., Khan A., Lorek A., Koncz A., Möhlmann D., and Spohn T. (2014) Adaptation of an Antarctic lichen to Martian niche conditions can occur within 34 days. *Planetary and Space Science*, 98: 182-190.
- Diaz B., and Schulze-Makuch D. (2006) Microbial survival rates of *Escherichia coli* and *Deinococcus radiodurans* under low temperature, low pressure, and UV-irradiation conditions, and their relevance to possible martian life. *Astrobiology*, 6: 332-347.
- Didyk B., Simoneit B., Brassell S. t., and Eglinton G. (1978) Organic geochemical indicators of palaeoenvironmental conditions of sedimentation. *Nature*, 272: 216-222.
- Dijkman N. A., Boschker H. T., Stal L. J., and Kromkamp J. C. (2010) Composition and heterogeneity of the microbial community in a coastal microbial mat as revealed by the analysis of pigments and phospholipid-derived fatty acids. *Journal of Sea Research*, 63: 62-70.
- Direito S. O., Ehrenfreund P., Marees A., Staats M., Foing B., and Röling W. F. (2011) A wide variety of putative extremophiles and large beta-diversity at the Mars Desert Research Station (Utah). *International Journal of Astrobiology*, 10: 191-207.
- Dolezel J., Bartos J., Voglmayr H., and Greilhuber J. (2003) Nuclear DNA content and genome size of trout and human. *Cytometry. Part A: the journal of the International Society for Analytical Cytology*, 51: 127.
- Dong H., Rech J. A., Jiang H., Sun H., and Buck B. J. (2007) Endolithic cyanobacteria in soil gypsum: Occurrences in Atacama (Chile), Mojave (United States), and Al-Jafr Basin (Jordan) Deserts. *Journal of Geophysical Research: Biogeosciences*, 112.
- Dong X., and Strous M. (2019) An integrated pipeline for annotation and visualization of metagenomic contigs. *Frontiers in genetics*, 10.
- Dorn R. I., and Oberlander T. M. (1981) Microbial origin of desert varnish. *Science*, 213: 1245-1247.
- Douki T. (2013) The variety of UV-induced pyrimidine dimeric photoproducts in DNA as shown by chromatographic quantification methods. *Photochemical & Photobiological Sciences*, 12: 1286-1302.
- Downs R. (2006) The RRUFF Project: an integrated study of the chemistry, crystallography, Raman and infrared spectroscopy of minerals. Program and Abstracts of the 19th General Meeting of the International Mineralogical Association in Kobe, Japan, 2006.
- Edwards A., Anesio A. M., Rassner S. M., Sattler B., Hubbard B., Perkins W. T., Young M., and Griffith G. W. (2011) Possible interactions between bacterial diversity, microbial activity and supraglacial hydrology of cryoconite holes in Svalbard. *The ISME journal*, 5: 150-160.
- Edwards A., Cameron K. A., Cook J. M., Debbonaire A. R., Furness E., Hay M. C., and Rassner S. M. (2020) Microbial genomics amidst the Arctic crisis. *Microbial Genomics*: mgen000375.
- Edwards A., Debbonaire A. R., Sattler B., Mur L. A., and Hodson A. J. (2016) Extreme metagenomics using nanopore DNA sequencing: a field report from Svalbard, 78 N. *bioRxiv*: 073965.
- Edwards A., Douglas B., Anesio A. M., Rassner S. M., Irvine-Fynn T. D., Sattler B., and Griffith G. W. (2013a) A distinctive fungal community inhabiting cryoconite holes on glaciers in Svalbard. *fungal ecology*, 6: 168-176.
- Edwards A., Mur L. A., Girdwood S. E., Anesio A. M., Stibal M., Rassner S. M., Hell K., Pachebat J. A., Post B., and Bussell J. S. (2014) Coupled cryoconite ecosystem structure–

- function relationships are revealed by comparing bacterial communities in alpine and Arctic glaciers. *FEMS microbiology ecology*, 89: 222-237.
- Edwards A., Pachebat J. A., Swain M., Hegarty M., Hodson A. J., Irvine-Fynn T. D., Rassner S. M., and Sattler B. (2013b) A metagenomic snapshot of taxonomic and functional diversity in an alpine glacier cryoconite ecosystem. *Environmental Research Letters*, 8: 035003.
- Edwards A., Rassner S. M., Anesio A. M., Worgan H. J., Irvine-Fynn T. D., Wyn Williams H., Sattler B., and Wyn Griffith G. (2013c) Contrasts between the cryoconite and ice-marginal bacterial communities of Svalbard glaciers. *Polar Research*, 32: 19468.
- Edwards A., Soares A., Rassner S., Green P., Felix J., and Mitchell A. (2017) Deep Sequencing: Intra-terrestrial metagenomics illustrates the potential of off-grid Nanopore DNA sequencing. *bioRxiv*: 133413.
- Edwards H. G., Hutchinson I., and Ingley R. (2012) The ExoMars Raman spectrometer and the identification of biogeological spectroscopic signatures using a flight-like prototype. *Analytical and bioanalytical chemistry*, 404: 1723-1731.
- Edwards H. G., Vandenabeele P., Jorge-Villar S. E., Carter E. A., Perez F. R., and Hargreaves M. D. (2007) The Rio Tinto Mars analogue site: an extremophilic Raman spectroscopic study. *Spectrochimica Acta Part A: Molecular and Biomolecular Spectroscopy*, 68: 1133-1137.
- Edwards H. G., Villar S. E. J., Parnell J., Cockell C. S., and Lee P. (2005) Raman spectroscopic analysis of cyanobacterial gypsum halotrophs and relevance for sulfate deposits on Mars. *Analyst*, 130: 917-923.
- Eglinton G., and Hamilton R. J. (1967) Leaf Epicuticular Waxes: The waxy outer surfaces of most plants display a wide diversity of fine structure and chemical constituents. *science*, 156: 1322-1335.
- Ehrenfreund P., Röling W., Thiel C., Quinn R., Sephton M., Stoker C., Kotler J., Direito S., Martins Z., and Orzechowska G. (2011) Astrobiology and habitability studies in preparation for future Mars missions: trends from investigating minerals, organics and biota. *International Journal of Astrobiology*, 10: 239-253.
- Eigenbrode J. L., Summons R. E., Steele A., Freissinet C., Millan M., Navarro-González R., Sutter B., McAdam A. C., Franz H. B., and Glavin D. P. (2018) Organic matter preserved in 3-billion-year-old mudstones at Gale crater, Mars. *Science*, 360: 1096-1101.
- Ellery A., Kolb C., Lammer H., Parnell J., Edwards H., Richter L., Patel M., Romstedt J., Dickensheets D., and Steele A. (2002) Astrobiological instrumentation for Mars—the only way is down. *International Journal of Astrobiology*, 1: 365-380.
- Emerson D., Weiss J. V., and Megonigal J. P. (1999) Iron-oxidizing bacteria are associated with ferric hydroxide precipitates (Fe-plaque) on the roots of wetland plants. *Applied and Environmental Microbiology*, 65: 2758-2761.
- Fairén A. G. (2010) A cold and wet Mars. *Icarus*, 208: 165-175.
- Fairén A. G., Davila A. F., Lim D., Bramall N., Bonaccorsi R., Zavaleta J., Uceda E. R., Stoker C., Wierzchos J., and Dohm J. M. (2010) Astrobiology through the ages of Mars: the study of terrestrial analogues to understand the habitability of Mars. *Astrobiology*, 10: 821-843.
- Fairén A. G., Parro V., Schulze-Makuch D., and Whyte L. (2017) Searching for life on Mars before it is too late. *Astrobiology*, 17: 962-970.

- Fajardo-Cavazos P., Schuerger A. C., and Nicholson W. L. (2010) Exposure of DNA and *Bacillus subtilis* spores to simulated martian environments: use of quantitative PCR (qPCR) to measure inactivation rates of DNA to function as a template molecule. *Astrobiology*, 10: 403-411.
- Falkner K. K., Steele M., Woodgate R. A., Swift J. H., Aagaard K., and Morison J. (2005) Dissolved oxygen extrema in the Arctic Ocean halocline from the North Pole to the Lincoln Sea. *Deep Sea Research Part I: Oceanographic Research Papers*, 52: 1138-1154.
- Feng X., Matranga C., Vidic R., and Borguet E. (2004) A vibrational spectroscopic study of the fate of oxygen-containing functional groups and trapped CO₂ in single-walled carbon nanotubes during thermal treatment. *The Journal of Physical Chemistry B*, 108: 19949-19954.
- Fernández-Gómez B., Díez B., Polz M. F., Arroyo J. I., Alfaro F. D., Marchandon G., Sanhueza C., Farías L., Trefault N., and Marquet P. A. (2019) Bacterial community structure in a sympagic habitat expanding with global warming: brackish ice brine at 85–90 N. *The ISME journal*, 13: 316-333.
- Fernández-Martínez M. Á., García-Villadangos M., Paz M. M., Gangloff V., Carrizo D., Blanco Y., González Herrero S., Sánchez-García L., Prieto-Ballesteros O., and Altshuler I. (2021) Geomicrobiological heterogeneity of lithic habitats in the extreme environment of Antarctic Nunataks: A potential early Mars analog. *Frontiers in Microbiology*, 12: 1568.
- Fisher D. A., Lacelle D., Pollard W., Davila A., and McKay C. P. (2016) Ground surface temperature and humidity, ground temperature cycles and the ice table depths in University Valley, McMurdo Dry Valleys of Antarctica. *Journal of Geophysical Research: Earth Surface*, 121: 2069-2084.
- Frawley E. R., and Fang F. C. (2014) The ins and outs of bacterial iron metabolism. *Molecular microbiology*, 93: 609-616.
- Friedberg E. C., Aguilera A., Gellert M., Hanawalt P. C., Hays J. B., Lehmann A. R., Lindahl T., Lowndes N., Sarasin A., and Wood R. D. (2006) DNA repair: from molecular mechanism to human disease. *DNA repair*, 5: 986-996.
- Friedmann E. I. (1982) Endolithic microorganisms in the Antarctic cold desert. *Science*, 215: 1045-1053.
- Gan H. M., Tan M. H., Austin C. M., Sherman C., Wong Y. T., Strugnell J., Gervis M., McPherson L., and Miller A. (2019) Best foot forward: Nanopore long reads, hybrid meta-assembly and haplotig purging optimises the first genome assembly for the Southern Hemisphere blacklip abalone (*Haliotis rubra*). *Frontiers in Genetics*, 10: 889.
- Garneau M.-È., Michel C., Meisterhans G., Fortin N., King T. L., Greer C. W., and Lee K. (2016) Hydrocarbon biodegradation by Arctic sea-ice and sub-ice microbial communities during microcosm experiments, Northwest Passage (Nunavut, Canada). *FEMS Microbiology Ecology*, 92: fiw130.
- Ghiglione J.-F., Richaume A., Philippot L., and Lensi R. (2002) Relative involvement of nitrate and nitrite reduction in the competitiveness of *Pseudomonas fluorescens* in the rhizosphere of maize under non-limiting nitrate conditions. *FEMS microbiology ecology*, 39: 121-127.
- Giovannetti R. (2012) The use of Spectrophotometry UV-Vis for the Study of Porphyrins. In: *Macro To Nano Spectroscopy*, InTech.

- Glavin D. P., Freissinet C., Miller K. E., Eigenbrode J. L., Brunner A. E., Buch A., Sutter B., Archer P. D., Atreya S. K., and Brinckerhoff W. B. (2013) Evidence for perchlorates and the origin of chlorinated hydrocarbons detected by SAM at the Rocknest aeolian deposit in Gale Crater. *Journal of Geophysical Research: Planets*, 118: 1955-1973.
- Goldstein S., Beka L., Graf J., and Klassen J. L. (2019) Evaluation of strategies for the assembly of diverse bacterial genomes using MinION long-read sequencing. *BMC genomics*, 20: 23.
- Gómez F., Mateo-Martí E., Prieto-Ballesteros O., Martín-Gago J., and Amils R. (2010) Protection of chemolithoautotrophic bacteria exposed to simulated Mars environmental conditions. *Icarus*, 209: 482-487.
- Goordial J., Altshuler I., Hindson K., Chan-Yam K., Marcoléfas E., and Whyte L. (2017) In situ field sequencing and life detection in remote (79° 26' N) Canadian High Arctic permafrost ice wedge microbial communities. *Frontiers in microbiology*, 8: 2594.
- Goordial J., Davila A., Lacelle D., Pollard W., Marinova M. M., Greer C. W., DiRuggiero J., McKay C. P., and Whyte L. G. (2016a) Nearing the cold-arid limits of microbial life in permafrost of an upper dry valley, Antarctica. *The ISME journal*, 10: 1613.
- Goordial J., Raymond-Bouchard I., Zolotarov Y., de Bethencourt L., Ronholm J., Shapiro N., Woyke T., Stromvik M., Greer C. W., and Bakermans C. (2016b) Cold adaptive traits revealed by comparative genomic analysis of the eurypsychrophile *Rhodococcus* sp. JG3 isolated from high elevation McMurdo Dry Valley permafrost, Antarctica. *FEMS microbiology ecology*, 92.
- Gosink J., Herwig R., and Staley J. (1997) *Octadecabacter arcticus* gen. nov., sp. nov., and *O. antarcticus*, sp. nov., nonpigmented, psychrophilic gas vacuolate bacteria from polar sea ice and water. *Systematic and applied microbiology*, 20: 356-365.
- Grimalt J. O., de Wit R., Teixidor P., and Albaigés J. (1992) Lipid biogeochemistry of Phormidium and Microcoleus mats. *Organic Geochemistry*, 19: 509-530.
- Guinness E. A., Arvidson R. E., Clark I. H., and Shepard M. K. (1997) Optical scattering properties of terrestrial varnished basalts compared with rocks and soils at the Viking Lander sites. *Journal of Geophysical Research: Planets*, 102: 28687-28703.
- Hansen A. A., Jensen L. L., Kristoffersen T., Mikkelsen K., Merrison J., Finster K. W., and Lomstein B. A. (2009) Effects of long-term simulated martian conditions on a freeze-dried and homogenized bacterial permafrost community. *Astrobiology*, 9: 229-240.
- Harwood J. (2012) *Lipids in plants and microbes*. Springer Science & Business Media.
- Hatam I., Charchuk R., Lange B., Beckers J., Haas C., and Lanoil B. (2014) Distinct bacterial assemblages reside at different depths in Arctic multiyear sea ice. *FEMS microbiology ecology*, 90: 115-125.
- Hays L. E., Graham H. V., Des Marais D. J., Hausrath E. M., Horgan B., McCollom T. M., Parenteau M. N., Potter-McIntyre S. L., Williams A. J., and Lynch K. L. (2017) Biosignature preservation and detection in Mars analog environments. *Astrobiology*, 17: 363-400.
- He Z., Gentry T. J., Schadt C. W., Wu L., Liebich J., Chong S. C., Huang Z., Wu W., Gu B., and Jardine P. (2007) GeoChip: a comprehensive microarray for investigating biogeochemical, ecological and environmental processes. *The ISME journal*, 1: 67.
- Hecht M., Kounaves S., Quinn R., West S., Young S., Ming D., Catling D., Clark B., Boynton W., and Hoffman J. (2009) Detection of perchlorate and the soluble chemistry of martian soil at the Phoenix lander site. *Science*, 325: 64-67.

- Hedges J. I., and Prahl F. G. (1993) Early diagenesis: consequences for applications of molecular biomarkers. In: *Organic geochemistry*, Springer, pp 237-253.
- Heldmann J., Pollard W., McKay C., Marinova M., Davila A., Williams K., Lacelle D., and Andersen D. (2013) The high elevation Dry Valleys in Antarctica as analog sites for subsurface ice on Mars. *Planetary and Space Science*, 85: 53-58.
- Hodson A., Cameron K., Bøggild C., Irvine-Fynn T., Langford H., Pearce D., and Banwart S. (2010) The structure, biological activity and biogeochemistry of cryoconite aggregates upon an Arctic valley glacier: Longyearbreen, Svalbard. *Journal of Glaciology*, 56: 349-362.
- Horne W. H., Volpe R. P., Korza G., DePratti S., Conze I. H., Shuryak I., Grebenc T., Matrosova V. Y., Gaidamakova E. K., and Tkavc R. (2022) Effects of Desiccation and Freezing on Microbial Ionizing Radiation Survivability: Considerations for Mars Sample Return. *Astrobiology*, 22: 1337-1350.
- Horneck G. (2000) The microbial world and the case for Mars. *Planetary and Space Science*, 48: 1053-1063.
- Huson D. H., Auch A. F., Qi J., and Schuster S. C. (2007) MEGAN analysis of metagenomic data. *Genome research*, 17: 377-386.
- Hutcherson J. A., Sinclair K. M., Belvin B. R., Gui Q., Hoffman P. S., and Lewis J. P. (2017) Amixicile, a novel strategy for targeting oral anaerobic pathogens. *Scientific reports*, 7: 1-14.
- Jain M., Koren S., Miga K. H., Quick J., Rand A. C., Sasani T. A., Tyson J. R., Beggs A. D., Dilthey A. T., and Fiddes I. T. (2018) Nanopore sequencing and assembly of a human genome with ultra-long reads. *Nature biotechnology*, 36: 338-345.
- Jain M., Tyson J. R., Loose M., Ip C. L., Eccles D. A., O'Grady J., Malla S., Leggett R. M., Wallerman O., and Jansen H. J. (2017) MinION Analysis and Reference Consortium: Phase 2 data release and analysis of R9.0 chemistry. *F1000Research*, 6.
- Jehlička J., Edwards H., and Oren A. (2013) Bacterioruberin and salinixanthin carotenoids of extremely halophilic Archaea and Bacteria: a Raman spectroscopic study. *Spectrochimica Acta Part A: Molecular and Biomolecular Spectroscopy*, 106: 99-103.
- Jehlicka J., and Oren A. (2013) Raman spectroscopy in halophile research. *Frontiers in microbiology*, 4: 380.
- Ji B., Yang K., Zhu L., Jiang Y., Wang H., Zhou J., and Zhang H. (2015) Aerobic denitrification: a review of important advances of the last 30 years. *Biotechnology and Bioengineering*, 20: 643-651.
- John K., Botkin D., Burton A., Castro-Wallace S., Chaput J., Dworkin J., Lehman N., Lupisella M., Mason C., and Smith D. (2016) The Biomolecule Sequencer Project: Nanopore sequencing as a dual-use tool for crew health and astrobiology investigations.
- Johnson A. P., Pratt L. M., Vishnivetskaya T., Pfiffner S., Bryan R. A., Dadachova E., Whyte L., Radtke K., Chan E., and Tronick S. (2011) Extended survival of several organisms and amino acids under simulated martian surface conditions. *Icarus*, 211: 1162-1178.
- Johnson S. S., Anslyn E. V., Graham H. V., Mahaffy P. R., and Ellington A. D. (2018) Fingerprinting non-terran biosignatures. *Astrobiology*, 18: 915-922.
- Johnson S. S., Zaikova E., Goerlitz D. S., Bai Y., and Tighe S. W. (2017) Real-Time DNA Sequencing in the Antarctic Dry Valleys Using the Oxford Nanopore Sequencer. *Journal of Biomolecular Techniques: JBT*, 28: 2.

- Jones M. M., Jones E. A., Harmon D. F., and Semmes R. T. (1961) A search for perchlorate complexes. Raman spectra of perchlorate solutions. *Journal of the American Chemical Society*, 83: 2038-2042.
- Jørgensen S. L., and Zhao R. (2016) Microbial inventory of deeply buried oceanic crust from a young ridge flank. *Frontiers in microbiology*, 7: 820.
- Kaczmarek Ł., Jakubowska N., Celewicz-Gołdyn S., and Zawierucha K. (2016) The microorganisms of cryoconite holes (algae, Archaea, bacteria, cyanobacteria, fungi, and Protista): a review. *Polar Record*, 52: 176-203.
- Kaczor A., and Baranska M. (2011) Structural changes of carotenoid astaxanthin in a single algal cell monitored in situ by Raman spectroscopy. *Analytical chemistry*, 83: 7763-7770.
- Kang D. D., Froula J., Egan R., and Wang Z. (2015) MetaBAT, an efficient tool for accurately reconstructing single genomes from complex microbial communities. *PeerJ*, 3: e1165.
- Kaplan M. (2012) DNA has a 521-year half-life [at 13.1 C]: genetic material can't be recovered from dinosaurs—but it lasts longer than thought. *Nature News*, 10.
- Kaštovská K., Elster J., Stibal M., and Šantrůčková H. (2005) Microbial assemblages in soil microbial succession after glacial retreat in Svalbard (High Arctic). *Microbial ecology*, 50: 396.
- Kim S. K., Kim M. S., and Suh S. W. (1987) Surface-enhanced Raman scattering (SERS) of aromatic amino acids and their glycyl dipeptides in silver sol. *Journal of Raman spectroscopy*, 18: 171-175.
- Kirchman D. L. (2002) The ecology of Cytophaga–Flavobacteria in aquatic environments. *FEMS microbiology ecology*, 39: 91-100.
- Kish A., Kirkali G., Robinson C., Rosenblatt R., Jaruga P., Dizdaroglu M., and DiRuggiero J. (2009) Salt shield: intracellular salts provide cellular protection against ionizing radiation in the halophilic archaeon, *Halobacterium salinarum* NRC-1. *Environmental microbiology*, 11: 1066-1078.
- Klein H. P. (1977) The Viking biological investigation: general aspects. *Journal of Geophysical Research*, 82: 4677-4680.
- Klein H. P. (1978a) The Viking biological experiments on Mars. *Icarus*, 34: 666-674.
- Klein H. P. (1978b) The Viking biological investigations: review and status. *Origins of life*, 9: 157-160.
- Koren S., Walenz B. P., Berlin K., Miller J. R., Bergman N. H., and Phillippy A. M. (2017) Canu: scalable and accurate long-read assembly via adaptive k-mer weighting and repeat separation. *Genome research*, 27: 722-736.
- Kottemann M., Kish A., Iloanusi C., Bjork S., and DiRuggiero J. (2005) Physiological responses of the halophilic archaeon *Halobacterium* sp. strain NRC1 to desiccation and gamma irradiation. *Extremophiles*, 9: 219-227.
- Kozich J. J., Westcott S. L., Baxter N. T., Highlander S. K., and Schloss P. D. (2013) Development of a dual-index sequencing strategy and curation pipeline for analyzing amplicon sequence data on the MiSeq Illumina sequencing platform. *Applied and environmental microbiology*: AEM. 01043-13.
- Krulwich T. A., Hicks D. B., and Ito M. (2009) Cation/proton antiporter complements of bacteria: why so large and diverse? *Molecular microbiology*, 74: 257-260.
- Kuypers M. M., Marchant H. K., and Kartal B. (2018) The microbial nitrogen-cycling network. *Nature Reviews Microbiology*, 16: 263.

- Lacap D. C., Warren-Rhodes K. A., McKay C. P., and Pointing S. B. (2011) Cyanobacteria and chloroflexi-dominated hypolithic colonization of quartz at the hyper-arid core of the Atacama Desert, Chile. *Extremophiles*, 15: 31-38.
- Lacelle D., Davila A. F., Pollard W. H., Andersen D., Heldmann J., Marinova M., and McKay C. P. (2011) Stability of massive ground ice bodies in University Valley, McMurdo Dry Valleys of Antarctica: Using stable O–H isotope as tracers of sublimation in hyper-arid regions. *Earth and Planetary Science Letters*, 301: 403-411.
- Lanoil B., Skidmore M., Priscu J. C., Han S., Foo W., Vogel S. W., Tulaczyk S., and Engelhardt H. (2009) Bacteria beneath the West Antarctic ice sheet. *Environmental Microbiology*, 11: 609-615.
- Larson D. (1983) The pattern of production within individual Umbilicaria lichen thalli. *New Phytologist*, 94: 409-419.
- Leask E. K., and Ehlmann B. L. (2022) Evidence for deposition of chloride on Mars from small-volume surface water events into the Late Hesperian-Early Amazonian. *AGU Advances*, 3: e2021AV000534.
- Lee K. C.-Y., Herbold C., Dunfield P. F., Morgan X. C., McDonald I. R., and Stott M. B. (2013) Phylogenetic delineation of the novel phylum Armatimonadetes (former candidate division OP10) and definition of two novel candidate divisions. *Appl. Environ. Microbiol.*, 79: 2484-2487.
- Lee M. D., Walworth N. G., Sylvan J. B., Edwards K. J., and Orcutt B. N. (2015) Microbial communities on seafloor basalts at Dorado Outcrop reflect level of alteration and highlight global lithic clades. *Frontiers in microbiology*, 6: 1470.
- Leggett R. M., and Clark M. D. (2017) A world of opportunities with nanopore sequencing. *Journal of Experimental Botany*.
- Levin G. V., and Straat P. A. (2016) The case for extant life on Mars and its possible detection by the Viking labeled release experiment. *Astrobiology*, 16: 798-810.
- Ley R. E., Harris J. K., Wilcox J., Spear J. R., Miller S. R., Bebout B. M., Maresca J. A., Bryant D. A., Sogin M. L., and Pace N. R. (2006) Unexpected diversity and complexity of the Guerrero Negro hypersaline microbial mat. *Applied and environmental microbiology*, 72: 3685-3695.
- Lezcano M. Á., Moreno-Paz M., Carrizo D., Prieto-Ballesteros O., Fernández-Martínez M. Á., Sánchez-García L., Blanco Y., Puente-Sánchez F., de Diego-Castilla G., and García-Villadangos M. (2019) Biomarker profiling of microbial mats in the geothermal band of Cerro Caliente, Deception Island (Antarctica): life at the edge of heat and cold. *Astrobiology*, 19: 1490-1504.
- Lezcano M. Á., Sanchez-Garcia L., Quesada A., Carrizo D., Fernández-Martínez M. Á., Cavalcante-Silva E., and Parro V. (2022) Comprehensive metabolic and taxonomic reconstruction of an ancient microbial mat from the McMurdo Ice Shelf (Antarctica) by integrating genetic, metaproteomics and lipid biomarker analyses. *Frontiers in Microbiology*: 1225.
- Li H. (2018) Minimap2: pairwise alignment for nucleotide sequences. *Bioinformatics*, 34: 3094-3100.
- Li H., Handsaker B., Wysoker A., Fennell T., Ruan J., Homer N., Marth G., Abecasis G., and Durbin R. (2009) The sequence alignment/map format and SAMtools. *Bioinformatics*, 25: 2078-2079.

- Lin X., Zhang Z., Zhang L., and Li X. (2017) Complete genome sequence of a denitrifying bacterium, *Pseudomonas* sp. CC6-YY-74, isolated from Arctic Ocean sediment. *Marine Genomics*, 35: 47-49.
- Linck E., Crane K. W., Zuckerman B. L., Corbin B. A., Myers R. M., Williams S. R., Carioscia S. A., Garcia R., and Lal B. (2019) Evaluation of a Human Mission to Mars by 2033. JSTOR.
- Lipson D. A., Jha M., Raab T. K., and Oechel W. C. (2010) Reduction of iron (III) and humic substances plays a major role in anaerobic respiration in an Arctic peat soil. *Journal of Geophysical Research: Biogeosciences*, 115.
- Liu R., and Ochman H. (2007) Origins of flagellar gene operons and secondary flagellar systems. *Journal of bacteriology*, 189: 7098-7104.
- Loman N. J., Quick J., and Simpson J. T. (2015) A complete bacterial genome assembled de novo using only nanopore sequencing data. *Nature methods*, 12: 733-735.
- Loman N. J., and Watson M. (2015) Successful test launch for nanopore sequencing. *Nature methods*, 12: 303-304.
- Luef B., Fakra S. C., Csencsits R., Wrighton K. C., Williams K. H., Wilkins M. J., Downing K. H., Long P. E., Comolli L. R., and Banfield J. F. (2013) Iron-reducing bacteria accumulate ferric oxyhydroxide nanoparticle aggregates that may support planktonic growth. *The ISME journal*, 7: 338.
- Luo G., Yang H., Algeo T. J., Hallmann C., and Xie S. (2019) Lipid biomarkers for the reconstruction of deep-time environmental conditions. *Earth-Science Reviews*, 189: 99-124.
- Maccario L., Sanguino L., Vogel T. M., and Larose C. (2015) Snow and ice ecosystems: not so extreme. *Research in microbiology*, 166: 782-795.
- Maggiore C., Stromberg J., Blanco Y., Goordial J., Cloutis E., García-Villadangos M., Parro V., and Whyte L. (2020) The Limits, Capabilities, and Potential for Life Detection with MinION Sequencing in a Paleochannel Mars Analog. *Astrobiology*, 20: 375-393.
- Magnuson E., Mykytczuk N. C., Pellerin A., Goordial J., Twine S. M., Wing B., Foote S. J., Fulton K., and Whyte L. G. (2020) Thiomicrobium streamers and sulfur cycling in perennial hypersaline cold springs in the Canadian high Arctic. *Environmental Microbiology*.
- Maiti N. C., Apetri M. M., Zagorski M. G., Carey P. R., and Anderson V. E. (2004) Raman spectroscopic characterization of secondary structure in natively unfolded proteins: α -synuclein. *Journal of the American Chemical Society*, 126: 2399-2408.
- Mangold N., Gupta S., Gasnault O., Dromart G., Tarnas J., Sholes S., Horgan B., Quantin-Nataf C., Brown A., and Le Mouélic S. (2021) Perseverance rover reveals an ancient delta-lake system and flood deposits at Jezero crater, Mars. *Science*, 374: 711-717.
- Manley L. J., Ma D., and Levine S. S. (2016) Monitoring error rates in Illumina sequencing. *Journal of biomolecular techniques: JBT*, 27: 125.
- Marchant H. K., Ahmerkamp S., Lavik G., Tegetmeyer H. E., Graf J., Klatt J. M., Holtappels M., Walpersdorf E., and Kuypers M. M. (2017) Denitrifying community in coastal sediments performs aerobic and anaerobic respiration simultaneously. *The ISME journal*, 11: 1799-1812.
- Margesin R., Spröer C., Zhang D.-C., and Busse H.-J. (2012) *Polaromonas glacialis* sp. nov. and *Polaromonas cryoconiti* sp. nov., isolated from alpine glacier cryoconite. *International journal of systematic and evolutionary microbiology*, 62: 2662-2668.

- Markowitz V. M., Chen I.-M. A., Palaniappan K., Chu K., Szeto E., Grechkin Y., Ratner A., Jacob B., Huang J., and Williams P. (2011) IMG: the integrated microbial genomes database and comparative analysis system. *Nucleic acids research*, 40: D115-D122.
- Marshall C. P., Carter E. A., Leuko S., and Javaux E. J. (2006) Vibrational spectroscopy of extant and fossil microbes: relevance for the astrobiological exploration of Mars. *Vibrational Spectroscopy*, 41: 182-189.
- Martin-Creuzburg D., and Merkel P. (2016) Sterols of freshwater microalgae: potential implications for zooplankton nutrition. *Journal of Plankton Research*, 38: 865-877.
- Martin J., Tremblay J.-É., Gagnon J., Tremblay G., Lapoussière A., Jose C., Poulin M., Gosselin M., Gratton Y., and Michel C. (2010) Prevalence, structure and properties of subsurface chlorophyll maxima in Canadian Arctic waters. *Marine Ecology Progress Series*, 412: 69-84.
- Martins Z. (2011) In situ biomarkers and the Life Marker Chip. *Astronomy & Geophysics*, 52: 1.34-1.35.
- Martins Z., Sephton M., Foing B., and Ehrenfreund P. (2011) Extraction of amino acids from soils close to the Mars Desert Research Station (MDRS), Utah. *International Journal of Astrobiology*, 10: 231-238.
- Mattes T. E., Alexander A. K., Richardson P. M., Munk A. C., Han C. S., Stothard P., and Coleman N. V. (2008) The genome of *Polaromonas* sp. strain JS666: insights into the evolution of a hydrocarbon- and xenobiotic-degrading bacterium, and features of relevance to biotechnology. *Applied and environmental microbiology*, 74: 6405-6416.
- Maurice S., Wiens R. C., Bernardi P., Caïs P., Robinson S., Nelson T., Gasnault O., Reess J.-M., Deleuze M., and Rull F. (2021) The SuperCam instrument suite on the Mars 2020 rover: Science objectives and Mast-Unit description. *Space Science Reviews*, 217: 1-108.
- McCammon S. A., and Bowman J. P. (2000) Taxonomy of Antarctic *Flavobacterium* species: description of *Flavobacterium gillisiae* sp. nov., *Flavobacterium tegetincola* sp. nov., and *Flavobacterium xanthum* sp. nov., nom. rev. and reclassification of [*Flavobacterium*] *salegens* as *Salegentibacter salegens* gen. nov., comb. nov. *International journal of systematic and evolutionary microbiology*, 50: 1055-1063.
- McCauley J., Breed C., El-Baz F., Whitney M., Grolier M., and Ward A. (1979) Pitted and fluted rocks in the Western Desert of Egypt: Viking comparisons. *Journal of Geophysical Research: Solid Earth*, 84: 8222-8232.
- McKay C. P., Andersen D., and Davila A. (2017) Antarctic environments as models of planetary habitats: University Valley as a model for modern Mars and Lake Untersee as a model for Enceladus and ancient Mars. *The Polar Journal*, 7: 303-318.
- McKay C. P., Friedman E. I., Wharton R. A., and Davies W. L. (1992) History of water on Mars: a biological perspective. *Advances in Space Research*, 12: 231-238.
- McLennan S., Sephton M., Beatty D., Hecht M., Pepin B., Leya I., Jones J., Weiss B., Race M., and Rummel J. (2012) Planning for Mars returned sample science: final report of the MSR End-to-End International Science Analysis Group (E2E-iSAG). *Astrobiology*, 12: 175-230.
- Meinert C., Myrgorodska I., De Marcellus P., Buhse T., Nahon L., Hoffmann S. V., d'Hendecourt L. L. S., and Meierhenrich U. J. (2016) Ribose and related sugars from ultraviolet irradiation of interstellar ice analogs. *Science*, 352: 208-212.

- Menegon M., Cantaloni C., Rodriguez-Prieto A., Centomo C., Abdelfattah A., Rossato M., Bernardi M., Xumerle L., Loader S., and Delledonne M. (2017) On site DNA barcoding by nanopore sequencing. *PloS one*, 12: e0184741.
- Menzel P., Ng K. L., and Krogh A. (2016) Fast and sensitive taxonomic classification for metagenomics with Kaiju. *Nature communications*, 7: 1-9.
- Mergelov N., Mueller C. W., Prater I., Shorkunov I., Dolgikh A., Zazovskaya E., Shishkov V., Krupskaya V., Abrosimov K., and Cherkinsky A. (2018) Alteration of rocks by endolithic organisms is one of the pathways for the beginning of soils on Earth. *Scientific Reports*, 8: 1-15.
- Meyers P. A. (1997) Organic geochemical proxies of paleoceanographic, paleolimnologic, and paleoclimatic processes. *Organic geochemistry*, 27: 213-250.
- Mileikowsky C., Cucinotta F. A., Wilson J. W., Gladman B., Horneck G., Lindegren L., Melosh J., Rickman H., Valtonen M., and Zheng J. (2000) Natural transfer of viable microbes in space: 1. From Mars to Earth and Earth to Mars. *Icarus*, 145: 391-427.
- Millan M., Szopa C., Buch A., Coll P., Glavin D. P., Freissinet C., Navarro-González R., François P., Coscia D., and Bonnet J.-Y. (2016) In situ analysis of martian regolith with the SAM experiment during the first mars year of the MSL mission: Identification of organic molecules by gas chromatography from laboratory measurements. *Planetary and Space Science*, 129: 88-102.
- Moreno-Vivián C., Cabello P., Martínez-Luque M., Blasco R., and Castillo F. (1999) Prokaryotic nitrate reduction: molecular properties and functional distinction among bacterial nitrate reductases. *Journal of bacteriology*, 181: 6573-6584.
- Mosca C., Rothschild L. J., Napoli A., Ferré F., Pietrosanto M., Fagliarone C., Baqué M., Rabbow E., Rettberg P., and Billi D. (2019) Over-expression of UV-damage DNA repair genes and ribonucleic acid persistence contribute to the resilience of dried biofilms of the desert cyanobacterium *Chroococcidiopsis* exposed to Mars-like UV flux and long-term desiccation. *Frontiers in Microbiology*, 10: 2312.
- Mueller D. R., Vincent W. F., Pollard W. H., and Fritsen C. H. (2001) Glacial cryoconite ecosystems: a bipolar comparison of algal communities and habitats. *Nova Hedwigia Beiheft*, 123: 173-198.
- Musk E. (2017) Making humans a multi-planetary species. *New Space*, 5: 46-61.
- Mustard J., Adler M., Allwood A., Bass D., Beaty D., and Bell J. (2013a) Appendices to the Report of the Mars 2020 Science Definition Team. *Mars Exploration Program Analysis Group*: 154.
- Mustard J., Adler M., Allwood A., Bass D., Beaty D., Bell J., Brinckerhoff W., Carr M., Des Marais D., and Brake B. (2013b) Report of the mars 2020 science definition team. *Mars Explor. Progr. Anal. Gr*: 155-205.
- Navarro-González R., Vargas E., de La Rosa J., Raga A. C., and McKay C. P. (2010) Reanalysis of the Viking results suggests perchlorate and organics at midlatitudes on Mars. *Journal of Geophysical Research: Planets*, 115.
- Nelson D. W., and Sommers L. E. (1996) Total carbon, organic carbon, and organic matter. *Methods of soil analysis: Part 3 Chemical methods*, 5: 961-1010.
- Neveu M., Hays L. E., Voytek M. A., New M. H., and Schulte M. D. (2018) The Ladder of Life Detection. *Astrobiology*.
- Nicholls S. M., Quick J. C., Tang S., and Loman N. J. (2019) Ultra-deep, long-read nanopore sequencing of mock microbial community standards. *Gigascience*, 8: giz043.

- Nicholson W. L., Schuerger A. C., and Douki T. (2018) The photochemistry of unprotected DNA and DNA inside *Bacillus subtilis* spores exposed to simulated Martian surface conditions of atmospheric composition, temperature, pressure, and solar radiation. *Astrobiology*, 18: 393-402.
- Niederberger T. D., Perreault N. N., Tille S., Lollar B. S., Lacrampe-Couloume G., Andersen D., Greer C. W., Pollard W., and Whyte L. G. (2010) Microbial characterization of a subzero, hypersaline methane seep in the Canadian High Arctic. *The ISME journal*, 4: 1326.
- Nordheim T., Hand K., and Paranicas C. (2018) Preservation of potential biosignatures in the shallow subsurface of Europa. *Nature Astronomy*, 2: 673-679.
- NRC. (2012) Vision and voyages for planetary science in the decade 2013-2022. National Academies Press.
- O'Connor B. R., Fernández-Martínez M. Á., Léveillé R. J., and Whyte L. G. (2021) Taxonomic characterization and microbial activity determination of cold-adapted microbial communities in lava tube ice caves from Lava Beds National Monument, a high-fidelity Mars analogue environment. *Astrobiology*, 21: 613-627.
- Oelgeschläger E., and Rother M. (2008) Carbon monoxide-dependent energy metabolism in anaerobic bacteria and archaea. *Archives of microbiology*, 190: 257-269.
- Onofri S., Barreca D., Selbmann L., Isola D., Rabbow E., Horneck G., De Vera J., Hatton J., and Zucconi L. (2013) Resistance of Antarctic black fungi and cryptoendolithic communities to simulated space and Martian conditions. *Studies in Mycology*, 75: 115-170.
- Oren A., Sørensen K. B., Canfield D. E., Teske A. P., Ionescu D., Lipski A., and Altendorf K. (2009) Microbial communities and processes within a hypersaline gypsum crust in a saltern evaporation pond (Eilat, Israel). *Hydrobiologia*, 626: 15-26.
- Orosei R., Lauro S., Pettinelli E., Cicchetti A., Coradini M., Cosciotti B., Di Paolo F., Flamini E., Mattei E., and Pajola M. (2018) Radar evidence of subglacial liquid water on Mars. *Science*, 361: 490-493.
- Osinski G. R., Battler M., Caudill C. M., Francis R., Haltigin T., Hipkin V. J., Kerrigan M., Pilles E., Pontefract A., and Tornabene L. L. (2018) The CanMars Mars Sample Return analogue mission. *Planetary and Space Science*, (in press).
- Otto A., Simoneit B. R., and Rember W. C. (2005) Conifer and angiosperm biomarkers in clay sediments and fossil plants from the Miocene Clarkia Formation, Idaho, USA. *Organic Geochemistry*, 36: 907-922.
- Overholt W. A., Hölzer M., Geesink P., Diezel C., Marz M., and Küsel K. (2020) Inclusion of Oxford Nanopore long reads improves all microbial and phage metagenome-assembled genomes from a complex aquifer system. *Environmental microbiology*, 22: 4000 - 4013.
- Pace N. R. (2001) The universal nature of biochemistry. *Proceedings of the National Academy of Sciences*, 98: 805-808.
- Pappalardo R., Vance S., Bagenal F., Bills B., Blaney D., Blankenship D., Brinckerhoff W., Connerney J., Hand K., and Hoehler T. M. (2013) Science potential from a Europa lander. *Astrobiology*, 13: 740-773.
- Parenteau M. N., Jahnke L. L., Farmer J. D., and Cady S. L. (2014) Production and early preservation of lipid biomarkers in iron hot springs. *Astrobiology*, 14: 502-521.
- Parks D. H., Chuvochina M., Waite D. W., Rinke C., Skarshewski A., Chaumeil P.-A., and Hugenholtz P. (2018) A standardized bacterial taxonomy based on genome phylogeny substantially revises the tree of life. *Nature biotechnology*, 36: 996-1004.

- Parks D. H., Imelfort M., Skennerton C. T., Hugenholtz P., and Tyson G. W. (2015) CheckM: assessing the quality of microbial genomes recovered from isolates, single cells, and metagenomes. *Genome research*, 25: 1043-1055.
- Parks D. H., Rinke C., Chuvochina M., Chaumeil P.-A., Woodcroft B. J., Evans P. N., Hugenholtz P., and Tyson G. W. (2017) Recovery of nearly 8,000 metagenome-assembled genomes substantially expands the tree of life. *Nature microbiology*, 2: 1533-1542.
- Parro V., de Diego-Castilla G., Rodríguez-Manfredi J. A., Rivas L. A., Blanco-López Y., Sebastián E., Romeral J., Compostizo C., Herrero P. L., and García-Marín A. (2011) SOLID3: a multiplex antibody microarray-based optical sensor instrument for in situ life detection in planetary exploration. *Astrobiology*, 11: 15-28.
- Parro V., Rivas L. A., and Gómez-Elvira J. (2008) Protein microarrays-based strategies for life detection in astrobiology. *Space science reviews*, 135: 293-311.
- Parro V., Rodríguez-Manfredi J., Briones C., Compostizo C., Herrero P., Vez E., Sebastián E., Moreno-Paz M., García-Villadangos M., and Fernández-Calvo P. (2005) Instrument development to search for biomarkers on Mars: terrestrial acidophile, iron-powered chemolithoautotrophic communities as model systems. *Planetary and Space Science*, 53: 729-737.
- Pontefract A., Hachey J., Zuber M. T., Ruvkun G., and Carr C. E. (2018) Sequencing Nothing: Exploring Failure Modes of Nanopore Sensing and Implications for Life Detection. *Life Sciences in Space Research*.
- Poretzky R., Rodriguez-R L. M., Luo C., Tsementzi D., and Konstantinidis K. T. (2014) Strengths and limitations of 16S rRNA gene amplicon sequencing in revealing temporal microbial community dynamics. *PloS one*, 9: e93827.
- Potts M. (1999) Mechanisms of desiccation tolerance in cyanobacteria. *European Journal of Phycology*, 34: 319-328.
- Quantin C., Popova O., Hartmann W. K., and Werner S. C. (2016) Young Martian crater Gratteri and its secondary craters. *Journal of Geophysical Research: Planets*, 121: 1118-1140.
- Raes J., Korbel J. O., Lercher M. J., Von Mering C., and Bork P. (2007) Prediction of effective genome size in metagenomic samples. *Genome biology*, 8: R10.
- Ranjan R., Rani A., Metwally A., McGee H. S., and Perkins D. L. (2016) Analysis of the microbiome: Advantages of whole genome shotgun versus 16S amplicon sequencing. *Biochemical and biophysical research communications*, 469: 967-977.
- Raymond-Bouchard I., Goordial J., Zolotarov Y., Ronholm J., Stromvik M., Bakermans C., and Whyte L. G. (2018) Conserved genomic and amino acid traits of cold adaptation in subzero-growing Arctic permafrost bacteria. *FEMS microbiology ecology*, 94: fiy023.
- Raymond-Bouchard I., Maggiori C., Brennan L., Altshuler I., Manchado J. M., Parro V., and Whyte L. G. (2021) Assessment of automated nucleic acid extraction systems in combination with MinION sequencing as potential tools for the detection of microbial biosignatures. *Astrobiology*, Submitted (Submission No. AST-2020-2349).
- Rhind T., Ronholm J., Berg B., Mann P., Applin D., Stromberg J., Sharma R., Whyte L., and Cloutis E. (2014) Gypsum-hosted endolithic communities of the Lake St. Martin impact structure, Manitoba, Canada: spectroscopic detectability and implications for Mars. *International Journal of Astrobiology*, 13: 366-377.

- Rinke C., Schwientek P., Sczyrba A., Ivanova N. N., Anderson I. J., Cheng J.-F., Darling A., Malfatti S., Swan B. K., and Gies E. A. (2013) Insights into the phylogeny and coding potential of microbial dark matter. *Nature*, 499: 431-437.
- Rivas L. A., Aguirre J., Blanco Y., González-Toril E., and Parro V. (2011) Graph-based deconvolution analysis of multiplex sandwich microarray immunoassays: applications for environmental monitoring. *Environmental microbiology*, 13: 1421-1432.
- Rivas L. A., García-Villadangos M., Moreno-Paz M., Cruz-Gil P., Gómez-Elvira J., and Parro V. (2008) A 200-antibody microarray biochip for environmental monitoring: searching for universal microbial biomarkers through immunoprofiling. *Analytical chemistry*, 80: 7970-7979.
- Rodriguez-R L. M., Gunturu S., Harvey W. T., Rosselló-Mora R., Tiedje J. M., Cole J. R., and Konstantinidis K. T. (2018) The Microbial Genomes Atlas (MiGA) webserver: taxonomic and gene diversity analysis of Archaea and Bacteria at the whole genome level. *Nucleic acids research*, 46: W282-W288.
- Ruan C., Wang W., and Gu B. (2006) Surface-enhanced Raman scattering for perchlorate detection using cystamine-modified gold nanoparticles. *Analytica chimica acta*, 567: 114-120.
- Rull F., Maurice S., Hutchinson I., Moral A., Perez C., Diaz C., Colombo M., Belenguer T., Lopez-Reyes G., and Sansano A. (2017) The Raman Laser Spectrometer for the ExoMars Rover Mission to Mars. *Astrobiology*, 17: 627-654.
- Rummel J. D., and Conley C. A. (2018) Inadvertently finding Earth contamination on Mars should not be a priority for anyone. *Astrobiology*, 18: 108-115.
- Sánchez-García L., Aeppli C., Parro V., Fernández-Remolar D., García-Villadangos M., Chong-Diaz G., Blanco Y., and Carrizo D. (2018a) Molecular biomarkers in the subsurface of the Salar Grande (Atacama, Chile) evaporitic deposits. *Biogeochemistry*, 140: 31-52.
- Sánchez-García L., Carrizo D., Molina A., Muñoz-Iglesias V., Lezcano M. Á., Fernández-Sampedro M., Parro V., and Prieto-Ballesteros O. (2020) Fingerprinting molecular and isotopic biosignatures on different hydrothermal scenarios of Iceland, an acidic and sulfur-rich Mars analog. *Scientific reports*, 10: 1-13.
- Sánchez-García L., Fernández M., García-Villadangos M., Blanco Y., Cady S., Hinman N., Bowden M., Pointing S., Lee K., Warren-Rhodes K. and others. (2018b) Microbial biomarker transition in high altitude sinter mounds from El Tatio (Chile) through different stages of hydrothermal activity. *Frontiers in microbiology*, (under review).
- Sandford S., and Allamandola L. (1990) The physical and infrared spectral properties of CO₂ in astrophysical ice analogs. *The Astrophysical Journal*, 355: 357-372.
- Santos S. P., Yang Y., Rosa M. T., Rodrigues M. A., La Tour D., Bouthier C., Sommer S., Teixeira M., Carrondo M. A., and Cloetens P. (2019) The interplay between Mn and Fe in *Deinococcus radiodurans* triggers cellular protection during paraquat-induced oxidative stress. *Scientific reports*, 9: 1-12.
- Schlesinger W. H., Phippen J. S., Wallenstein M. D., Hofmockel K. S., Klepeis D. M., and Mahall B. E. (2003) Community composition and photosynthesis by photoautotrophs under quartz pebbles, southern Mojave Desert. *Ecology*, 84: 3222-3231.
- Schmidt M. H.-W., Vogel A., Denton A. K., Istace B., Wormit A., van de Geest H., Bolger M. E., Alseekh S., Maß J., and Pfaff C. (2017) De novo assembly of a new *Solanum pennellii* accession using nanopore sequencing. *The Plant Cell*, 29: 2336-2348.

- Schneider K., Peyraud R., Kiefer P., Christen P., Delmotte N., Massou S., Portais J.-C., and Vorholt J. A. (2012) The ethylmalonyl-CoA pathway is used in place of the glyoxylate cycle by *Methylobacterium extorquens* AM1 during growth on acetate. *Journal of Biological Chemistry*, 287: 757-766.
- Schuenger A. (2015) Ultraviolet irradiation on the surface of Mars: Implications for EVA activities during future human missions. *Planetary Protection Knowledge Gaps for Human Extraterrestrial Missions*, 1845: 1011.
- Schuenger A. C., Mancinelli R. L., Kern R. G., Rothschild L. J., and McKay C. P. (2003) Survival of endospores of *Bacillus subtilis* on spacecraft surfaces under simulated martian environments: implications for the forward contamination of Mars. *Icarus*, 165: 253-276.
- Schuenger A. C., and Nicholson W. L. (2006) Interactive effects of hypobaria, low temperature, and CO₂ atmospheres inhibit the growth of mesophilic *Bacillus* spp. under simulated martian conditions. *Icarus*, 185: 143-152.
- Schwieterman E. W., Kiang N. Y., Parenteau M. N., Harman C. E., DasSarma S., Fisher T. M., Arney G. N., Hartnett H. E., Reinhard C. T., and Olson S. L. (2018) Exoplanet biosignatures: a review of remotely detectable signs of life. *Astrobiology*, 18: 663-708.
- Segawa T., Yonezawa T., Edwards A., Akiyoshi A., Tanaka S., Uetake J., Irvine-Fynn T., Fukui K., Li Z., and Takeuchi N. (2017) Biogeography of cryoconite forming cyanobacteria on polar and Asian glaciers. *Journal of biogeography*, 44: 2849-2861.
- Sephton M. A. (2018) Selecting Mars samples to return to Earth. *Astronomy & Geophysics*, 59: 1.36-1.38.
- Sevim V., Lee J., Egan R., Clum A., Hundley H., Lee J., Everroad R. C., Detweiler A. M., Bebout B. M., and Pett-Ridge J. (2019) Shotgun metagenome data of a defined mock community using Oxford Nanopore, PacBio and Illumina technologies. *Scientific data*, 6: 1-9.
- Shin S. C., Kim H., Lee J. H., Kim H.-W., Park J., Choi B.-S., Lee S.-C., Kim J. H., Lee H., and Kim S. (2019) Nanopore sequencing reads improve assembly and gene annotation of the *Parochlus steinenii* genome. *Scientific Reports*, 9: 1-10.
- Simon C., Wiezer A., Strittmatter A. W., and Daniel R. (2009) Phylogenetic diversity and metabolic potential revealed in a glacier ice metagenome. *Applied and Environmental Microbiology*, 75: 7519-7526.
- Sims M. R., Cullen D. C., Rix C. S., Buckley A., Derveni M., Evans D., García-Con L. M., Rhodes A., Rato C. C., and Stefinovic M. (2012) Development status of the life marker chip instrument for ExoMars. *Planetary and Space Science*, 72: 129-137.
- Singh P., Hanada Y., Singh S. M., and Tsuda S. (2014) Antifreeze protein activity in Arctic cryoconite bacteria. *FEMS microbiology letters*, 351: 14-22.
- Sobrado J. M., Martín-Soler J., and Martín-Gago J. A. (2014) Mimicking Mars: A vacuum simulation chamber for testing environmental instrumentation for Mars exploration. *Review of Scientific Instruments*, 85: 035111.
- Somerville V., Lutz S., Schmid M., Frei D., Moser A., Irmeler S., Frey J. E., and Ahrens C. H. (2019) Long-read based de novo assembly of low-complexity metagenome samples results in finished genomes and reveals insights into strain diversity and an active phage system. *BMC microbiology*, 19: 143.
- Spry J. A., Race M., Kminek G., Siegel B., and Conley C. (2018) Planetary Protection Knowledge Gaps for Future Mars Human Missions: Stepwise Progress in Identifying and

- Integrating Science and Technology Needs. 48th International Conference on Environmental Systems.
- Stewart R. D., Auffret M. D., Warr A., Walker A. W., Roehe R., and Watson M. (2019) Compendium of 4,941 rumen metagenome-assembled genomes for rumen microbiome biology and enzyme discovery. *Nature biotechnology*, 37: 953.
- Stoker C. R., Clarke J., Direito S. O., Blake D., Martin K. R., Zavaleta J., and Foing B. (2011) Mineralogical, chemical, organic and microbial properties of subsurface soil cores from Mars Desert Research Station (Utah, USA): Phyllosilicate and sulfate analogues to Mars mission landing sites. *International Journal of Astrobiology*, 10: 269-289.
- Stromberg J., Applin D., Cloutis E., Rice M., Berard G., and Mann P. (2014) The persistence of a chlorophyll spectral biosignature from Martian evaporite and spring analogues under Mars-like conditions. *International Journal of Astrobiology*, 13: 203-223.
- Suija A., Ertz D., Lawrey J. D., and Diederich P. (2015) Multiple origin of the lichenicolous life habit in Helotiales, based on nuclear ribosomal sequences. *Fungal Diversity*, 70: 55-72.
- Summons R., Sessions A., Allwood A., Barton H., Beaty D., Blakkolb B., Canham J., Clark B., Dworkin J., and Lin Y. (2014) Planning considerations related to the organic contamination of Martian samples and implications for the Mars 2020 rover. *Astrobiology*, 14: 969-1027.
- Sutton M. A., Burton A. S., Zaikova E., Sutton R. E., Brinckerhoff W. B., Bevilacqua J. G., Weng M. M., Mumma M. J., and Johnson S. S. (2019) Radiation tolerance of Nanopore sequencing technology for life detection on Mars and Europa. *Scientific reports*, 9: 1-10.
- Tahon G., Tytgat B., Lebbe L., Carlier A., and Willems A. (2018) *Abditibacterium utsteinense* sp. nov., the first cultivated member of candidate phylum FBP, isolated from ice-free Antarctic soil samples. *Systematic and applied microbiology*, 41: 279-290.
- Tan M. H., Austin C. M., Hammer M. P., Lee Y. P., Croft L. J., and Gan H. M. (2018) Finding Nemo: hybrid assembly with Oxford Nanopore and Illumina reads greatly improves the clownfish (*Amphiprion ocellaris*) genome assembly. *GigaScience*, 7: gix137.
- Team R. C. (2013) R: A language and environment for statistical computing.
- Tessler M., Neumann J. S., Afshinnekoo E., Pineda M., Hersch R., Velho L. F. M., Segovia B. T., Lansac-Toha F. A., Lemke M., and DeSalle R. (2017) Large-scale differences in microbial biodiversity discovery between 16S amplicon and shotgun sequencing. *Scientific reports*, 7: 6589.
- Thiel C. S., Ehrenfreund P., Foing B., Pletser V., and Ullrich O. (2011) PCR-based analysis of microbial communities during the EuroGeoMars campaign at Mars Desert Research Station, Utah. *International Journal of Astrobiology*, 10: 177-190.
- Thomas G. J., Prescott B., and Urry D. W. (1987) Raman amide bands of type-II β -turns in cyclo-(VPGVG) 3 and poly-(VPGVG), and implications for protein secondary-structure analysis. *Biopolymers*, 26: 921-934.
- Trivedi C. B., Lau G. E., Grasby S. E., Templeton A. S., and Spear J. R. (2018) Low-temperature sulfidic-ice microbial communities, Borup Fiord Pass, Canadian high Arctic. *Frontiers in microbiology*, 9: 1622.
- Vago J. L., Westall F., Coates A. J., Jaumann R., Korablev O., Ciarletti V., Mitrofanov I., Josset J.-L., De Sanctis M. C., and Bibring J.-P. (2017) Habitability on early Mars and the search for biosignatures with the ExoMars Rover. *Astrobiology*, 17: 471-510.
- Van Acker H., and Coenye T. (2017) The role of reactive oxygen species in antibiotic-mediated killing of bacteria. *Trends in microbiology*, 25: 456-466.

- van der Valk T., Pečnerová P., Díez-del-Molino D., Bergström A., Oppenheimer J., Hartmann S., Xenikoudakis G., Thomas J. A., Dehasque M., and Sağlıcan E. (2021) Million-year-old DNA sheds light on the genomic history of mammoths. *Nature*, 591: 265-269.
- Van Etten J., Graves M., Müller D., Boland W., and Delaroque N. (2002) Phycodnaviridae—large DNA algal viruses. *Archives of virology*, 147: 1479-1516.
- Van Lith Y., Warthmann R., Vasconcelos C., and Mckenzie J. A. (2003) Sulphate-reducing bacteria induce low-temperature Ca-dolomite and high Mg-calcite formation. *Geobiology*, 1: 71-79.
- Van Trappen S., Vandecandelaere I., Mergaert J., and Swings J. (2004) *Flavobacterium degerlachei* sp. nov., *Flavobacterium frigidis* sp. nov. and *Flavobacterium micromati* sp. nov., novel psychrophilic bacteria isolated from microbial mats in Antarctic lakes. *International journal of systematic and evolutionary microbiology*, 54: 85-92.
- Varin T., Lovejoy C., Jungblut A. D., Vincent W. F., and Corbeil J. (2012) Metagenomic analysis of stress genes in microbial mat communities from Antarctica and the High Arctic. *Applied and environmental microbiology*, 78: 549-559.
- Vaser R., Sović I., Nagarajan N., and Šikić M. (2017) Fast and accurate de novo genome assembly from long uncorrected reads. *Genome research*, 27: 737-746.
- Vega-García S., Sánchez-García L., Prieto-Ballesteros O., and Carrizo D. (2021) Molecular and isotopic biogeochemistry on recently-formed soils on King George Island (Maritime Antarctica) after glacier retreat upon warming climate. *Science of the Total Environment*, 755: 142662.
- Velázquez D., Lezcano M. Á., Frias A., and Quesada A. (2013) Ecological relationships and stoichiometry within a Maritime Antarctic watershed. *Antarctic Science*, 25: 191-197.
- Vicente-Retortillo Á., Valero F., Vázquez L., and Martínez G. M. (2015) A model to calculate solar radiation fluxes on the Martian surface. *Journal of Space Weather and Space Climate*, 5: A33.
- Volkman J., Johns R., Gillan F., Perry G., and Bavor Jr H. (1980) Microbial lipids of an intertidal sediment—I. Fatty acids and hydrocarbons. *Geochimica et Cosmochimica Acta*, 44: 1133-1143.
- Volkman J. K. (1986) A review of sterol markers for marine and terrigenous organic matter. *Organic geochemistry*, 9: 83-99.
- Volkman J. K., Barrett S. M., Blackburn S. I., Mansour M. P., Sikes E. L., and Gelin F. (1998) Microalgal biomarkers: a review of recent research developments. *Organic Geochemistry*, 29: 1163-1179.
- Vollmers J., Voget S., Dietrich S., Gollnow K., Smits M., Meyer K., Brinkhoff T., Simon M., and Daniel R. (2013) Poles apart: Arctic and Antarctic Octadecabacter strains share high genome plasticity and a new type of xanthorhodopsin. *PLoS One*, 8: e63422.
- Walker J. J., Spear J. R., and Pace N. R. (2005) Geobiology of a microbial endolithic community in the Yellowstone geothermal environment. *Nature*, 434: 1011-1014.
- Warren-Rhodes K. A., Rhodes K. L., Pointing S. B., Ewing S. A., Lacap D. C., Gomez-Silva B., Amundson R., Friedmann E. I., and McKay C. P. (2006) Hypolithic cyanobacteria, dry limit of photosynthesis, and microbial ecology in the hyperarid Atacama Desert. *Microbial ecology*, 52: 389-398.
- Weisleitner K., Perras A., Moissl-Eichinger C., Andersen D. T., and Sattler B. (2019) Source environments of the microbiome in perennially ice-covered Lake Untersee, Antarctica. *Frontiers in microbiology*, 10: 1019.

- Wick R. R., Judd L. M., Gorrie C. L., and Holt K. E. (2017) Completing bacterial genome assemblies with multiplex MinION sequencing. *Microbial genomics*, 3.
- Wierzchos J., Cámara B., de Los Ríos A., Davila A., Sánchez Almazo I., Artieda O., Wierzchos K., Gomez-Silva B., McKay C., and Ascaso C. (2011) Microbial colonization of Calcium sulfate crusts in the hyperarid core of the Atacama Desert: implications for the search for life on Mars. *Geobiology*, 9: 44-60.
- Wierzchos J., Davila A. F., Artieda O., Cámara-Gallego B., de los Ríos A., Neelson K. H., Valea S., García-González M. T., and Ascaso C. (2013) Ignimbrite as a substrate for endolithic life in the hyper-arid Atacama Desert: implications for the search for life on Mars. *Icarus*, 224: 334-346.
- Wierzchos J., DiRuggiero J., Vitek P., Artieda O., Souza-Egipsy V., Skaloud P., Tisza M., Davila A. F., Vílchez C., and Garbayo I. (2015) Adaptation strategies of endolithic chlorophototrophs to survive the hyperarid and extreme solar radiation environment of the Atacama Desert. *Frontiers in microbiology*, 6: 934.
- Wierzchos J., Ríos A. d. I., and Ascaso C. (2012) Microorganisms in desert rocks: the edge of life on Earth.
- Wight J., Varin M.-P., Robertson G. J., Huot Y., and Lang A. S. (2020) Microbiology in the field: construction and validation of a portable incubator for real-time quantification of coliforms and other bacteria. *Frontiers in public health*, 8.
- Wilhelm M. B., Davila A. F., Eigenbrode J. L., Parenteau M. N., Jahnke L. L., Liu X.-L., Summons R. E., Wray J. J., Stamos B. N., and O'Reilly S. S. (2017) Xeropreservation of functionalized lipid biomarkers in hyperarid soils in the Atacama Desert. *Organic geochemistry*, 103: 97-104.
- Williams R. M., Chidsey Jr T. C., and Eby D. E. (2007) Exhumed paleochannels in central Utah—Analogues for raised curvilinear features on Mars.
- Williams R. M., Irwin III R. P., Burr D. M., Harrison T., and McClelland P. (2013) Variability in Martian sinuous ridge form: Case study of Aeolis Serpens in the Aeolis Dorsa, Mars, and insight from the Mirackina paleoriver, South Australia. *Icarus*, 225: 308-324.
- Williams R. M., Irwin R. P., and Zimbelman J. R. (2009) Evaluation of paleohydrologic models for terrestrial inverted channels: Implications for application to martian sinuous ridges. *Geomorphology*, 107: 300-315.
- Xu D., Kong H., Yang E.-J., Li X., Jiao N., Warren A., Wang Y., Lee Y., Jung J., and Kang S.-H. (2020) Contrasting community composition of active microbial eukaryotes in melt ponds and sea water of the Arctic Ocean revealed by high throughput sequencing. *Frontiers in Microbiology*, 11: 1170.
- Ye T., Wang B., Li C., Bian P., Chen L., and Wang G. (2021) Exposure of cyanobacterium *Nostoc* sp. to the Mars-like stratosphere environment. *Journal of Photochemistry and Photobiology B: Biology*, 224: 112307.
- Yergeau E., Michel C., Tremblay J., Niemi A., King T. L., Wyglinski J., Lee K., and Greer C. W. (2017) Metagenomic survey of the taxonomic and functional microbial communities of seawater and sea ice from the Canadian Arctic. *Scientific reports*, 7: 42242.
- Zawierucha K., Ostrowska M., and Kolicka M. (2017) Applicability of cryoconite consortia of microorganisms and glacier-dwelling animals in astrobiological studies. *Contemporary Trends in Geoscience*, 6.

- Ziolkowski L., Mykytczuk N., Omelon C., Johnson H., Whyte L., and Slater G. (2013) Arctic gypsum endoliths: a biogeochemical characterization of a viable and active microbial community.
- Zucconi L., Onofri S., Cecchini C., Isola D., Ripa C., Fenice M., Madonna S., Reboleiro-Rivas P., and Selbmann L. (2016) Mapping the lithic colonization at the boundaries of life in Northern Victoria Land, Antarctica. *Polar Biology*, 39: 91-102.

Chapter 5. Discussion and Conclusion

Detection of unambiguous biosignatures such as DNA will be essential for future astrobiology missions. DNA can be detected with MinION sequencing, in which DNA is ratcheted through a protein nanopore and an ionic current is generated for sequence determination. The MinION is a miniaturized, low energy, and low cost sequencing device that could be adapted for use in space missions. In the preceding chapters, the MinION was used to detect DNA from all three domains of life, as well as viruses, in a diverse suite of Mars and icy moons analogue environments (i.e. the Hanksville paleochannels, University Valley cryptoendoliths, and Allen Bay sea ice cryoconites). The results from this thesis further establish the MinION's ability to detect life in analogue samples exposed to Mars-like conditions, as well as act as a reliable tool for genome reconstruction from metagenomes in analogue environments.

5.1 The taxonomy of Mars analogue environments as revealed by MinION sequencing

MinION sequencing of the Hanksville paleochannels revealed a variable community, depending on the sample type (i.e. endolith, sediment, or rock). In general, Proteobacteria, Actinobacteria, Cyanobacteria, and Bacteroidetes were the most prominent phyla encountered (Figure 2.2). Most endolith samples (samples E3, E4, and E5) were heavily dominated by Cyanobacteria ($\geq 76\%$) as Nostocales, a common order in endolithic samples (Sigler *et al.* 2003; Ye *et al.* 2021). The other two endolith samples (E1 and E2) were more dominated by Firmicutes and Proteobacteria, respectively. Most sediment and rock samples (S1, S2, S3, R1, and R2) contained Actinobacteria, Bacteroidetes, and Proteobacteria as the dominant taxa, save sample R3,

which like endoliths E3, E4, and E5 contained primarily Cyanobacteria as Nostocales. This sample had no visible endoliths; instead, the outer rock layer was covered with a dark, oxidized coating that may have been desert varnish. Desert varnish (aka “rock rust” or “desert patina”) is a μm -thick surface layer containing clay, organic matter, and oxides of iron and manganese (Engel and Sharp 1958). It has been observed on Mars previously (Guinness *et al.* 1997; McCauley *et al.* 1979) and its formation may be microbially mediated (Dorn and Oberlander 1981). MinION sequencing was also able to detect genes from putatively extremophilic taxa in all three sample types, including UV-resistant and halophilic Halobacteria, methanogens Methanobacteria and Methanomicrobia, desiccation-tolerant *Chroococcidiopsis*, and polyextremophilic Deinococcus-Thermus.

These results are consistent with previous surveys of the Hanksville paleochannel area. A PCR-based detection survey of soil from the neighbouring Mars Desert Research Station (MDRS) showed that the area is largely dominated by Bacteria (Thiel *et al.* 2011). A separate 16S and 18S rRNA-based assessment also showed a dominance of Bacteria, specifically as Actinobacteria, Proteobacteria, Bacteroidetes, and Gemmatimonadetes (Direito *et al.* 2011). Eukaryotic taxa present were also moderately diverse as fungi (Blastocladiomycota, Zygomycota), green algae (Chlorophyta), bacterivorous flagellates (*Heteromita globosa*), and other protozoans (e.g. ciliophores) (Direito *et al.* 2011). Low archaeal diversity was present, like the results produced in this work. The lack of Cyanobacteria present in these previous works can be attributed to the sample types examined; Thiel *et al.* (2011) and Direito *et al.* (2011) analyzed soils rather than endoliths and rocks. Similar to the MinION results presented here, Direito *et al.* (2011) also detected putatively extremophilic taxa, including desiccation-tolerant *Chroococcidiopsis* and polyextremophilic Deinococcus-Thermus.

When the MinION sequencing results were directly compared with 16S rRNA Illumina sequencing results, some overlap was found. The OTUs present were most abundant from the phyla Acidobacteria, Actinobacteria, Cyanobacteria, Proteobacteria, Deinococcus-Thermus, Planctomycetes, and Chloroflexi (Figure 2.3). Like the MinION results, three of the endolith samples were largely dominated by Cyanobacteria (Nostocales), but were samples E1, E2, and E4 (rather than E3, E4, and E5). Samples E3 and E5 contained higher proportions of Actinobacteria and Deinococcus-Thermus (mostly Deinococcales) instead of Cyanobacteria. Sediment and rock samples were dominated by Actinobacteria, Proteobacteria, and Chloroflexi. Further, the 16S amplicons revealed more diversity in the Hanksville paleochannels than the shotgun metagenome produced by MinION sequencing. In particular, the candidate phylum FBP was detected in 16S rRNA dataset but was absent in the MinION data. Intrinsic differences between the two sequencing techniques and datasets can account for this variance, including reduced shotgun metagenome database size, lower read output from the MinION, and the MinION's inherently high error rate (i.e. 0.7 – 14.5% for MinION sequencing, <0.1% for Illumina sequencing) (Jain *et al.* 2017; Manley *et al.* 2016). This type of discrepancy is not uncommon; a previous large-scale comparison of floodplain environments showed that <50% of phyla from 16S rRNA amplicon datasets were detected in the corresponding shotgun metagenomes (Tessler *et al.* 2017).

MinION sequencing of the University Valley cryptoendoliths showed a variable microbial community (Figures 3.4 and 3.5). The initial communities prior to MARTE or strong UV exposure (T_{0M} and T_{0UV}, respectively) were not identical, which may be due to a combination of different classification pipelines (JGI IMG/M ER vs. Kaiju) and natural variation within cryptoendolithic samples (Mergelov *et al.* 2018; Wierzchos *et al.* 2015). T_{0M} contained primarily phototrophic algae as Cyanobacteria (Synechococcales, Nostocales) and Chlorophyta (Chlamydomonadales,

Trebouxiophyceae), while T_{UV} contained instead Ascomycota (Helotiales, Eurotiales, and Umbiliciales), Proteobacteria (Hyphomicrobiales, Burkholderiales), and Acidobacteria. Helotiales and Umbiliciales are lichenizing fungi (Larson 1983; Suija *et al.* 2015), a common constituent in Antarctic cryptoendoliths (Friedmann 1982; Zucconi *et al.* 2016). Previous surveys of University Valley cryptoendoliths have produced similar results; a 16S/18S rRNA survey of the University Valley cryptoendoliths found that Cyanobacteria were dominant (Archer *et al.* 2017), while Goordial *et al.* (2016) observed that the University Valley cryptoendolith community was composed of heterotrophic bacteria (Acidobacteria) and fungi (Lecanoromycetes) (Goordial *et al.* 2016a). This difference in community composition within our samples implies that the University Valley cryptoendoliths may be alternately Cyanobacteria- or lichen-dominated, depending on the localized sampling area (Mergelov *et al.* 2018; Wierzos *et al.* 2015).

When used on sea ice cryoconites from Allen Bay, MinION sequencing showed a community largely dominated (>90%) by Bacteroidetes as Flavobacteriales, primarily *Flavobacterium* sp. ALD4, *Flavobacterium* sp. ACAM 123, *Flavobacterium frigoris*, and *Flavobacterium gillisiae* (Figure 4.2). These bacterial heterotrophs are ubiquitous in polar aquatic environments (Kirchman 2002; McCammon and Bowman 2000; Van Trappen *et al.* 2004). This lack of sequence diversity is not uncommon in sea ice and cryoconite communities, where a small number of key taxa dominate but vary spatially and temporally (Maccario *et al.* 2015). Indeed, the low amount of archaeal sequences present may be due to the summer sampling time; archaeal taxa often increase over winter in sea ice (Collins *et al.* 2010). While cryoconites in glacial and alpine environments frequently contain high amounts of Cyanobacteria and Proteobacteria, cryoconites comprising predominantly heterotrophic community members like *Flavobacterium* spp. and other Bacteroidetes are not uncommon and are instead supported by allochthonous carbon inputs

(Collins *et al.* 2010; Edwards *et al.* 2020; Edwards *et al.* 2019; Edwards *et al.* 2016; Edwards *et al.* 2013b). Sea ice communities in the Canadian high Arctic regularly contain high amounts of Bacteroidetes as *Flavobacterium* spp., as well (Garneau *et al.* 2016; Hatam *et al.* 2014; Yergeau *et al.* 2017).

A HiSeq-generated metagenome from the Allen Bay sea ice cryoconites also showed a dominance of Bacteroidetes as *Flavobacterium* spp., but in a lower quantity (~55%) than in the MinION dataset (Figure 4.2). Like the Hanksville paleochannels, the Illumina dataset of this environment was more diverse than the corresponding MinION metagenome, containing some taxa lacking from the MinION dataset (e.g. Caulobacterales, Chlorellales, Desulfovibrionales), although the most dominant community members are represented in both metagenomes. This discrepancy can be attributed to inherent differences in the techniques (i.e. reduced shotgun metagenome database size, lower read output from the MinION, the MinION's inherently high error rate) (Jain *et al.* 2017; Manley *et al.* 2016; Tessler *et al.* 2017).

5.2 MinION utility in space science

In addition to real-time DNA detection, the MinION can detect DNA in quantities relevant to putative extraterrestrial microbial habitats. The lowest DNA input currently recommended by Oxford Nanopore Technologies (ONT) is 50 ng of high molecular weight (HMW) genomic DNA without PCR amplification and >1 ng of genomic DNA with PCR amplification. Using an average bacterial genome size of ~2 – 5 Mbp and ~1.5 – 5.4 fg of DNA per bacterial genome, 1 ng of genomic DNA corresponds to a biomass of ~10⁶ – 10⁷ cells/g (Dolezel *et al.* 2003; Raes *et al.* 2007). This value is higher than Mars and icy world analogue environmental biomasses (e.g.

University Valley permafrost with 10^3 cells/g, Lost Hammer Spring sediment with 10^5 cells/g) (Goordial *et al.* 2016a; Niederberger *et al.* 2010). Thus, I chose to explore MinION DNA detection limits beyond amounts endorsed by ONT.

Using a high biomass endolith sample from the Hanksville paleochannels (E4), I determined putative lower detection limits for MinION DNA detection (Table 2.2, Figure 2.5). Starting with 0.110 ng of DNA ($\sim 1/10^{\text{th}}$ of the minimum input required with PCR), 253 188 total reads were generated and showed a community dominated by Cyanobacteria, similar to the community shown in the MinION metagenome and Illumina 16S rRNA profile of sample E4 (Figures 2.2 and 2.3). I then tested inputs of 0.0408 ng, 0.0106 ng, and 0.00106 ng of DNA, and the total number of sequences produced per trial decreased with DNA concentration. Cyanobacteria became less dominant as the DNA input decreased and was completely absent from the final 0.00106 ng trial. 0.00106 ng corresponds to a biomass of ~ 100 cells/g, a biomass common in strong Mars and icy worlds analogue environments (Goordial *et al.* 2016a; Niederberger *et al.* 2010).

Sequencing a sample containing zero DNA (i.e. nuclease-free water) produced 121 reads, but none of these reads were able to be classified by JGI IMG/M ER, suggesting that these reads were barcodes and adapter dimers produced during the library preparation. Examining the quality score distribution of the DNA detection trials showed that PHRED score for the 0 ng run had a seemingly random quality distribution (Supplementary Figure 2.1), indicating that a low sequence number, lack of sequence classification, and random quality score distribution are strong indicators of a sample with zero DNA present and that the MinION will not produce false positives. Separate studies have also shown that the MinION also does not produce sequencing artifacts or ionic current noise that could be confused for positive DNA detection (Pontefract *et al.* 2018).

The MinION is also able to detect DNA from samples exposed to Mars-like environmental conditions. When University Valley cryptoendoliths were exposed to Martian temperature, atmospheric pressure, atmospheric composition, and UV radiation in MARTE, DNA remained detectable and sequenceable (Figure 3.4, Table 3.2). UVC chamber exposure also did not prevent MinION detection and sequencing of these samples (Figure 3.5, Table 3.6). The longer exposure in the UVC chamber vs. MARTE (~278 Martian years vs. ~58 Martian sols, respectively) showed a general decrease in DNA concentration with exposure time. However, ~278 Martian years' worth of UVC radiation was not enough to completely prevent DNA detection and sequencing, demonstrating that the MinION could be used to detect extant or recently extinct Martian life from samples collected during missions for future caching or samples that have been exposed to the Martian surface naturally (e.g. relatively young craters) (Quantin *et al.* 2016).

When combined with the MinION's ability to produce sequences in real-time, this assurance that the MinION does not generate false positives enables confidence in definitive life detection, as well as the ability to select optimal samples to cache for future sample return to Earth (Goordial *et al.* 2017). Despite the MinION's relatively high error rate (i.e. 0.7 – 14.5%) (Jain *et al.* 2017), it is a reliable tool for identifying common laboratory contaminants, pathogens, and lineages (Castro-Wallace *et al.* 2017; Tyler *et al.* 2018); real-time detection and comparison with a systematic database of common contaminants would therefore prevent potential forward contamination in future astrobiology missions. The MinION can also identify non-standard bases in nucleic acids (i.e. inosine), producing a reliable, diagnostic signature for potential non-Earth-based life (Carr *et al.* 2017). Even with the potential for shared terrestrial ancestry based on past meteoritic exchange between Earth and Mars, the divergence would have occurred ~4 billion years

ago, indicating that potential Martian life would be an independent, unclassified lineage but still possess a repeating and detectable charge (Fairén *et al.* 2017).

5.3 MinION sequencing complements and supports results from other space mission techniques

As a standalone tool, the MinION was able to produce reliable signs of life (i.e. DNA sequences) from all three analogue environments examined in this thesis: the Hanksville paleochannels, University Valley cryptoendoliths, and sea ice cryoconites from Allen Bay. When combined with other techniques and instruments used in space missions or space mission concepts, results from the MinION can be used to contextualize and increase understanding of environments and their microbial populations. In my survey of the Hanksville paleochannels, X-ray diffraction (XRD), reflectance spectroscopy, Raman spectroscopy, and Life Detector Chip (LDChip) microarray immunoassays were also performed in conjunction with MinION sequencing. These techniques are the same as or approximations of those used in past, current, and potential future missions; XRD is used by *Curiosity's* CheMin instrument, reflectance spectroscopy will be used by the Mars Multispectral Imager for Subsurface Studies (MA-MISS) instrument aboard *Rosalind Franklin*, and Raman spectroscopy will be a component of *Rosalind Franklin's* Raman Laser Spectrometer (RLS) and is utilized by *Perseverance's* SuperCam and SHERLOC (Scanning Habitable Environments with Raman and Luminescence for Organics and Chemicals) instruments (Maurice *et al.* 2021; Rull *et al.* 2017). The LDChip is analogous to the Life Marker Chip (LMC), an antibody microarray for protein detection and a former candidate payload for *ExoMars* (Martins 2011; Sims *et al.* 2012).

XRD data from the Hanksville paleochannels showed a quartz-rich environment, with some minor signatures of gypsum, calcite, and montmorillonite (Supplementary Table 2.1). Reflectance spectra were largely dominated by hydrated mineral absorption features, including montmorillonite, calcite, and Fe-bearing oxyhydroxides (i.e. goethite). Unlike the XRD data, the reflectance spectra also showed various organic matter signatures, including chlorophyll *a* indicated by an absorption band at 670 nm, a preceding “chlorophyll bump”, and “red edge” at 800 nm (Rhind *et al.* 2014; Stromberg *et al.* 2014) (Figure 2.6). Other pigment features were present in the reflectance spectra, including porphyrin and carotenoids (Berg *et al.* 2014). The Raman spectra also contained organic features, including peaks representing chlorophyll, carotenoids, and potentially parietin (Edwards *et al.* 2005; Rhind *et al.* 2014) (Figure 2.7). Quartz and gypsum are represented in the Raman spectra by peaks at $\sim 470\text{ cm}^{-1}$ and $\sim 1006\text{ cm}^{-1}$, respectively (Edwards *et al.* 2007). The LDChip detected signals from Actinobacteria, Cyanobacteria, iron/sulfur bacteria from Acidithiobacillia, Nitrospirae, and crude environmental extracts from the Río Tinto that are rich in iron and sulfur (Figures 2.8 and 2.9).

The XRD, reflectance, and Raman data provide geological context to the Hanksville paleochannels and detected some features related to life (e.g. pigments). The LDChip can detect definitive signs of life (i.e. proteins) but with a broad range of classification. The polyclonal antibodies of the LDChip may detect closely related taxa or similar epitopes as well as their target. However, when combined with MinION sequencing, these techniques form a suite of instrumentation for life detection with results that complement and support each other (Table 2.3). The presence of quartz in the diffraction and spectral data corroborates the detection of Cyanobacteria in the MinION and LDChip data, as quartz is a common component of samples hosting cyanobacterial communities in desert environments (Lacap *et al.* 2011; Schlesinger *et al.*

2003). Calcite is precipitated by many bacterial taxa and its presence in the Hanksville paleochannel samples could be mediated by sulfate-reducing bacteria (SRBs; e.g. Desulfobacterales, Desulfovibrionales) and *Bacillus* spp. detected by the MinION and LDChip (Boquet *et al.* 1973; Castanier *et al.* 1999; Van Lith *et al.* 2003). SRBs can also be validated by the presence of gypsum in the diffraction and spectral data, and gypsum is further known to harbour various cyanobacterial and archaeal halophiles (Jehlička *et al.* 2013; Oren *et al.* 2009; Ziolkowski *et al.* 2013). Pigments detected in the spectral data (e.g. chlorophyll *a*, carotenoids) are indicated by the MinION and LDChip as Cyanobacteria and photosystem genes. The MinION and LDChip also detected genes and proteins indicative of potential metabolisms in the Hanksville paleochannels; together, the two datasets detected a wider set of metabolic features than either technique alone. These metabolisms include nitrogen metabolism (e.g. *nir* and *nif* genes, nitrate reductase) and methane metabolism (e.g. Methanomicrobia, Methanobacteria).

MinION sequencing results can also be used to support other methods for definitive life detection. When used in conjunction with gas chromatography-mass spectroscopy (GC-MS) and the LDChip for cell membrane-derived lipid and protein detection, respectively, a more detailed picture of the University Valley cryptoendolith community was generated. GC-MS has been included on previous mission payloads (e.g. the *Viking* biological experiments, SAM on *Curiosity*) (Klein 1978a; Millan *et al.* 2016). MinION sequencing showed that T0_M and T3_M were dominated by photoautotrophs, primarily as Cyanobacteria and Chlorophyta, and secondarily containing Proteobacteria and Streptophyta (Figure 3.4). Photoautotrophs are indicated in the lipid profile by the presence of high molecular weight (HMW) linear and saturated compounds (Carrizo *et al.* 2019; Johnson *et al.* 2020; Sánchez-García *et al.* 2018; Volkman *et al.* 1998) (Figure 3.7). Algae are further signified via monomethyl-HMW alkanes and 2-alkanones. Monounsaturated LMW

alkanes, pristane, mono- and diunsaturated C18 acids denote the presence of Cyanobacteria (Carrizo *et al.* 2019; Cranwell 1978; Parenteau *et al.* 2014; Sánchez-García *et al.* 2018; Sánchez-García *et al.* 2020; Volkman *et al.* 1980). Phytol, phytosterol, and campesterol were also present, potentially from photoautotrophs (Didyk *et al.* 1978; Luo *et al.* 2019; Sánchez-García *et al.* 2018; Sánchez-García *et al.* 2020). The LDChip results supported the lesser presence of non-photoautotrophs in the MinION data, exhibiting strong signals for Proteobacteria as Alphaproteobacteria, Betaproteobacteria, and Gammaproteobacteria. Thus, when combined with the MinION, the potential for biosignature detection, environmental and community characterization with the techniques used in Chapters 2 and 4 (i.e. XRD, reflectance spectroscopy, Raman spectroscopy, LDChip immunoassays, GC-MS) is greatly increased and forms an effective suite of instrumentation for life detection in astrobiology analogue environments.

5.4 Utility of MinION sequencing in microbial ecology

The long reads generated by the MinION can often be genome-sized and span repetitive regions, enabling simpler contig assembly and genome reconstruction (Goldstein *et al.* 2019; Jain *et al.* 2018). Producing metagenome-assembled genomes (MAGs) (i.e. genome bins) is more complicated than reconstructing individual genomes from culture due to intergenomic repeats, chimeric reads, and a higher diversity of genomes present (Somerville *et al.* 2019); as such, I wanted to determine if it was possible to produce MAGs from MinION reads and if the longer reads would facilitate MAG generation (Jain *et al.* 2017). Using samples from the Allen Bay sea ice cryoconites, I attempted to produce MAGs with MinION reads only; however, these MAGs had extremely high contamination and medium-to-low completeness (Supplementary Table 3.1).

Short-read polishing and frameshift correction was also performed (MinION_RD MAGs), but the completeness and contamination remained so poor that taxonomic designations were irrelevant.

I also wanted to determine if using a combination MinION+Illumina HiSeq (i.e. hybrid) dataset would produce higher quality contigs and MAGs than either constituent dataset alone. Hybrid assemblies have previously produced metagenomes with higher quality contigs and MAGs in mock microbial communities and natural environments (Bertrand *et al.* 2019; Brown *et al.* 2021; Nicholls *et al.* 2019; Overholt *et al.* 2020; Sevim *et al.* 2019), but hybrid assembly had not yet been evaluated as a tool for genome reconstruction in a low biomass, extreme environment like the sea ice cryoconites from Allen Bay. This environment is a strong astrobiology analogue for the icy moons Enceladus and Europa and is becoming increasingly transient with climate change; thus, a greater understanding of microbial life in sea ice cryoconite holes is needed.

The MinION-only metagenome largely contained (>90%) Bacteroidetes as *Flavobacterium* spp. Similarly, the HiSeq and hybrid metagenomes were also dominated by Bacteroidetes but in a smaller proportion (~55%); these datasets also contained Proteobacteria as Burkholderiales (*Polaromonas* spp.), Pseudomonadales (*Pseudomonas* spp., *Psychrobacter* spp.), and Rhodobacterales (*Loktanella salsilacus*, *Octadecabacter* spp.) (Figure 4.2). The hybrid and HiSeq metagenomes differed somewhat in the proportions of taxa present but contained all the same taxa at the phylum level, with one exception; Candidatus Gracilibacteria was detected only in the hybrid and MinION metagenomes. This phylum is an uncultured lineage with restricted metabolisms, previously detected in deep-sea sediment and microbial mats (Ley *et al.* 2006). The hybrid dataset also contained more unique genes in higher abundances than those in the HiSeq dataset. This increase in information with the addition of MinION reads to the hybrid dataset

demonstrates the value of hybrid datasets for enhancing understanding of extreme astrobiology analogue environments.

A direct comparison of the MinION, hybrid, and HiSeq assemblies shows that the MinION-only dataset had the longest average contig length and the highest proportion of ultra-long (>50 000 bp) contigs in its dataset (Table 4.2). The hybrid dataset had a higher contig length, an increased number of ultra-long contigs, more classified coding sequences (CDSs), higher N50 values, and more total MAGs produced than the HiSeq dataset. Hybrid assembly also produced more total MAGs than the HiSeq-only dataset (44 vs. 37, respectively) (Table 4.3). Hybrid assembly produced one high-quality (i.e. > 90% complete, < 5% contaminated, presence of the 23S, 16S, and 5S rRNA genes and at least 18 tRNAs) (Bowers *et al.* 2017) and five medium-quality bins (i.e. \geq 50% complete, < 5% contaminated) (Bowers *et al.* 2017). HiSeq assembly produced six medium-quality MAGs. Similar taxonomies were produced with each method. Directly comparing HiSeq and hybrid MAGs of the same taxonomic assignment showed that in nearly all cases, the hybrid MAGs possessed higher completeness, N50 values, mean contig length, longest contig, and lower contamination (Supplementary Figure 4.1). The taxonomies of the MAGs produced reflects those present in the cryoconite metagenomes. Full complements of rRNA were present in just four MAGs, all of which contain MinION reads: Hybrid_5, MinION_3, MinION_RD_2, and MinION_RD_3. rRNA is often difficult to retrieve from metagenomes and binning programs (Alneberg *et al.* 2018), but the MinION's ability to generate long reads that span repetitive regions enables increased recovery of this important microbial marker (Case *et al.* 2007; Somerville *et al.* 2019; Stewart *et al.* 2019).

I also assessed if the disadvantages of MinION sequencing (i.e. high error rate) would effect the quality of hybrid contigs and hybrid MAGs. The most common error generated during

MinION sequencing is insertion-deletions (i.e. indels). Indels introduce premature stop codons, causing truncated open reading frames (ORFs) and reducing the lengths of predicted proteins from the sequences produced. When comparing predicted protein length to the length of its best match, this ratio will be <1 if there are many details present in the dataset. Plots of query length:hit length (i.e. predicted protein:best match) vs. frequency for each assembly method and the highest quality hybrid and HiSeq MAGs show that the hybrid plots do not differ significantly from the HiSeq plots (Figure 4.3). The majority of contigs in both the hybrid and HiSeq plots show have a query length:hit length ratio of ~ 1 ; thus, the effect of indels in these datasets is marginal. Conversely, the MinION metagenome has a query length:hit length ratio of <1 , signifying that indels are strongly present in this dataset. When polished with the HiSeq reads, the query length:hit length ratio is increased to ~ 1 , demonstrating that the effect of indels is minimized when paired with HiSeq reads or HiSeq read polishing. The addition of MinION reads increases the quality of a hybrid metagenome (e.g. higher average contig length, higher MAG completeness) without impacting the error rate.

Included in the hybrid MAGs is a putatively novel member of the *Octadecabacter* genus: Hybrid_5. Hybrid_5 was the most complete (90.9%) and least contaminated (0.6%) bin produced by any assembly method and was assigned to the *Octadecabacter* genus by both GTDB and MiGA. Hybrid_5 also contained a complete 16S rRNA gene mapping to *O. arcticus* with 98% identity and had an average nucleotide identity (ANI) of 93.51% with *O. arcticus*; this ANI is below the threshold of 95% similarity for identical species, suggesting that Hybrid_5 represents a potential novel species of *Octadecabacter*. *Octadecabacter* is exemplified by *O. arcticus* and *O. antarcticus*, marine psychrophiles with a bipolar distribution. *Octadecabacter* is common in

marine environments, implying that Hybrid_5 may have entered the cryoconite environment via the surrounding seawater.

Like *O. arcticus*, Hybrid_5's metabolic genes suggest an aerobic/microaerophilic and heterotrophic lifestyle. Hybrid_5's genome encodes for a complete tricarboxylic acid (TCA) cycle, Embden-Meyerhof glycolysis, oxidative phosphorylation, the acetyl-CoA pathway, the Entner-Doudoroff pathway, and glyoxylate shunt (Figure 4.5). Hybrid_5 also possesses anaerobic metabolic capabilities, including full lactic acid and ethanol fermentation pathways, and pyruvate:ferredoxin oxidoreductase for anaerobic oxidation of pyruvate. Complete pathways for assimilatory sulfate reduction, assimilatory nitrate reduction, dissimilatory nitrate reduction, and nitrate reduction are also present. Three nitrate reductases are encoded in the Hybrid_5 genome (*nar*, *nap*, and *nas*), suggesting that Hybrid_5 can use nitrate for redox balancing, as a terminal electron acceptor, and as a nitrogen source, respectively (Moreno-Vivián *et al.* 1999). The presence of periplasmic *nap* indicates aerobic denitrification capabilities; thus, Hybrid_5 may be able to co-respire oxygen and nitrate (Ji *et al.* 2015). Hybrid_5 also encodes for many stress response and cold adaptation genes, including cold shock response genes (e.g. *csp*, molecular chaperones), osmotic stress response genes (e.g. compatible solute transporters), carotenoid production (e.g. phytoene synthase), and UV damage repair (e.g. *phrB*).

There are no other species of *Octadecabacter* that contain genes for full assimilatory nitrate reduction, denitrification, assimilatory sulfate reduction, lactic acid fermentation, or ethanol fermentation, further signifying that Hybrid_5 is a novel member of this genus and functions as a facultative anaerobe in the sea ice cryoconite environment (Parks *et al.* 2018; Simon *et al.* 2009; Vollmers *et al.* 2013). Hybrid_5 also differs from its HiSeq-only counterpart, HiSeq_31, via its possession of more stress response genes; in particular, HiSeq_31 lacks *murB*, catalase peroxidase,

an Na⁺:H⁺ antiporter, and peroxidase. The addition of MinION data to the hybrid dataset thus produced potential novel species of *Octadecabacter* that possessed features absent in the HiSeq-only dataset, leading to a greater understanding of this extreme analogue environment and its inhabitants.

5.5 Future work

The results from this thesis suggest that MinION sequencing may be a viable tool for life detection and metagenome studies in extreme analogue environments. However, there are several paths for future research emanating from this work, including determining exact detection limits for DNA with MinION sequencing. Chapter 2 of this thesis established a putative lower limit of 0.001 ng for successful DNA detection and that the MinION will not generate a false positive when there is no DNA present. While this value corresponds to ~100 cells/g (Dolezel *et al.* 2003; Raes *et al.* 2007), a value similar to biomasses found in Mars analogue environments (Goordial *et al.* 2016a; Niederberger *et al.* 2010), it is not an exact limit of detection and the absolute lower limit for MinION detection of DNA needs to be defined. This value also applies to a library preparation protocol that includes a PCR amplification step; detection limits without PCR have not been published. The minimum DNA input without PCR is currently 50 ng for the Rapid Barcoding Kit 96 (SQK-RBK110.96). I previously was able to perform a successful MinION sequencing run with ~32.6 ng of DNA without PCR and using the Field Sequencing Kit (SQK-LRK001) on a glacial ice core sample (data not shown); however, this amount is far higher than Mars and icy moons analogue environmental biomasses, signifying that PCR-free detection limits for MinION sequencing also need to be determined. Lower limits of detection will be strongly

dependent of the use of PCR and DNA extraction efficiency. Additionally, extant life detection with the MinION is possible even after sample exposure to ~58 Martian sols of Mars-like environmental conditions and ~278 years of Mars-like UVC. PCR amplification of the exposed DNA is possible, as well. However, exposure times to Mars simulated conditions should ideally be extended to include longer time scales. Future experiments should also include more time points to enable construction of a robust model for DNA detection with the MinION vs. exposure time and extrapolation over geological timescales.

Automation and integration of the entire MinION sequencing process need also be explored. This exploration includes testing and optimization of thermocyclers, DNA extraction methods, and DNA library preparation methods to an appropriately high technology readiness level (TRL). Miniaturized and field-ready thermocyclers have previously been used in extreme environments, including in conjunction with MinION sequencing. The miniPCR system was used with the MinION on the ISS as part of the Biomolecule Sequencer Project (Burton *et al.* 2020; Stahl-Rommel *et al.* 2021), but this device needs to be tested in combination with lower limits of DNA. DNA extraction also needs to be automated and optimized to reduce the required human input for cell lysis and DNA purification. Previous research has shown that the semi-automated SuperFastPrep2, ClaremontX1, and SOLID-Sample Preparation Unit (SOLID-SPU) are all viable DNA extraction devices for use with MinION sequencing, although devices that utilize bead beating for cellular lysis (i.e. SuperFastPrep2 and ClaremontX1) tend to produce the highest quality and quantity of DNA from environmental samples (Raymond-Bouchard *et al.* 2022). An automated library preparation device currently exists in ONT's VolTRAX. The VolTRAX is a USB-powered, portable microfluidics device that performs the required DNA adapter attachment, fragmentation, and amplification. DNA extractions and required reagents are loaded into the

VolTRAX's microfluidics chips and the library produced can be loaded directly into a MinION flow cell. However, VolTRAX users have reported numerous operating issues affecting its performance, including difficulty pipetting into and from the VolTRAX chips and software problems (Raymond-Bouchard *et al.* 2022). The VolTRAX also requires a relatively high input of DNA (≥ 475 ng). Full automation for DNA extraction and optimization of library preparation, as well as development of a microfluidics system for connecting these instruments, remains unresolved.

The MinION uses a protein nanopore for DNA detection and sequencing; as such, MinION flow cells have a definitive shelf life and require refrigeration. A non-biodegradable nanopore is required for the long trips necessary to Mars (~7–9 months), Enceladus (~3–7 years), and Europa (~3–6 years) and is presently being explored by NASA's Concepts for Ocean worlds Life Detection Technology program (COLDTech) (Bywaters *et al.* 2017) and the Search for Extraterrestrial Genomes project (SETG) (Carr *et al.* 2020; Carr *et al.* 2017). SETG is further investigating "nanogaps," which are lower bandwidth solid state nanopores that can detect and distinguish amino acids, as well as nucleic acids. Protein and RNA sequencing should be further explored as options for life detection with the MinION, as they are unambiguous biosignatures possessing a definitive, repeating charge able to be detected with nanopore sequencing.

In terms of microbial ecology studies, this thesis has shown that MinION sequences add valuable information to a hybrid dataset and enable detailed studies of MAGs that would not be produced otherwise. However, generating MAGs from low biomass, extreme environments with solely MinION sequences remains challenging. This process could be improved through the reduction of the MinION's high error rate via instrumentation development and bioinformatics pipelines. Previous MinION studies have produced contig assemblies that represent complete or

near-complete whole genomes (Stewart *et al.* 2019), but these single contigs are from high biomass environments and an input ~ 2 μg of DNA. Methods to effectively concentrate DNA could also improve MAG generation, in addition to technology development from ONT.

Conclusion

Searching for extraterrestrial life is a crucial objective for both scientific exploration and human interest. This curiosity necessitates the development and testing of life detection instrumentation and techniques for potential use on Mars, Enceladus, Europa, and their associated terrestrial analogue environments. The Oxford Nanopore Technologies' (ONT) MinION sequencer is one such instrument; the MinION is a miniaturized and portable sequencing device that can detect unambiguous biosignatures (i.e. DNA). The overall goal of this thesis was to test the MinION on a diverse set of analogue environmental samples and determine its efficacy for life detection and genome reconstruction in extreme analogue environments.

In Chapter 2, my goals were to establish that the MinION could detect life from a Mars analogue environment, the MinION's minimum DNA detection limits, and show how data from the MinION could support results from other techniques used in space missions. I found that the MinION could definitively detect life from the Hanksville paleochannels down to 0.001 ng of DNA. This input corresponds to ~100 cells/g, a biomass common in extreme Mars analogue environments. When combined with results from other space mission analogue instruments (i.e. X-ray diffraction, reflectance spectroscopy, Raman spectroscopy, immunoassay microarrays), the MinION results generated a clearer picture of the Hanksville paleochannel environment and its associated biosignatures.

In Chapter 3, following this proof-of-concept use of the MinION for life detection in Chapter 2, my goal was to determine if the MinION could detect DNA from Mars analogue samples after exposure to Mars-like environmental conditions (i.e. a Mars environmental chamber) as well as a separate exposure to strong UVC light. A ~58 sol exposure in the Mars environmental

chamber did not prevent successful DNA detection with the MinION and other definitive biosignatures (i.e. proteins and cell membrane-derived lipids) remained detectable after this exposure. UVC exposure corresponding to ~278 Martian sols also did not prevent DNA detection with the MinION, signifying the MinION's potential use for future extant life detection studies.

In Chapter 4, my goal was to ascertain if long reads produced from the MinION could be used to aid in genome reconstruction from metagenomes. I thus compared approaches for contig assembly and metagenome-assembled genome (MAG) construction using samples from Allen Bay sea ice cryoconites: MinION-only, HiSeq-only, and a hybrid (i.e. MinION + HiSEQ) dataset. I determined that the hybrid approach produced longer contigs, more coding sequences, and more total MAGs. These hybrid MAGs had the highest completeness, lowest contamination, and highest N50 of all datasets, and contained a MAG representing a potentially novel species of *Octadecabacter*. The hybrid dataset contained information unavailable in the HiSeq-only dataset, demonstrating the utility of including MinION sequencing data in genome reconstruction projects.

Going forward, the MinION should continue to be tested in a wide variety of analogue environments to definitively establish its minimum detection limits with and without PCR. Additionally, automation and integration of the entire sequencing process (i.e. DNA extraction, library preparation) needs to be explored. Use in microbial ecology studies necessitates further technology developments to reduce the MinION's error rate, as well. However, this thesis has shown that the MinION is a robust instrument for DNA detection and genome reconstruction in Mars and icy worlds analogue environments and represents a positive future for direct life detection missions.

References

- Alneberg J., Karlsson C. M., Divne A.-M., Bergin C., Homa F., Lindh M. V., Hugerth L. W., Ettema T. J., Bertilsson S., and Andersson A. F. (2018) Genomes from uncultivated prokaryotes: a comparison of metagenome-assembled and single-amplified genomes. *Microbiome*, 6: 173.
- Alonso-Sáez L., Sánchez O., Gasol J. M., Balagué V., and Pedrós-Alio C. (2008) Winter-to-summer changes in the composition and single-cell activity of near-surface Arctic prokaryotes. *Environmental Microbiology*, 10: 2444-2454.
- Anesio A. M., Lutz S., Christmas N. A., and Benning L. G. (2017) The microbiome of glaciers and ice sheets. *npj Biofilms and Microbiomes*, 3: 1-11.
- Archer S. D., de los Ríos A., Lee K. C., Niederberger T. S., Cary S. C., Coyne K. J., Douglas S., Lacap-Bugler D. C., and Pointing S. B. (2017) Endolithic microbial diversity in sandstone and granite from the McMurdo Dry Valleys, Antarctica. *Polar Biology*, 40: 997-1006.
- Balme M., Grindrod P., Sefton-Nash E., Davis J., Gupta S., and Fawdon P. (2016) Aram Dorsum, Candidate ExoMars Rover Landing Site: a Noachian Inverted Fluvial Channel System in Arabia Terra Mars. EGU General Assembly Conference Abstracts.
- Balme M. R., Gupta S., Davis J. M., Fawdon P., Grindrod P. M., Bridges J. C., Sefton-Nash E., and Williams R. M. (2020) Aram Dorsum: An Extensive Mid-Noachian Age Fluvial Depositional System in Arabia Terra, Mars. *Journal of Geophysical Research: Planets*, 125: e2019JE006244.
- Banfield D., Stern J., Davila A., Johnson S. S., Brain D., Wordsworth R., Horgan B., Williams R. M., Niles P., and Rucker M. (2021) Summary of the Mars Science Goals, Objectives, Investigations, and Priorities. *Bulletin of the American Astronomical Society*, 53: 142.
- Baqué M., Scalzi G., Rabbow E., Rettberg P., and Billi D. (2013) Biofilm and planktonic lifestyles differently support the resistance of the desert cyanobacterium *Chroococcidiopsis* under space and Martian simulations. *Origins of Life and Evolution of Biospheres*, 43: 377-389.
- Baqué M., Verseux C., Böttger U., Rabbow E., de Vera J.-P. P., and Billi D. (2016) Preservation of biomarkers from cyanobacteria mixed with Marslike regolith under simulated Martian atmosphere and UV flux. *Origins of Life and Evolution of Biospheres*, 46: 289-310.
- Barber D. J., and Scott E. R. (2002) Origin of supposedly biogenic magnetite in the Martian meteorite Allan Hills 84001. *Proceedings of the National Academy of Sciences*, 99: 6556-6561.
- Bauermeister A., Leon F., Rettberg P., Reitz G., Sand W., and Flemming H.-C. (2010) Mars-relevant microorganisms in simulated subsurface environments under hydration/dehydration conditions. *Origins of Life and Evolution of Biospheres*, 40: 552.
- Benner S. A. (2017) Detecting Darwinism from molecules in the Enceladus plumes, Jupiter's moons, and other planetary water lagoons. *Astrobiology*, 17: 840-851.
- Benner S. A., Devine K. G., Matveeva L. N., and Powell D. H. (2000) The missing organic molecules on Mars. *Proceedings of the National Academy of Sciences*, 97: 2425-2430.

- Berg B., Ronholm J., Applin D., Mann P., Izawa M., Cloutis E., and Whyte L. (2014) Spectral features of biogenic calcium carbonates and implications for astrobiology. *International Journal of Astrobiology*, 13: 353-365.
- Berger T., Hajek M., Bilski P., Körner C., Vanhavere F., and Reitz G. (2012) Cosmic radiation exposure of biological test systems during the EXPOSE-E mission. *Astrobiology*, 12: 387-392.
- Berry B. J., Jenkins D. G., and Schuerger A. C. (2010) Effects of simulated Mars conditions on the survival and growth of *Escherichia coli* and *Serratia liquefaciens*. *Applied and Environmental Microbiology*, 76: 2377-2386.
- Bertrand D., Shaw J., Kalathiyappan M., Ng A. H. Q., Kumar M. S., Li C., Dvornicic M., Soldo J. P., Koh J. Y., and Tong C. (2019) Hybrid metagenomic assembly enables high-resolution analysis of resistance determinants and mobile elements in human microbiomes. *Nature biotechnology*, 37: 937-944.
- Biemann K. (1979) The implications and limitations of the findings of the Viking organic analysis experiment. *Journal of Molecular Evolution*, 14: 65-70.
- Biemann K., Oro J., Toulmin III P., Orgel L., Nier A., Anderson D., Simmonds P., Flory D., Diaz A., and Rushneck D. (1977) The search for organic substances and inorganic volatile compounds in the surface of Mars. *Journal of Geophysical Research*, 82: 4641-4658.
- Billi D., Friedmann E. I., Hofer K. G., Caiola M. G., and Ocampo-Friedmann R. (2000) Ionizing-radiation resistance in the desiccation-tolerant cyanobacterium *Chroococcidiopsis*. *Applied and environmental microbiology*, 66: 1489-1492.
- Blachowicz A., Chiang A. J., Elsaesser A., Kalkum M., Ehrenfreund P., Stajich J. E., Torok T., Wang C. C., and Venkateswaran K. (2019) Proteomic and metabolomic characteristics of extremophilic fungi under simulated Mars conditions. *Frontiers in microbiology*, 10: 1013.
- Boquet E., Boronat A., and Ramos-Cormenzana A. (1973) Production of calcite (calcium carbonate) crystals by soil bacteria is a general phenomenon. *Nature*, 246: 527.
- Bower D. M., Hummer D. R., Steele A., and Kyono A. (2015) The co-evolution of Fe-oxides, Ti-oxides, and other microbially induced mineral precipitates in sandy sediments: Understanding the role of cyanobacteria in weathering and early diagenesis. *Journal of Sedimentary Research*, 85: 1213-1227.
- Bowers R. M., Kyrpides N. C., Stepanauskas R., Harmon-Smith M., Doud D., Reddy T., Schulz F., Jarett J., Rivers A. R., and Eloie-Fadrosch E. A. (2017) Minimum information about a single amplified genome (MISAG) and a metagenome-assembled genome (MIMAG) of bacteria and archaea. *Nature biotechnology*, 35: 725-731.
- Brandt A., de Vera J.-P., Onofri S., and Ott S. (2015) Viability of the lichen *Xanthoria elegans* and its symbionts after 18 months of space exposure and simulated Mars conditions on the ISS. *International Journal of Astrobiology*, 14: 411-425.
- Brown C. L., Keenum I. M., Dai D., Zhang L., Vikesland P. J., and Pruden A. (2021) Critical evaluation of short, long, and hybrid assembly for contextual analysis of antibiotic resistance genes in complex environmental metagenomes. *Scientific reports*, 11: 1-12.
- Büdel B., Bendix J., Bicker F. R., and Allan Green T. (2008) DEWFALL AS A WATER SOURCE FREQUENTLY ACTIVATES THE ENDOLITHIC CYANOBACTERIAL COMMUNITIES IN THE GRANITES OF TAYLOR VALLEY, ANTARCTICA 1. *Journal of Phycology*, 44: 1415-1424.

- Bulat S. A., Alekhina I. A., Marie D., Martins J., and Petit J. R. (2011) Searching for life in extreme environments relevant to Jovian's Europa: Lessons from subglacial ice studies at Lake Vostok (East Antarctica). *Advances in Space Research*, 48: 697-701.
- Burton A. S., Stahl S. E., John K. K., Jain M., Juul S., Turner D. J., Harrington E. D., Stoddart D., Paten B., and Akeson M. (2020) Off Earth identification of bacterial populations using 16S rDNA nanopore sequencing. *Genes*, 11: 76.
- Bywaters K., Schmidt H., Vercoutere W., Deamer D., Hawkins A., Quinn R., Burton A., and Mckay C. (2017) Development of Solid-State Nanopore Technology for Life Detection.
- Carr C. E., Bryan N. C., Saboda K. N., Bhattaru S. A., Ruvkun G., and Zuber M. T. (2020) Nanopore sequencing at Mars, Europa, and microgravity conditions. *npj Microgravity*, 6: 1-6.
- Carr C. E., Mojarro A., Hachey J., Saboda K., Tani J., Bhattaru S. A., Smith A., Pontefract A., Zuber M. T., and Doebler R. (2017) Towards in situ sequencing for life detection. Aerospace Conference, 2017 IEEE. IEEE.
- Carrizo D., Sánchez-García L., Rodríguez N., and Gómez F. (2019) Lipid Biomarker and carbon stable isotope survey on the dallol hydrothermal system in Ethiopia. *Astrobiology*, 19: 1474-1489.
- Case R. J., Boucher Y., Dahllöf I., Holmström C., Doolittle W. F., and Kjelleberg S. (2007) Use of 16S rRNA and rpoB genes as molecular markers for microbial ecology studies. *Applied and environmental microbiology*, 73: 278-288.
- Castanier S., Le Métayer-Levrel G., and Perthuisot J.-P. (1999) Ca-carbonates precipitation and limestone genesis—the microbiogeologist point of view. *Sedimentary geology*, 126: 9-23.
- Castro-Wallace S. L., Chiu C. Y., John K. K., Stahl S. E., Rubins K. H., McIntyre A. B., Dworkin J. P., Lupisella M. L., Smith D. J., and Botkin D. J. (2017) Nanopore DNA sequencing and genome assembly on the International Space Station. *Scientific reports*, 7: 18022.
- Cesur R. M., Ansari I. M., Chen F., Clark B. C., and Schneegurt M. A. (2022) Bacterial Growth in Brines Formed by the Deliquescence of Salts Relevant to Cold Arid Worlds. *Astrobiology*, 22: 104-115.
- Chan M. A., Hinman N. W., Potter-McIntyre S. L., Schubert K. E., Gillams R. J., Awramik S. M., Boston P. J., Bower D. M., Des Marais D. J., and Farmer J. D. (2019) Deciphering biosignatures in planetary contexts. *Astrobiology*, 19: 1075-1102.
- Clark B. C., and Kounaves S. P. (2016) Evidence for the distribution of perchlorates on Mars. *International Journal of Astrobiology*, 15: 311-318.
- Clarke J. D., and Stoker C. R. (2011) Concretions in exhumed and inverted channels near Hanksville Utah: implications for Mars. *International Journal of Astrobiology*, 10: 161-175.
- Cloutis E., Casson N., Applin D., Poitras J., Moreras Marti A., Morison M., Maggiori C., Cousins C., Whyte L., and Kruzelecky R. (2017) A Hydrologic-and Biosignature-Driven Field Campaign at an Inverted Fluvial Channel Site: Hanksville, UT, USA. Lunar and Planetary Science Conference.
- Cloutis E. A., Craig M. A., Mustard J. F., Kruzelecky R. V., Jamroz W. R., Scott A., Bish D. L., Poulet F., Bibring J. P., and King P. L. (2007) Stability of hydrated minerals on Mars. *Geophysical Research Letters*, 34.

- Cockell C. S., Rettberg P., Rabbow E., and Olsson-Francis K. (2011) Exposure of phototrophs to 548 days in low Earth orbit: microbial selection pressures in outer space and on early earth. *The ISME journal*, 5: 1671-1682.
- Cockell C. S., Schuenger A. C., Billi D., Friedmann E. I., and Panitz C. (2005) Effects of a simulated martian UV flux on the cyanobacterium, *Chroococcidiopsis* sp. 029. *Astrobiology*, 5: 127-140.
- Coleine C., Biagioli F., de Vera J. P., Onofri S., and Selbmann L. (2021a) Endolithic microbial composition in Helliwell Hills, a newly investigated Mars-like area in Antarctica. *Environmental Microbiology*, 23: 4002-4016.
- Coleine C., Stajich J. E., de Los Ríos A., and Selbmann L. (2021b) Beyond the extremes: Rocks as ultimate refuge for fungi in drylands. *Mycologia*, 113: 108-133.
- Coleine C., Stajich J. E., Pombubpa N., Zucconi L., Onofri S., Canini F., and Selbmann L. (2019) Altitude and fungal diversity influence the structure of Antarctic cryptoendolithic Bacteria communities. *Environmental microbiology reports*, 11: 718-726.
- Coleine C., Stajich J. E., Zucconi L., Onofri S., Pombubpa N., Egidi E., Franks A., Buzzini P., and Selbmann L. (2018) Antarctic cryptoendolithic fungal communities are highly adapted and dominated by Lecanoromycetes and Dothideomycetes. *Frontiers in microbiology*, 9: 1392.
- Collins R. E., Rocap G., and Deming J. W. (2010) Persistence of bacterial and archaeal communities in sea ice through an Arctic winter. *Environmental microbiology*, 12: 1828-1841.
- Cook J., Edwards A., Takeuchi N., and Irvine-Fynn T. (2016) Cryoconite: the dark biological secret of the cryosphere. *Progress in Physical Geography*, 40: 66-111.
- Cook J., Hodson A., Telling J., Anesio A., Irvine-Fynn T., and Bellas C. (2010) The mass–area relationship within cryoconite holes and its implications for primary production. *Annals of Glaciology*, 51: 106-110.
- Cortese M., Fuchs F. M., Commichau F. M., Eichenberger P., Schuenger A. C., Nicholson W. L., Setlow P., and Moeller R. (2019) *Bacillus subtilis* spore resistance to simulated Mars surface conditions. *Frontiers in microbiology*, 10: 333.
- Council N. R. (2019) The limits of organic life in planetary systems. The national academy of press.
- Craig M., Cloutis E., and Mueller T. (2001) ME and mini-ME: Two Mars environmental simulation chambers for reflectance spectroscopy. Lunar and Planetary Science Conference.
- Cranwell P. (1978) Extractable and bound lipid components in a freshwater sediment. *Geochimica et Cosmochimica Acta*, 42: 1523-1532.
- Crits-Christoph A., Gelsinger D. R., Ma B., Wierzchos J., Ravel J., Davila A., Casero M. C., and DiRuggiero J. (2016) Functional interactions of archaea, bacteria and viruses in a hypersaline endolithic community. *Environmental Microbiology*, 18: 2064-2077.
- Crosby C. H., and Bailey J. V. (2018) Experimental precipitation of apatite pseudofossils resembling fossil embryos. *Geobiology*, 16: 80-87.
- Cuscó A., Pérez D., Viñes J., Fàbregas N., and Francino O. (2021) Long-read metagenomics retrieves complete single-contig bacterial genomes from canine feces. *BMC genomics*, 22: 1-15.

- Davila A. F., Duport L. G., Melchiorri R., Jaenchen J., Valea S., de Los Rios A., Fairen A. G., Moehlmann D., McKay C. P., and Ascaso C. (2010) Hygroscopic salts and the potential for life on Mars. *Astrobiology*, 10: 617-628.
- Davis J., Balme M., Grindrod P., Williams R., and Gupta S. (2016) Extensive Noachian fluvial systems in Arabia Terra: Implications for early Martian climate. *Geology*, 44: 847-850.
- De La Torre Noetzel R., Miller A. Z., de la Rosa J. M., Pacelli C., Onofri S., Garcia Sancho L., Cubero B., Lorek A., Wolter D., and De Vera J. P. (2018) Cellular responses of the lichen *Circinaria gyrosa* in Mars-like conditions. *Frontiers in Microbiology*, 9: 308.
- de la Vega U. P., Rettberg P., and Reitz G. (2007) Simulation of the environmental climate conditions on martian surface and its effect on *Deinococcus radiodurans*. *Advances in Space Research*, 40: 1672-1677.
- De Los Ríos A., Wierzchos J., and Ascaso C. (2014) The lithic microbial ecosystems of Antarctica's McMurdo Dry Valleys. *Antarctic Science*, 26: 459-477.
- De Maio N., Shaw L. P., Hubbard A., George S., Sanderson N. D., Swann J., Wick R., AbuOun M., Stubberfield E., and Hoosdally S. J. (2019) Comparison of long-read sequencing technologies in the hybrid assembly of complex bacterial genomes. *Microbial genomics*, 5.
- De Vera J.-P., Dulai S., Kereszturi A., Koncz L., Lorek A., Mohlmann D., Marschall M., and Pocs T. (2014a) Results on the survival of cryptobiotic cyanobacteria samples after exposure to Mars-like environmental conditions. *International Journal of Astrobiology*, 13: 35-44.
- De Vera J.-P., Horneck G., Rettberg P., and Ott S. (2004) The potential of the lichen symbiosis to cope with the extreme conditions of outer space II: germination capacity of lichen ascospores in response to simulated space conditions. *Advances in Space Research*, 33: 1236-1243.
- de Vera J.-P., Schulze-Makuch D., Khan A., Lorek A., Koncz A., Möhlmann D., and Spohn T. (2014b) Adaptation of an Antarctic lichen to Martian niche conditions can occur within 34 days. *Planetary and Space Science*, 98: 182-190.
- Deamer D., and Damer B. (2017) Can life begin on Enceladus? A perspective from hydrothermal chemistry. *Astrobiology*, 17: 834-839.
- Demets R., Schulte W., and Baglioni P. (2005) The past, present and future of Biopan. *Advances in Space Research*, 36: 311-316.
- Diaz B., and Schulze-Makuch D. (2006) Microbial survival rates of *Escherichia coli* and *Deinococcus radiodurans* under low temperature, low pressure, and UV-irradiation conditions, and their relevance to possible martian life. *Astrobiology*, 6: 332-347.
- Didyk B., Simoneit B., Brassell S. t., and Eglinton G. (1978) Organic geochemical indicators of palaeoenvironmental conditions of sedimentation. *Nature*, 272: 216-222.
- Direito S. O., Ehrenfreund P., Marees A., Staats M., Foing B., and Röling W. F. (2011) A wide variety of putative extremophiles and large beta-diversity at the Mars Desert Research Station (Utah). *International Journal of Astrobiology*, 10: 191-207.
- Dolezel J., Bartos J., Voglmayr H., and Greilhuber J. (2003) Nuclear DNA content and genome size of trout and human. *Cytometry. Part A: the journal of the International Society for Analytical Cytology*, 51: 127.
- Doran P. T., Fritsen C. H., McKay C. P., Priscu J. C., and Adams E. E. (2003) Formation and character of an ancient 19-m ice cover and underlying trapped brine in an "ice-sealed" east Antarctic lake. *Proceedings of the National Academy of Sciences*, 100: 26-31.

- Dorn R. I., and Oberlander T. M. (1981) Microbial origin of desert varnish. *Science*, 213: 1245-1247.
- Douki T. (2013) The variety of UV-induced pyrimidine dimeric photoproducts in DNA as shown by chromatographic quantification methods. *Photochemical & Photobiological Sciences*, 12: 1286-1302.
- Dwyer D. J., Camacho D. M., Kohanski M. A., Callura J. M., and Collins J. J. (2012) Antibiotic-induced bacterial cell death exhibits physiological and biochemical hallmarks of apoptosis. *Molecular cell*, 46: 561-572.
- Edwards A., Anesio A. M., Rassner S. M., Sattler B., Hubbard B., Perkins W. T., Young M., and Griffith G. W. (2011) Possible interactions between bacterial diversity, microbial activity and supraglacial hydrology of cryoconite holes in Svalbard. *The ISME journal*, 5: 150-160.
- Edwards A., Cameron K. A., Cook J. M., Debonnaire A. R., Furness E., Hay M. C., and Rassner S. M. (2020) Microbial genomics amidst the Arctic crisis. *Microbial Genomics*: mgen000375.
- Edwards A., Debonnaire A. R., Nicholls S. M., Rassner S. M., Sattler B., Cook J. M., Davy T., Soares A., Mur L. A., and Hodson A. J. (2019) In-field metagenome and 16S rRNA gene amplicon nanopore sequencing robustly characterize glacier microbiota. *BioRxiv*: 073965.
- Edwards A., Debonnaire A. R., Sattler B., Mur L. A., and Hodson A. J. (2016) Extreme metagenomics using nanopore DNA sequencing: a field report from Svalbard, 78 N. *bioRxiv*: 073965.
- Edwards A., Douglas B., Anesio A. M., Rassner S. M., Irvine-Fynn T. D., Sattler B., and Griffith G. W. (2013a) A distinctive fungal community inhabiting cryoconite holes on glaciers in Svalbard. *fungus ecology*, 6: 168-176.
- Edwards A., Mur L. A., Girdwood S. E., Anesio A. M., Stibal M., Rassner S. M., Hell K., Pachebat J. A., Post B., and Bussell J. S. (2014) Coupled cryoconite ecosystem structure–function relationships are revealed by comparing bacterial communities in alpine and Arctic glaciers. *FEMS microbiology ecology*, 89: 222-237.
- Edwards A., Pachebat J. A., Swain M., Hegarty M., Hodson A. J., Irvine-Fynn T. D., Rassner S. M., and Sattler B. (2013b) A metagenomic snapshot of taxonomic and functional diversity in an alpine glacier cryoconite ecosystem. *Environmental Research Letters*, 8: 035003.
- Edwards A., Rassner S. M., Anesio A. M., Worgan H. J., Irvine-Fynn T. D., Wyn Williams H., Sattler B., and Wyn Griffith G. (2013c) Contrasts between the cryoconite and ice-marginal bacterial communities of Svalbard glaciers. *Polar Research*, 32: 19468.
- Edwards H. G., Vandenabeele P., Jorge-Villar S. E., Carter E. A., Perez F. R., and Hargreaves M. D. (2007) The Rio Tinto Mars analogue site: an extremophilic Raman spectroscopic study. *Spectrochimica Acta Part A: Molecular and Biomolecular Spectroscopy*, 68: 1133-1137.
- Edwards H. G., Villar S. E. J., Parnell J., Cockell C. S., and Lee P. (2005) Raman spectroscopic analysis of cyanobacterial gypsum halotrophs and relevance for sulfate deposits on Mars. *Analyst*, 130: 917-923.
- Ehlmann B. L., Mustard J. F., Fassett C. I., Schon S. C., Head III J. W., Des Marais D. J., Grant J. A., and Murchie S. L. (2008) Clay minerals in delta deposits and organic preservation potential on Mars. *Nature Geoscience*, 1: 355-358.

- Eigenbrode J. L., Summons R. E., Steele A., Freissinet C., Millan M., Navarro-González R., Sutter B., McAdam A. C., Franz H. B., and Glavin D. P. (2018) Organic matter preserved in 3-billion-year-old mudstones at Gale crater, Mars. *Science*, 360: 1096-1101.
- Ellery A., Kolb C., Lammer H., Parnell J., Edwards H., Richter L., Patel M., Romstedt J., Dickensheets D., and Steele A. (2002) Astrobiological instrumentation for Mars—the only way is down. *International Journal of Astrobiology*, 1: 365-380.
- Engel C. G., and Sharp R. P. (1958) Chemical data on desert varnish. *Geological Society of America Bulletin*, 69: 487-518.
- Erental A., Kalderon Z., Saada A., Smith Y., and Engelberg-Kulka H. (2014) Apoptosis-like death, an extreme SOS response in *Escherichia coli*. *MBio*, 5: e01426-14.
- Fairén A. G., Davila A. F., Lim D., Bramall N., Bonaccorsi R., Zavaleta J., Uceda E. R., Stoker C., Wierzchos J., and Dohm J. M. (2010) Astrobiology through the ages of Mars: the study of terrestrial analogues to understand the habitability of Mars. *Astrobiology*, 10: 821-843.
- Fairén A. G., Parro V., Schulze-Makuch D., and Whyte L. (2017) Searching for life on Mars before it is too late. *Astrobiology*, 17: 962-970.
- Fajardo-Cavazos P., Schuerger A. C., and Nicholson W. L. (2010) Exposure of DNA and *Bacillus subtilis* spores to simulated martian environments: use of quantitative PCR (qPCR) to measure inactivation rates of DNA to function as a template molecule. *Astrobiology*, 10: 403-411.
- Faria N. R., Sabino E. C., Nunes M. R., Alcantara L. C. J., Loman N. J., and Pybus O. G. (2016) Mobile real-time surveillance of Zika virus in Brazil. *Genome medicine*, 8: 1-4.
- Fassett C. I., and Head III J. W. (2008) Valley network-fed, open-basin lakes on Mars: Distribution and implications for Noachian surface and subsurface hydrology. *Icarus*, 198: 37-56.
- Fernández-Gómez B., Díez B., Polz M. F., Arroyo J. I., Alfaro F. D., Marchandon G., Sanhueza C., Farías L., Trefault N., and Marquet P. A. (2019) Bacterial community structure in a sympagic habitat expanding with global warming: brackish ice brine at 85–90 N. *The ISME journal*, 13: 316-333.
- Fernández-Martínez M. Á., García-Villadangos M., Paz M. M., Gangloff V., Carrizo D., Blanco Y., González Herrero S., Sánchez-García L., Prieto-Ballesteros O., and Altshuler I. (2021) Geomicrobiological heterogeneity of lithic habitats in the extreme environment of Antarctic Nunataks: A potential early Mars analog. *Frontiers in Microbiology*, 12: 1568.
- Fisher D. A., Lacelle D., Pollard W., Davila A., and McKay C. P. (2016) Ground surface temperature and humidity, ground temperature cycles and the ice table depths in University Valley, McMurdo Dry Valleys of Antarctica. *Journal of Geophysical Research: Earth Surface*, 121: 2069-2084.
- Friedberg E. C., Aguilera A., Gellert M., Hanawalt P. C., Hays J. B., Lehmann A. R., Lindahl T., Lowndes N., Sarasin A., and Wood R. D. (2006) DNA repair: from molecular mechanism to human disease. *DNA repair*, 5: 986-996.
- Friedmann E. I. (1982) Endolithic microorganisms in the Antarctic cold desert. *Science*, 215: 1045-1053.
- Fulton J. D. (1958) Survival of terrestrial microorganisms under simulated Martian conditions. *Physics and Medicine of the Atmosphere and Space*: 606-613.
- Gan H. M., Tan M. H., Austin C. M., Sherman C., Wong Y. T., Strugnell J., Gervis M., McPherson L., and Miller A. (2019) Best foot forward: Nanopore long reads, hybrid

- meta-assembly and haplotig purging optimises the first genome assembly for the Southern Hemisphere blacklip abalone (*Haliotis rubra*). *Frontiers in Genetics*, 10: 889.
- Garneau M.-È., Michel C., Meisterhans G., Fortin N., King T. L., Greer C. W., and Lee K. (2016) Hydrocarbon biodegradation by Arctic sea-ice and sub-ice microbial communities during microcosm experiments, Northwest Passage (Nunavut, Canada). *FEMS Microbiology Ecology*, 92: fiw130.
- Garvin J. B. (2001) The emerging face of Mars: A synthesis from Viking to Mars Global Surveyor. *Astrobiology*, 1: 513-521.
- Glass B., Davila A., Parro V., Quinn R., Willis P., Brinckherhoff W., Zacny K., DiRuggiero J., Williams M., and Fong T. (2018) Atacama Rover Astrobiology Drilling Studies Project: second year. In: *Earth and Space 2018: Engineering for Extreme Environments*, American Society of Civil Engineers Reston, VA, pp 337-347.
- Glavin D. P., Burton A. S., Elsila J. E., Aponte J. C., and Dworkin J. P. (2019) The search for chiral asymmetry as a potential biosignature in our solar system. *Chemical reviews*, 120: 4660-4689.
- Glavin D. P., Elsila J. E., Burton A. S., Callahan M. P., Dworkin J. P., Hilts R. W., and Herd C. D. (2012) Unusual nonterrestrial l-proteinogenic amino acid excesses in the Tagish Lake meteorite. *Meteoritics & Planetary Science*, 47: 1347-1364.
- Glavin D. P., Freissinet C., Miller K. E., Eigenbrode J. L., Brunner A. E., Buch A., Sutter B., Archer P. D., Atreya S. K., and Brinckerhoff W. B. (2013) Evidence for perchlorates and the origin of chlorinated hydrocarbons detected by SAM at the Rocknest aeolian deposit in Gale Crater. *Journal of Geophysical Research: Planets*, 118: 1955-1973.
- Godfrey A. E. (1997) Wind erosion of Mancos Shale badland ridges by sudden drops in pressure. *Earth Surface Processes and Landforms: The Journal of the British Geomorphological Group*, 22: 345-352.
- Godfrey A. E., Everitt B. L., and Duque J. F. M. (2008) Episodic sediment delivery and landscape connectivity in the Mancos Shale badlands and Fremont River system, Utah, USA. *Geomorphology*, 102: 242-251.
- Goldstein S., Beka L., Graf J., and Klassen J. L. (2019) Evaluation of strategies for the assembly of diverse bacterial genomes using MinION long-read sequencing. *BMC genomics*, 20: 23.
- Gómez F., Mateo-Martí E., Prieto-Ballesteros O., Martín-Gago J., and Amils R. (2010) Protection of chemolithoautotrophic bacteria exposed to simulated Mars environmental conditions. *Icarus*, 209: 482-487.
- Goordial J., Altshuler I., Hindson K., Chan-Yam K., Marcolefes E., and Whyte L. (2017) In situ field sequencing and life detection in remote (79° 26' N) Canadian High Arctic permafrost ice wedge microbial communities. *Frontiers in microbiology*, 8: 2594.
- Goordial J., Davila A., Lacelle D., Pollard W., Marinova M. M., Greer C. W., DiRuggiero J., McKay C. P., and Whyte L. G. (2016a) Nearing the cold-arid limits of microbial life in permafrost of an upper dry valley, Antarctica. *The ISME journal*, 10: 1613.
- Goordial J., Raymond-Bouchard I., Zolotarov Y., de Bethencourt L., Ronholm J., Shapiro N., Woyke T., Stromvik M., Greer C. W., and Bakermans C. (2016b) Cold adaptive traits revealed by comparative genomic analysis of the eurypsychrophile *Rhodococcus* sp. JG3 isolated from high elevation McMurdo Dry Valley permafrost, Antarctica. *FEMS microbiology ecology*, 92.

- Guinness E. A., Arvidson R. E., Clark I. H., and Shepard M. K. (1997) Optical scattering properties of terrestrial varnished basalts compared with rocks and soils at the Viking Lander sites. *Journal of Geophysical Research: Planets*, 102: 28687-28703.
- Hagen C., Hawrylewicz E., and Ehrlich R. (1967) Survival of microorganisms in a simulated martian environment: II. Moisture and oxygen requirements for germination of *Bacillus cereus* and *Bacillus subtilis* var. *niger* spores. *Applied microbiology*, 15: 285-291.
- Hansen A. A., Jensen L. L., Kristoffersen T., Mikkelsen K., Merrison J., Finster K. W., and Lomstein B. A. (2009) Effects of long-term simulated martian conditions on a freeze-dried and homogenized bacterial permafrost community. *Astrobiology*, 9: 229-240.
- Hansen A. A., Merrison J., Nørnberg P., Lomstein B. A., and Finster K. (2005) Activity and stability of a complex bacterial soil community under simulated Martian conditions. *International Journal of Astrobiology*, 4: 135-144.
- Haskin L. A., Wang A., Jolliff B. L., McSween H. Y., Clark B. C., Des Marais D. J., McLennan S. M., Tosca N. J., Hurowitz J. A., and Farmer J. D. (2005) Water alteration of rocks and soils on Mars at the Spirit rover site in Gusev crater. *Nature*, 436: 66-69.
- Hatam I., Charchuk R., Lange B., Beckers J., Haas C., and Lanoil B. (2014) Distinct bacterial assemblages reside at different depths in Arctic multiyear sea ice. *FEMS microbiology ecology*, 90: 115-125.
- Hawrylewicz E., Gowdy B., and Ehrlich R. (1962) Micro-organisms under a simulated Martian environment. *Nature*, 193: 497-497.
- Hawrylewicz E., Hagen C., Tolkacz V., Anderson B., and Ewing M. (1968) Probability of growth (pG) of viable microorganisms in Martian environments. *Life Sci. Space Res*, 6: 146-156.
- Hays L. E., Graham H. V., Des Marais D. J., Hausrath E. M., Horgan B., McCollom T. M., Parenteau M. N., Potter-McIntyre S. L., Williams A. J., and Lynch K. L. (2017) Biosignature preservation and detection in Mars analog environments. *Astrobiology*, 17: 363-400.
- Hecht M., Kounaves S., Quinn R., West S., Young S., Ming D., Catling D., Clark B., Boynton W., and Hoffman J. (2009) Detection of perchlorate and the soluble chemistry of martian soil at the Phoenix lander site. *Science*, 325: 64-67.
- Heldmann J., Pollard W., McKay C., Marinova M., Davila A., Williams K., Lacelle D., and Andersen D. (2013) The high elevation Dry Valleys in Antarctica as analog sites for subsurface ice on Mars. *Planetary and Space Science*, 85: 53-58.
- Hendrix A. R., Hurford T. A., Barge L. M., Bland M. T., Bowman J. S., Brinckerhoff W., Buratti B. J., Cable M. L., Castillo-Rogez J., and Collins G. C. (2019) The NASA roadmap to ocean worlds. *Astrobiology*, 19: 1-27.
- Higashibata A., Szewczyk N. J., Conley C. A., Imamizo-Sato M., Higashitani A., and Ishioka N. (2006) Decreased expression of myogenic transcription factors and myosin heavy chains in *Caenorhabditis elegans* muscles developed during spaceflight. *Journal of Experimental Biology*, 209: 3209-3218.
- Hodson A., Cameron K., Bøggild C., Irvine-Fynn T., Langford H., Pearce D., and Banwart S. (2010) The structure, biological activity and biogeochemistry of cryoconite aggregates upon an Arctic valley glacier: Longyearbreen, Svalbard. *Journal of Glaciology*, 56: 349-362.

- Horne, W. H., Volpe, R. P., Korza, G., DePratti, S., Conze, I. H., Shuryak, I., ... & Daly, M. J. (2022) Effects of Desiccation and Freezing on Microbial Ionizing Radiation Survivability: Considerations for Mars Sample Return. *Astrobiology*, 22(11): 1337-1350.
- Horneck G. (2000) The microbial world and the case for Mars. *Planetary and Space Science*, 48: 1053-1063.
- Horneck G., Klaus D. M., and Mancinelli R. L. (2010) Space microbiology. *Microbiology and Molecular Biology Reviews*, 74: 121-156.
- Horowitz N., Hobby G., and Hubbard J. S. (1977) Viking on Mars: the carbon assimilation experiments. *Journal of Geophysical Research*, 82: 4659-4662.
- Hotchin J., Lorenz P., and Hemenway C. (1965) Survival of micro-organisms in space. *Nature*, 206: 442-445.
- House C. H., Wong G. M., Webster C. R., Flesch G. J., Franz H. B., Stern J. C., Pavlov A., Atreya S. K., Eigenbrode J. L., and Gilbert A. (2022) Depleted carbon isotope compositions observed at Gale crater, Mars. *Proceedings of the National Academy of Sciences*, 119: e2115651119.
- Iess L., Stevenson D., Parisi M., Hemingway D., Jacobson R., Lunine J., Nimmo F., Armstrong J., Asmar S., and Ducci M. (2014) The gravity field and interior structure of Enceladus. *Science*, 344: 78-80.
- Ilardo M., Meringer M., Freeland S., Rasulev B., and Cleaves II H. J. (2015) Extraordinarily adaptive properties of the genetically encoded amino acids. *Scientific reports*, 5: 1-6.
- Imshenetskiĭ A., Murzakov B., Evdokimova M., and Dorofeeva I. (1984) Survival of bacteria in the artificial Mars unit. *Mikrobiologiya*, 53: 731-737.
- Irwin III R. P., Maxwell T. A., Howard A. D., Craddock R. A., and Leverington D. W. (2002) A large paleolake basin at the head of Ma'adim Vallis, Mars. *Science*, 296: 2209-2212.
- Jain M., Koren S., Miga K. H., Quick J., Rand A. C., Sasani T. A., Tyson J. R., Beggs A. D., Dilthey A. T., and Fiddes I. T. (2018) Nanopore sequencing and assembly of a human genome with ultra-long reads. *Nature biotechnology*, 36: 338-345.
- Jain M., Tyson J. R., Loose M., Ip C. L., Eccles D. A., O'Grady J., Malla S., Leggett R. M., Wallerman O., and Jansen H. J. (2017) MinION Analysis and Reference Consortium: Phase 2 data release and analysis of R9. 0 chemistry. *F1000Research*, 6.
- Jänchen J., Feyh N., Szewzyk U., and de Vera J.-P. P. (2016) Provision of water by halite deliquescence for Nostoc commune biofilms under Mars relevant surface conditions. *International Journal of Astrobiology*, 15: 107-118.
- Jehlička J., Edwards H., and Oren A. (2013) Bacterioruberin and salinixanthin carotenoids of extremely halophilic Archaea and Bacteria: a Raman spectroscopic study. *Spectrochimica Acta Part A: Molecular and Biomolecular Spectroscopy*, 106: 99-103.
- Jensen L. L., Merrison J., Hansen A. A., Mikkelsen K. A., Kristoffersen T., Nørnberg P., Lomstein B. A., and Finster K. (2008) A facility for long-term Mars simulation experiments: the Mars Environmental Simulation Chamber (MESCH). *Astrobiology*, 8: 537-548.
- Ji B., Yang K., Zhu L., Jiang Y., Wang H., Zhou J., and Zhang H. (2015) Aerobic denitrification: a review of important advances of the last 30 years. *Biotechnology and Bioprocess Engineering*, 20: 643-651.
- Johnson A. P., Pratt L. M., Vishnivetskaya T., Pfiffner S., Bryan R. A., Dadachova E., Whyte L., Radtke K., Chan E., and Tronick S. (2011) Extended survival of several organisms and amino acids under simulated martian surface conditions. *Icarus*, 211: 1162-1178.

- Johnson S. S., Anslyn E. V., Graham H. V., Mahaffy P. R., and Ellington A. D. (2018) Fingerprinting non-terran biosignatures. *Astrobiology*, 18: 915-922.
- Johnson S. S., Millan M., Graham H., Benison K. C., Williams A. J., McAdam A., Knudson C. A., Andrejkovičová S., and Achilles C. (2020) Lipid biomarkers in ephemeral acid salt lake mudflat/sandflat sediments: implications for Mars. *Astrobiology*, 20: 167-178.
- Johnson S. S., Zaikova E., Goerlitz D. S., Bai Y., and Tighe S. W. (2017) Real-Time DNA Sequencing in the Antarctic Dry Valleys Using the Oxford Nanopore Sequencer. *Journal of Biomolecular Techniques: JBT*, 28: 2.
- Jönsson K. I., Rabbow E., Schill R. O., Harms-Ringdahl M., and Rettberg P. (2008) Tardigrades survive exposure to space in low Earth orbit. *Current biology*, 18: R729-R731.
- Jönsson K. I., and Wojcik A. (2017) Tolerance to X-rays and heavy ions (Fe, He) in the tardigrade *Richtersius coronifer* and the bdelloid rotifer *Mniobia russeola*. *Astrobiology*, 17: 163-167.
- Kaczmarek Ł., Jakubowska N., Celewicz-Gołdyn S., and Zawierucha K. (2016) The microorganisms of cryoconite holes (algae, Archaea, bacteria, cyanobacteria, fungi, and Protista): a review. *Polar Record*, 52: 176-203.
- Kawaguchi Y., Hashimoto H., Yokobori S.-i., Yamagishi A., Shibuya M., Kinoshita I., Hayashi R., Yatabe J., Narumi I., and Fujiwara D. (2018) Survival and DNA damage of cell-aggregate of *Deinococcus* spp. exposed to space for two-years in Tanpopo mission. *42nd COSPAR Scientific Assembly*, 42: F3. 1-5-18.
- Kawaguchi Y., Shibuya M., Kinoshita I., Yatabe J., Narumi I., Shibata H., Hayashi R., Fujiwara D., Murano Y., and Hashimoto H. (2020) DNA damage and survival time course of deinococcal cell pellets during 3 years of exposure to outer space. *Frontiers in microbiology*, 11: 2050.
- Kawaguchi Y., Yokobori S.-i., Hashimoto H., Yano H., Tabata M., Kawai H., and Yamagishi A. (2016) Investigation of the interplanetary transfer of microbes in the Tanpopo mission at the exposed facility of the international space station. *Astrobiology*, 16: 363-376.
- Khan N., Tuffin M., Stafford W., Cary C., Lacap D. C., Pointing S. B., and Cowan D. (2011) Hypolithic microbial communities of quartz rocks from Miers Valley, McMurdo dry valleys, Antarctica. *Polar biology*, 34: 1657-1668.
- Khawaja N., Postberg F., Hillier J., Klenner F., Kempf S., Nölle L., Reviol R., Zou Z., and Srama R. (2019) Low-mass nitrogen-, oxygen-bearing, and aromatic compounds in Enceladean ice grains. *Monthly Notices of the Royal Astronomical Society*, 489: 5231-5243.
- Khurana K., Kivelson M., Stevenson D., Schubert G., Russell C., Walker R., and Polanskey C. (1998) Induced magnetic fields as evidence for subsurface oceans in Europa and Callisto. *Nature*, 395: 777-780.
- Kirchman D. L. (2002) The ecology of Cytophaga–Flavobacteria in aquatic environments. *FEMS microbiology ecology*, 39: 91-100.
- Kish A., Kirkali G., Robinson C., Rosenblatt R., Jaruga P., Dizdaroglu M., and DiRuggiero J. (2009) Salt shield: intracellular salts provide cellular protection against ionizing radiation in the halophilic archaeon, *Halobacterium salinarum* NRC-1. *Environmental microbiology*, 11: 1066-1078.
- Klein H. P. (1977) The Viking biological investigation: general aspects. *Journal of Geophysical Research*, 82: 4677-4680.
- Klein H. P. (1978a) The Viking biological experiments on Mars. *Icarus*, 34: 666-674.

- Klein H. P. (1978b) The Viking biological investigations: review and status. *Origins of life*, 9: 157-160.
- Koike J., Hori T., Katahira Y., Koike K., Tanaka K., Kobayashi K., and Kawasaki Y. (1996) Fundamental studies concerning planetary quarantine in space. *Advances in Space Research*, 18: 339-344.
- Kottemann M., Kish A., Iloanusi C., Bjork S., and DiRuggiero J. (2005) Physiological responses of the halophilic archaeon *Halobacterium* sp. strain NRC1 to desiccation and gamma irradiation. *Extremophiles*, 9: 219-227.
- Krissansen-Totton J., Bergsman D. S., and Catling D. C. (2016) On detecting biospheres from chemical thermodynamic disequilibrium in planetary atmospheres. *Astrobiology*, 16: 39-67.
- Kvenvolden K., Lawless J., Pering K., Peterson E., Flores J., Ponnampereuma C., Kaplan I. R., and Moore C. (1970) Evidence for extraterrestrial amino-acids and hydrocarbons in the Murchison meteorite. *Nature*, 228: 923-926.
- Lacap D. C., Warren-Rhodes K. A., McKay C. P., and Pointing S. B. (2011) Cyanobacteria and chloroflexi-dominated hypolithic colonization of quartz at the hyper-arid core of the Atacama Desert, Chile. *Extremophiles*, 15: 31-38.
- Larson D. (1983) The pattern of production within individual *Umbilicaria* lichen thalli. *New Phytologist*, 94: 409-419.
- Leask E. K., and Ehlmann B. L. (2022) Evidence for deposition of chloride on Mars from small-volume surface water events into the Late Hesperian-Early Amazonian. *AGU Advances*, 3: e2021AV000534.
- Leggett R. M., and Clark M. D. (2017) A world of opportunities with nanopore sequencing. *Journal of Experimental Botany*.
- Leuko S., Bohmeier M., Hanke F., Böettger U., Rabbow E., Parpart A., Rettberg P., and de Vera J.-P. P. (2017) On the stability of deinoxanthin exposed to Mars conditions during a long-term space mission and implications for biomarker detection on other planets. *Frontiers in microbiology*, 8: 1680.
- Levin G. V., and Straat P. A. (1976) Viking labeled release biology experiment: interim results. *Science*, 194: 1322-1329.
- Levin G. V., and Straat P. A. (1977) Recent results from the Viking labeled release experiment on Mars. *Journal of Geophysical Research*, 82: 4663-4667.
- Levin G. V., and Straat P. A. (2016) The case for extant life on Mars and its possible detection by the Viking labeled release experiment. *Astrobiology*, 16: 798-810.
- Ley R. E., Harris J. K., Wilcox J., Spear J. R., Miller S. R., Bebout B. M., Maresca J. A., Bryant D. A., Sogin M. L., and Pace N. R. (2006) Unexpected diversity and complexity of the Guerrero Negro hypersaline microbial mat. *Applied and environmental microbiology*, 72: 3685-3695.
- Linck E., Crane K. W., Zuckerman B. L., Corbin B. A., Myers R. M., Williams S. R., Carioscia S. A., Garcia R., and Lal B. (2019) Evaluation of a Human Mission to Mars by 2033. JSTOR.
- Loman N. J., Quick J., and Simpson J. T. (2015) A complete bacterial genome assembled de novo using only nanopore sequencing data. *Nature methods*, 12: 733-735.
- Loman N. J., and Watson M. (2015) Successful test launch for nanopore sequencing. *Nature methods*, 12: 303-304.

- Luo G., Yang H., Algeo T. J., Hallmann C., and Xie S. (2019) Lipid biomarkers for the reconstruction of deep-time environmental conditions. *Earth-Science Reviews*, 189: 99-124.
- Maccario L., Sanguino L., Vogel T. M., and Larose C. (2015) Snow and ice ecosystems: not so extreme. *Research in microbiology*, 166: 782-795.
- Macey M. C., Fox-Powell M., Ramkissoon N. K., Stephens B., Barton T., Schwenzer S., Pearson V., Cousins C., and Olsson-Francis K. (2020) The identification of sulfide oxidation as a potential metabolism driving primary production on late Noachian Mars. *Scientific reports*, 10: 1-13.
- MacKenzie S. M., Neveu M., Davila A. F., Lunine J. I., Craft K. L., Cable M. L., Phillips-Lander C. M., Hofgartner J. D., Eigenbrode J. L., and Waite J. H. (2021) The Enceladus Orbilander Mission Concept: balancing return and resources in the search for life. *The Planetary Science Journal*, 2: 77.
- Magnuson E., Mykytczuk N. C., Pellerin A., Goordial J., Twine S. M., Wing B., Foote S. J., Fulton K., and Whyte L. G. (2020) Thiomicrobhabdus streamers and sulfur cycling in perennial hypersaline cold springs in the Canadian high Arctic. *Environmental Microbiology*.
- Malin M. C., and Edgett K. S. (2000) Evidence for recent groundwater seepage and surface runoff on Mars. *Science*, 288: 2330-2335.
- Malin M. C., and Edgett K. S. (2001) Mars global surveyor Mars orbiter camera: interplanetary cruise through primary mission. *Journal of Geophysical Research: Planets*, 106: 23429-23570.
- Mancinelli R. (2015) The affect of the space environment on the survival of Halorubrum chaoviator and Synechococcus (Nägeli): data from the Space Experiment OSMO on EXPOSE-R. *International Journal of Astrobiology*, 14: 123-128.
- Mancinelli R., White M., and Rothschild L. J. (1998) Biopan-survival I: exposure of the osmophiles Synechococcus sp.(Nageli) and Haloarcula sp. to the space environment. *Advances in Space Research*, 22: 327-334.
- Mangold N., Gupta S., Gasnault O., Dromart G., Tarnas J., Sholes S., Horgan B., Quantin-Nataf C., Brown A., and Le Mouélic S. (2021) Perseverance rover reveals an ancient delta-lake system and flood deposits at Jezero crater, Mars. *Science*, 374: 711-717.
- Manley L. J., Ma D., and Levine S. S. (2016) Monitoring error rates in Illumina sequencing. *Journal of biomolecular techniques: JBT*, 27: 125.
- Martins Z. (2011) In situ biomarkers and the Life Marker Chip. *Astronomy & Geophysics*, 52: 1.34-1.35.
- Martins Z., Sephton M., Foing B., and Ehrenfreund P. (2011) Extraction of amino acids from soils close to the Mars Desert Research Station (MDRS), Utah. *International Journal of Astrobiology*, 10: 231-238.
- Mateo-Martí E., Prieto-Ballesteros O., Sobrado J., Gómez-Elvira J., and Martín-Gago J. (2006) A chamber for studying planetary environments and its applications to astrobiology. *Measurement Science and Technology*, 17: 2274.
- Matthes U., Turner S. J., and Larson D. W. (2001) Light attenuation by limestone rock and its constraint on the depth distribution of endolithic algae and cyanobacteria. *International Journal of Plant Sciences*, 162: 263-270.

- Maurice S., Wiens R. C., Bernardi P., Caïs P., Robinson S., Nelson T., Gasnault O., Reess J.-M., Deleuze M., and Rull F. (2021) The SuperCam instrument suite on the Mars 2020 rover: Science objectives and Mast-Unit description. *Space Science Reviews*, 217: 1-108.
- Maus D., Heinz J., Schirmack J., Airo A., Kounaves S. P., Wagner D., and Schulze-Makuch D. (2020) Methanogenic archaea can produce methane in deliquescence-driven Mars analog environments. *Scientific Reports*, 10: 1-7.
- McCammon S. A., and Bowman J. P. (2000) Taxonomy of Antarctic Flavobacterium species: description of Flavobacterium gillisiae sp. nov., Flavobacterium tegetincola sp. nov., and Flavobacterium xanthum sp. nov., nom. rev. and reclassification of [Flavobacterium] salegens as Salegentibacter salegens gen. nov., comb. nov. *International journal of systematic and evolutionary microbiology*, 50: 1055-1063.
- McCauley J., Breed C., El-Baz F., Whitney M., Grolier M., and Ward A. (1979) Pitted and fluted rocks in the Western Desert of Egypt: Viking comparisons. *Journal of Geophysical Research: Solid Earth*, 84: 8222-8232.
- McEwen A. S., Dundas C. M., Mattson S. S., Toigo A. D., Ojha L., Wray J. J., Chojnacki M., Byrne S., Murchie S. L., and Thomas N. (2014) Recurring slope lineae in equatorial regions of Mars. *Nature geoscience*, 7: 53-58.
- McKay C. P., Anbar A. D., Porco C., and Tsou P. (2014) Follow the plume: the habitability of Enceladus. *Astrobiology*, 14: 352-355.
- McKay C. P., Andersen D., and Davila A. (2017) Antarctic environments as models of planetary habitats: University Valley as a model for modern Mars and Lake Untersee as a model for Enceladus and ancient Mars. *The Polar Journal*, 7: 303-318.
- McKay C. P., Friedman E. I., Wharton R. A., and Davies W. L. (1992) History of water on Mars: a biological perspective. *Advances in Space Research*, 12: 231-238.
- Meadows V. S., Reinhard C. T., Arney G. N., Parenteau M. N., Schwieterman E. W., Domagal-Goldman S. D., Lincowski A. P., Stapelfeldt K. R., Rauer H., and DasSarma S. (2018) Exoplanet biosignatures: understanding oxygen as a biosignature in the context of its environment. *Astrobiology*, 18: 630-662.
- Meeßen J., Wuthenow P., Schille P., Rabbow E., de Vera J.-P., and Ott S. (2015) Resistance of the lichen Buellia frigida to simulated space conditions during the preflight tests for BIOMEX—viability assay and morphological stability. *Astrobiology*, 15: 601-615.
- Meinert C., Myrgorodska I., De Marcellus P., Buhse T., Nahon L., Hoffmann S. V., d’Hendecourt L. L. S., and Meierhenrich U. J. (2016) Ribose and related sugars from ultraviolet irradiation of interstellar ice analogs. *Science*, 352: 208-212.
- Menon L. R., McIlroy D., Liu A. G., and Brasier M. D. (2016) The dynamic influence of microbial mats on sediments: fluid escape and pseudofossil formation in the Ediacaran Longmyndian Supergroup, UK. *Journal of the Geological Society*, 173: 177-185.
- Mergelov N., Mueller C. W., Prater I., Shorkunov I., Dolgikh A., Zazovskaya E., Shishkov V., Krupskaya V., Abrosimov K., and Cherkinsky A. (2018) Alteration of rocks by endolithic organisms is one of the pathways for the beginning of soils on Earth. *Scientific Reports*, 8: 1-15.
- Mezzasoma A., Coleine C., Sannino C., and Selbmann L. (2022) Endolithic Bacterial Diversity in Lichen-Dominated Communities Is Shaped by Sun Exposure in McMurdo Dry Valleys, Antarctica. *Microbial ecology*, 83: 328-339.

- Mileikowsky C., Cucinotta F. A., Wilson J. W., Gladman B., Horneck G., Lindegren L., Melosh J., Rickman H., Valtonen M., and Zheng J. (2000) Natural transfer of viable microbes in space: 1. From Mars to Earth and Earth to Mars. *Icarus*, 145: 391-427.
- Millan M., Szopa C., Buch A., Coll P., Glavin D. P., Freissinet C., Navarro-González R., François P., Coscia D., and Bonnet J.-Y. (2016) In situ analysis of martian regolith with the SAM experiment during the first mars year of the MSL mission: Identification of organic molecules by gas chromatography from laboratory measurements. *Planetary and Space Science*, 129: 88-102.
- Millar J. L., Bagshaw E. A., Edwards A., Poniecka E. A., and Jungblut A. D. (2021) Polar cryoconite associated microbiota is dominated by hemispheric specialist genera. *Frontiers in microbiology*, 12.
- Minelli G., Ricco A., Beasley C., Hines J., Agasid E., Yost B., Squires D., Friedericks C., Piccini M., and Defouw G. (2010) O/OREOS nanosatellite: A multi-payload technology demonstration.
- Moeller R., Schuerger A. C., Reitz G., and Nicholson W. L. (2012) Protective role of spore structural components in determining *Bacillus subtilis* spore resistance to simulated mars surface conditions. *Applied and environmental microbiology*, 78: 8849-8853.
- Moore J. M., and Howard A. D. (2005) Large alluvial fans on Mars. *Journal of Geophysical Research: Planets*, 110.
- Moreno-Vivián C., Cabello P., Martínez-Luque M., Blasco R., and Castillo F. (1999) Prokaryotic nitrate reduction: molecular properties and functional distinction among bacterial nitrate reductases. *Journal of bacteriology*, 181: 6573-6584.
- Morgan A., Howard A., Hobley D. E., Moore J. M., Dietrich W. E., Williams R. M., Burr D. M., Grant J. A., Wilson S. A., and Matsubara Y. (2014) Sedimentology and climatic environment of alluvial fans in the martian Saheki crater and a comparison with terrestrial fans in the Atacama Desert. *Icarus*, 229: 131-156.
- Morozova D., Möhlmann D., and Wagner D. (2007) Survival of methanogenic archaea from Siberian permafrost under simulated Martian thermal conditions. *Origins of Life and Evolution of Biospheres*, 37: 189-200.
- Motamedi K., Colin A., Hooijschuur J., Postma O., Lootens R., Pruijser D., Stoevelaar R., Ariese F., Hutchinson I., and Ingley R. (2015) Design of a Mars atmosphere simulation chamber and testing a Raman Laser Spectrometer (RLS) under conditions pertinent to Mars rover missions. *EPJ Techniques and Instrumentation*, 2: 1-15.
- Mueller D. R., Vincent W. F., Pollard W. H., and Fritsen C. H. (2001) Glacial cryoconite ecosystems: a bipolar comparison of algal communities and habitats. *Nova Hedwigia Beiheft*, 123: 173-198.
- Murray A. E., Kenig F., Fritsen C. H., McKay C. P., Cawley K. M., Edwards R., Kuhn E., McKnight D. M., Ostrom N. E., and Peng V. (2012) Microbial life at -13 C in the brine of an ice-sealed Antarctic lake. *Proceedings of the National Academy of Sciences*, 109: 20626-20631.
- Musk E. (2017) Making humans a multi-planetary species. *New Space*, 5: 46-61.
- Mustard J., Adler M., Allwood A., Bass D., Beaty D., Bell J., Brinckerhoff W., Carr M., Des Marais D., and Brake B. (2013) Report of the mars 2020 science definition team. *Mars Explor. Progr. Anal. Gr*: 155-205.

- Mustard J. F., Murchie S. L., Pelkey S., Ehlmann B., Milliken R., Grant J. A., Bibring J.-P., Poulet F., Bishop J., and Dobreá E. N. (2008) Hydrated silicate minerals on Mars observed by the Mars Reconnaissance Orbiter CRISM instrument. *Nature*, 454: 305-309.
- Navarro-González R., Navarro K. F., de la Rosa J., Iñiguez E., Molina P., Miranda L. D., Morales P., Cienfuegos E., Coll P., and Raulin F. (2006) The limitations on organic detection in Mars-like soils by thermal volatilization–gas chromatography–MS and their implications for the Viking results. *Proceedings of the National Academy of Sciences*, 103: 16089-16094.
- Navarro-González R., Vargas E., de La Rosa J., Raga A. C., and McKay C. P. (2010) Reanalysis of the Viking results suggests perchlorate and organics at midlatitudes on Mars. *Journal of Geophysical Research: Planets*, 115.
- Neveu M., Hays L. E., Voytek M. A., New M. H., and Schulte M. D. (2018) The Ladder of Life Detection. *Astrobiology*.
- Nicholls S. M., Quick J. C., Tang S., and Loman N. J. (2019) Ultra-deep, long-read nanopore sequencing of mock microbial community standards. *Gigascience*, 8: giz043.
- Nicholson W., Gilichinsky D., Schuerger A., Mironov V., Fajardo-Cavazos P., Kerney K., Krivushin K., Oliveira R., and Waters S. (2014) Isolation of bacteria from Siberian permafrost capable of growing under simulated Mars atmospheric pressure and composition. *40th COSPAR Scientific Assembly*, 40: F3. 3-10-14.
- Nicholson W. L., Krivushin K., Gilichinsky D., and Schuerger A. C. (2013) Growth of *Carnobacterium* spp. from permafrost under low pressure, temperature, and anoxic atmosphere has implications for Earth microbes on Mars. *Proceedings of the National Academy of Sciences*, 110: 666-671.
- Nicholson W. L., Ricco A. J., Agasid E., Beasley C., Diaz-Aguado M., Ehrenfreund P., Friedericks C., Ghassemieh S., Henschke M., and Hines J. W. (2011) The O/OREOS mission: first science data from the Space Environment Survivability of Living Organisms (SESLO) payload. *Astrobiology*, 11: 951-958.
- Nicholson W. L., Schuerger A. C., and Douki T. (2018) The photochemistry of unprotected DNA and DNA inside *Bacillus subtilis* spores exposed to simulated Martian surface conditions of atmospheric composition, temperature, pressure, and solar radiation. *Astrobiology*, 18: 393-402.
- Niederberger T. D., Perreault N. N., Tille S., Lollar B. S., Lacrampe-Couloume G., Andersen D., Greer C. W., Pollard W., and Whyte L. G. (2010) Microbial characterization of a subzero, hypersaline methane seep in the Canadian High Arctic. *The ISME journal*, 4: 1326.
- Nienow J. A., McKay C. P., and Friedmann E. I. (1988) The cryptoendolithic microbial environment in the Ross Desert of Antarctica: light in the photosynthetically active region. *Microbial ecology*, 16: 271-289.
- Nimmo F., and Pappalardo R. (2016) Ocean worlds in the outer solar system. *Journal of Geophysical Research: Planets*, 121: 1378-1399.
- Nordheim T., Hand K., and Paranicas C. (2018) Preservation of potential biosignatures in the shallow subsurface of Europa. *Nature Astronomy*, 2: 673-679.
- Northup D., Melim L., Spilde M., Hathaway J., Garcia M., Moya M., Stone F., Boston P., Dapkevicius M., and Riquelme C. (2011) Lava cave microbial communities within mats and secondary mineral deposits: implications for life detection on other planets. *Astrobiology*, 11: 601-618.

- Novikova N., Deshevaya E., Levinskikh M., Polikarpov N., Poddubko S., Gusev O., and Sychev V. (2015) Study of the effects of the outer space environment on dormant forms of microorganisms, fungi and plants in the 'Expose-R' experiment. *International Journal of Astrobiology*, 14: 137-142.
- O'Connor B. R., Fernández-Martínez M. Á., Léveillé R. J., and Whyte L. G. (2021) Taxonomic characterization and microbial activity determination of cold-adapted microbial communities in lava tube ice caves from Lava Beds National Monument, a high-fidelity Mars analogue environment. *Astrobiology*, 21: 613-627.
- Ojha L., Wilhelm M. B., Murchie S. L., McEwen A. S., Wray J. J., Hanley J., Massé M., and Chojnacki M. (2015) Spectral evidence for hydrated salts in recurring slope lineae on Mars. *Nature Geoscience*, 8: 829-832.
- Olsson-Francis K., and Cockell C. S. (2010) Experimental methods for studying microbial survival in extraterrestrial environments. *Journal of microbiological methods*, 80: 1-13.
- Olsson-Francis K., de La Torre R., Towner M. C., and Cockell C. S. (2009) Survival of akinetes (resting-state cells of cyanobacteria) in low Earth orbit and simulated extraterrestrial conditions. *Origins of Life and Evolution of Biospheres*, 39: 565-579.
- Onofri S., Barreca D., Selbmann L., Isola D., Rabbow E., Horneck G., De Vera J., Hatton J., and Zucconi L. (2013) Resistance of Antarctic black fungi and cryptoendolithic communities to simulated space and Martian conditions. *Studies in Mycology*, 75: 115-170.
- Onofri S., Selbmann L., Pacelli C., Zucconi L., Rabbow E., and de Vera J.-P. (2019) Survival, DNA, and ultrastructural integrity of a cryptoendolithic Antarctic fungus in Mars and Lunar rock analogs exposed outside the International Space Station. *Astrobiology*, 19: 170-182.
- Oren A., Sørensen K. B., Canfield D. E., Teske A. P., Ionescu D., Lipski A., and Altendorf K. (2009) Microbial communities and processes within a hypersaline gypsum crust in a saltern evaporation pond (Eilat, Israel). *Hydrobiologia*, 626: 15-26.
- Orosei R., Lauro S., Pettinelli E., Cicchetti A., Coradini M., Cosciotti B., Di Paolo F., Flamini E., Mattei E., and Pajola M. (2018) Radar evidence of subglacial liquid water on Mars. *Science*, 361: 490-493.
- Ortiz M., Leung P. M., Shelley G., Jirapanjawan T., Nauer P. A., Van Goethem M. W., Bay S. K., Islam Z. F., Jordaan K., and Vikram S. (2021) Multiple energy sources and metabolic strategies sustain microbial diversity in Antarctic desert soils. *Proceedings of the National Academy of Sciences*, 118.
- Osinski G. R., Battler M., Caudill C. M., Francis R., Haltigin T., Hipkin V. J., Kerrigan M., Pilles E., Pontefract A., and Tornabene L. L. (2018) The CanMars Mars Sample Return analogue mission. *Planetary and Space Science*, (in press).
- Overholt W. A., Hölzer M., Geesink P., Diezel C., Marz M., and Küsel K. (2020) Inclusion of Oxford Nanopore long reads improves all microbial and phage metagenome-assembled genomes from a complex aquifer system. *Environmental microbiology*, 22: 4000 - 4013.
- Oyama V. I., and Berdahl B. J. (1977) The Viking gas exchange experiment results from Chryse and Utopia surface samples. *Journal of Geophysical Research*, 82: 4669-4676.
- Pace A., Bourillot R., Bouton A., Vennin E., Galaup S., Bundeleva I., Patrier P., Dupraz C., Thomazo C., and Sansjofre P. (2016) Microbial and diagenetic steps leading to the mineralisation of Great Salt Lake microbialites. *Scientific Reports*, 6: 1-12.
- Pace N. R. (2001) The universal nature of biochemistry. *Proceedings of the National Academy of Sciences*, 98: 805-808.

- Pacelli C., Selbmann L., Zucconi L., De Vera J.-P., Rabbow E., Horneck G., de la Torre R., and Onofri S. (2017) BIOMEX experiment: ultrastructural alterations, molecular damage and survival of the fungus *Cryomyces antarcticus* after the experiment verification tests. *Origins of Life and Evolution of Biospheres*, 47: 187-202.
- Panitz C., Rettberg P., Frösler J., Flemming H.-C., Rabbow E., and Reitz G. (2013) BOSS on EXPOSE-R2-Comparative Investigations on Biofilm and Planktonic cells of *Deinococcus geothermalis* as Mission Preparation Tests. European Planetary Science Congress.
- Pappalardo R., Vance S., Bagenal F., Bills B., Blaney D., Blankenship D., Brinckerhoff W., Connerney J., Hand K., and Hoehler T. M. (2013) Science potential from a Europa lander. *Astrobiology*, 13: 740-773.
- Parenteau M. N., Jahnke L. L., Farmer J. D., and Cady S. L. (2014) Production and early preservation of lipid biomarkers in iron hot springs. *Astrobiology*, 14: 502-521.
- Parfenov G., and Lukin A. (1973) Results and prospects of microbiological studies in outer space. *Space life sciences*, 4: 160-179.
- Park C. H., Kim K. M., Kim O.-S., Jeong G., and Hong S. G. (2016) Bacterial communities in Antarctic lichens. *Antarctic Science*, 28: 455-461.
- Parks D. H., Chuvochina M., Waite D. W., Rinke C., Skarshewski A., Chaumeil P.-A., and Hugenholtz P. (2018) A standardized bacterial taxonomy based on genome phylogeny substantially revises the tree of life. *Nature biotechnology*, 36: 996-1004.
- Parro V., and Munoz-Caro G. (2010) Solid carbonaceous and organic matter in space, macromolecular complexes, biomarkers, and microarray-based instrumentation for in situ detection. *Astrobiology: Emergence, Search and Detection of Life*, edited by VA Basiuk, American Scientific Publishers, Los Angeles: 376-398.
- Perri E., Tucker M. E., and Mawson M. (2013) Biotic and abiotic processes in the formation and diagenesis of Permian dolomitic stromatolites (Zechstein Group, NE England). *Journal of Sedimentary Research*, 83: 896-914.
- Plesivkova D., Richards R., and Harbison S. (2019) A review of the potential of the MinION™ single-molecule sequencing system for forensic applications. *Wiley Interdisciplinary Reviews: Forensic Science*, 1: e1323.
- Pointing S. B., and Belnap J. (2012) Microbial colonization and controls in dryland systems. *Nature Reviews Microbiology*, 10: 551-562.
- Pointing S. B., Chan Y., Lacap D. C., Lau M. C., Jurgens J. A., and Farrell R. L. (2009) Highly specialized microbial diversity in hyper-arid polar desert. *Proceedings of the National Academy of Sciences*, 106: 19964-19969.
- Pontefract A., Hachey J., Zuber M. T., Ruvkun G., and Carr C. E. (2018) Sequencing Nothing: Exploring Failure Modes of Nanopore Sensing and Implications for Life Detection. *Life Sciences in Space Research*.
- Qu E. B., Omelon C. R., Oren A., Meslier V., Cowan D. A., Maggs-Kölling G., and DiRuggiero J. (2020) Trophic selective pressures organize the composition of endolithic microbial communities from global deserts. *Frontiers in microbiology*, 10: 2952.
- Quantin C., Popova O., Hartmann W. K., and Werner S. C. (2016) Young Martian crater Gratteri and its secondary craters. *Journal of Geophysical Research: Planets*, 121: 1118-1140.
- Quick J., Grubaugh N. D., Pullan S. T., Claro I. M., Smith A. D., Gangavarapu K., Oliveira G., Robles-Sikisaka R., Rogers T. F., and Beutler N. A. (2017) Multiplex PCR method for

- MinION and Illumina sequencing of Zika and other virus genomes directly from clinical samples. *Nature protocols*, 12: 1261-1276.
- Quick J., Loman N. J., Duraffour S., Simpson J. T., Severi E., Cowley L., Bore J. A., Koundouno R., Dudas G., and Mikhail A. (2016) Real-time, portable genome sequencing for Ebola surveillance. *Nature*, 530: 228-232.
- Rabbow E., Rettberg P., Barczyk S., Bohmeier M., Parpart A., Panitz C., Horneck G., von Heise-Rotenburg R., Hoppenbrouwers T., and Willnecker R. (2012) EXPOSE-E: an ESA astrobiology mission 1.5 years in space. *Astrobiology*, 12: 374-386.
- Raes J., Korbel J. O., Lercher M. J., Von Mering C., and Bork P. (2007) Prediction of effective genome size in metagenomic samples. *Genome biology*, 8: R10.
- Raggio J., Pintado A., Ascaso C., De La Torre R., De Los Ríos A., Wierzchos J., Horneck G., and Sancho L. (2011) Whole lichen thalli survive exposure to space conditions: results of Lithopanspermia experiment with *Aspicilia fruticulosa*. *Astrobiology*, 11: 281-292.
- Rapin W., Ehlmann B. L., Dromart G., Schieber J., Thomas N., Fischer W. W., Fox V., Stein N. T., Nachon M., and Clark B. C. (2019) An interval of high salinity in ancient Gale crater lake on Mars. *Nature Geoscience*, 12: 889-895.
- Raymond-Bouchard I., Maggiori C., Brennan L., Altshuler I., Manchado J. M., Parro V., and Whyte L. G. (2022) Assessment of automated nucleic acid extraction systems in combination with MinION sequencing as potential tools for the detection of microbial biosignatures. *Astrobiology*, 22: 87-103.
- Rhind T., Ronholm J., Berg B., Mann P., Applin D., Stromberg J., Sharma R., Whyte L., and Cloutis E. (2014) Gypsum-hosted endolithic communities of the Lake St. Martin impact structure, Manitoba, Canada: spectroscopic detectability and implications for Mars. *International Journal of Astrobiology*, 13: 366-377.
- Rivera-Valentín E. G., Chevriér V. F., Soto A., and Martínez G. (2020) Distribution and habitability of (meta) stable brines on present-day Mars. *Nature astronomy*, 4: 756-761.
- Roth L., Saur J., Retherford K. D., Strobel D. F., Feldman P. D., McGrath M. A., and Nimmo F. (2014) Transient water vapor at Europa's south pole. *science*, 343: 171-174.
- Roy R., Shilpa P. P., and Bagh S. (2016) A systems biology analysis unfolds the molecular pathways and networks of two proteobacteria in spaceflight and simulated microgravity conditions. *Astrobiology*, 16: 677-689.
- Rull F., Maurice S., Hutchinson I., Moral A., Perez C., Diaz C., Colombo M., Belenguer T., Lopez-Reyes G., and Sansano A. (2017) The Raman Laser Spectrometer for the ExoMars Rover Mission to Mars. *Astrobiology*, 17: 627-654.
- Rummel J. D., and Conley C. A. (2018) Inadvertently finding Earth contamination on Mars should not be a priority for anyone. *Astrobiology*, 18: 108-115.
- Rutishauser A., Blankenship D. D., Sharp M., Skidmore M. L., Greenbaum J. S., Grima C., Schroeder D. M., Dowdeswell J. A., and Young D. A. (2018) Discovery of a hypersaline subglacial lake complex beneath Devon Ice Cap, Canadian Arctic. *Science Advances*, 4: eaar4353.
- Sagan C., and Fox P. (1975) The canals of Mars: an assessment after Mariner 9. *Icarus*, 25: 602-612.
- Sagan C., and Lederberg J. (1976) The prospects for life on Mars: A pre-Viking assessment. *Icarus*, 28: 291-300.

- Sánchez-García L., Aeppli C., Parro V., Fernández-Remolar D., García-Villadangos M., Chong-Díaz G., Blanco Y., and Carrizo D. (2018) Molecular biomarkers in the subsurface of the Salar Grande (Atacama, Chile) evaporitic deposits. *Biogeochemistry*, 140: 31-52.
- Sánchez-García L., Fernández-Martínez M. A., Moreno-Paz M., Carrizo D., García-Villadangos M., Manchado J. M., Stoker C. R., Glass B., and Parro V. (2020) Simulating Mars drilling mission for searching for life: ground-truthing lipids and other complex microbial biomarkers in the iron-sulfur rich Río Tinto analog. *Astrobiology*, 20: 1029-1047.
- Sánchez F. J., Meeßen J., ^a del Carmen Ruiz M., Leopoldo G., Ott S., Vílchez C., Horneck G., Sadowsky A., and de la Torre R. (2014) UV-C tolerance of symbiotic *Trebouxia* sp. in the space-tested lichen species *Rhizocarpon geographicum* and *Circinaria gyrosa*: role of the hydration state and cortex/screening substances. *International Journal of Astrobiology*, 13: 1-18.
- Sancho L. G., De la Torre R., Horneck G., Ascaso C., de Los Rios A., Pintado A., Wierzos J., and Schuster M. (2007) Lichens survive in space: results from the 2005 LICHENS experiment. *Astrobiology*, 7: 443-454.
- Sarantopoulou E., Gomoiu I., Kollia Z., and Cefalas A. (2011) Interplanetary survival probability of *Aspergillus terreus* spores under simulated solar vacuum ultraviolet irradiation. *Planetary and Space Science*, 59: 63-78.
- Sarantopoulou E., Stefi A., Kollia Z., Palles D., Petrou P., Bourkoula A., Koukouvinos G., Velentzas A., Kakabakos S., and Cefalas A. (2014) Viability of *Cladosporium herbarum* spores under 157 nm laser and vacuum ultraviolet irradiation, low temperature (10 K) and vacuum. *Journal of Applied Physics*, 116: 104701.
- Saunders R., Arvidson R., Badhwar G., Boynton W., Christensen P., Cucinotta F., Feldman W., Gibbs R., Kloss C., and Landano M. (2004) 2001 Mars Odyssey mission summary. *Space Science Reviews*, 110: 1-36.
- Scheller E., Ehlmann B., Hu R., Adams D., and Yung Y. (2021) Long-term drying of Mars by sequestration of ocean-scale volumes of water in the crust. *Science*, 372: 56-62.
- Schlesinger W. H., Phipps J. S., Wallenstein M. D., Hofmockel K. S., Klepeis D. M., and Mahall B. E. (2003) Community composition and photosynthesis by photoautotrophs under quartz pebbles, southern Mojave Desert. *Ecology*, 84: 3222-3231.
- Schmidt B., Blankenship D., Patterson G., and Schenk P. (2011) Active formation of 'chaos terrain' over shallow subsurface water on Europa. *Nature*, 479: 502-505.
- Schmidt M. H.-W., Vogel A., Denton A. K., Istace B., Wormit A., van de Geest H., Bolger M. E., Alseekh S., Maß J., and Pfaff C. (2017) De novo assembly of a new *Solanum pennellii* accession using nanopore sequencing. *The Plant Cell*, 29: 2336-2348.
- Schrodinger E. (1951) What is life? The physical aspect of the living cell. At the University Press.
- Schuenger A. (2015) Ultraviolet irradiation on the surface of Mars: Implications for EVA activities during future human missions. *Planetary Protection Knowledge Gaps for Human Extraterrestrial Missions*, 1845: 1011.
- Schuenger A. C., Mancinelli R. L., Kern R. G., Rothschild L. J., and McKay C. P. (2003) Survival of endospores of *Bacillus subtilis* on spacecraft surfaces under simulated martian environments: implications for the forward contamination of Mars. *Icarus*, 165: 253-276.

- Schuerger A. C., Mickol R. L., and Schwendner P. (2020) The hypopiezotolerant bacterium, *Serratia liquefaciens*, failed to grow in Mars analog soils under simulated Martian conditions at 7 hPa. *Life*, 10: 77.
- Schuerger A. C., and Nicholson W. L. (2006) Interactive effects of hypobaria, low temperature, and CO₂ atmospheres inhibit the growth of mesophilic *Bacillus* spp. under simulated martian conditions. *Icarus*, 185: 143-152.
- Schwieterman E. W., Kiang N. Y., Parenteau M. N., Harman C. E., DasSarma S., Fisher T. M., Arney G. N., Hartnett H. E., Reinhard C. T., and Olson S. L. (2018) Exoplanet biosignatures: a review of remotely detectable signs of life. *Astrobiology*, 18: 663-708.
- Segawa T., Yonezawa T., Edwards A., Akiyoshi A., Tanaka S., Uetake J., Irvine-Fynn T., Fukui K., Li Z., and Takeuchi N. (2017) Biogeography of cryoconite forming cyanobacteria on polar and Asian glaciers. *Journal of biogeography*, 44: 2849-2861.
- Selbmann L., Onofri S., Coleine C., Buzzini P., Canini F., and Zucconi L. (2017) Effect of environmental parameters on biodiversity of the fungal component in lithic Antarctic communities. *Extremophiles*, 21: 1069-1080.
- Sephton M. A. (2018) Selecting Mars samples to return to Earth. *Astronomy & Geophysics*, 59: 1.36-1.38.
- Sevim V., Lee J., Egan R., Clum A., Hundley H., Lee J., Everroad R. C., Detweiler A. M., Bebout B. M., and Pett-Ridge J. (2019) Shotgun metagenome data of a defined mock community using Oxford Nanopore, PacBio and Illumina technologies. *Scientific data*, 6: 1-9.
- Shin S. C., Kim H., Lee J. H., Kim H.-W., Park J., Choi B.-S., Lee S.-C., Kim J. H., Lee H., and Kim S. (2019) Nanopore sequencing reads improve assembly and gene annotation of the *Parochlus steinenii* genome. *Scientific Reports*, 9: 1-10.
- Shoji D., Hussmann H., Sohl F., and Kurita K. (2014) Non-steady state tidal heating of Enceladus. *Icarus*, 235: 75-85.
- Sigler W. V., Bachofen R., and Zeyer J. (2003) Molecular characterization of endolithic cyanobacteria inhabiting exposed dolomite in central Switzerland. *Environmental microbiology*, 5: 618-627.
- Sikorsky J. A., Primerano D. A., Fenger T. W., and Denvir J. (2004) Effect of DNA damage on PCR amplification efficiency with the relative threshold cycle method. *Biochemical and biophysical research communications*, 323: 823-830.
- Simon C., Wiezer A., Strittmatter A. W., and Daniel R. (2009) Phylogenetic diversity and metabolic potential revealed in a glacier ice metagenome. *Applied and Environmental Microbiology*, 75: 7519-7526.
- Simpson J. T., Workman R. E., Zuzarte P., David M., Dursi L., and Timp W. (2017) Detecting DNA cytosine methylation using nanopore sequencing. *Nature methods*, 14: 407-410.
- Sims M. R., Cullen D. C., Rix C. S., Buckley A., Derveni M., Evans D., García-Con L. M., Rhodes A., Rato C. C., and Stefinovic M. (2012) Development status of the life marker chip instrument for ExoMars. *Planetary and Space Science*, 72: 129-137.
- Slatko B. E., Gardner A. F., and Ausubel F. M. (2018) Overview of next-generation sequencing technologies. *Current protocols in molecular biology*, 122: e59.
- Smith A. (1988) The USSR space astronomy programme. In: *Hot Thin Plasmas in Astrophysics*, Springer, pp 415-427.

- Smith D. J., Schuerger A. C., Davidson M. M., Pacala S. W., Bakermans C., and Onstott T. C. (2009) Survivability of *Psychrobacter cryohalolentis* K5 under simulated martian surface conditions. *Astrobiology*, 9: 221-228.
- Sobrado J. M., Martín-Soler J., and Martín-Gago J. A. (2014) Mimicking Mars: A vacuum simulation chamber for testing environmental instrumentation for Mars exploration. *Review of Scientific Instruments*, 85: 035111.
- Sobron P., and Wang A. (2012) A planetary environment and analysis chamber (PEACh) for coordinated Raman–LIBS–IR measurements under planetary surface environmental conditions. *Journal of Raman Spectroscopy*, 43: 212-227.
- Somerville V., Lutz S., Schmid M., Frei D., Moser A., Irmeler S., Frey J. E., and Ahrens C. H. (2019) Long-read based de novo assembly of low-complexity metagenome samples results in finished genomes and reveals insights into strain diversity and an active phage system. *BMC microbiology*, 19: 143.
- Spencer J., Pearl J., Segura M., Flasar F., Mamoutkine A., Romani P., Buratti B., Hendrix A., Spilker L., and Lopes R. (2006) Cassini encounters Enceladus: Background and the discovery of a south polar hot spot. *science*.
- Spry J. A., Race M., Kminek G., Siegel B., and Conley C. (2018) Planetary Protection Knowledge Gaps for Future Mars Human Missions: Stepwise Progress in Identifying and Integrating Science and Technology Needs. 48th International Conference on Environmental Systems.
- Squyres S. W., Knoll A. H., Arvidson R. E., Ashley J. W., Bell III J. F., Calvin W. M., Christensen P. R., Clark B. C., Cohen B. A., and de Souza Jr P. A. (2009) Exploration of Victoria crater by the Mars rover Opportunity. *Science*, 324: 1058-1061.
- Stahl-Rommel S., Jain M., Nguyen H. N., Arnold R. R., Aunon-Chancellor S. M., Sharp G. M., Castro C. L., John K. K., Juul S., and Turner D. J. (2021) Real-time culture-independent microbial profiling onboard the international space station using nanopore sequencing. *Genes*, 12: 106.
- Stan-Lotter H., Radax C., Gruber C., Legat A., Pfaffenhuemer M., Wieland H., Leuko S., Weidler G., Kömle N., and Kargl G. (2002) Astrobiology with haloarchaea from Permo-Triassic rock salt. *International Journal of Astrobiology*, 1: 271-284.
- Steinbrügge G., Voigt J. R., Wolfenbarger N. S., Hamilton C., Soderlund K., Young D., Blankenship D. D., Vance S. D., and Schroeder D. M. (2020) Brine migration and impact-induced cryovolcanism on Europa. *Geophysical Research Letters*, 47: e2020GL090797.
- Stern J. C., Malespin C. A., Eigenbrode J. L., Webster C. R., Flesch G., Franz H. B., Graham H. V., House C. H., Sutter B., and Archer Jr P. D. (2022) Organic carbon concentrations in 3.5-billion-year-old lacustrine mudstones of Mars. *Proceedings of the National Academy of Sciences*, 119: e2201139119.
- Stewart R. D., Auffret M. D., Warr A., Walker A. W., Roehe R., and Watson M. (2019) Compendium of 4,941 rumen metagenome-assembled genomes for rumen microbiome biology and enzyme discovery. *Nature biotechnology*, 37: 953.
- Stoker C. R., Clarke J., Direito S. O., Blake D., Martin K. R., Zavaleta J., and Foing B. (2011) Mineralogical, chemical, organic and microbial properties of subsurface soil cores from Mars Desert Research Station (Utah, USA): Phyllosilicate and sulfate analogues to Mars mission landing sites. *International Journal of Astrobiology*, 10: 269-289.

- Stromberg J., Applin D., Cloutis E., Rice M., Berard G., and Mann P. (2014) The persistence of a chlorophyll spectral biosignature from Martian evaporite and spring analogues under Mars-like conditions. *International Journal of Astrobiology*, 13: 203-223.
- Stüder F., Petit J.-L., Engelen S., and Mendoza-Parra M. A. (2021) Real-time SARS-CoV-2 diagnostic and variants tracking over multiple candidates using nanopore DNA sequencing. *Scientific reports*, 11: 1-11.
- Suija A., Ertz D., Lawrey J. D., and Diederich P. (2015) Multiple origin of the lichenicolous life habit in Helotiales, based on nuclear ribosomal sequences. *Fungal Diversity*, 70: 55-72.
- Summons R. E., Amend J. P., Bish D., Buick R., Cody G. D., Des Marais D. J., Dromart G., Eigenbrode J. L., Knoll A. H., and Sumner D. Y. (2011) Preservation of martian organic and environmental records: final report of the Mars Biosignature Working Group. *Astrobiology*, 11: 157-181.
- Szopa C., Freissinet C., Glavin D. P., Millan M., Buch A., Franz H. B., Summons R. E., Sumner D. Y., Sutter B., and Eigenbrode J. L. (2020) First detections of dichlorobenzene isomers and trichloromethylpropane from organic matter indigenous to Mars mudstone in Gale Crater, Mars: results from the Sample Analysis at Mars instrument onboard the Curiosity rover. *Astrobiology*, 20: 292-306.
- Takada A., Matsushita K., Horioka S., Furuichi Y., and Sumi Y. (2017) Bactericidal effects of 310 nm ultraviolet light-emitting diode irradiation on oral bacteria. *BMC Oral Health*, 17: 1-10.
- Takeuchi N., Kohshima S., Goto-Azuma K., and Koerner R. M. (2001) Biological characteristics of dark colored material (cryoconite) on Canadian Arctic glaciers (Devon and Penny ice caps).
- Tan M. H., Austin C. M., Hammer M. P., Lee Y. P., Croft L. J., and Gan H. M. (2018) Finding Nemo: hybrid assembly with Oxford Nanopore and Illumina reads greatly improves the clownfish (*Amphiprion ocellaris*) genome assembly. *GigaScience*, 7: gix137.
- Tanaka H., Matsuo Y., Nakagawa S., Nishi K., Okamoto A., Kai S., Iwai T., Tabata Y., Tajima T., and Komatsu Y. (2019) Real-time diagnostic analysis of MinION™-based metagenomic sequencing in clinical microbiology evaluation: a case report. *JA clinical reports*, 5: 1-2.
- Taylor G., Bailey J., and Benton E. (2022) Physical dosimetric evaluations in the Apollo 16 microbial response experiment. In: *13. São Paulo, SP, Brazil-June 1974*, De Gruyter, pp 135-143.
- Taylor J. S., and Cohrs M. P. (1987) DNA, light, and Dewar pyrimidinones: the structure and biological significance to TpT3. *Journal of the American Chemical Society*, 109: 2834-2835.
- Telling J., Anesio A. M., Tranter M., Stibal M., Hawkings J., Irvine-Fynn T., Hodson A., Butler C., Yallop M., and Wadham J. (2012) Controls on the autochthonous production and respiration of organic matter in cryoconite holes on high Arctic glaciers. *Journal of Geophysical Research: Biogeosciences*, 117.
- Tessler M., Neumann J. S., Afshinnekoo E., Pineda M., Hersch R., Velho L. F. M., Segovia B. T., Lansac-Toha F. A., Lemke M., and DeSalle R. (2017) Large-scale differences in microbial biodiversity discovery between 16S amplicon and shotgun sequencing. *Scientific reports*, 7: 6589.

- Thiel C. S., Ehrenfreund P., Foing B., Pletser V., and Ullrich O. (2011) PCR-based analysis of microbial communities during the EuroGeoMars campaign at Mars Desert Research Station, Utah. *International Journal of Astrobiology*, 10: 177-190.
- Thompson J. F., and Milos P. M. (2011) The properties and applications of single-molecule DNA sequencing. *Genome biology*, 12: 1-10.
- Trokhimovskiy A., Fedorova A., Olsen K., Alday J., Korablev O., Montmessin F., Lefèvre F., Patrakeevev A., Belyaev D., and Shakun A. (2021) Isotopes of chlorine from HCl in the Martian atmosphere. *Astronomy and Astrophysics*, 651.
- Trumbo S. K., Brown M. E., and Hand K. P. (2019) Sodium chloride on the surface of Europa. *Science advances*, 5: eaaw7123.
- Tyler A. D., Mataseje L., Urfano C. J., Schmidt L., Antonation K. S., Mulvey M. R., and Corbett C. R. (2018) Evaluation of Oxford Nanopore's MinION sequencing device for microbial whole genome sequencing applications. *Scientific reports*, 8: 1-12.
- Vago J. L., Westall F., Coates A. J., Jaumann R., Korablev O., Ciarletti V., Mitrofanov I., Josset J.-L., De Sanctis M. C., and Bibring J.-P. (2017) Habitability on early Mars and the search for biosignatures with the ExoMars Rover. *Astrobiology*, 17: 471-510.
- Van Goethem M. W., Makhalyane T. P., Valverde A., Cary S. C., and Cowan D. A. (2016) Characterization of bacterial communities in lithobionts and soil niches from Victoria Valley, Antarctica. *FEMS microbiology ecology*, 92: fiw051.
- Van Lith Y., Warthmann R., Vasconcelos C., and Mckenzie J. A. (2003) Sulphate-reducing bacteria induce low-temperature Ca-dolomite and high Mg-calcite formation. *Geobiology*, 1: 71-79.
- Van Trappen S., Vandecandelaere I., Mergaert J., and Swings J. (2004) *Flavobacterium degerlachei* sp. nov., *Flavobacterium frigidis* sp. nov. and *Flavobacterium micromati* sp. nov., novel psychrophilic bacteria isolated from microbial mats in Antarctic lakes. *International journal of systematic and evolutionary microbiology*, 54: 85-92.
- Vera J.-P. d., Möhlmann D., Butina F., Lorek A., Wernecke R., and Ott S. (2010) Survival potential and photosynthetic activity of lichens under Mars-like conditions: a laboratory study. *Astrobiology*, 10: 215-227.
- Volkman J., Johns R., Gillan F., Perry G., and Bavor Jr H. (1980) Microbial lipids of an intertidal sediment—I. Fatty acids and hydrocarbons. *Geochimica et Cosmochimica Acta*, 44: 1133-1143.
- Volkman J. K., Barrett S. M., Blackburn S. I., Mansour M. P., Sikes E. L., and Gelin F. (1998) Microalgal biomarkers: a review of recent research developments. *Organic Geochemistry*, 29: 1163-1179.
- Vollmers J., Voget S., Dietrich S., Gollnow K., Smits M., Meyer K., Brinkhoff T., Simon M., and Daniel R. (2013) Poles apart: Arctic and Antarctic Octadecabacter strains share high genome plasticity and a new type of xanthorhodopsin. *PLoS One*, 8: e63422.
- Wan W., Wang C., Li C., and Wei Y. (2020) China's first mission to Mars. *Nature Astronomy*, 4: 721-721.
- Wassmann M., Moeller R., Rabbow E., Panitz C., Horneck G., Reitz G., Douki T., Cadet J., Stan-Lotter H., and Cockell C. S. (2012) Survival of spores of the UV-resistant *Bacillus subtilis* strain MW01 after exposure to low-earth orbit and simulated martian conditions: data from the space experiment ADAPT on EXPOSE-E. *Astrobiology*, 12: 498-507.
- Waters S. M., Ledford S. M., Wacker A., Verma S., Serda B., McKaig J., Varelas J., Nicoll P. M., Venkateswaran K., and Smith D. J. (2021) Long-read sequencing reveals increased

- occurrence of genomic variants and adenosine methylation in *Bacillus pumilus* SAFR-032 after long-duration flight exposure onboard the International Space Station. *International Journal of Astrobiology*, 20: 435-444.
- Weisleitner K., Perras A., Moissl-Eichinger C., Andersen D. T., and Sattler B. (2019) Source environments of the microbiome in perennially ice-covered Lake Untersee, Antarctica. *Frontiers in microbiology*, 10: 1019.
- Westall F., Loizeau D., Foucher F., Bost N., Bertrand M., Vago J., and Kminek G. (2013) Habitability on Mars from a microbial point of view. *Astrobiology*, 13: 887-897.
- Wick R. R., Judd L. M., Gorrie C. L., and Holt K. E. (2017) Completing bacterial genome assemblies with multiplex MinION sequencing. *Microbial genomics*, 3.
- Wierzchos J., Cámara B., de Los Ríos A., Davila A., Sánchez Almazo I., Artieda O., Wierzchos K., Gomez-Silva B., McKay C., and Ascaso C. (2011) Microbial colonization of Calcium sulfate crusts in the hyperarid core of the Atacama Desert: implications for the search for life on Mars. *Geobiology*, 9: 44-60.
- Wierzchos J., Davila A. F., Artieda O., Cámara-Gallego B., de los Ríos A., Neelson K. H., Valea S., García-González M. T., and Ascaso C. (2013) Ignimbrite as a substrate for endolithic life in the hyper-arid Atacama Desert: implications for the search for life on Mars. *Icarus*, 224: 334-346.
- Wierzchos J., DiRuggiero J., Vitek P., Artieda O., Souza-Egipsy V., Skaloud P., Tisza M., Davila A. F., Vílchez C., and Garbayo I. (2015) Adaptation strategies of endolithic chlorophototrophs to survive the hyperarid and extreme solar radiation environment of the Atacama Desert. *Frontiers in microbiology*, 6: 934.
- Wierzchos J., Ríos A. d. I., and Ascaso C. (2012) Microorganisms in desert rocks: the edge of life on Earth.
- Wight J., Varin M.-P., Robertson G. J., Huot Y., and Lang A. S. (2020) Microbiology in the field: construction and validation of a portable incubator for real-time quantification of coliforms and other bacteria. *Frontiers in public health*, 8.
- Williams R. M., Chidsey Jr T. C., and Eby D. E. (2007) Exhumed paleochannels in central Utah—Analogues for raised curvilinear features on Mars.
- Williams R. M., Irwin R. P., and Zimbelman J. R. (2009) Evaluation of paleohydrologic models for terrestrial inverted channels: Implications for application to martian sinuous ridges. *Geomorphology*, 107: 300-315.
- Wu Z., Ling Z., Zhang J., Fu X., Liu C., Xin Y., Li B., and Qiao L. (2021) A Mars Environment Chamber Coupled with Multiple In Situ Spectral Sensors for Mars Exploration. *Sensors*, 21: 2519.
- Ye T., Wang B., Li C., Bian P., Chen L., and Wang G. (2021) Exposure of cyanobacterium *Nostoc* sp. to the Mars-like stratosphere environment. *Journal of Photochemistry and Photobiology B: Biology*, 224: 112307.
- Yergeau E., Michel C., Tremblay J., Niemi A., King T. L., Wyglinski J., Lee K., and Greer C. W. (2017) Metagenomic survey of the taxonomic and functional microbial communities of seawater and sea ice from the Canadian Arctic. *Scientific reports*, 7: 42242.
- Zawierucha K., Ostrowska M., and Kolicka M. (2017) Applicability of cryoconite consortia of microorganisms and glacier-dwelling animals in astrobiological studies. *Contemporary Trends in Geoscience*, 6.
- Zhukova A., and Kondratyev I. (1965) On artificial Martian conditions reproduced for microbiological research. *Life sciences and space research*, 3: 120-126.

- Ziolkowski L., Mykytczuk N., Omelon C., Johnson H., Whyte L., and Slater G. (2013) Arctic gypsum endoliths: a biogeochemical characterization of a viable and active microbial community.
- Zucconi L., Onofri S., Cecchini C., Isola D., Ripa C., Fenice M., Madonna S., Reboleiro-Rivas P., and Selbmann L. (2016) Mapping the lithic colonization at the boundaries of life in Northern Victoria Land, Antarctica. *Polar Biology*, 39: 91-102.

Appendix

Supplementary Table 2.1. XRD results of the mineralogy of the Hanksville paleochannel samples. Major and minor sample constituents are indicated.

Sample type	Sample name	Major mineral	Minor minerals
Endolith	E1	Quartz	Albite (Ca)
Endolith	E2	Quartz	N/A
Endolith	E3	Quartz	N/A
Endolith	E4	Quartz	N/A
Endolith	E5	Quartz	Calcite
Regolith	S1	Quartz	Albite, montmorillonite
Regolith	S2	Quartz	Montmorillonite, albite (Ca)
Regolith	S3	Quartz	Calcite, gypsum, montmorillonite, albite (Ca)
Rock	R1	Quartz	Gypsum, apatite
Rock	R2	Quartz, calcite	Nontronite, fluoroapatite (carbonate-rich)
Rock	R3	Quartz	Calcite

Supplementary Table 3.1. UVC irradiation values for the UVC chamber. These values assume Ls 323, an assumed opacity of 0.42, the length of a Martian year = 668.6 sols, and a maximum total UV irradiation per sol of 1.0619 MJ/m².

Sample	Exposure time (days)	Irradiance (W/m²)	Irradiation (MJ/m²)	Equivalent exposure time based on UVC dose (sols/ Martian years)
T0 _{UV}	0	0	0	0/0
T1 _{UV}	14	32.94	39.844224	25 301.43726/ 37.84
T2 _{UV}	28	36.18	87.526656	55 580.20643/ 83.13
T3 _{UV}	42	47.71	173.130048	109 939.1231/ 164.38
T4 _{UV}	56	60.42	292.336128	185 636.046/ 277.65

Supplementary Table 4.1. MAGs produced with MinION assembly and MinION assembly+short read polishing with Racon+frameshift correction with DIAMOND. MAG parameters were determined with CheckM. Metaerg taxonomy is determined via predicted ORFs which inherited their taxonomy from GTDB. The following bins had contigs removed: MinION_3 below coverage 20x, MinION_RD_2 below coverage 15x and above 60x, MinION_RD_3 below coverage 18x and above 60x.

Assembly type	MAG ID	Genome size (bp)	Longest contig (bp)	Mean contig length (bp)	N50	Completeness (%)	Contamination (%)	Metaerg GTDB-based taxonomy
MinION	MinION_3	9 763 258	105 216	12 663	17 423	62.3	63.8	<i>Flavobacterium</i> sp.
	MinION_1	645 498	130 460	26 895	66 719	4.1	0	Unknown
	MinION_4	466 879	235 857	66 697	235 857	1.3	0.1	Unknown
	MinION_2	619 656	41 561	8488	11 508	1.6	0	Unknown
MinION+ Racon+ DIAMOND	MinION_RD_4	521 910	42 192	9663	12 724	3.9	3.1	Unknown
	MinION_RD_5	470 838	238 237	67 246	238 237	4.4	0.5	Unknown
	MinION_RD_6	386 987	192 920	16 097	28 604	0	0	Unknown
	MinION_RD_2	6 130 373	83 218	10 997	14 970	76.3	89.6	<i>Flavobacterium</i> sp.
	MinION_RD_1	635 010	130 059	28 852	66 485	4.1	0	Unknown
	MinION_RD_3	4 149 228	106 479	13 310	17 514	68.2	46.4	<i>Flavobacterium</i> sp.

Supplementary Table 4.2. Stress response genes present in Hybrid_5.

Stress response category	KEGG orthology / Enzyme Commission number	Gene name
General stress response	K01356 / EC:3.4.21.88	SOS-response transcriptional repressor LexA, <i>lexA</i>
Osmotic stress	K02000+K02001+K02002 / EC:7.6.2.9	Glycine betaine ABC transport system, <i>proVWX</i>
	K03762	Proline betaine transporter, <i>proP</i>
	K00130 / EC:1.2.1.8	Betaine-aldehyde dehydrogenase, <i>betB</i> and <i>gbsA</i>
	K02168	Choline/glycine/proline betaine transporter, <i>betT</i> and <i>betS</i>
	K00108 / EC:1.1.99.1	Choline dehydrogenase, <i>betA</i>
	K03451	Carnitine/betaine transporter, BCCT family
	K00301+ K00302+ K00303+ K00304+ K00305 / EC:1.5.3.1	Sarcosine oxidase, <i>soxABDG</i>
	EC:3.1.6.6	Choline-sulfatase
	K03313	Na ⁺ :H ⁺ antiporter, NhaA family
	K07646 / EC:2.7.13.3	Osmosensitive K ⁺ channel histidine kinase, <i>kdpD</i>
	K10227+K10229	Sorbitol/mannitol transport system substrate-binding and permease proteins, <i>smoE</i> and <i>smoG</i>
	K00284 / EC:1.4.7.1	Glutamate synthase (ferredoxin)
	K00264 / EC:1.4.1.14	Glutamate synthase (NADH)
	K00266+K00265 / EC:1.4.1.13	Glutamate synthase (NADPH) small chain and large chain
Oxidative stress	K04564 / EC:1.15.11	Superoxide dismutase
	K03782 / EC:1.11.1.21	Catalase-peroxidase, <i>katG</i>
	K19511 / EC:1.11.1.7	Peroxidase
	K01420	Transcription regulator, Crp/Fnr family
	K03386 / EC:1.11.1.15	Peroxioredoxin (alkyl hydroperoxide reductase subunit C), <i>ahpC</i>
	K03808	Paraquat-inducible protein A, <i>pqiA</i>
	K00681 / EC:2.3.2.2	Gamma-glutamyltranspeptidase
	K03396 / EC:6.3.2.3	Glutathione synthase, <i>gshB</i>

	K13892+K13889+ K13890	Glutathione transport system, <i>gsiABC</i>
	K00799 / EC:2.5.1.18	Glutathione S-transferase, <i>gst</i>
	K00383 / EC:1.8.1.7	Glutathione reductase (NADPH), <i>gor</i>
	K00432 / EC:1.11.1.9	Glutathione peroxidase, <i>gpx</i>
	K00384 / EC:1.8.1.9	Thioredoxin reductase, <i>trxB</i>
	K01637 / EC:4.1.3.1	Isocitrate lyase, <i>aceA</i>
	K00036 / EC:1.1.1.49	Glucose-6-phosphate 1- dehydrogenase, <i>G6PD/zwf</i>
Cold and heat shock	K03704	Cold shock protein, <i>cspA</i>
	K03686	Molecular chaperone DnaJ, <i>dnaJ</i>
	K05801	DnaJ-like chaperone, <i>djlA</i>
	K04043	Molecular chaperone DnaK, <i>dnaK</i>
	K03687	Molecular chaperone GrpE
	K04080	Molecular chaperone IbpA, <i>ibpA</i>
	K04083	Molecular chaperone Hsp33, <i>hslO</i>
	K04078 K04077	Chaperonin GroES, <i>groES</i> Chaperonin GroEL, <i>groEL</i>
Protein folding	K03775 / EC:5.2.1.8	Peptidyl-prolyl <i>cis-trans</i> isomerase
	K03545	Trigger factor, <i>tig</i>
Carotenoids	K02291 / EC:2.5.1.32	Phytoene synthase
Membrane / peptidoglycan alteration	K00647 / EC:2.3.1.41	3-oxoacyl-[acyl-carrier-protein] synthase I, <i>fabB</i>
	K09458 / EC:2.3.1.179	3-oxoacyl-[acyl-carrier-protein] synthase II, <i>fabF</i>
	K00648 / EC:2.3.1.180	3-oxoacyl-[acyl-carrier-protein] synthase III, <i>fabH</i>
	K00059 / EC:1.1.1.100	3-oxoacyl-[acyl-carrier protein] reductase, <i>fabG</i>
	K01286 / EC:3.4.16.4	D-alanyl-D-alanine carboxypeptidase
	K07516 / EC:1.1.1.35	3-hydroxyacyl-CoA dehydrogenase, <i>fadN</i>
	K00790 / EC:2.5.1.7	UDP-N-acetylglucosamine 1- carboxyvinyltransferase, <i>murA</i>
	K00075 / EC:1.3.1.98	UDP-N-acetylmuramate dehydrogenase, <i>murB</i>
	K01924 / EC:6.3.2.8	UDP-N-acetylmuramate—alanine ligase, <i>murC</i>
	K01925 / EC:6.3.2.9	UDP-N-acetylmuramoylalanine-- D-glutamate ligase, <i>murD</i>
	K05362 / EC:6.3.2.7	UDP-N-acetylmuramoyl-L-alanyl- D-glutamate-L-lysine ligase, <i>murE</i>

	K01929 / EC:6.3.2.10	UDP-N-acetylmuramoyl-tripeptide--D-alanyl-D-alanine ligase, <i>murF</i>
UV stress	K01669 / EC:4.1.99.3	Deoxyribodipyrimidine photolyase, <i>phrB</i> [EC:4.1.99.3]
	K06876	Deoxyribodipyrimidine photolyase-related protein
Storage and starvation response	K06217	Phosphate starvation-inducible protein PhoH and related proteins, <i>phoH</i> and <i>phoL</i>
	K07636 / EC:2.7.13.3	Phosphate regulon sensor histidine kinase PhoR, <i>phoR</i>
	K07657	Phosphate regulon response regulator, <i>phoB</i>
	K02039	Phosphate transport system protein, <i>phoU</i>
	K00631 / EC:2.3.1.15	Glycerol-3-phosphate O-acyltransferase, <i>plsB</i>
DNA replication and repair	K02469+K02470 / EC:5.6.2.2	DNA gyrase, <i>gyrAB</i>
	K03553	Recombination protein RecA, <i>recA</i>
	K06187	Recombination protein RecR, <i>recR</i>
	K03631	DNA repair protein RecN, <i>recN</i>
	K03584	DNA repair protein RecO, <i>recO</i>
	K04485	DNA repair protein RadA/Sms, <i>radA/sms</i>
	K03630	DNA repair protein RadC, <i>radC</i>
	K03655	ATP-dependent DNA helicase RecG, <i>recG</i>
	K03654 / EC:3.6.4.12	ATP-dependent DNA helicase RecQ, <i>recQ</i>
	K07462	Single-stranded-DNA-specific exonuclease, <i>recJ</i>
	K03550 / EC:3.6.4.12	Holliday junction DNA helicase RuvA, <i>ruvA</i>
	K03551 / EC:3.6.4.12	Holliday junction DNA helicase RuvB, <i>ruvB</i>
K01159 / EC:3.1.22.4	Crossover junction endodeoxyribonuclease RuvC, <i>ruvC</i>	
Polysaccharide capsule	K19421	Polysaccharide biosynthesis protein EpsC, <i>epsC</i>
Transcription and translation factors	K05539	tRNA-dihydrouridine synthase, <i>dusA</i>
	K03628	Transcription termination factor Rho, <i>rho</i>

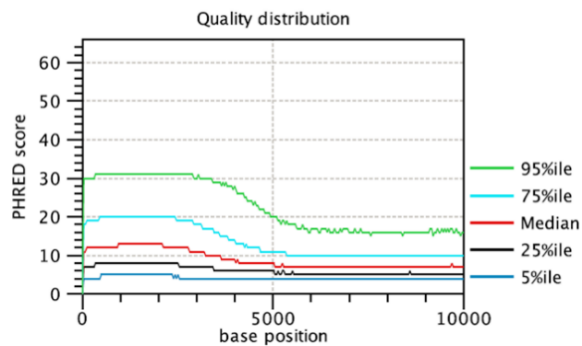
	K02600	Transcription termination/antitermination protein NusA, <i>nusA</i>
	K03625	Transcription antitermination protein NusB, <i>nusB</i>
	K02601	Transcription termination/antitermination protein NusG, <i>nusG</i>
	K03257	Translation initiation factor 4A
	K02518	Translation initiation factor IF-1, <i>infA</i>
	K02519	Translation initiation factor IF-2, <i>infB</i>
	K02520	Translation initiation factor IF-3, <i>infC</i>
	K03723 / EC:3.6.4.-	Transcription-repair coupling factor (superfamily II helicase)
	K05592 / EC:3.6.4.13	ATP-dependent RNA helicase DeaD, <i>deaD</i>
	K12573 / EC:3.1.13.1	Cold shock-induced ribonuclease R, <i>rnr</i>
	K02834	Ribosome-binding factor A, <i>rbfA</i>
Pyruvate metabolism	K00163 / EC:1.2.4.1	Pyruvate dehydrogenase E1 component, <i>aceE</i>
	K00627 / EC:2.3.1.12	Pyruvate dehydrogenase E2 component (dihydrolipoamide acetyltransferase), <i>aceF</i>

Supplementary Table 4.3. DNA extraction details for MinION-sequenced cryoconites.

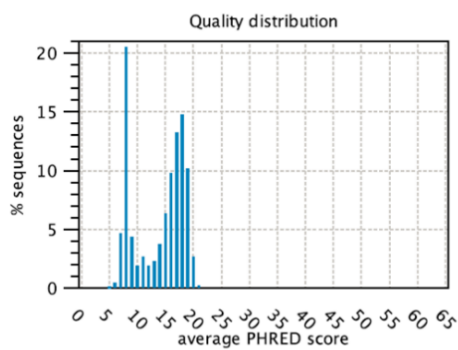
Sample	Extraction method	MinION sequencing kit	Cryoconite
Crude	Lysing with the SuperFastPrep-2™ and filtration with a 0.45 µm filter	SQK-RPB004	3
C3FullM	Lysing with the SuperFastPrep-2™ and purification as outlined in the DNeasy protocol (steps #5 – 19)	SQK-RPB004	3
VolTRAX	Lysing with the SuperFastPrep-2™ and purification as outlined in the DNeasy protocol (steps #5 – 19)	VSK-VSK002	3
C3Claremont	Claremont SimplePrep X1	SQK-RPB004	3

Supplementary Table 4.4. DNA extraction details for HiSeq-sequenced samples.

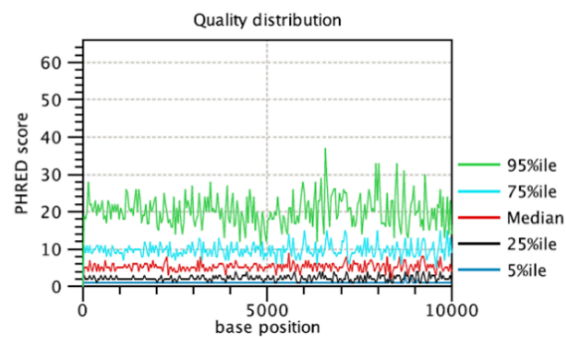
Sample	Extraction method	Cryoconite
C1Crude	Lysing with the SuperFastPrep-2™ and filtration with a 0.45 µm filter	1
C1FullM	Lysing with the SuperFastPrep-2™ and purification as outlined in the DNeasy protocol (steps #5 – 19)	1
C1Full	Full and purified extraction with the DNeasy kit according to the manufacturer's instructions	1
C2FullM	Lysing with the SuperFastPrep-2™ and purification as outlined in the DNeasy protocol (steps #5 – 19)	2
C2Full1	Full and purified extraction with the DNeasy kit according to the manufacturer's instructions	2
C2Full2	Full and purified extraction with the DNeasy kit according to the manufacturer's instructions	2
C3FullM	Lysing with the SuperFastPrep-2™ and purification as outlined in the DNeasy protocol (steps #5 – 19)	3
C3Full1	Full and purified extraction with the DNeasy kit according to the manufacturer's instructions	3
C3Full2	Full and purified extraction with the DNeasy kit according to the manufacturer's instructions	3
C3Claremont	Claremont SimplePrep X1	3

A

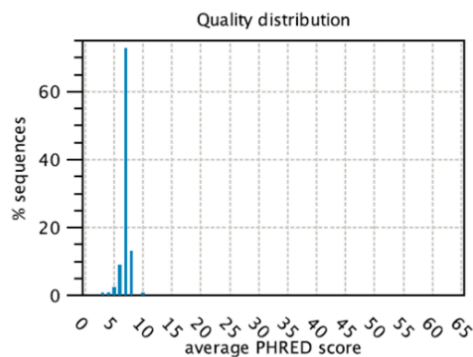
Base-quality distribution along the base positions.
 x: base position
 y: median & percentiles of quality scores observed at that base position



Distribution of average sequence quality scores. The quality of a sequence is calculated as the arithmetic mean of its base qualities.
 x: PHRED-score
 y: number of sequences observed at that qual. score normalized to the total number of sequences

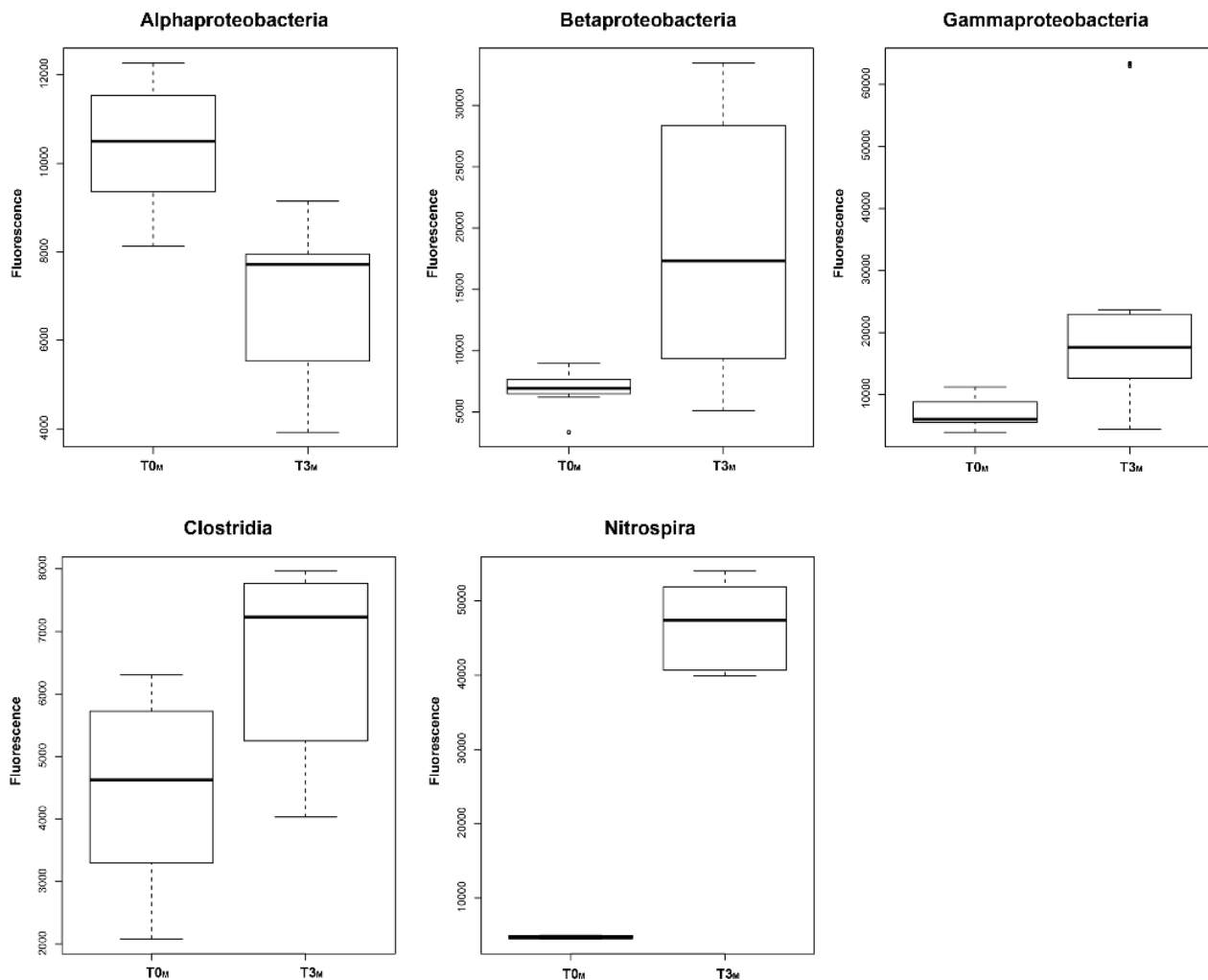
B

Base-quality distribution along the base positions.
 x: base position
 y: median & percentiles of quality scores observed at that base position

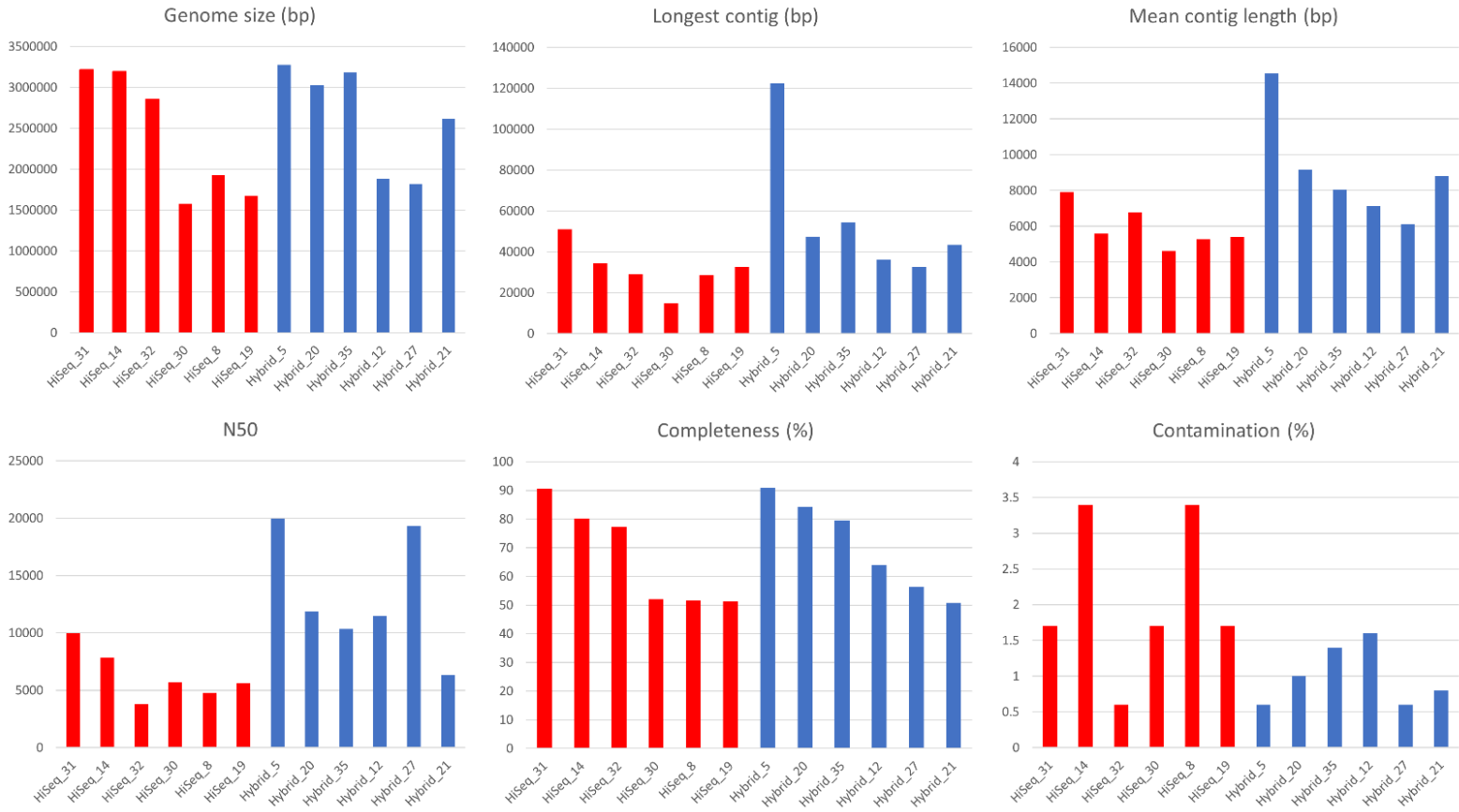


Distribution of average sequence quality scores. The quality of a sequence is calculated as the arithmetic mean of its base qualities.
 x: PHRED-score
 y: number of sequences observed at that qual. score normalized to the total number of sequences

Supplementary Figure 2.1. PHRED quality distribution of the detection limit trials with endolith sample E4. (A) Quality distribution in the first 0.110 ng trial. (B) Quality distribution in the trial containing no DNA.



Supplementary Figure 3.1. Statistically significant differences between antibodies from the LDChip exhibiting positive detection in samples T0_M and T3_M. These antibodies were compared via T-test and visualized on the boxplots above.



Supplementary Figure 4.1. Details of the hybrid and HiSeq high-quality and medium-quality MAGs. This information is outlined in Table 3.